ISSN 1007-9327
CN 14-1219/R

WJG

World Journal of Gastroenterology®

Indexed and Abstracted in:

Current Contents®/Clinical Medicine, Science Citation Index Expanded (also known as SciSearch®) and Journal Citation Reports/Science Edition, *Index Medicus*, MEDLINE and PubMed, Chemical Abstracts, EMBASE/Excerpta Medica, Abstracts Journals, PubMed Central, Digital Object Identifier, CAB Abstracts and Global Health.

ISI JCR 2003-2000 IF: 3.318, 2.532, 1.445 and 0.993.

Volume 15 Number 22
June 14, 2009
World J Gastroenterol
2009 June 14; 15(22): 2689-2816

Online Submissions
wjg.wjgnet.com
www.wjgnet.com

Printed on Acid-free Paper
世界胃肠病学杂志

A Weekly Journal of Gastroenterology and Hepatology

World Journal of Gastroenterology ®

Editorial Board

2007-2009

百世登
Baishideng™©

Editorial Office: *World Journal of Gastroenterology*
Room 903, Building D, Ocean International Center
No. 62 Dongsihuan Zhonglu, Chaoyang District, Beijing 100025, China
E-mail: wjg@wjgnet.com http://www.wjgnet.com Telephone: 0086-10-5908-0039 Fax: 0086-10-8538-1893

The *World Journal of Gastroenterology* Editorial Board consists of 1179 members, representing a team of worldwide experts in gastroenterology and hepatology. They are from 60 countries, including Albania (1), Argentina (4), Australia (38), Austria (11), Belarus (1), Belgium (15), Brazil (2), Bulgaria (1), Canada (25), Chile (1), China (59), Croatia (2), Cuba (1), Czech (2), Denmark (7), Egypt (4), Estonia (1), Finland (4), France (42), Germany (106), Greece (9), Hungary (2), Iceland (1), India (12), Iran (4), Ireland (4), Israel (8), Italy (94), Japan (168), Lebanon (3), Lithuania (1), Macedonia (1), Malaysia (3), Mexico (6), Monaco (1), Morocco (1), The Netherlands (27), New Zealand (1), Nigeria (1), Norway (3), Pakistan (2), Peru (1), Poland (6), Portugal (1), Russia (3), Saudi Arabia (2), Serbia (1), Singapore (4), Slovakia (2), Slovenia (1), South Africa (2), South Korea (14), Spain (36), Sweden (15), Switzerland (13), Turkey (8), United Arab Emirates (1), United Kingdom (80), United States (308), and Uruguay (2).

Andrew V Biankin, *Sydney*
Filip Braet, *Sydney*
Andrew D Clouston, *Sydney*
Graham Cooksley, *Queensland*
Darrell HG Crawford, *Brisbane*
Adrian G Cummins, *Woodville South*
Guy D Eslick, *Sydney*
Michael A Fink, *Melbourne*
Robert JL Fraser, *Daw Park*
Peter Raymond Gibson, *Victoria*
Jacob George, *Westmead*
Mark D Gorrell, *Sydney*
Yik-Hong Ho, *Townsville*
Gerald J Holtmann, *Adelaide*
Michael Horowitz, *Adelaide*
John E Kellow, *Sydney*
Rupert Leong, *Concord*
Geoffrey W McCaughan, *Sydney*
Finlay A Macrae, *Victoria*
Daniel Markovich, *Brisbane*
Phillip S Oates, *Perth*
Jacqui Richmond, *Victoria*
Stephen M Riordan, *Sydney*
Ian C Roberts-Thomson, *Adelaide*
Devanshi Seth, *Camperdown*
Arthur Shulkes, *Melbourne*
Ross C Smith, *Sydney*
Kevin J Spring, *Brisbane*
Huy A Tran, *New South Wales*
Debbie Trinder, *Fremantle*
Martin J Veysey, *Gosford*
Daniel L Worthley, *Bedford*

Austria

Peter Ferenci, *Vienna*
Valentin Fuhrmann, *Vienna*
Alfred Gangl, *Vienna*
Christoph Gasche, *Vienna*
Kurt Lenz, *Linz*
Markus Peck-Radosavljevic, *Vienna*
Rudolf E Stauber, *Auenbruggerplatz*
Herbert Tilg, *Innsbruck*
Michael Trauner, *Graz*
Harald Vogelsang, *Vienna*
Guenter Weiss, *Innsbruck*

Belarus

Yury K Marakhouski, *Minsk*

Belgium

Rudi Beyaert, *Gent*
Bart Rik De Geest, *Leuven*
Inge I Depoortere, *Leuven*
Olivier Detry, *Liège*
Benedicte Y De Winter, *Antwerp*
Karel Geboes, *Leuven*
Thierry Gustot, *Brussels*
Yves J Horsmans, *Brussels*
Geert G Leroux-Roels, *Ghent*
Louis Libbrecht, *Leuven*
Etienne M Sokal, *Brussels*
Marc Peeters, *De Pintelaan*
Gert A Van Assche, *Leuven*
Yvan Vandenplas, *Brussels*
Eddie Wisse, *Keerbergen*

Brazil

Heitor Rosa, *Goiania*
Ana Cristina Simões e Silva, *Belo Horizonte*

Bulgaria

Zahariy Krastev, *Sofia*

Canada

Fernando Alvarez, *Québec*
David Armstrong, *Ontario*
Jeffrey P Baker, *Toronto*
Olivier Barbier, *Québec*
Nancy Baxter, *Toronto*
Frank J Burczynski, *Manitoba*
Michael F Byrne, *Vancouver*
Wang-Xue Chen, *Ottawa*
Samuel S Lee, *Calgary*
Gary A Levy, *Toronto*
Andrew L Mason, *Alberta*
John K Marshall, *Ontario*
Donna-Marie McCafferty, *Calgary*
Thomas I Michalak, *St. John's*
Gerald Y Minuk, *Manitoba*
Paul Moayyedi, *Hamilton*
Kostas Pantopoulos, *Québec*
William G Paterson, *Kingston*
Eldon Shaffer, *Calgary*
Martin Storr, *Calgary*
Elena F Verdu, *Ontario*
Waliul Khan, *Ontario*
John L Wallace, *Calgary*
Eric M Yoshida, *Vancouver*

Chile

Silvana Zanlungo, *Santiago*

China

Henry LY Chan, *Hong Kong*
Xiao-Ping Chen, *Wuhan*
Zong-Jie Cui, *Beijing*
Da-Jun Deng, *Beijing*
Er-Dan Dong, *Beijing*
Sheung-Tat Fan, *Hong Kong*
Jin Gu, *Beijing*
Xin-Yuan Guan, *Pokfulam*
De-Wu Han, *Taiyuan*
Ming-Liang He, *Hong Kong*
Wayne HC Hu, *Hong Kong*
Chee-Kin Hui, *Hong Kong*
Ching-Lung Lai, *Hong Kong*
Kam Chuen Lai, *Hong Kong*
James YW Lau, *Hong Kong*
Yuk-Tong Lee, *Hong Kong*
Suet-Yi Leung, *Hong Kong*
Wai-Keung Leung, *Hong Kong*
John M Luk, *Pokfulam*
Chung-Mau Lo, *Hong Kong*
Jing-Yun Ma, *Beijing*
Ronnie Tung Ping Poon, *Hong Kong*
Lun-Xiu Qin, *Shanghai*
Yu-Gang Song, *Guangzhou*
Qin Su, *Beijing*
Wai-Man Wong, *Hong Kong*
Hong Xiao, *Shanghai*
Dong-Liang Yang, *Wuhan*
Winnie Yeo, *Hong Kong*
Yuan Yuan, *Shenyang*
Man-Fung Yuen, *Hong Kong*
Jian-Zhong Zhang, *Beijing*
Xin-Xin Zhang, *Shanghai*
Bo-Jian Zheng, *Hong Kong*
Shu Zheng, *Hangzhou*

Croatia

Tamara Cacev, *Zagreb*
Marko Duvnjak, *Zagreb*

Cuba

Damian C Rodriguez, *Havana*

Czech

Milan Jirsa, *Praha*
Pavel Trunečka, *Prague*

Denmark

Peter Bytzer, *Copenhagen*
Asbjørn M Drewes, *Aalborg*
Hans Gregersen, *Aalborg*
Jens H Henriksen, *Hvidovre*
Claus P Hovendal, *Odense*
Fin S Larsen, *Copenhagen*
Søren Møller, *Hvidovre*

Egypt

Abdel-Rahman El-Zayadi, *Giza*
Amr M Helmy, *Cairo*
Ayman Yosry, *Cairo*

Estonia

Riina Salupere, *Tartu*

Finland

Irma E Jarvela, *Helsinki*
Katri M Kaukinen, *Tampere*
Minna Nyström, *Helsinki*
Pentti Sipponen, *Espoo*

France

Bettaieb Ali, *Dijon*
Anne Corlu, *Rennes*
Denis Ardid, *Clermont-Ferrand*
Charles P Balabaud, *Bordeaux*
Soumeya Bekri, *Rouen*
Jacques Belghiti, *Clichy*
Jacques Bernuau, *Clichy Cedex*
Pierre Brissot, *Rennes*
Patrice P Cacoub, *Paris*
Franck Carbonnel, *Besancon*
Laurent Castera, *Pessac*
Bruno Clément, *Rennes*
Benoit Coffin, *Colombes*
Thomas Decaens, *Cedex*
Francoise L Fabiani, *Angers*

Gérard Feldmann, *Paris*
Jean Fioramonti, *Toulouse*
Jean-Noël Freund, *Strasbourg*
Catherine Guettier, *Villejuif*
Chantal Housset, *Paris*
Juan L Iovanna, *Marseille*
Rene Lambert, *Lyon*
Patrick Marcellin, *Paris*
Philippe Mathurin, *Lille*
Tamara Matysiak-Budnik, *Paris*
Francis Mégraud, *Bordeaux*
Richard Moreau, *Clichy*
Thierry Piche, *Nice*
Raoul Poupon, *Paris*
Jean Rosenbaum, *Bordeaux*
Dominique Marie Roulot, *Bobigny*
Thierry Poynard, *Paris*
Jean-Philippe Salier, *Rouen*
Didier Samuel, *Villejuif*
Jean-Yves Scoazec, *Lyon*
Alain L Servin, *Châtenay-Malabry*
Khalid A Tazi, *Clichy*
Emmanuel Tiret, *Paris*
Baumert F Thomas, *Strasbourg*
Jean-Pierre H Zarski, *Grenoble*
Jessica Zucman-Rossi, *Paris*

Germany

Hans-Dieter Allescher, *G-Partenkirchen*
Martin Anlauf, *Kiel*
Rudolf Arnold, *Marburg*
Max G Bachem, *Ulm*
Thomas F Baumert, *Freiburg*
Daniel C Baumgart, *Berlin*
Hubert Blum, *Freiburg*
Thomas Bock, *Tuebingen*
Katja Breitkopf, *Mannheim*
Dunja Bruder, *Braunschweig*
Markus W Büchler, *Heidelberg*
Christa Buechler, *Regensburg*
Reinhard Buettner, *Bonn*
Elke Cario, *Essen*
Uta Dahmen, *Essen*
Christoph F Dietrich, *Bad Mergentheim*
Arno J Dormann, *Koeln*
Rainer J Duchmann, *Berlin*
Volker F Eckardt, *Wiesbaden*
Fred Fändrich, *Kiel*
Ulrich R Fölsch, *Kiel*
Helmut Friess, *Heidelberg*
Peter R Galle, *Mainz*
Nikolaus Gassler, *Aachen*
Andreas Geier, *Aachen*
Markus Gerhard, *Munich*
Wolfram H Gerlich, *Giessen*
Dieter Glebe, *Giessen*
Burkhard Göke, *Munich*
Florian Graepler, *Tuebingen*
Axel M Gressner, *Aachen*
Veit Gülberg, *Munich*
Rainer Haas, *Munich*
Eckhart G Hahn, *Erlangen*
Stephan Hellmig, *Kiel*
Martin Hennenberg, *Bonn*
Johannes Herkel, *Hamburg*
Klaus R Herrlinger, *Stuttgart*
Eva Herrmann, *Homburg/Saar*
Eberhard Hildt, *Berlin*
Joerg C Hoffmann, *Berlin*
Ferdinand Hofstaedter, *Regensburg*
Werner Hohenberger, *Erlangen*
Jörg C Kalff, *Bonn*
Ralf Jakobs, *Ludwigshafen*
Jutta Keller, *Hamburg*
Andrej Khandoga, *Munich*
Sibylle Koletzko, *München*
Stefan Kubicka, *Hannover*
Joachim Labenz, *Siegen*
Frank Lammert, *Bonn*
Thomas Langmann, *Regensburg*
Christian Liedtke, *Aachen*
Matthias Löhr, *Mannheim*
Christian Maaser, *Muenster*
Ahmed Madisch, *Dresden*
Peter Malfertheiner, *Magdeburg*
Michael P Manns, *Hannover*
Helmut Messmann, *Augsburg*
Stephan Miehlke, *Dresden*
Sabine Mihm, *Göttingen*
Silvio Nadalin, *Essen*
Markus F Neurath, *Mainz*
Johann Ockenga, *Berlin*
Florian Obermeier, *Regensburg*
Gustav Paumgartner, *Munich*
Ulrich KS Peitz, *Magdeburg*
Markus Reiser, *Bochum*
Emil C Reisinger, *Rostock*
Steffen Rickes, *Magdeburg*
Tilman Sauerbruch, *Bonn*
Dieter Saur, *Munich*
Hans Scherubl, *Berlin*
Joerg Schirra, *Munich*
Roland M Schmid, *München*
Volker Schmitz, *Bonn*
Andreas G Schreyer, *Regensburg*
Tobias Schroeder, *Essen*
Henning Schulze-Bergkamen, *Mainz*
Hans Seifert, *Oldenburg*
Norbert Senninger, *Muenster*
Manfred V Singer, *Mannheim*
Gisela Sparmann, *Rostock*
Christian J Steib, *München*
Jurgen M Stein, *Frankfurt*
Ulrike S Stein, *Berlin*
Manfred Stolte, *Bayreuth*
Christian P Strassburg, *Hannover*
Wolfgang R Stremmel, *Heidelberg*
Harald F Teutsch, *Ulm*
Robert Thimme, *Freiburg*
Hans L Tillmann, *Leipzig*
Tung-Yu Tsui, *Regensburg*
Axel Ulsenheimer, *Munich*
Patrick Veit-Haibach, *Essen*
Claudia Veltkamp, *Heidelberg*
Siegfried Wagner, *Deggendorf*
Henning Walczak, *Heidelberg*
Heiner Wedemeyer, *Hannover*
Fritz von Weizsacker, *Berlin*
Jens Werner, *Heidelberg*
Bertram Wiedenmann, *Berlin*
Reiner Wiest, *Regensburg*
Stefan Wirth, *Wuppertal*
Stefan JP Zeuzem, *Homburg*

Greece

Alexandra A Alexopoulou, *Athens*
George N Dalekos, *Larissa*
Christos Dervenis, *Athens*
Melanie Maria Deutsch, *Athens*
Tsianos Epameinondas, *Ioannina*
Elias A Kouroumalis, *Heraklion*
George Papatheodoridis, *Athens*
Spiros Sgouros, *Athens*

Hungary

Peter L Lakatos, *Budapest*
Zsuzsa Szondy, *Debrecen*

Iceland

Hallgrimur Gudjonsson, *Reykjavik*

India

Philip Abraham, *Mumbai*
Rakesh Aggarwal, *Lucknow*
Kunissery A Balasubramanian, *Vellore*
Deepak Kumar Bhasin, *Chandigarh*
Sujit K Bhattacharya, *Kolkata*
Yogesh K Chawla, *Chandigarh*
Radha K Dhiman, *Chandigarh*
Sri Prakash Misra, *Allahabad*
Ramesh Roop Rai, *Jaipur*
Nageshwar D Reddy, *Hyderabad*
Rakesh Kumar Tandon, *New Delhi*

Iran

Mohammad Abdollahi, *Tehran*
Seyed-Moayed Alavian, *Tehran*
Reza Malekzadeh, *Tehran*
Seyed A Taghavi, *Shiraz*

Ireland

Billy Bourke, *Dublin*
Ronan A Cahill, *Cork*
Anthony P Moran, *Galway*

Israel

Simon Bar-Meir, *Hashomer*
Abraham R Eliakim, *Haifa*
Zvi Fireman, *Hadera*
Yaron Ilan, *Jerusalem*
Avidan U Neumann, *Ramat-Gan*
Yaron Niv, *Pardesia*
Ran Oren, *Tel Aviv*
Ami D Sperber, *Beer-Sheva*

Italy

Giovanni Addolorato, *Roma*
Luigi E Adinolfi, *Naples*
Domenico Alvaro, *Rome*
Vito Annese, *San Giovanni Rotond*
Filippo Ansaldi, *Genoa*
Adolfo F Attili, *Roma*
Giovanni Barbara, *Bologna*
Claudio Bassi, *Verona*
Gabrio Bassotti, *Perugia*
Pier M Battezzati, *Milan*
Stefano Bellentani, *Carpi*
Antomio Benedetti, *Ancona*
Mauro Bernardi, *Bologna*
Livia Biancone, *Rome*
Luigi Bonavina, *Milano*
Flavia Bortolotti, *Padova*
Giuseppe Brisinda, *Rome*
Elisabetta Buscarini, *Crema*
Giovanni Cammarota, *Roma*

Antonino Cavallari, *Bologna*
Giuseppe Chiarioni, *Valeggio*
Michele Cicala, *Rome*
Massimo Colombo, *Milan*
Amedeo Columbano, *Cagliari*
Massimo Conio, *Sanremo*
Dario Conte, *Milano*
Gino R Corazza, *Pavia*
Francesco Costa, *Pisa*
Antonio Craxi, *Palermo*
Silvio Danese, *Milan*
Roberto de Franchis, *Milano*
Roberto De Giorgio, *Bologna*
Maria Stella De Mitri, *Bologna*
Giovanni D De Palma, *Naples*
Fabio Farinati, *Padua*
Giammarco Fava, *Ancona*
Francesco Feo, *Sassari*
Fiorucci Stefano, *Perugia*
Andrea Galli, *Firenze*
Valeria Ghisett, *Turin*
Gianluigi Giannelli, *Bari*
Edoardo G Giannini, *Genoa*
Paolo Gionchetti, *Bologna*
Fabio Grizzi, *Milan*
Salvatore Gruttadauria, *Palermo*
Mario Guslandi, *Milano*
Pietro Invernizzi, *Milan*
Ezio Laconi, *Cagliari*
Giacomo Laffi, *Firenze*
Giovanni Maconi, *Milan*
Lucia Malaguarnera, *Catania*
Emanuele D Mangoni, *Napoli*
Paolo Manzoni, *Torino*
Giulio Marchesini, *Bologna*
Fabio Marra, *Florence*
Marco Marzioni, *Ancona*
Roberto Mazzanti, *Florence*
Giuseppe Mazzella, *Bologna*
Giuseppe Montalto, *Palermo*
Giovanni Monteleone, *Rome*
Giovanni Musso, *Torino*
Gerardo Nardone, *Napoli*
Valerio Nobili, *Rome*
Fabio Pace, *Milano*
Luisi Pagliaro, *Palermo*
Francesco Pallone, *Rome*
Fabrizio R Parente, *Milan*
Maurizio Parola, *Torino*
Francesco Perri, *San Giovanni Rotondo*
Raffaele Pezzilli, *Bologna*
Alberto Pilotto, *San Giovanni Rotondo*
Alberto Piperno, *Monza*
Mario Pirisi, *Novara*
Anna C Piscaglia, *Roma*
Paolo Del Poggio, *Treviglio*
Gabriele B Porro, *Milano*
Piero Portincasa, *Bari*
Cosimo Prantera, *Roma*
Bernardino Rampone, *Siena*
Oliviero Riggio, *Rome*
Claudio Romano, *Messina*
Marco Romano, *Napoli*
Gerardo Rosati, *Potenza*
Mario Del Tacca, *Pisa*
Gloria Taliani, *Rome*
Pier A Testoni, *Milan*
Enrico Roda, *Bologna*
Domenico Sansonno, *Bari*
Vincenzo Savarino, *Genova*
Vincenzo Stanghellini, *Bologna*
Giovanni Tarantino, *Naples*
Roberto Testa, *Genoa*
Dino Vaira, *Bologna*

Japan

Kyoichi Adachi, *Izumo*
Yasushi Adachi, *Sapporo*
Taiji Akamatsu, *Matsumoto*
Sk Md Fazle Akbar, *Ehime*
Takafumi Ando, *Nagoya*
Akira Andoh, *Otsu*
Taku Aoki, *Tokyo*
Masahiro Arai, *Tokyo*
Tetsuo Arakawa, *Osaka*
Yasuji Arase, *Tokyo*
Hitoshi Asakura, *Tokyo*
Takeshi Azuma, *Fukui*
Takahiro Fujimori, *Tochigi*
Jiro Fujimoto, *Hyogo*
Kazuma Fujimoto, *Saga*
Mitsuhiro Fujishiro, *Tokyo*
Yoshihide Fujiyama, *Otsu*
Hiroyuki Fukui, *Tochigi*
Hiroyuki Hanai, *Hamamatsu*
Naohiko Harada, *Fukuoka*
Makoto Hashizume, *Fukuoka*
Tetsuo Hayakawa, *Nagoya*
Toru Hiyama, *Higashihiroshima*
Kazuhide Higuchi, *Osaka*
Keisuke Hino, *Ube*
Keiji Hirata, *Kitakyushu*
Yuji Iimuro, *Nishinomiya*
Kenji Ikeda, *Tokyo*
Toru Ikegami, *Fukuoka*
Kenichi Ikejima, *Bunkyo-ku*
Fumio Imazeki, *Chiba*
Yutaka Inagaki, *Kanagawa*
Yasuhiro Inokuchi, *Yokohama*
Haruhiro Inoue, *Yokohama*
Masayasu Inoue, *Osaka*
Hiromi Ishibashi, *Nagasaki*
Shunji Ishihara, *Izumo*
Toru Ishikawa, *Niigata*
Kei Ito, *Sendai*
Masayoshi Ito, *Tokyo*
Hiroaki Itoh, *Akita*
Ryuichi Iwakiri, *Saga*
Yoshiaki Iwasaki, *Okayama*
Terumi Kamisawa, *Tokyo*
Hiroshi Kaneko, *Aichi-Gun*
Shuichi Kaneko, *Kanazawa*
Takashi Kanematsu, *Nagasaki*
Mitsuo Katano, *Fukuoka*
Mototsugu Kato, *Sapporo*
Shinzo Kato, *Tokyo*
Norifumi Kawada, *Osaka*
Sunao Kawano, *Osaka*
Mitsuhiro Kida, *Kanagawa*
Yoshikazu Kinoshita, *Izumo*
Tsuneo Kitamura, *Chiba*
Seigo Kitano, *Oita*
Kazuhiko Koike, *Tokyo*
Norihiro Kokudo, *Tokyo*
Shoji Kubo, *Osaka*
Masatoshi Kudo, *Osaka*
Shigeki Kuriyama, *Kagawa*[2]
Katsunori Iijima, *Sendai*
Shin Maeda, *Tokyo*
Shigeru Marubashi, *Suita*
Masatoshi Makuuchi, *Tokyo*
Osamu Matsui, *Kanazawa*
Yasuhiro Matsumura, *Kashiwa*
Yasushi Matsuzaki, *Tsukuba*
Kiyoshi Migita, *Omura*
Kenji Miki, *Tokyo*
Tetsuya Mine, *Kanagawa*
Hiroto Miwa, *Hyogo*
Masashi Mizokami, *Nagoya*
Yoshiaki Mizuguchi, *Tokyo*
Motowo Mizuno, *Hiroshima*
Morito Monden, *Suita*
Hisataka Moriwaki, *Gifu*
Yasuaki Motomura, *Iizuka*
Yoshiharu Motoo, *Kanazawa*
Naofumi Mukaida, *Kanazawa*
Kazunari Murakami, *Oita*
Kunihiko Murase, *Tusima*
Hiroaki Nagano, *Suita*
Masahito Nagaki, *Gifu*
Yujl Naito, *Kyoto*
Atsushi Nakajima, *Yokohama*
Hisato Nakajima, *Tokyo*
Hiroki Nakamura, *Yamaguchi*
Shotaro Nakamura, *Fukuoka*
Mikio Nishioka, *Niihama*
Shuji Nomoto, *Nagoya*
Susumu Ohmada, *Maebashi*
Hirohide Ohnishi, *Akita*
Masayuki Ohta, *Oita*
Tetsuo Ohta, *Kanazawa*
Kazuichi Okazaki, *Osaka*
Katsuhisa Omagari, *Nagasaki*
Saburo Onishi, *Nankoku*
Morikazu Onji, *Ehime*
Satoshi Osawa, *Hamamatsu*
Masanobu Oshima, *Kanazawa*
Hiromitsu Saisho, *Chiba*
Hidetsugu Saito, *Tokyo*
Yutaka Saito, *Tokyo*
Michiie Sakamoto, *Tokyo*
Yasushi Sano, *Chiba*
Hiroki Sasaki, *Tokyo*
Iwao Sasaki, *Sendai*
Motoko Sasaki, *Kanazawa*
Chifumi Sato, *Tokyo*
Shuichi Seki, *Osaka*
Hiroshi Shimada, *Yokohama*
Mitsuo Shimada, *Tokushima*
Tomohiko Shimatan, *Hiroshima*
Hiroaki Shimizu, *Chiba*
Ichiro Shimizu, *Tokushima*
Yukihiro Shimizu, *Kyoto*
Shinji Shimoda, *Fukuoka*
Tooru Shimosegawa, *Sendai*
Tadashi Shimoyama, *Hirosaki*
Ken Shirabe, *Iizuka City*
Yoshio Shirai, *Niigata*
Katsuya Shiraki, *Mie*
Yasushi Shiratori, *Okayama*
Masayuki Sho, *Nara*
Yasuhiko Sugawara, *Tokyo*
Hidekazu Suzuki, *Tokyo*
Minoru Tada, *Tokyo*
Tadatoshi Takayama, *Tokyo*
Tadashi Takeda, *Osaka*
Kiichi Tamada, *Tochigi*
Akira Tanaka, *Kyoto*
Eiji Tanaka, *Matsumoto*
Noriaki Tanaka, *Okayama*
Shinji Tanaka, *Hiroshima*
Hideki Taniguchi, *Yokohama*
Kyuichi Tanikawa, *Kurume*
Akira Terano, *Shimotsugagun*
Hitoshi Togash, *Yamagata*
Shinji Togo, *Yokohama*
Kazunari Tominaga, *Osaka*
Takuji Torimura, *Fukuoka*
Minoru Toyota, *Sapporo*

Akihito Tsubota, *Chiba*
Takato Ueno, *Kurume*
Shinichi Wada, *Tochigi*
Hiroyuki Watanabe, *Kanazawa*
Toshio Watanabe, *Osaka*
Yuji Watanabe, *Ehime*
Toshiaki Watanabe, *Tokyo*
Chun-Yang Wen, *Nagasaki*
Satoshi Yamagiwa, *Niigata*
Koji Yamaguchi, *Fukuoka*
Takayuki Yamamoto, *Yokkaichi*
Takashi Yao, *Fukuoka*
Masashi Yoneda, *Tochigi*
Hiroshi Yoshida, *Tokyo*
Masashi Yoshida, *Tokyo*
Norimasa Yoshida, *Kyoto*
Hitoshi Yoshiji, *Nara*
Kentaro Yoshika, *Toyoake*
Masahide Yoshikawa, *Kashihara*
Katsutoshi Yoshizato, *Higashihiroshima*

Lebanon
Bassam N Abboud, *Beirut*
Ala I Sharara, *Beirut*
Joseph D Boujaoude, *Beirut*

Lithuania
Limas Kupcinskas, *Kaunas*

Macedonia
Vladimir C Serafimoski, *Skopje*

Malaysia
Andrew Seng Boon Chua, *Ipoh*
Khean-Lee Goh, Kuala *Lumpur*
Jayaram Menon, *Sabah*

Mexico
Diego Garcia-Compean, *Monterrey*
Eduardo R Marin-Lopez, *Jesús García*
Nahum Méndez-Sánchez, *Mexico*
Saúl Villa-Treviño, *México*

Monaco
Patrick Rampal, *Monaco*

Morocco
Abdellah Essaid, *Rabat*

The Netherlands
Ulrich Beuers, *Amsterdam*
Gerd Bouma, *Amsterdam*
Lee Bouwman, *Leiden*
J Bart A Crusius, *Amsterdam*
NKH de Boer, *Amsterdam*
Koert P de Jong, *Groningen*
Henrike Hamer, *Maastricht*
Frank Hoentjen, *Haarlem*
Janine K Kruit, *Groningen*
Ernst J Kuipers, *Rotterdam*
CBHW Lamers, *Leiden*
Ton Lisman, *Utrecht*
Yi Liu, *Amsterdam*
Jeroen Maljaars, *Maastricht*
Servaas Morré, *Amsterdam*
Chris JJ Mulder, *Amsterdam*
Michael Müller, *Wageningen*
Amado S Peña, *Amsterdam*
Robert J Porte, *Groningen*
Ingrid B Renes, *Rotterdam*
Andreas Smout, *Utrecht*
Paul E Sijens, *Groningen*
Reinhold W Stockbrugger, *Maastricht*
Luc JW van der Laan, *Rotterdam*
Karel van Erpecum, *Utrecht*
Gerard P VanBerge-Henegouwen,*Utrecht*

New Zealand
Ian D Wallace, *Auckland*

Nigeria
Samuel B Olaleye, *Ibadan*

Norway
Trond Berg, *Oslo*
Tom H Karlsen, *Oslo*
Helge L Waldum, *Trondheim*

Pakistan
Muhammad S Khokhar, *Lahore*
Syed MW Jafri, *Karachi*

Peru
Hector H Garcia, *Lima*

Poland
Tomasz Brzozowski, *Cracow*
Robert Flisiak, *Bialystok*
Hanna Gregorek, *Warsaw*
Dariusz M Lebensztejn, *Bialystok*
Wojciech G Polak, *Wroclaw*
Marek Hartleb, *Katowice*

Portugal
Miguel C De Moura, *Lisbon*

Russia
Vladimir T Ivashkin, *Moscow*
Leonid Lazebnik, *Moscow*
Vasiliy I Reshetnyak, *Moscow*

Saudi Arabia
Ibrahim A Al Mofleh, *Riyadh*
Ahmed Helmy, *Riyadh*

Serbia
Dusan M Jovanovic, *Sremska Kamenica*

Singapore
Bow Ho, *Singapore*
Khek-Yu Ho, *Singapore*
Fock Kwong Ming, *Singapore*
Francis Seow-Choen, *Singapore*

Slovakia
Silvia Pastorekova, *Bratislava*
Anton Vavrecka, *Bratislava*

Slovenia
Sasa Markovic, *Ljubljana*

South Africa
Rosemary Joyce Burnett, *Pretoria*
Michael C Kew, *Parktown*

South Korea
Byung Ihn Choi, *Seoul*
Ho Soon Choi, *Seoul*
Marie Yeo, *Suwon*
Sun Pyo Hong, *Gyeonggi-do*
Jae J Kim, *Seoul*
Jin-Hong Kim, *Suwon*
Myung-Hwan Kim, *Seoul*
Chang Hong Lee, *Seoul*
Jeong Min Lee, *Seoul*
Jong Kyun Lee, *Seoul*
Eun-Yi Moon, *Seoul*
Jae-Gahb Park, *Seoul*
Dong Wan Seo, *Seoul*
Byung Chul Yoo, *Seoul*

Spain
Juan G Abraldes, *Barcelona*
Agustin Albillos, *Madrid*
Raul J Andrade, *Málaga*
Luis Aparisi, *Valencia*
Fernando Azpiroz, *Barcelona*
Ramon Bataller, *Barcelona*
Josep M Bordas, *Barcelona*
Jordi Camps, *Catalunya*
Andres Cardenas, *Barcelona*
Vicente Carreño, *Madrid*
Jose Castellote, *Barcelona*
Antoni Castells, *Barcelona*
Vicente Felipo, *Valencia*
Juan C Garcia-Pagán, *Barcelona*
Jaime B Genover, *Barcelona*
Javier P Gisbert, *Madrid*
Jaime Guardia, *Barcelona*
Isabel Fabregat, *Barcelona*
Mercedes Fernandez, *Barcelona*
Angel Lanas, *Zaragoza*
Juan-Ramón Larrubia, *Guadalajara*
Laura Lladóa, *Barcelona*
María IT López, *Jaén*
José M Mato, *Derio*
Juan F Medina, *Pamplona*
Miguel A Muñoz-Navas, *Pamplona*
Julian Panes, *Barcelona*
Miguel M Perez, *Valencia*
Miguel Perez-Mateo, *Alicante*

Josep M Pique, *Barcelona*
Jesús M Prieto, *Pamplona*
Sabino Riestra, *Pola De Siero*
Luis Rodrigo, *Oviedo*
Manuel Romero-Gómez, *Sevilla*
Joan Roselló-Catafau, *Barcelona*

Sweden

Einar S Björnsson, *Gothenburg*
Curt Einarsson, *Huddinge*
Per M Hellström, *Stockholm*
Ulf Hindorf, *Lund*
Elisabeth Hultgren-Hörnquist, *Örebro*
Anders E Lehmann, *Mölndal*
Hanns-Ulrich Marschall, *Stockholm*
Lars C Olbe, *Molndal*
Lars A Pahlman, *Uppsala*
Matti Sallberg, *Stockholm*
Magnus Simrén, *Göteborg*
Xiao-Feng Sun, *Linköping*
Ervin Tóth, *Malmö*
Weimin Ye, *Stockholm*
Christer S von Holstein, *Lund*

Switzerland

Chrish Beglinger, *Basel*
Pierre A Clavien, *Zurich*
Jean-Francois Dufour, *Bern*
Franco Fortunato, *Zurich*
Jean L Frossard, *Geneva*
Gerd A Kullak-Ublick, *Zurich*
Pierre Michetti, *Lausanne*
Francesco Negro, *Genève*
Bruno Stieger, *Zurich*
Radu Tutuian, *Zurich*
Stephan R Vavricka, *Zurich*
Gerhard Rogler, *Zurich*
Arthur Zimmermann, *Berne*

Turkey

Yusuf Bayraktar, *Ankara*
Figen Gurakan, *Ankara*
Aydin Karabacakoglu, *Konya*
Serdar Karakose, *Konya*
Hizir Kurtel, *Istanbul*
Osman C Ozdogan, *Istanbul*
Özlem Yilmaz, *Izmir*
Cihan Yurdaydin, *Ankara*

United Arab Emirates

Sherif M Karam, *Al-Ain*

United Kingdom

David H Adams, *Birmingham*
Simon Afford, *Birmingham*
Navneet K Ahluwalia, *Stockport*
Ahmed Alzaraa, *Manchester*
Lesley A Anderson, *Belfast*
Charalambos G Antoniades, *London*
Anthony TR Axon, *Leeds*
Qasim Aziz, *Manchester*
Nicholas M Barnes, *Birmingham*
Jim D Bell, *London*
Mairi Brittan, *London*
Alastair D Burt, *Newcastle*
Simon S Campbell, *Manchester*
Simon R Carding, *Leeds*
Paul J Ciclitira, *London*
Eithne Costello, *Liverpool*
Tatjana Crnogorac-Jurcevic, *London*
Harry Dalton, *Truro*
Amar P Dhillon, *London*
William Dickey, *Londonderry*
James E East, *London*
Emad M El-Omar, *Aberdeen*
Ahmed M Elsharkawy, *Newcastle Upon Tyne*
Annette Fristscher-Ravens, *London*
Elizabeth Furrie, *Dundee*
Daniel R Gaya, *Edinburgh*
Subrata Ghosh, *London*
William Greenhalf, *Liverpool*
Indra N Guha, *Southampton*
Gwo-Tzer Ho, *Edinburgh*
Anthony R Hobson, *Salford*
Lesley A Houghton, *Manchester*
Stefan G Hübscher, *Birmingham*
Robin Hughes, *London*
Pali Hungin, *Stockton*
David P Hurlstone, *Sheffield*
Rajiv Jalan, *London*
Janusz AZ Jankowski, *Oxford*
Brian T Johnston, *Belfast*
David EJ Jones, *Newcastle*
Roger Jones, *London*
Michael A Kamm, *Harrow*
Peter Karayiannis, *London*
Laurens Kruidenier, *Harlow*
Patricia F Lalor, *Birmingham*
Chee Hooi Lim, *Midlands*
Hong-Xiang Liu, *Cambridge*
Yun Ma, *London*
Kenneth E L McColl, *Glasgow*
Stuart AC McDonald, *London*
Dermot P Mcgovern, *Oxford*
Giorgina Mieli-Vergani, *London*
Nikolai V Naoumov, *London*
John P Neoptolemos, *Liverpool*
James Neuberger, *Birmingham*
Philip Noel Newsome, *Birmingham*
Mark S Pearce, *Newcastle Upon Tyne*
D Mark Pritchard, *Liverpool*
Sakhawat Rahman, *London*
Stephen E Roberts, *Swansea*
Marco Senzolo, *Padova*
Soraya Shirazi-Beechey, *Liverpool*
Robert Sutton, *Liverpool*
Simon D Taylor-Robinson, *London*
Paris P Tekkis, *London*
Ulrich Thalheimer, *London*
David G Thompson, *Salford*
Nick P Thompson, *Newcastle*
Frank I Tovey, *London*
Chris Tselepis, *Birmingham*
Diego Vergani, *London*
Geoffrey Warhurst, *Salford*
Alastair John Watson, *Liverpool*
Peter J Whorwell, *Manchester*
Roger Williams, *London*
Karen L Wright, *Bath*
Min Zhao, *Foresterhill*

United States

Manal F Abdelmalek, *Durham*
Gary A Abrams, *Birmingham*
Maria T Abreu, *New York*
Reid B Adams, *Virginia*
Golo Ahlenstiel, *Bethesda*
BS Anand, *Houston*
M Ananthanarayanan, *New York*
Gavin E Arteel, *Louisville*
Jasmohan S Bajaj, *Milwaukee*
Shashi Bala, *Worcester*
Subhas Banerjee, *Palo Alto*
Peter A Banks, *Boston*
Jamie S Barkin, *Miami Beach*
Kim E Barrett, *San Diego*
Marc D Basson, *Detroit*
Anthony J Bauer, *Pittsburgh*
Wallace F Berman, *Durham*
Timothy R Billiar, *Pittsburgh*
Edmund J Bini, *New York*
David G Binion, *Milwaukee*
Jennifer D Black, *Buffalo*
Herbert L Bonkovsky, *Charlotte*
Carla W Brady, *Durham*
Andrea D Branch, *New York*
Robert S Bresalier, *Houston*
Alan L Buchman, *Chicago*
Ronald W Busuttil, *Los Angeles*
Alan Cahill, *Philadelphia*
John M Carethers, *San Diego*
David L Carr-Locke, *Boston*
Maurice A Cerulli, *New York*
Ravi S Chari, *Nashville*
Anping Chen, *St. Louis*
Jiande Chen, *Galveston*
Xian-Ming Chen, *Omaha*
Xin Chen, *San Francisco*
Ramsey Chi-man Cheung, *Palo Alto*
William D Chey, *Ann Arbor*
John Y Chiang, *Rootstown*
Parimal Chowdhury, *Arkansas*
Raymond T Chung, *Boston*
James M Church, *Cleveland*
Ram Chuttani, *Boston*
Mark G Clemens, *Charlotte*
Ana J Coito, *Los Angeles*
Vincent Coghlan, *Beaverton*
David Cronin II, *New Haven*
John Cuppoletti, *Cincinnati*
Mark J Czaja, *New York*
Peter V Danenberg, *Los Angeles*
Kiron M Das, New *Brunswick*
Conor P Delaney, *Cleveland*
Jose L del Pozo, *Rochester*
Sharon DeMorrow, *Temple*
Deborah L Diamond, *Seattle*
Douglas A Drossman, *Chapel Hill*
Katerina Dvorak, *Tucson*
Bijan Eghtesad, *Cleveland*
Hala El-Zimaity, *Houston*
Michelle Embree-Ku, *Providence*
Sukru Emre, New *Haven*
Douglas G Farmer, *Los Angeles*
Alessio Fasano, *Baltimore*
Ariel E Feldstein, *Cleveland*
Alessandro Fichera, *Chicago*
Robert L Fine, *New York*
Chris E Forsmark, *Gainesville*
Glenn T Furuta, *Aurora*
Chandrashekhar R Gandhi, *Pittsburgh*
Susan L Gearhart, *Baltimore*
Xupeng Ge, *Boston*
Xin Geng, *New Brunswick*
M Eric Gershwin, *Suite*
Jean-Francois Geschwind, *Baltimore*
Ignacio Gil-Bazo, *New York*
Shannon S Glaser, *Temple*
Ajay Goel, *Dallas*

Richard M Green, *Chicago*
Julia B Greer, *Pittsburgh*
James H Grendell, *New York*
David R Gretch, *Seattle*
Stefano Guandalini, *Chicago*
Anna S Gukovskaya, *Los Angeles*
Sanjeev Gupta, *Bronx*
David J Hackam, *Pittsburgh*
Stephen B Hanauer, *Chicago*
Gavin Harewood, *Rochester*
Margaret M Heitkemper, *Washington*
Alan W Hemming, *Gainesville*
Samuel B Ho, *San Diego*
Peter R Holt, *New York*
Colin W Howden, *Chicago*
Hongjin Huang, *Alameda*
Jamal A Ibdah, *Columbia*
Atif Iqbal, *Omaha*
Hajime Isomoto, *Rochester*
Hartmut Jaeschke, *Tucson*
Cheng Ji, *Los Angeles*
Leonard R Johnson, *Memphis*
Peter J Kahrilas, *Chicago*
Anthony N Kalloo, *Baltimore*
Marshall M Kaplan, *Boston*
Neil Kaplowitz, *Los Angeles*
Serhan Karvar, *Los Angeles*
Rashmi Kaul, *Tulsa*
Jonathan D Kaunitz, *Los Angeles*
Ali Keshavarzian, *Chicago*
Miran Kim, *Providence*
Joseph B Kirsner, *Chicago*
Leonidas G Koniaris, *Miami*
Burton I Korelitz, *New York*
Robert J Korst, *New York*
Richard A Kozarek, *Seattle*
Alyssa M Krasinskas, *Pittsburgh*
Michael Kremer, *Chapel Hill*
Shiu-Ming Kuo, *Buffalo*
Paul Y Kwo, *Indianapolis*
Daryl Tan Yeung Lau, *Galvesto*
Stephen J Lanspa, *Omaha*
Joel E Lavine, *San Diego*
Bret Lashner, *Cleveland*
Dirk J van Leeuwen, *Lebanon*
Glen A Lehman, *Indianapolis*
Alex B Lentsch, *Cincinnati*
Andreas Leodolter, *La Jolla*
Gene LeSage, *Houston*
Josh Levitsky, *Chicago*
Cynthia Levy, *Gainesville*
Ming Li, *New Orleans*
Zhiping Li, *Baltimore*
Zhe-Xiong Lian, *Davis*
Lenard M Lichtenberger, *Houston*
Gary R Lichtenstein, *Philadelphia*
Otto Schiueh-Tzang Lin, *Seattle*
Martin Lipkin, *New York*
Chen Liu, *Gainesville*
Edward V Loftus, *Rocheste*
Robin G Lorenz, *Birmingham*
Michael R Lucey, *Madison*
James D Luketich, *Pittsburgh*
Guangbin Luo, *Cheveland*
Henry T Lynch, *Omaha*
Patrick M Lynch, *Houston*
John S Macdonald, *New York*
Bruce V MacFadyen, *Augusta*
Willis C Maddrey, *Dallas*
Ashok Malani, *Los Angeles*
Mercedes Susan Mandell, *Aurora*
Peter J Mannon, *Bethesda*
Charles M Mansbach, *Tennessee*
John F Di Mari, *Texas*
John M Mariadason, *Bronx*
Jorge A Marrero, *Ann Arbor*
Paul Martin, *New York*
Paulo Ney Aguiar Martins, *Boston*
Wendy M Mars, *Pittsburgh*
Laura E Matarese, *Pittsburgh*
Richard W McCallum, *Kansas*
Beth A McCormick, *Charlestown*
Lynne V McFarland, *Washington*
Kevin McGrath, *Pittsburgh*
Harihara Mehendale, *Monroe*
Ali Mencin, *New York*
Fanyin Meng, *Ohio*
Stephan Menne, *New York*
Didier Merlin, *Atlanta*
Howard Mertz, *Nashville*
George W Meyer, *Sacramento*
George Michalopoulos, *Pittsburgh*
James M Millis, *Chicago*
Albert D Min, *New York*
Pramod K Mistry, *New Haven*
Emiko Mizoguchi, *Boston*
Smruti R Mohanty, *Chicago*
Satdarshan S Monga, *Pittsburgh*
Timothy H Moran, *Baltimore*
Peter L Moses, *Burlington*
Steven F Moss, *Providence*
Andrew J Muir, *Durham*
Milton G Mutchnick, *Detroit*
Masaki Nagaya, *Boston*
Victor Navarro, *Philadelphia*
Laura E Nagy, *Cleveland*
Hiroshi Nakagawa, *Philadelphia*
Douglas B Nelson, *Minneapolis*
Justin H Nguyen, *Florida*
Christopher O'Brien, *Miami*
Robert D Odze, *Boston*
Brant K Oelschlager, *Washington*
Curtis T Okamoto, *Los Angeles*
Stephen JD O'Keefe, *Pittsburgh*
Dimitry Oleynikov, *Omaha*
Stephen J Pandol, *Los Angeles*
Georgios Papachristou, *Pittsburgh*
Pankaj J Pasricha, *Galveston*
Zhiheng Pei, *New York*
CS Pitchumoni, *New Brunswiuc*
Paul J Pockros, *La Jolla*
Jay Pravda, *Gainesville*
Massimo Raimondo, *Jacksonville*
GS Raju, *Galveston*
Raymund R Razonable, *Minnesota*
Murray B Resnick, *Providence*
Adrian Reuben, *Charleston*
Douglas K Rex, *Indianapolis*
Victor E Reyes, *Galveston*
Basil Rigas, *New York*
Yehuda Ringel, *Chapel Hill*
Richard A Rippe, *Chapel Hill*
Maribel Rodriguez-Torres, *Santurce*
Marcos Rojkind, *Washington*
Philip Rosenthal, *San Francisco*
Barry Rosser, *Jacksonville Florida*
Hemant K Roy, *Evanston*
Sammy Saab, *Los Angeles*
Shawn D Safford, *Norfolk*
Dushyant V Sahani, *Boston*
James M Scheiman, *Ann Arbor*
Eugene R Schiff, *Miami*
Nicholas J Shaheen, *Chapel Hill*
Vanessa M Shami, *Charlottesville*
Prateek Sharma, *Kansas City*
Harvey L Sharp, *Minneapolis*
Stuart Sherman, *Indianapolis*
Shivendra Shukla, *Columbia*
Alphonse E Sirica, *Virginia*
Shanthi V Sitaraman, *Atlanta*
Bronislaw L Slomiany, *Newark*
Stuart J Spechler, *Dallas*
Subbaramiah Sridhar, *Augusta*
Shanthi Srinivasan, *Atlanta*
Peter D Stevens, *New York*
Charmaine A Stewart, *Rochester*
Christian D Stone, *Saint Louis*
Gary D Stoner, *Columbus*
R Todd Stravitz, *Richmond*
Liping Su, *Chicago*
Christina Surawicz, *Seattle*
Robert W Summers, *Iowa City*
Wing-Kin Syn, *Durham*
Gyongyi Szabo, *Worcester*
Yvette Taché, *Los Angeles*
Toku Takahashi, *Milwaukee*
Andrzej S Tarnawski, *Orange*
K-M Tchou-Wong, *New York*
Jonathan P Terdiman, *San Francisco*
Christopher C Thompson, *Boston*
Swan N Thung, *New York*
Michael Torbenson, *Baltimore*
Natalie J Torok, *Sacramento*
RA Travagli, *Baton Rouge*
George Triadafilopoulos, *Stanford*
Chung-Jyi Tsai, *Lexington*
Janet Elizabeth Tuttle-Newhall, *Durham*
Andrew Ukleja, *Florida*
Michael F Vaezi, *Nashville*
Hugo E Vargas, *Phoenix*
Arnold Wald, *Wisconsin*
Scott A Waldman, *Philadelphia*
Jian-Ying Wang, *Baltimore*
Junru Wang, *Little Rock*
Timothy C Wang, *New York*
Irving Waxman, *Chicago*
Steven A Weinman, *Galveston*
Steven D Wexner, *Weston*
Keith T Wilson, *Baltimore*
Jacqueline L Wolf, *Boston*
Jackie Wood, *Ohio*
George Y Wu, *Farmington*
Jian Wu, *Sacramento*
Samuel Wyllie, *Houston*
Wen Xie, *Pittsburgh*
Vijay Yajnik, *Boston*
Vincent W Yang, *Atlanta*
Francis Y Yao, *San Francisco*
Hal F Yee, *San Francisco*
Xiao-Ming Yin, *Pittsburgh*
Min You, *Tampa*
Zobair M Younossi, *Virginia*
Liqing Yu, *Winston-Salem*
David Yule, *Rochester*
Ruben Zamora, *Pittsburgh*
Michael E Zenilman, *New York*
Zhi Zhong, *Chapel Hill*
Michael A Zimmerman, *Colorado*
Stephen D Zucker, *Cincinnati*

Uruguay

Henry Cohen, *Montevideo*

[1]Passed away on October 20, 2007
[2]Passed away on June 11, 2007
[3]Passed away on June 14, 2008

World Journal of
Gastroenterology®
Weekly Established in October 1995
Volume 15 Number 22
June 14, 2009

Contents

Contents

World Journal of Gastroenterology
Volume 15 **Number** 22 **June** 14, 2009

Contents

World Journal of Gastroenterology
Volume 15 **Number** 22 **June** 14, 2009

INTRODUCTION

World Journal of Gastroenterology is an international, open-access, peer-reviewed, and multidisciplinary weekly journal that serves gastroenterologists and hepatologists. The biggest advantage of the open access model is that it provides free, full-text articles in PDF and other formats for experts and the public without registration, which eliminates the obstacle that traditional journals possess and usually delays the speed of the propagation and communication of scientific research results. The open access model has been proven to be a true approach that may achieve the ultimate goal of the journals, i.e. the maximization of the values of the readers, the authors and the society.

Maximization of the value of the readers can be comprehended in two ways. First, the journal publishes articles that can be directly read or downloaded free of charge at any time, which attracts more readers. Second, the readers can apply the knowledge in clinical practice without delay after reading and understanding the information in their fields. In addition, the readers are encouraged to propose new ideas based on those of the authors, or to provide viewpoints that are different from those of the authors. Such discussions or debates among different schools of thought will definitely boost advancements and developments in the fields. Maximization of the value of the authors refers to the fact that these journals provide a platform that promotes the speed of propagation and communication to a maximum extent. This is also what the authors really need. Maximization of the value of the society refers to the maximal extent of the social influences and impacts produced by the high quality original articles published in the journal. This is also the main purpose of many journals around the world.

NAME OF JOURNAL
World Journal of Gastroenterology

RESPONSIBLE INSTITUTION
Department of Science and Technology of Shanxi Province

SPONSOR
Taiyuan Research and Treatment Center for Digestive Diseases, 77 Shuangta Xijie, Taiyuan 030001, Shanxi Province, China

EDITING
Editorial Board of *World Journal of Gastroenterology,* Room 903, Building D, Ocean International Center, No.62 Dongsihuan Zhonglu, Chaoyang District, Beijing 100025, China
Telephone: +86-10-59080039
Fax: +86-10-85381893
E-mail: wjg@wjgnet.com
http://www.wjgnet.com

PUBLISHING
The WJG Press and Beijing Baishideng BioMed Scientific Co., Ltd.. Room 903, Building D, Ocean International Center, No.62 Dongsihuan Zhonglu, Chaoyang District, Beijing 100025, China
Telephone: +86-10-59080039
Fax: +86-10-85381893
E-mail: wjg@wjgnet.com
http://www.wjgnet.com

PRINTING
Beijing Kexin Printing House

OVERSEAS DISTRIBUTOR
Beijing Bureau for Distribution of Newspapers and Journals
(Code No. 82-261)
China International Book Trading Corporation PO Box 399, Beijing, China (Code No. M4481)

PUBLICATION DATE
June 14, 2009

EDITOR-IN-CHIEF
Lian-Sheng Ma, *Beijing*

SUBSCRIPTION
RMB 50 Yuan for each issue, RMB 2400 Yuan for one year

CSSN
ISSN 1007-9327
CN 14-1219/R

INSTRUCTIONS TO AUTHORS
Full instructions are available online at http://www.wjgnet.com/wjg/help/instructions.jsp. If you do not have web access please contact the editorial office.

ONLINE SUBMISSION
http://wjg.wjgnet.com

Online Submissions: wjg.wjgnet.com
wjg@wjgnet.com
doi:10.3748/wjg.15.2689

World J Gastroenterol 2009 June 14; 15(22): 2689-2692
World Journal of Gastroenterology ISSN 1007-9327

EDITORIAL

New perspectives in the treatment of advanced or metastatic gastric cancer

Gerardo Rosati, Domenica Ferrara, Luigi Manzione

Gerardo Rosati, Domenica Ferrara, Luigi Manzione, Medical Oncology Unit, S. Carlo Hospital, Potenza 85100, Italy
Author contributions: Rosati G designed the research, analyzed the data and wrote the paper; Manzione L and Ferrara D participated in this work.
Correspondence to: Gerardo Rosati, MD, Medical Oncology Unit, S. Carlo Hospital, Via P. Petrone, 1, Potenza 85100, Italy. rosatiger@yahoo.com
Telephone: +39-971-612273 Fax: +39-971-613000
Received: March 5, 2009 Revised: April 12, 2009
Accepted: April 19, 2009
Published online: June 14, 2009

Abstract

Metastatic gastric cancer remains an incurable disease, with a relative 5-year survival rate of 7%-27%. Chemotherapy, which improves overall survival (OS) and quality of life, is the main treatment option. Meta-analysis has demonstrated that the best survival results obtained in earlier randomized studies were achieved with three-drug regimens containing a fluoropyrimidine, an anthracycline, and cisplatin (ECF). Although there has been little progress in improving median OS times beyond the 9-mo plateau achievable with the standard regimens, the availability of newer agents has provided some measure of optimism. A number of new combinations incorporating docetaxel, oxaliplatin, capecitabine, and S-1 have been explored in randomized trials. Some combinations, such as epirubicin-oxaliplatin-capecitabine, have been shown to be as effective as (or perhaps more effective than) ECF, and promising early data have been derived for S-1 in combination with cisplatin. One factor that might contribute to extending median OS is the advancement whenever possible to second-line cytotoxic treatments. However, the biggest hope for significant survival advances in the near future would be the combination of new targeted biological agents with existing chemotherapy first-line regimens.

Key words: Advanced gastric cancer; Biological agents; Chemotherapy

Peer reviewer: Emad M El-Omar, Professor, Department of Medicine & Therapeutics, Aberdeen AB25 2ZD, United Kingdom

Rosati G, Ferrara D, Manzione L. New perspectives in the treatment of advanced or metastatic gastric cancer. *World J Gastroenterol* 2009; 15(22): 2689-2692 Available from: URL: http://www.wjgnet.com/1007-9327/15/2689.asp DOI: http://dx.doi.org/10.3748/wjg.15.2689

INTRODUCTION

Gastric cancer is the fourth most common cancer worldwide, with about 700 000 confirmed deaths annually. Despite an overall global decrease in incidence, gastric cancer is more prevalent in east Asia, eastern Europe, and central and south America than in other countries[1,2].

Chemotherapy is the main treatment option for patients with advanced disease. Median overall survival (OS) of 8-12 mo has been reported in patients undergoing chemotherapy compared with 3-5 mo for those treated with best supportive care[3]. Several drugs have shown good single-agent activity. The response rates range from 10% to 25% and the median duration of response is relatively short. Fluorouracil (5-FU), cisplatin, docetaxel, and, less commonly, paclitaxel, epirubicin, and irinotecan are major components of conventional regimens. Oxaliplatin, capecitabine, S-1, and UFT are also being used in combination chemotherapy. To date, although a large number of trials have been performed, there is no standard treatment for advanced disease.

Intravenous 5-FU remains the most widely used agent and has been the cornerstone of old combination regimens such as FAM (5-FU, doxorubicin, and mitomycin C), FAMTX (5-FU, doxorubicin, and methotrexate), ELF (etoposide, leucovorin, and 5-FU), and ECF (epirubicin, cisplatin, and continuous infusion 5-FU). Although these regimens yield overall response rates (ORRs) of up to 51%, the median survival time in patients with advanced disease has remained irredeemably below 10 mo[4]. Evidently, there is a clear need for more active new agents and regimens.

Combination chemotherapy has been shown to be associated with a statistically significant ($P = 0.001$) survival benefit compared with monotherapy in a meta-analysis of several clinical trials[5]. This corresponded to a small but clinically relevant 1-mo mean average survival benefit. This meta-analysis also evaluated the role of anthracyclines as part of combination chemotherapy. The authors found that including anthracyclines in a 5-FU-cisplatin combination had a modest advantage

over cisplatin-5-FU alone (HR 0.77). Finally, the meta-analysis also showed that three-drug combinations have a significant survival benefit compared with two-drug combinations.

In this context, Van Cutsem *et al*[6] have performed a large-scale random assignment trial comparing the docetaxel, cisplatin, 5-FU (DCF) combination to a control arm of cisplatin plus 5-FU alone (the TAX325 trial). The primary end point of the study was time to progression (TTP) and it was powered to detect an increase in median TTP from 4 mo to 6 mo. The two arms of the study were well balanced for the usual prognostic factors, including weight loss, performance status (PS), and extent of disease. The median TTP was 3.7 mo for patients receiving cisplatin-5-FU, and 5.6 mo for those receiving DCF (HR 1.47; $P = 0.0004$). As a secondary end point, survival was also modestly increased from 8.6 mo for cisplatin-5-FU to 9.2 mo for DCF. The 2-year survival rate was, however, more than doubled for DCF (8.8% for cisplatin-5-FU and 18.4% for DCF). Another measure of efficacy favoring DCF was response rate (37% for DCF, 25% for cisplatin-5-FU). Although this study indicated an efficacy advantage for the three drug combination of DCF, toxicity was also increased and was very substantial. Eighty-one percent of all patients receiving DCF had at least one grade 3 or 4 non-hematologic toxicity, as well as substantially more hematologic toxicity. Despite this, the use of DCF was associated with a better preservation of quality of life and maintenance of clinical benefit compared with cisplatin-5-FU. On the other hand, there was no difference in the treatment-related mortality rate for the two arms. Therefore, like epirubicin, docetaxel, when added to cisplatin-5-FU, produces a modest improvement in efficacy.

ORAL FLUOROPYRIMIDINES

Treatment with oral fluoropyrimidines seems to offer new hope for patients with gastric cancer, which is surprising when only a few years ago, such patients were not thought to be ideal candidates for an oral treatment. In fact, difficulties with the location of primary tumors, surgery (gastrectomy), or presence of metastatic sites affecting intestinal transit (ie. metastases in the peritoneum), made the hypothetic use of an oral treatment a remote possibility. Nonetheless, findings from recent trials that assessed the role of oral fluoropyrimidines seem to place this assumption into a new promising perspective.

Accordingly, capecitabine has been shown to be effective in the treatment of advanced esophagogastric cancer in a phase Ⅲ study comparing capecitabine with fluorouracil and oxaliplatin with cisplatin (the REAL trial)[7]. Patients were randomly assigned to one of four regimens: ECF, epirubicin plus oxaliplatin and 5-FU (EOF), epirubicin plus cisplatin and capecitabine (ECX), or epirubicin plus oxaliplatin and capecitabine (EOX). Comparing ECF to EOF, ECX, and EOX, there were no significant differences in ORRs (41%, 42%, 46%, and 48%, respectively) and grade 3/4 non-hematologic toxicity (36%, 42%, 33%, and 45%, respectively). Non-inferiority in OS was established in both oxaliplatin/cisplatin and capecitabine/5-FU comparisons in this largest randomized controlled trial. Notably, EOX resulted in a significantly improved survival time compared with the control arm ECF. A median survival time of 11.2 mo in the EOX arm was amongst the longest achieved in this setting of patients. Therefore, EOX should now be regarded as one of the standard first-line treatment options for advanced disease. Another trial that compared treatment with 5-FU plus cisplatin with capecitabine plus cisplatin confirmed that efficacy of capecitabine is equivalent to that of 5-FU[8]. Furthermore, although both of these trials were designed to assess whether capecitabine was no worse than 5-FU, the findings generally suggested better outcome in patients who received oral capecitabine.

S-1 is a new oral anticancer drug comprised of tegafur, 5-chloro-2,4-dihydroxypyrimidine, and oteracil potassium. This drug was designed to enhance the efficacy of tegafur, a prodrug of 5-FU. Koizumi *et al*[9] report findings of the S-1 plus cisplatin *vs* S-1 alone for first-line treatment of advanced gastric cancer (SPIRITS trial). Median progression-free survival (6.0 mo *vs* 4.0 mo; $P < 0.0001$) and OS (13.0 mo *vs* 11.0 mo; $P = 0.04$) were significantly longer in the combination group. Response was also significantly improved in patients having target tumors and assigned to S-1 plus cisplatin (54% *vs* 31%). On the basis of these findings, the standard of treatment in Japan has changed, and treatment with combined S-1 plus cisplatin has become the standard of care. The findings from this trial are clearly relevant: for the first time, in a randomized study, the apparently insurmountable wall of 12 mo survival in advanced gastric cancer was crumbled. However, some considerations must be taken into account before combination S-1 plus cisplatin is implemented as standard treatment in western countries. The SPIRITS trial gives no information about the advantage of S-1 over 5-FU when each was combined with cisplatin. The First-Line Advanced Gastric Cancer Study (FLAGS), which compared S-1 with 5-FU, both combined with cisplatin, has responded to this question[10]. This multicenter phase Ⅲ trial has randomized 1053 patients primarily in the USA, Europe, and South America. Median OS was 8.6 mo in the cisplatin/S-1 arm and 7.9 mo in the cisplatin/5-FU arm ($P = 0.1983$). Statistically significant safety advantages for the S-1-based combination were observed regarding the rates of severe neutropenia (18.6% *vs* 40.0%), stomatitis (1.3% *vs* 13.8%), hypokalemia (3.6% *vs* 10.8%), and renal adverse events (all grades: 18.8% *vs* 33.5%). However, this study has not confirmed the efficacy results of the SPIRITS trial in western populations. Thus, the future role of S-1 in gastric cancer could be the inclusion of this oral drug into a three-drug regimen making DCF or ECF better tolerated. What more can we do to increase median OS?

SECOND-LINE CYTOTOXIC TREATMENT

First-line chemotherapy for the treatment of advanced gastric cancer can provide high response rates which are

of a similar magnitude to those achievable with the newer first-line combinations in colorectal cancer. However, a corresponding improvement in the median OS time has not yet been delivered by the currently available gastric cancer regimens. This lack of progress in relation to markedly improving OS times may be a result, in part, of the more limited efficacy of the currently available second- and third-line treatments for advanced disease, although it should be noted that only one third to one half of the gastric cancer patients in clinical studies may actually receive second-line treatments[11]. Data published to date relating to this are restricted to phase Ⅱ studies of small patient populations, and these investigations are therefore not able to provide definitive results. However, second-line treatments are clearly effective to some degree, with ORRs in the region of 11%-32%, median TTP of 2.5-4.5 mo, and median OS times of 5.4-9.3 mo[12-15].

TARGETED BIOLOGICAL AGENTS

The main hope for significant advances in the near future is the combination of new targeted biological agents with existing chemotherapy first-line regimens. A number of different classes of targeted agents have shown promising activity in clinical studies of advanced gastric cancer, including epidermal growth factor receptor (EGFR) and human epidermal growth factor (HER)-2-targeted monoclonal antibodies, antiangiogenic and antiangiogenic/antitumor compounds, and the proteasome inhibitor bortezomib[16-20].

High response and/or disease control rates have been reported for EGFR-targeted cetuximab combined with irinotecan and infusional 5-FU and leucovorin[16-17] and VEGF-targeted bevacizumab combined with irinotecan and cisplatin[19]. In particular, the FOLCETUX study has demonstrated that the addition of cetuximab to the FOLFIRI regimen increased survival in 38 untreated patients with confirmed advanced gastric/gastroesophageal adenocarcinoma. The treatment was delivered for a maximum of 24 wk, and then cetuximab alone was allowed in patients with a complete response (CR), partial response (PR) or stable disease (SD). Consequently, the overall response rate (ORR) was 44% with a CR in four patients and a PR in 11 patients. Sixteen patients had SD. Median expected OS was 16 mo[16]. In another multicenter phase Ⅱ study, 47 patients with metastatic or unresectable gastric cancer received bevacizumab plus irinotecan and cisplatin. With a median follow-up of 12.2 mo among 34 assessable patients, the ORR was 65%, with 20 patients achieving a PR and two patients a CR. Twelve patients had SD. Median survival was 12.3 mo[19].

Trastuzumab exhibits activity in human gastric cancer cells that overexpress HER2/neu. A phase Ⅱ trial has determined the efficacy and tolerability of trastuzumab plus cisplatin in patients with advanced gastric cancer with HER2/neu overexpression/amplification. Preliminary results showed that 6 (35%) out of 17 assessable patients achieved response, 3 (17%) stabilization. There was no grade 4 toxicity[18]. In considering such studies, it is notable that the first-line cytotoxic regimens that have been selected for combination with biological agents tend to be those that are generally considered not to be optimal for the treatment of advanced gastric cancer. This begs the question as to whether the impressive potential of these targeted agents might be more profitably explored in the future within combinations that include standard cytotoxic backbones such as ECF, DCF, EOX, or perhaps S-1 plus cisplatin. Indeed, a number of randomized phase Ⅲ studies incorporating targeted agents in first-line regimens have recently been initiated: the ToGA (Trastuzumab with Chemotherapy in HER2-Positive Advanced Gastric Cancer) study is investigating the effect on progression-free survival of trastuzumab in combination with a fluoropyrimidine plus cisplatin *versus* chemotherapy alone in patients with HER-2-positive advanced gastric cancer, AVAGAST (Avastin® in Gastric Cancer) is investigating OS time in advanced gastric cancer patients receiving either capecitabine and cisplatin plus bevacizumab or chemotherapy alone plus placebo, and the REAL-3 study is investigating the benefit of adding panitumumab to an EOX regimen in patients with locally advanced or metastatic esophagogastric adenocarcinoma.

However, new biological agents could be useful in the management of advanced disease after the failure of first-line treatment. In this context, it is possible that targeted agents may have a future role as single-agent maintenance treatments. Two recent phase Ⅱ studies have pursued this concept[21-22]. A Japanese study has evaluated the activity and safety of everolimus (RAD001), an oral inhibitor of the mammalian target of rapamycin serine-threonine kinase, in 54 pretreated patients with metastatic gastric cancer. At interim analysis, no objective responses were observed but disease control rate was 55% and median TTP was 83 d. Main adverse events were stomatitis (74%), anorexia (51%), fatigue (47%), rash (45%), peripheral edema (23%), thrombocytopenia (21%), diarrhea (19%), pneumonitis (13%), and hyperglycemia (9%). The multicenter AIO phase Ⅱ trial has evaluated tolerability and efficacy of sunitinib in highly pretreated Caucasian patients with unresectable metastatic cancer of stomach, esophagogastric junction or lower esophagus. Among 14 response-evaluable patients, 5 of them showed tumor control for at least 6 wk. With regard to survival, 5 patients experienced early death caused by progressive disease, 7 patients survived > 60 d. Twelve patients were still in follow-up or withdrew informed consent within 60 d after start of therapy. Again, 3 of them survived > 60 d. No serious adverse events occurred.

In conclusion, these studies constitute a potentially important advance, indicating a role for biological agents in the treatment of advanced gastric cancer. Further trials are now needed to clarify their respective position with reference to chemotherapy.

REFERENCES

1 **Muñoz N**, Franceschi S. Epidemiology of gastric cancer

and perspectives for prevention. *Salud Publica Mex* 1997; **39**: 318-330

2 **Kamangar F**, Dores GM, Anderson WF. Patterns of cancer incidence, mortality, and prevalence across five continents: defining priorities to reduce cancer disparities in different geographic regions of the world. *J Clin Oncol* 2006; **24**: 2137-2150

3 **Glimelius B**, Ekström K, Hoffman K, Graf W, Sjödén PO, Haglund U, Svensson C, Enander LK, Linné T, Sellström H, Heuman R. Randomized comparison between chemotherapy plus best supportive care with best supportive care in advanced gastric cancer. *Ann Oncol* 1997; **8**: 163-168

4 **Webb A**, Cunningham D, Scarffe JH, Harper P, Norman A, Joffe JK, Hughes M, Mansi J, Findlay M, Hill A, Oates J, Nicolson M, Hickish T, O'Brien M, Iveson T, Watson M, Underhill C, Wardley A, Meehan M. Randomized trial comparing epirubicin, cisplatin, and fluorouracil versus fluorouracil, doxorubicin, and methotrexate in advanced esophagogastric cancer. *J Clin Oncol* 1997; **15**: 261-267

5 **Wagner AD**, Grothe W, Haerting J, Kleber G, Grothey A, Fleig WE. Chemotherapy in advanced gastric cancer: a systematic review and meta-analysis based on aggregate data. *J Clin Oncol* 2006; **24**: 2903-2909

6 **Van Cutsem E**, Moiseyenko VM, Tjulandin S, Majlis A, Constenla M, Boni C, Rodrigues A, Fodor M, Chao Y, Voznyi E, Risse ML, Ajani JA. Phase III study of docetaxel and cisplatin plus fluorouracil compared with cisplatin and fluorouracil as first-line therapy for advanced gastric cancer: a report of the V325 Study Group. *J Clin Oncol* 2006; **24**: 4991-4997

7 **Cunningham D**, Starling N, Rao S, Iveson T, Nicolson M, Coxon F, Middleton G, Daniel F, Oates J, Norman AR. Capecitabine and oxaliplatin for advanced esophagogastric cancer. *N Engl J Med* 2008; **358**: 36-46

8 **Kang Y**, Kang WK, Shin DB, Chen J, Xiong J, Wang J, Lichinitser M, Salas MP, Suarez T, Santamaria J. Randomized phase III trial of capecitabine/cisplatin (XP) vs. continuous infusion of 5-FU/cisplatin (FP) as first-line therapy in patients (pts) with advanced gastric cancer (AGC): efficacy and safety results. Proceedings of the 42nd Annual Meeting of American Society of Clinical Oncology; 2006 June 1-5; Chicago, USA. Alexandria: American Society of Clinical Oncology, 2006: 18s

9 **Koizumi W**, Narahara H, Hara T, Takagane A, Akiya T, Takagi M, Miyashita K, Nishizaki T, Kobayashi O, Takiyama W, Toh Y, Nagaie T, Takagi S, Yamamura Y, Yanaoka K, Orita H, Takeuchi M. S-1 plus cisplatin versus S-1 alone for first-line treatment of advanced gastric cancer (SPIRITS trial): a phase III trial. *Lancet Oncol* 2008; **9**: 215-221

10 **Ajani JA**, Rodriguez W, Bodoky G, Moiseyenko V, Lichinitser M, Gorbunova V, Vynnychenko I, Garin A, Lang I, Falcon S. Multicenter phase III comparison of cisplatin/S-1 (CS) with cisplatin/5-FU (CF) as first-line therapy in patients with advanced gastric cancer (FLAGS). Presented at the American Society of Clinical Oncology Gastrointestinal Cancers Symposium; 2009 January 15-17; San Francisco, USA

11 **Pozzo C**, Barone C. Is there an optimal chemotherapy regimen for the treatment of advanced gastric cancer that will provide a platform for the introduction of new biological agents? *Oncologist* 2008; **13**: 794-806

12 **Lee JL**, Ryu MH, Chang HM, Kim TW, Yook JH, Oh ST, Kim BS, Kim M, Chun YJ, Lee JS, Kang YK. A phase II study of docetaxel as salvage chemotherapy in advanced gastric cancer after failure of fluoropyrimidine and platinum combination chemotherapy. *Cancer Chemother Pharmacol* 2008; **61**: 631-637

13 **Kodera Y**, Ito S, Mochizuki Y, Fujitake S, Koshikawa K, Kanyama Y, Matsui T, Kojima H, Takase T, Ohashi N, Fujiwara M, Sakamoto J, Akimasa N. A phase II study of weekly paclitaxel as second-line chemotherapy for advanced gastric Cancer (CCOG0302 study). *Anticancer Res* 2007; **27**: 2667-2671

14 **Rosati G**, Bilancia D, Germano D, Dinota A, Romano R, Reggiardo G, Manzione L. Reduced dose intensity of docetaxel plus capecitabine as second-line palliative chemotherapy in patients with metastatic gastric cancer: a phase II study. *Ann Oncol* 2007; **18** Suppl 6: vi128-vi132

15 **Giuliani F**, Molica S, Maiello E, Battaglia C, Gebbia V, Di Bisceglie M, Vinciarelli G, Gebbia N, Colucci G. Irinotecan (CPT-11) and mitomycin-C (MMC) as second-line therapy in advanced gastric cancer: a phase II study of the Gruppo Oncologico dell' Italia Meridionale (prot. 2106). *Am J Clin Oncol* 2005; **28**: 581-585

16 **Pinto C**, Di Fabio F, Siena S, Cascinu S, Rojas Llimpe FL, Ceccarelli C, Mutri V, Giannetta L, Giaquinta S, Funaioli C, Berardi R, Longobardi C, Piana E, Martoni AA. Phase II study of cetuximab in combination with FOLFIRI in patients with untreated advanced gastric or gastroesophageal junction adenocarcinoma (FOLCETUX study). *Ann Oncol* 2007; **18**: 510-517

17 **Moehler MH**, Trarbach T, Seufferlein T, Kubicka S, Lordick F, Geissler M, Daum S, Kanzler S, Galle P. Cetuximab with irinotecan/FA/5FU as first-line treatment in advanced gastric cancer: Preliminary results of a non-randomized multicenter AIO phase II study. Presented at the American Society of Clinical Oncology Gastrointestinal Cancers Symposium; 2008 January 25-27; Orlando, USA

18 **Cortés-Funes H**, Rivera F, Alés I, Márquez A, Velasco A, Colomer R, García-Carbonero R, Sastre J, Guerra J, Grávalos C. Phase II of trastuzumab and cisplatin in patients (pts) with advanced gastric cancer (AGC) with HER2/neu overexpression/amplification. Proceedings of the 43rd Annual Meeting of American Society of Clinical Oncology; 2007 June 1-5; Chicago, USA. Alexandria: American Society of Clinical Oncology, 2007: 4613a

19 **Shah MA**, Ramanathan RK, Ilson DH, Levnor A, D'Adamo D, O'Reilly E, Tse A, Trocola R, Schwartz L, Capanu M, Schwartz GK, Kelsen DP. Multicenter phase II study of irinotecan, cisplatin, and bevacizumab in patients with metastatic gastric or gastroesophageal junction adenocarcinoma. *J Clin Oncol* 2006; **24**: 5201-5206

20 **Ocean AJ**, Schnoll-Sussman F, Chen XE, Keresztes R, Holloway S, Matthews N, O'Brien K, Christos P, Mazumdar M, Wadler S. Recent results of phase II study of PS-341 (bortezomib) with or without irinotecan in patients (pts) with advanced gastric adenocarcinomas (AGA). Proceedings of the 43rd Annual Meeting of American Society of Clinical Oncology; 2007 June 1-5; Chicago, USA. Alexandria: American Society of Clinical Oncology, 2007: 45a

21 **Yamada Y**, Doi T, Muro K, Boku N, Nishina T, Takiuchi H, Komatsu Y, Hamamoto Y, Ohno N, Fujita Y, Ohtsu Y. Multicenter phase II study of everolimus in patients with previously treated metastatic gastric cancer: main results. Presented at the American Society of Clinical Oncology Gastrointestinal Cancers Symposium; 2009 January 15-19; San Francisco, USA

22 **Moehler M**, Hartmann JT, Lordick F, Al-Batran S, Reimer P, Trarbach T, Ebert M, Daum S, Weihrauch M, Galle PR. AIO Upper GI Group. Sunitinib in patients with chemo-refractory metastatic gastric cancer: Preliminary results of an open-label, prospective nonrandomized multicenter AIO phase II trial. Presented at the American Society of Clinical Oncology Gastrointestinal Cancers Symposium; 2009 January 15-19; San Francisco, USA

S- Editor Li LF **L- Editor** Logan S **E- Editor** Yin DH

Online Submissions: wjg.wjgnet.com
wjg@wjgnet.com
doi:10.3748/wjg.15.2693

World J Gastroenterol 2009 June 14; 15(22): 2693-2700
World Journal of Gastroenterology ISSN 1007-9327

EDITORIAL

Role of scintigraphy in inflammatory bowel disease

Maria I Stathaki, Sophia I Koukouraki, Nikolaos S Karkavitsas, Ioannis E Koutroubakis

Maria I Stathaki, Sophia I Koukouraki, Nikolaos S Karkavitsas, Department of Nuclear Medicine, University Hospital of Heraklion, 71110 Heraklion, Crete, Greece
Ioannis E Koutroubakis, Department of Gastroenterology, University Hospital of Heraklion, 71110 Heraklion, Crete, Greece
Author contributions: Stathaki MI, Koukouraki SI reviewed the literature, wrote the first draft of the paper; Karkavitsas NS and Koutroubakis IE provided the idea, performed the review, and edited the manuscript.
Correspondence to: Ioannis E Koutroubakis, MD, PhD, Department of Gastroenterology, Medicine University Hospital of Heraklion, PO Box 1352, 71110 Heraklion, Crete, Greece. ktjohn@her.forthnet.gr
Telephone: +30-2810-392253 Fax: +30-2810-542085
Received: February 1, 2009 Revised: March 25, 2009
Accepted: April 1, 2009
Published online: June 14, 2009

Abstract

The diagnosis of inflammatory bowel disease (IBD) depends on direct endoscopic visualization of the colonic and ileal mucosa and the histological study of the obtained samples. Radiological and scintigraphic methods are mainly used as an adjunct to endoscopy. In this review, we focus on the diagnostic potential of nuclear medicine procedures. The value of all radiotracers is described with special reference to those with greater experience and more satisfactory results. Tc-99m hexamethylpropylene amine oxime white blood cells remain a widely acceptable scintigraphic method for the diagnosis of IBD, as well as for the evaluation of disease extension and severity. Recently, pentavalent Tc-99m dimercaptosuccinic acid has been recommended as an accurate variant and a complementary technique to endoscopy for the follow-up and assessment of disease activity. Positron emission tomography alone or with computed tomography using fluorine-18 fluorodeoxyglucose appears to be a promising method of measuring inflammation in IBD patients.

Key words: Crohn's disease; Technetium-99m pentavalent dimercaptosuccinic acid; Intestinal inflammation; Scintigraphy; Ulcerative colitis

Peer reviewer: Tsianos Epameinondas, MD, PhD, Professor, 1st Division of Internal Medicine & Hepato-Gastroenterology Unit, Medical school University of Ioannina, PO Box 1186, Ioannina 45110, Greece

Stathaki MI, Koukouraki SI, Karkavitsas NS, Koutroubakis IE. Role of scintigraphy in inflammatory bowel disease. *World J Gastroenterol* 2009; 15(22): 2693-2700 Available from: URL: http://www.wjgnet.com/1007-9327/15/2693.asp DOI: http://dx.doi.org/10.3748/wjg.15.2693

INTRODUCTION

The diagnosis and follow-up of patients with inflammatory bowel disease (IBD) is mainly based on endoscopy and the histological study of the obtained biopsy specimens[1,2]. Ileocolonoscopy, gastroscopy and evaluation of small bowel by wireless capsule endoscopy or double balloon enteroscopy offer a successful diagnostic approach in the majority of IBD patients[3,4].

Radiological methods have a secondary role and they are used additionally to endoscopy. They are indicated in cases of suspected complications or small bowel involvement in patients with Crohn's disease (CD)[4-6]. They include conventional radiological methods such as double-contrast barium studies and cross-sectional imaging modalities such as computed tomography (CT), magnetic resonance imaging (MRI), and ultrasound[6-9]. All of them have been proven valuable techniques for evaluation of the effects of the inflammatory process, not only on the bowel wall, but also on other structures within the abdomen[6,8].

Unfortunately, endoscopy as well as the majority of the aforementioned radiological methods are not well tolerated by patients, because of the necessity for adequate bowel preparation and the increased risk of complications, especially when used during the acute phase of bowel inflammation[1,3,8,10].

Alternatively, several studies have demonstrated the reliability of scintigraphic imaging in the diagnosis and assessment of disease activity in IBD. In comparison with other modalities, they are non-invasive techniques and produce no patient discomfort related to instrumentation and preparation, they are not contraindicated in the acute phase and can visualize active disease both in the small and the large bowel[2,11]. Technetium-99m hexamethylpropylene amine oxime labelled white blood cells (Tc-99m HMPAO WBC) have been accepted widely as a reliable method for the diagnosis of IBD, assessment of disease activity

and treatment response[12-14]. Pentavalent Tc-99m dimercaptosuccinic acid [Tc-99m (V) DMSA] seems to be an accurate scintigraphic variant and has been suggested as a complementary technique to colonoscopy for the follow-up and assessment of disease activity[15-17]. Finally, fluorine-18 fluorodeoxyglucose (F-18 FDG) is a promising method for the detection of inflammation in the small and large bowel[18,19].

In this article, we review the current data and future prospects on the role of scintigraphy in diagnosis and evaluation of disease activity in patients with IBD.

THE ROLE OF NUCLEAR MEDICINE IN IBD

Nuclear medicine imaging has played a major role in the diagnosis and detection of inflammation, and has a wide availability of radiotracers. However, its contribution to the localization of small and large bowel pathology in IBD is still under investigation.

Indium-111 oxine labeled leukocytes

Indium-111 (In-111) oxine was the first agent used for *in vitro* leucocyte labeling[2]. The method has been validated by different research groups as a sensitive and specific test for the detection of active intestinal inflammation. However, the high radiation dose, limited availability and poor image quality comprise major disadvantages associated with In-111[2,11,13,14].

Recently, a dedicated whole-body counter has been proposed as an alternative technique to whole-body gamma-camera counting for quantification of disease activity in IBD. It relies on the assumption that all granulocytes migrating into the bowel wall in IBD do in fact end up in the feces, therefore In-111 retention in IBD patients is less compared to that in normal volunteers[20].

Tc-99m HMPAO labeled leukocytes

Tc-99m HMPAO has been used clinically as a cerebral perfusion agent. In 1986, Peters *et al*[21] used it as an alternative to leukocytes labeling and inflammation imaging. Since then, several groups have verified the utility of this imaging technique for IBD. The published data show that it provides a sensitivity of 95%-100%, a specificity of 85%-100% and an accuracy of 92%-100% in the detection, localization and assessment of disease activity. Therefore, its widespread acceptance has been based on the aforementioned favorable results and the advantages of Tc-99m, such as low radiation dose, availability, cost and superior image quality[2,22-24]. It plays an important role in the diagnosis of complications, assessment of disease activity and establishing the extent of small intestine affected. Moreover, it allows a true evaluation of inflammation activity, even during clinical remission or treatment response[2,23,24].

In 2007, Almer *et al*[25] compared leucocyte scintigraphy to intraoperative small bowel enteroscopy and laparotomy findings in CD. They confirmed the reliability of Tc-99m HMPAO WBC in the early diagnosis of small bowel inflammation, and proposed its utility as a first-line investigation modality, especially in children and vulnerable adults.

Despite the wide utility of Tc-99m HMPAO WBC in IBD, controversy still exists about the advantageous imaging time. Early scanning (30-60 min) has been recommended by some authors in order to avoid false positive results caused by intestinal migration of the radionuclide, whereas others favor late scanning because of higher sensitivity. Recently, Sans *et al*[24] have evaluated the optimal scanning sequence for identification of active disease, evaluation of IBD extent, and quantification of disease activity. They reported only slightly lower specificity but higher sensitivity (85% *vs* 100%) and accuracy (85% *vs* 95%) of late scanning (3 h) when compared to early scanning.

Various biomarkers of inflammation have been suggested in selecting patients with suspected IBD for white cell scanning. Given that C-reactive protein constitutes a reliable indicator for the evaluation of inflammatory activity in IBD, patients with $\geqslant$ 5 mg/L should be selected for white cell scanning in order to reduce the number of false negative results[26].

Alonso *et al*[27,28] have applied Tc-99m HMPAO WBC to patients with subclinical gut inflammation. This group studied patients with seronegative spondyloarthropathy without clinical evidence of IBD. They confirmed the utility of the method in the assessment of bowel inflammation, even if it remains subclinical. Moreover, they described a possible role of labeled leukocytes in identifying the patients who are suitable for therapy with sulfasalazine, and in assessing treatment effectiveness and disease relapse[27,28]. El Maghraoui *et al*[29] have certified the aforementioned results and demonstrated a statistically significant correlation between Tc-99m HMPAO-labeled leukocytes and ileocolonoscopy.

The usefulness of this technique in early detection of postoperative asymptomatic recurrence of CD has been suggested. Biancone *et al*[30] have demonstrated that, in patients with CD who had an ileocecal resection in the previous 6 mo, the perianastomotic 30 min Tc-99m HMPAO WBC uptake was significantly associated with disease recurrence.

The role of Tc-99m HMPAO-labeled leukocytes single photon emission computerized tomography (SPECT) in IBD has also been investigated. SPECT images provide accurate assessment of inflammation in both the small and large bowel and precise anatomical details of CD lesions. Moreover, they are independent of bone marrow activity, thus allowing detailed disease evaluation within the pelvis[31,32].

The aim of several groups has been to evaluate and compare the diagnostic accuracy of Tc-99m HMPAO-labeled leukocytes and CT in IBD. They have demonstrated the superiority of scintigraphy in detecting segmental inflammatory activity and proximal extension of bowel involvement. CT displays excellent suitability for the localization of fibrostenotic bowel disease and the recognition of complications, but has a four-fold higher radiation exposure[33-35].

Several studies have supported the utility of Tc-

Table 1 Summary of published studies evaluating the use of Tc-99m HMPAO WBC in IBD

Study	*n*	Study design	Sensitivity	Specificity
Adult population				
Sciarretta *et al*[23]	103	Known active CD compared with colonoscopy	95%	100%
Mairal *et al*[50]	27	Known IBD compared with In-111 HIG	100%	85%
Giaffer *et al*[13]	31	Suspected IBD compared with In-111 oxine labeled leukocytes	85% at 40 min 94% at 120 min	87% at 40 min 71% at 120 min
Kolkman *et al*[33]	32	Known IBD compared with CT	79% for CD 81% for UC	98% for CD 86% for UC
Molnár *et al*[34]	28	Known active CD compared with spiral CT	76.1%	91%
Almer *et al*[25]	48	Known active CD with small bowel inflammation compared with intraoperative small bowel enteroscopy and laparotomy findings	85%	81%
Pediatric population				
Charron *et al*[40]	215	Acute intestinal inflammation in patients with and without IBD	90%	97%
Cucchiara *et al*[38]	48	Suspected IBD compared with colonoscopy	76.2%	NA
Charron *et al*[42]	130	Exclude inflammation in suspected IBD compared with colonoscopy	94%	99%
Alberini *et al*[37]	28	Known IBD compared with endoscopy, ultrasonography and contrast radiology	75%	92%
Charron *et al*[35]	313	Known IBD compared with colonoscopy	92%	94%

NA: Not applicable; CD: Crohn's disease; CT: Computed tomography; IBD: Inflammatory bowel disease; UC: Ulcerative colitis.

99m HMPAO WBC in pediatric patients with IBD. They have suggested that labeled leukocytes cannot replace endoscopy for initial diagnosis but they do have a place in the decision for colonoscopy[36,37]. Patients with negative Tc-99m HMPAO WBC scans may avoid unnecessary colonoscopy. However, Cucchiara *et al*[38], after evaluating 48 children, have concluded that a positive test indicates the presence of inflammation but a negative result does not rule out inflammation, since the technique may miss cases with mild disease.

Moreover leukocytes scintigraphy can be considered a reference method for clarifying the extent of inflammation when colonoscopy is not completed successfully, or the findings in contrast radiography are negative[36,37,39]. Although SPECT allows the identification of additional involved segments over planar images, its performance in children seems to be rather difficult[37,40].

The accuracy of Tc-99m HMPAO WBC in differentiating continuous from discontinuous colitis has also been examined[37,41]. In 77 children with active CD, discontinuous uptake was revealed in 63, and among 29 children with ulcerative colitis (UC), continuous uptake was revealed in 23[41]. It should also play an important role in the follow-up of patients and it could be used as a diagnostic tool for assessing recurrence or response to therapy, thus reducing the need for repeated colonoscopy[36,37].

In a report by Charron *et al*[35], the accuracy of CT and Tc-99m HMPAO WBC scintigraphy versus colonoscopy in IBD has been compared. After evaluating 313 consecutive children who underwent a labeled leucocyte test and comparing with colonoscopy, the sensitivity of scintigraphy was 92%, specificity was 94%, positive predictive value was 96%, negative predictive value was 93% and accuracy was 94%. Tc-99m HMPAO WBC scan is unlikely to miss significant inflammation, while CT has lower sensitivity for detecting inflammation in the bowel wall. However, similar to the adult population, the incidence of complications detected by CT is higher than with scintigraphy[35].

Compared to other modalities, Tc-99m HMPAO WBC scintigraphy is non-invasive, practical, safe, rapid and has excellent diagnostic sensitivity (Figure 1). It requires no bowel preparation, causes no discomfort and exposes patients to less radiation, namely the effective radiation dose for Tc-99m HMPAO WBC imaging is 3 mSv, for barium small bowel follow-through, 6 mSv, and for barium enema, 8.5 mSv[36,39,40,42]. Additional important advantages are the ability to evaluate the small and the large bowel simultaneously and the superiority over small bowel follow-through and CT, in the initial screening and detection of inflammation in patients with IBD[35,36,42]. A concise form of the published data is presented in Table 1.

The high cost, time-consuming *in vitro* labeling procedure, radiation microdosimetry, as well as the handling and reinjection of blood constitute the main shortcomings of the procedure when compared to other scintigraphic modalities.

Tc-99m (V) DMSA

Tc-99m (V) DMSA is a tumor-seeking agent of low molecular weight developed in 1981. It has been used successfully in the scintigraphic diagnosis of various malignant tumors[43-47]. Moreover, it has been proven advantageous in the diagnosis of inflammatory diseases such as osteomyelitis, psoas muscle abscess, and bone and joint infection[48,49].

The mechanism of Tc-99m (V) DMSA localization in tumors and inflammation remains unclear. In some cases, it resembles the phosphate ion because it accumulates in lesions where calcification is present. However, the increased capillary permeability followed by infiltration of the radiotracer into the interstitial space seems to be the most probable mechanism of uptake in inflammatory lesions[16,17,48,49].

Tc-99m (V) DMSA scintigraphy requires no bowel preparation, no blood manipulation and causes no patient discomfort. Moreover it has a low cost, ideal physical characteristics, and simple preparation procedure from cold kits[15-17]. Its utility in the diagnosis

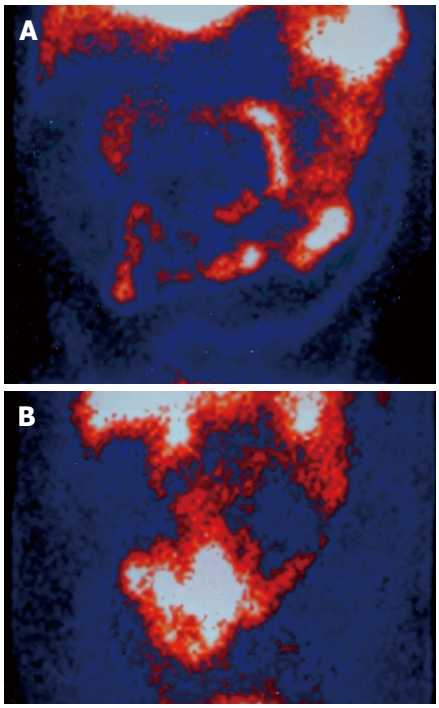

Figure 1 Tc-99m HMPAO WBC scintigram. A: Ulcerative colitis (UC) with intense inflammation of the entire large bowel; B: Crohn's disease (CD) with intense inflammation in the small bowel and the descending colon.

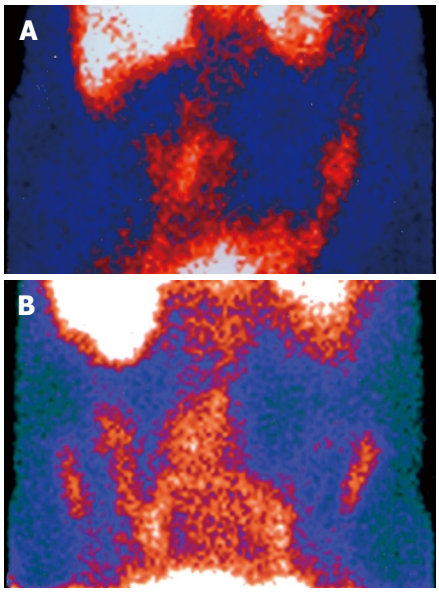

Figure 2 Tc-99m (V) DMSA scintigram. A: UC with intense inflammation mainly in the transverse and the descending colon; B: CD with intense inflammation of the terminal ileum and the ascending colon.

of inflammation combined with the aforementioned advantages have given a new impulse to research groups to evaluate its role in IBD.

In 2001, Lee *et al*[15] appraised the potential use of Tc-99m (V) DMSA scintigraphy in the detection and localization of intestinal inflammation. The study enrolled 62 patients with suspected intestinal inflammation, namely IBD, appendicitis, and antibiotic-associated, infective, eosinophilic and ischemic colitis. The scintigraphic findings were compared to colonoscopy and biopsy results. The overall sensitivity was 95%, specificity, 94%, and accuracy, 95%. The three false negative cases were attributed to a mild degree of inflammation. Findings were false positive in two cases as a result of coexisting active bleeding from the gastrointestinal tract and colonic adenocarcinoma, seen at colonoscopy with biopsy[15].

In 2003, Koutroubakis *et al*[16] evaluated the use of Tc-99m (V) DMSA for the assessment of disease activity in patients with IBD. They examined three groups of patients. The first group enrolled 36 patients who had an exacerbation of previously demonstrated disease or had a first attack of IBD. The second group included 28 patients who were in remission from IBD. The third group included 12 patients with miscellaneous bowel disease, namely ischemic, infectious or segmental colitis associated with diverticulosis. The scintigraphic findings were compared to colonoscopy and biopsy results. In the detection of active disease, the sensitivity was 92%, the specificity was 86%, the negative predictive value was 85.1% and the positive predictive value was 91.9%. A high correlation of the scintigraphic activity index with the endoscopic and histological inflammatory activity was found. Findings were false negative in three cases with active disease because of a mild degree of inflammation[16].

A direct comparison of Tc-99m (V) DMSA with Tc-99m HMPAO WBC scintigraphy in the evaluation of IBD has been undertaken by Stathaki *et al*[17] in 2008. The favorable results of the two previous studies, in combination with the advantages of the method, could establish it as an ideal alternative scintigraphic method. The study enrolled 23 patients who had an exacerbation of previously proven IBD or a first attack of the disease. Tc-99m (V) DMSA scintigraphy was performed after clinical and endoscopic confirmation of active disease and true positive labeled leucocyte scintigraphy. The full agreement among the scintigraphic modalities was 72.5%. The agreement among endoscopy and scintigraphy was 91.9% and 84.4% for Tc-99m HMPAO WBC and Tc-99m (V) DMSA, respectively. The overall sensitivity was 91% for Tc-99m HMPAO WBC and 84% for Tc-99m (V) DMSA. False negative results for Tc-99m (V) DMSA scintigraphy were seen in two patients with UC, probably because of a mild degree of bowel inflammation[17].

Data suggest that Tc-99m (V) DMSA scintigraphy provides a useful approach in the diagnosis of active disease and assessment of disease activity (Figure 2). Despite that, it cannot replace Tc-99m HMPAO WBC for the evaluation of disease localization. Probably, it is not the ideal method for the diagnosis of IBD but it has a place in the follow-up and assessment of disease activity, progression and treatment response[17]. A concise form of the published data is presented in Table 2.

Other radiotracers

A variety of radionuclides has been applied to IBD investigation. Some of them have not gained widespread clinical use because of limitations and disappointing results, while others seem to have a definite role.

Table 2 Summary of published studies evaluating the use of Tc-99m (V) DMSA in IBD

Study	*n*	Study design	Sensitivity (%)	Specificity (%)
Lee *et al*[15]	62	Intestinal inflammation compared with colonoscopy	95	94
Koutroubakis *et al*[16]	76	Active and inactive IBD compared with colonoscopy	92	86
Stathaki *et al*[17]	23	Active IBD compared with Tc-99m HMPAO WBC and colonoscopy	84	NA

In-111 or Tc-99m human polyclonal immunoglobulin (HIG) has been used in the diagnosis of inflammation and it has been evaluated in IBD. Comparative studies have demonstrated sensitivity, specificity and accuracy of 100%, 85% and 96%, respectively, for labeled leukocytes and 70%, 85% and 74% for In-111 HIG[50]. Tc-99m HIG scintigraphy had 33% sensitivity while Tc-99m HMPAO WBC imaging had 100% sensitivity in the detection of active IBD[51]. On the basis of these results, the role of In-111 HIG is confined to the diagnosis of inflammation only when there is no other alternative modality[50]. On the other hand, Tc-99m HIG has no role in the evaluation of patients with IBD[51].

In vivo specific labeling of granulocytes using Tc-99m labeled anti-granulocyte monoclonal antibodies (AGAb) comprises a different approach. They do not require leucocyte isolation, are stored as cold kits and can selectively label granulocytes. Different AGAb have been designed, among them BW 250/183 and Leukoscan[52-55]. Tc-99m BW 250/183 was found to be inferior to Tc-99m HMPAO WBC in the detection of small bowel involvement, although the accuracy between the two scintigraphic methods for the localization of disease in the large bowel was comparable[52]. With respect to Tc-99m Leukoscan, its diagnostic value in IBD is low[53,54]. However, a recent study by Kerry *et al*[55] has found that Tc-99m Leukoscan has higher sensitivity and specificity at 2 h (44% and 100% respectively) and 4 h (75% and 50% respectively) planar imaging compared to that in previous publications. SPECT images at 4 h showed additional areas of uptake, raising the sensitivity to a value similar to that of Tc-99m HMPAO WBC, namely 88%. Although sensitivity is high, the low specificity limits its application for the investigation of IBD[55].

Research groups have evaluated the role of AGAb imaging in pediatric patients with IBD. Bruno *et al*[56] have found that the overall sensitivity of Tc-99m BW 250/183 was 94% for CD and 85% for UC. Sensitivity of scintigraphy compared to colonoscopy, radiology and ultrasonography was 90%, 76%, 75% and 55%, respectively. However, it did not appear sufficiently specific in identifying clinical remission, probably because of the presence of tissue inflammation in about 50% of biopsy samples, although patients were considered to be in clinical remission and with negative colonoscopy. The authors have recommended Tc-99m BW 250/183 as a useful tool in the detection of intestinal inflammation in children and young patients with IBD. However, because of its low specificity, endoscopic and histological confirmation is mandatory for all positive cases[56]. The efficacy of Tc-99m Leukoscan has been evaluated in a small series of pediatric patients with IBD. The reported sensitivity per patient was 90% and per bowel segment, 57%. The latter was improved with the use of SPECT[57].

In 1984, Hanna *et al*[58] worked on the labeling of leukocytes with Tc-99m stannous colloid, and reported the clinical application of this new imaging modality in IBD. Despite its usefulness as an alternative when other agents are not available, the activation of leukocytes, which reduces the *in vivo* viability, constitutes a shortcoming[59]. Recently, its use in the initial evaluation of children with suspected IBD has been assessed. The combination of the reported results (sensitivity 88%, specificity 90%) and the aforesaid advantages support its utility in the initial assessment of childhood IBD[59].

The primary data on the role of In-111 anti E-selectin monoclonal antibodies are encouraging, given that it can identify areas of inflammation in CD and UC. Still, they are not supported sufficiently to gain acceptance in the field of IBD[60].

Positron emission tomography (PET)

PET with F-18 FDG is a functional imaging modality which identifies areas of increased glucose metabolism. It has been found to be effective in the evaluation of malignancies, inflammation and infection. Preliminary studies have shown favorable results in the assessment of disease activity in IBD[19].

In a small study of four patients with CD and two with UC, PET scanning demonstrated high radionuclide uptake in the inflamed segments, which had been detected on endoscopy and confirmed by histology. The potential utility of this non-invasive modality, as well as its usefulness for follow-up was suggested[61]. Neurath *et al*[18] have compared F-18 FDG, hydro-MRI and granulocyte scintigraphy with labeled antibodies (Tc-99m BW 250/183) in the detection of disease activity in 59 patients with CD. The sensitivity and specificity reported for F-18 FDG was 85% and 89%, for hydro-MRI, 67% and 93%, and for Tc-99m BW 250/183, 41% and 100%. It appears to be an accurate modality for detecting inflammation, considering that it allows a simultaneous non-invasive analysis of affected segments in both small and large bowel. Moreover, it is helpful in evaluating possible inflammatory activity in detected stenosis, which is important for its therapeutic application[18].

Recent studies have assessed the role of PET in the investigation of pediatric IBD. It diagnosed active disease in 80% of childhood cases with known IBD, and F-18 FDG uptake correlated with the endoscopic findings in 83.8% of the patients. PET recognized diseased segments that were not detected by other diagnostic methods, probably because of the limited accessibility at endoscopy. Moreover, it is the least invasive technique, can provide additional information to the diagnostic data obtained by other modalities, and exposes patients to

lower radiation doses[62]. Löffler *et al*[63], using histology as a reference standard, reported F-18 FDG PET sensitivity, specificity and accuracy to be 98%, 68% and 83%, respectively, for large bowel, and 100%, 86% and 90% for small bowel involvement. Based on these favorable results, the authors have recommended the inclusion of PET in the initial investigative algorithm for the evaluation of bowel inflammation and treatment response. On the other hand, its moderate specificity renders indispensable the endoscopic and histological confirmation of all positive cases[63].

Coupling CT to PET combines the functional data obtained from PET with the anatomical data provided by CT. Its role in the detection and localization of disease activity in IBD has been evaluated. In a pilot study, Meisner *et al*[64] have validated the results of previous reports concerning the role of PET in IBD, and they have investigated the use of sequential CT. In most cases, the simultaneous transaction of CT was not essential but it allowed better anatomical analysis in patients who had been surgically treated, and in those with inflammation of the small bowel. There was a high correlation between PET activity and disease activity, as determined by other currently used modalities[64].

Louis *et al*[65] have similarly concluded that coupling PET with CT allows a more accurate anatomical identification and evaluation of F-18 FDG uptake, and it gives more morphological information, namely, the presence of strictures. The technique can detect almost all bowel segments with moderate and severe lesions and a significant proportion with only mild lesions. Of great scientific interest were the combined findings of increased F-18 FDG uptake and bowel wall thickening in PET/CT, which were observed in some segments without endoscopic evidence of lesions. One explanation might be the detection of active disease deeper in the bowel wall, which is an additional benefit of this diagnostic modality[65].

Recently, the role of PET/CT in patients with UC in remission has been evaluated. Although clinical remission was strictly defined, four out of the 10 patients who participated in the study had increased F-18 FDG uptake in the colon. This may be explained by the presence of asymptomatic inflammation, attributed to chronic low-grade activity or to the succession of flare and quiescence. The possibility of representing a normal variant or a false positive result could not be excluded. This finding necessitates further understanding of disease remission. The authors have suggested that PET/CT is a highly sensitive method, however, future studies will define its precise role among all available diagnostic modalities in disease evaluation and treatment monitoring[66].

At present, published data have suggested a high diagnostic value of F-18 FDG PET alone or PET/CT in adult and pediatric patients with IBD. However, the physiological distribution of the radionuclide, mainly in the urinary tract, and to a minor degree in the gastrointestinal tract, may compromise abdominal PET imaging of patients with IBD. In order to avoid any false results, the utility of quantitative analysis using the standardized uptake value (SUV) has been suggested. A cutoff RSUV (ratio between SUV of inflamed bowel and SUV of liver) value of 1.47 seems to be reliable for the identification of areas with significant bowel inflammation[19]. Recently, various methods of labeling leukocytes with F-18 FDG have been reported. F-18 FDG WBC are taken up in the reticuloendothelial tissue and follow the normal leukocyte distribution *in vivo*. Its role as a method for non-invasive quantification of IBD has been evaluated mainly in animal models[67]. The localization of the inflammatory process and the degree of tracer uptake are correlated with the endoscopic and histological findings. In the future, the method may be useful in determining the cause of pathological abdominopelvic tracer uptake, namely, inflammation *versus* malignancy. These are preliminary results that require further investigation in humans[67].

CONCLUSION

In this review, we have presented the role and the future prospects of nuclear medicine in IBD. Although it has no primary role in the diagnosis, it might be considered when colonoscopy is not completed successfully or other imaging modalities are negative. However, its contribution to the assessment of disease extent and activity, monitoring treatment response, and differentiating between active CD and UC is well established. Tc-99m HMPAO WBC have gain widespread clinical use while Tc-99m (V) DMSA seems to provide an accurate scintigraphic variant and a complementary technique to colonoscopy for follow-up and assessment of disease activity. The preliminary results on the role of F-18 FDG PET or PET/CT in the diagnosis and follow up of patients with IBD are encouraging. F-18 FDG WBC seem to be a promising future prospect, given that they can differentiate between the cause of pathological tracer uptake, namely, inflammation *versus* malignancy. Further investigation is essential in order to verify all the aforementioned favorable preliminary results.

REFERENCES

1 **Hommes DW**, van Deventer SJ. Endoscopy in inflammatory bowel diseases. *Gastroenterology* 2004; **126**: 1561-1573
2 **Martin-Comin J**, Prats E. Clinical applications of radiolabeled blood elements in inflammatory bowel disease. *Q J Nucl Med* 1999; **43**: 74-82
3 **Nikolaus S**, Schreiber S. Diagnostics of inflammatory bowel disease. *Gastroenterology* 2007; **133**: 1670-1689
4 **Albert JG**, Martiny F, Krummenerl A, Stock K, Lesske J, Göbel CM, Lotterer E, Nietsch HH, Behrmann C, Fleig WE. Diagnosis of small bowel Crohn's disease: a prospective comparison of capsule endoscopy with magnetic resonance imaging and fluoroscopic enteroclysis. *Gut* 2005; **54**: 1721-1727
5 **Toms AP**, Barltrop A, Freeman AH. A prospective randomised study comparing enteroclysis with small bowel follow-through examinations in 244 patients. *Eur Radiol* 2001; **11**: 1155-1160
6 **Ambrosini R**, Barchiesi A, Di Mizio V, Di Terlizzi M, Leo L, Filippone A, Canalis L, Fossaceca R, Carriero A.

Inflammatory chronic disease of the colon: how to image. *Eur J Radiol* 2007; **61**: 442-448
7 **Parente F**, Greco S, Molteni M, Anderloni A, Bianchi Porro G. Imaging inflammatory bowel disease using bowel ultrasound. *Eur J Gastroenterol Hepatol* 2005; **17**: 283-291
8 **Horsthuis K**, Bipat S, Bennink RJ, Stoker J. Inflammatory bowel disease diagnosed with US, MR, scintigraphy, and CT: meta-analysis of prospective studies. *Radiology* 2008; **247**: 64-79
9 **Madsen SM**, Thomsen HS, Munkholm P, Davidsen B, Dorph S, Nielsen SL, Schlichting P. Inflammatory bowel disease evaluated by low-field magnetic resonance imaging. Comparison with endoscopy, 99mTc-HMPAO leucocyte scintigraphy, conventional radiography and surgery. *Scand J Gastroenterol* 2002; **37**: 307-316
10 **Gan SI**, Beck PL. A new look at toxic megacolon: an update and review of incidence, etiology, pathogenesis, and management. *Am J Gastroenterol* 2003; **98**: 2363-2371
11 **Györke T**, Duffek L, Bártfai K, Makó E, Karlinger K, Mester A, Tarján Z. The role of nuclear medicine in inflammatory bowel disease. A review with experiences of aspecific bowel activity using immunoscintigraphy with 99mTc anti-granulocyte antibodies. *Eur J Radiol* 2000; **35**: 183-192
12 **Schölmerich J**, Schmidt E, Schümichen C, Billmann P, Schmidt H, Gerok W. Scintigraphic assessment of bowel involvement and disease activity in Crohn's disease using technetium 99m-hexamethyl propylene amine oxine as leukocyte label. *Gastroenterology* 1988; **95**: 1287-1293
13 **Giaffer MH**, Tindale WB, Holdsworth D. Value of technetium-99m HMPAO-labelled leucocyte scintigraphy as an initial screening test in patients suspected of having inflammatory bowel disease. *Eur J Gastroenterol Hepatol* 1996; **8**: 1195-1200
14 **Weldon MJ**, Lowe C, Joseph AE, Maxwell JD. Review article: quantitative leucocyte scanning in the assessment of inflammatory bowel disease activity and its response to therapy. *Aliment Pharmacol Ther* 1996; **10**: 123-132
15 **Lee BF**, Chiu NT, Wu DC, Tsai KB, Liu GC, Yu HS, Wang ST. Use of 99mTc (V) DMSA scintigraphy in the detection and localization of intestinal inflammation: comparison of findings and colonoscopy and biopsy. *Radiology* 2001; **220**: 381-385
16 **Koutroubakis IE**, Koukouraki SI, Dimoulios PD, Velidaki AA, Karkavitsas NS, Kouroumalis EA. Active inflammatory bowel disease: evaluation with 99mTc (V) DMSA scintigraphy. *Radiology* 2003; **229**: 70-74
17 **Stathaki MI**, Koutroubakis IE, Koukouraki SI, Karmiris KP, Moschandreas JA, Kouroumalis EA, Karkavitsas NS. Active inflammatory bowel disease: head-to-head comparison between 99mTc-hexamethylpropylene amine oxime white blood cells and 99mTc(V)-dimercaptosuccinic acid scintigraphy. *Nucl Med Commun* 2008; **29**: 27-32
18 **Neurath MF**, Vehling D, Schunk K, Holtmann M, Brockmann H, Helisch A, Orth T, Schreckenberger M, Galle PR, Bartenstein P. Noninvasive assessment of Crohn's disease activity: a comparison of 18F-fluorodeoxyglucose positron emission tomography, hydromagnetic resonance imaging, and granulocyte scintigraphy with labeled antibodies. *Am J Gastroenterol* 2002; **97**: 1978-1985
19 **Halpenny DF**, Burke JP, Lawlor GO, O'Connell M. Role of PET and combination PET/CT in the evaluation of patients with inflammatory bowel disease. *Inflamm Bowel Dis* 2009; Epub ahead of print
20 **Cheow HK**, Voutnis DD, Evans JW, Szczepura KR, Swift EA, Bird NJ, Ruparelia P, Solanki CK, Ballinger JR, Chilvers ER, Middleton SJ, Peters AM. Quantification of disease activity in patients undergoing leucocyte scintigraphy for suspected inflammatory bowel disease. *Eur J Nucl Med Mol Imaging* 2005; **32**: 329-337
21 **Peters AM**, Danpure HJ, Osman S, Hawker RJ, Henderson BL, Hodgson HJ, Kelly JD, Neirinckx RD, Lavender JP. Clinical experience with 99mTc-hexamethylpropylene-amineoxime for labelling leucocytes and imaging inflammation. *Lancet* 1986; **2**: 946-949
22 **Allan RA**, Sladen GE, Bassingham S, Lazarus C, Clarke SE, Fogelman I. Comparison of simultaneous 99mTc-HMPAO and 111In oxine labelled white cell scans in the assessment of inflammatory bowel disease. *Eur J Nucl Med* 1993; **20**: 195-200
23 **Sciarretta G**, Furno A, Mazzoni M, Basile C, Malaguti P. Technetium-99m hexamethyl propylene amine oxime granulocyte scintigraphy in Crohn's disease: diagnostic and clinical relevance. *Gut* 1993; **34**: 1364-1369
24 **Sans M**, Fuster D, Llach J, Lomeña F, Bordas JM, Herranz R, Piqué JM, Panés J. Optimization of technetium-99m-HMPAO leukocyte scintigraphy in evaluation of active inflammatory bowel disease. *Dig Dis Sci* 2000; **45**: 1828-1835
25 **Almer S**, Granerus G, Ström M, Olaison G, Bonnet J, Lémann M, Smedh K, Franzén L, Bertheau P, Cattan P, Rain JD, Modigliani R. Leukocyte scintigraphy compared to intraoperative small bowel enteroscopy and laparotomy findings in Crohn's disease. *Inflamm Bowel Dis* 2007; **13**: 164-174
26 **Kerry JE**, Marshall C, Griffiths PA, Scott BB, Griffiths G. White cell scanning for inflammatory bowel disease: are biochemical markers useful referral criteria? *Nucl Med Commun* 2003; **24**: 1145-1148
27 **Alonso JC**, Lopez-Longo FJ, Lampreave JL, González CM, Vegazo O, Carreño L, Almoguera I. Abdominal scintigraphy using 99mTc-HMPAO-labelled leucocytes in patients with seronegative spondylarthropathies without clinical evidence of inflammatory bowel disease. *Eur J Nucl Med* 1996; **23**: 243-246
28 **Alonso JC**, Soriano A, Rubio C, Cuadra JL, Zarca M, Guerra P, Garcia A, Molino C. Technetium-99m-HMPAO-labeled leukocyte imaging in patients with seronegative spondyloarthropathies. *J Nucl Med Technol* 1999; **27**: 204-206
29 **El Maghraoui A**, Dougados M, Freneaux E, Chaussade S, Amor B, Breban M. Concordance between abdominal scintigraphy using technetium-99m hexamethylpropylene amine oxime-labelled leucocytes and ileocolonoscopy in patients with spondyloarthropathies and without clinical evidence of inflammatory bowel disease. *Rheumatology* (Oxford) 1999; **38**: 543-546
30 **Biancone L**, Scopinaro F, Ierardi M, Paoluzi P, Marcheggiano A, Di Paolo MC, Porowska B, Colella AC, Pallone F. 99mTc-HMPAO granulocyte scintigraphy in the early detection of postoperative asymptomatic recurrence in Crohn's disease. *Dig Dis Sci* 1997; **42**: 1549-1556
31 **Weldon MJ**, Masoomi AM, Britten AJ, Gane J, Finlayson CJ, Joseph AE, Maxwell JD. Quantification of inflammatory bowel disease activity using technetium-99m HMPAO labelled leucocyte single photon emission computerised tomography (SPECT). *Gut* 1995; **36**: 243-250
32 **Biancone L**, Schillaci O, Capoccetti F, Bozzi RM, Fina D, Petruzziello C, Geremia A, Simonetti G, Pallone F. Technetium-99m-HMPAO labeled leukocyte single photon emission computerized tomography (SPECT) for assessing Crohn's disease extent and intestinal infiltration. *Am J Gastroenterol* 2005; **100**: 344-354
33 **Kolkman JJ**, Falke TH, Roos JC, Van Dijk DH, Bannink IM, Den Hollander W, Cuesta MA, Peña AS, Meuwissen SG. Computed tomography and granulocyte scintigraphy in active inflammatory bowel disease. Comparison with endoscopy and operative findings. *Dig Dis Sci* 1996; **41**: 641-650
34 **Molnár T**, Papós M, Gyulai C, Ambrus E, Kardos L, Nagy F, Palkó A, Pávics L, Lonovics J. Clinical value of technetium-99m-HMPAO-labeled leukocyte scintigraphy and spiral computed tomography in active Crohn's disease. *Am J Gastroenterol* 2001; **96**: 1517-1521
35 **Charron M**, Di Lorenzo C, Kocoshis S. CT and 99mTc-WBC vs colonoscopy in the evaluation of inflammation and complications of inflammatory bowel diseases. *J*

Gastroenterol 2002; **37**: 23-28
36 **Charron M**. Technetium leukocyte imaging in inflammatory bowel disease. *Curr Gastroenterol Rep* 1999; **1**: 245-252
37 **Alberini JL**, Badran A, Freneaux E, Hadji S, Kalifa G, Devaux JY, Dupont T. Technetium-99m HMPAO-labeled leukocyte imaging compared with endoscopy, ultrasonography, and contrast radiology in children with inflammatory bowel disease. *J Pediatr Gastroenterol Nutr* 2001; **32**: 278-286
38 **Cucchiara S**, Celentano L, de Magistris TM, Montisci A, Iula VD, Fecarotta S. Colonoscopy and technetium-99m white cell scan in children with suspected inflammatory bowel disease. *J Pediatr* 1999; **135**: 727-732
39 **Charron M**. Pediatric inflammatory bowel disease imaged with Tc-99m white blood cells. *Clin Nucl Med* 2000; **25**: 708-715
40 **Charron M**, del Rosario FJ, Kocoshis SA. Pediatric inflammatory bowel disease: assessment with scintigraphy with 99mTc white blood cells. *Radiology* 1999; **212**: 507-513
41 **Charron M**, del Rosario JF, Kocoshis S. Use of technetium-tagged white blood cells in patients with Crohn's disease and ulcerative colitis: is differential diagnosis possible? *Pediatr Radiol* 1998; **28**: 871-877
42 **Charron M**, Di Lorenzo C, Kocoshis S. Are 99mTc leukocyte scintigraphy and SBFT studies useful in children suspected of having inflammatory bowel disease? *Am J Gastroenterol* 2000; **95**: 1208-1212
43 **Mojiminiyi OA**, Udelsman R, Soper ND, Shepstone BJ, Dudley NE. Pentavalent Tc-99m DMSA scintigraphy. Prospective evaluation of its role in the management of patients with medullary carcinoma of the thyroid. *Clin Nucl Med* 1991; **16**: 259-262
44 **Ohta H**, Endo K, Fujita T, Nakajima T, Sakahara H, Torizuka K, Shimizu Y, Hata N, Masuda H, Horiuchi K. Imaging of soft tissue tumors with Tc(V)-99m dimercaptosuccinic acid. A new tumor-seeking agent. *Clin Nucl Med* 1984; **9**: 568-573
45 **Kobayashi H**, Kotoura Y, Hosono M, Sakahara H, Hosono M, Yao ZS, Tsuboyama T, Yamamuro T, Endo K, Konishi J. Diagnostic value of Tc-99m (V) DMSA for chondrogenic tumors with positive Tc-99m HMDP uptake on bone scintigraphy. *Clin Nucl Med* 1995; **20**: 361-364
46 **Banci M**, Bianchi PL, Gianni W, Romani AM, De Vincentis G, Ierardi M, Scopinaro F. Preliminary evaluation of the usefulness of Tc-99m (V) DMSA in pancreatic neuroendocrine tumors. *Clin Nucl Med* 1996; **21**: 122-124
47 **Kobayashi H**, Sakahara H, Hosono M, Shirato M, Endo K, Kotoura Y, Yamamuro T, Konishi J. Soft-tissue tumors: diagnosis with Tc-99m (V) dimercaptosuccinic acid scintigraphy. *Radiology* 1994; **190**: 277-280
48 **Lee BF**, Chiu NT, Chang JK, Liu GC, Yu HS. Technetium-99m(V)-DMSA and gallium-67 in the assessment of bone and joint infection. *J Nucl Med* 1998; **39**: 2128-2131
49 **Ercan MT**, Gülaldi NC, Unsal IS, Aydin M, Peksoy I, Hasçelik Z. Evaluation of Tc-99m(V) DMSA for imaging inflammatory lesions: an experimental study. *Ann Nucl Med* 1996; **10**: 419-423
50 **Mairal L**, de Lima PA, Martin-Comin J, Baliellas C, Xiol X, Roca M, Ricart Y, Ramos M. Simultaneous administration of 111In-human immunoglobulin and 99mTc-HMPAO labelled leucocytes in inflammatory bowel disease. *Eur J Nucl Med* 1995; **22**: 664-670
51 **Delgado Castro M**, Lancha C, Prats E, Mitjavilla M, Abós D, Martín-Curto LM, Crespo A, Banzo J. The diagnostic value of Tc-99m human polyclonal immunoglobulin imaging compared to Tc-99m HMPAO labeled leukocytes in inflammatory bowel disease. *Clin Nucl Med* 1997; **22**: 17-20
52 **Papos M**, Nagy F, Narai G, Rajtar M, Szantai G, Lang J, Csernay L. Anti-granulocyte immunoscintigraphy and [99mTc]hexamethylpropyleneamine-oxime-labeled leukocyte scintigraphy in inflammatory bowel disease. *Dig Dis Sci* 1996; **41**: 412-420
53 **Stokkel MP**, Reigman HE, Pauwels EK. Scintigraphic head-to-head comparison between 99mTc-WBCs and 99mTc-LeukoScan in the evaluation of inflammatory bowel disease: a pilot study. *Eur J Nucl Med Mol Imaging* 2002; **29**: 251-254
54 **Kapsoritakis AN**, Koutroubakis IE, Kouroumalis EA, Koukouraki SI, Karkavitsas N. (99m)Tc-Leucoscan in the evaluation of inflammatory bowel disease. *Eur J Nucl Med Mol Imaging* 2002; **29**: 1098
55 **Kerry JE**, Marshall C, Griffiths PA, James MW, Scott BB. Comparison between Tc-HMPAO labelled white cells and Tc LeukoScan in the investigation of inflammatory bowel disease. *Nucl Med Commun* 2005; **26**: 245-251
56 **Bruno I**, Martelossi S, Geatti O, Maggiore G, Guastalla P, Povolato M, Ventura A. Antigranulocyte monoclonal antibody immunoscintigraphy in inflammatory bowel disease in children and young adolescents. *Acta Paediatr* 2002; **91**: 1050-1055
57 **Charron M**, Di Lorenzo C, Kocoshis SA, Hickeson MP, Orenstein SR, Goyal A, Kahn S, Collins L. (99m)Tc antigranulocyte monoclonal antibody imaging for the detection and assessment of inflammatory bowel disease newly diagnosed by colonoscopy in children. *Pediatr Radiol* 2001; **31**: 796-800
58 **Hanna R**, Braun T, Levendel A, Lomas F. Radiochemistry and biostability of autologous leucocytes labelled with 99mTc-stannous colloid in whole blood. *Eur J Nucl Med* 1984; **9**: 216-219
59 **Peacock K**, Porn U, Howman-Giles R, O'Loughlin E, Uren R, Gaskin K, Dorney S, Kamath R. 99mTc-stannous colloid white cell scintigraphy in childhood inflammatory bowel disease. *J Nucl Med* 2004; **45**: 261-265
60 **Bhatti M**, Chapman P, Peters M, Haskard D, Hodgson HJ. Visualising E-selectin in the detection and evaluation of inflammatory bowel disease. *Gut* 1998; **43**: 40-47
61 **Bicik I**, Bauerfeind P, Breitbach T, von Schulthess GK, Fried M. Inflammatory bowel disease activity measured by positron-emission tomography. *Lancet* 1997; **350**: 262
62 **Lemberg DA**, Issenman RM, Cawdron R, Green T, Mernagh J, Skehan SJ, Nahmias C, Jacobson K. Positron emission tomography in the investigation of pediatric inflammatory bowel disease. *Inflamm Bowel Dis* 2005; **11**: 733-738
63 **Löffler M**, Weckesser M, Franzius C, Schober O, Zimmer KP. High diagnostic value of 18F-FDG-PET in pediatric patients with chronic inflammatory bowel disease. *Ann N Y Acad Sci* 2006; **1072**: 379-385
64 **Meisner RS**, Spier BJ, Einarsson S, Roberson EN, Perlman SB, Bianco JA, Taylor AJ, Einstein M, Jaskowiak CJ, Massoth KM, Reichelderfer M. Pilot study using PET/CT as a novel, noninvasive assessment of disease activity in inflammatory bowel disease. *Inflamm Bowel Dis* 2007; **13**: 993-1000
65 **Louis E**, Ancion G, Colard A, Spote V, Belaiche J, Hustinx R. Noninvasive assessment of Crohn's disease intestinal lesions with (18)F-FDG PET/CT. *J Nucl Med* 2007; **48**: 1053-1059
66 **Rubin DT**, Surma BL, Gavzy SJ, Schnell KM, Bunnag AP, Huo D, Appelbaum DE. Positron emission tomography (PET) used to image subclinical inflammation associated with ulcerative colitis (UC) in remission. *Inflamm Bowel Dis* 2009; **15**: 750-755
67 **Pio BS**, Byrne FR, Aranda R, Boulay G, Spicher K, Song MH, Birnbaumer L, Phelps ME, Czernin J, Silverman DH. Noninvasive quantification of bowel inflammation through positron emission tomography imaging of 2-deoxy-2-[18F]fluoro-D-glucose-labeled white blood cells. *Mol Imaging Biol* 2003; **5**: 271-277

S- Editor Li LF **L- Editor** Kerr C **E- Editor** Yin DH

Online Submissions: wjg.wjgnet.com
wjg@wjgnet.com
doi:10.3748/wjg.15.2701

World J Gastroenterol 2009 June 14; 15(22): 2701-2707
World Journal of Gastroenterology ISSN 1007-9327

REVIEW

Helicobacter pylori infection and endocrine disorders: Is there a link?

Konstantinos X Papamichael, Garyphallia Papaioannou, Helen Karga, Anastasios Roussos, Gerassimos J Mantzaris

Konstantinos X Papamichael, Anastasios Roussos, Gerassimos J Mantzaris, First Department of Gastroenterology, Evaggelismos Hospital, Kolonaki-10676 Athens, Greece
Garyphallia Papaioannou, Helen Karga, B' Department of Endocrinology, Alexandra Hospital, Vas. Sofias & Lourou-115 28 Athens, Greece
Author contributions: Papamichael KX, Mantzaris GJ and Karga H wrote the paper; Papaioannou G and Roussos A undertook the acquisition, analysis and interpretation of the data.
Correspondence to: Konstantinos X Papamichael, MD, PhD, First Department of Gastroenterology, Evaggelismos Hospital, 45-47 Ypsilantou street, Kolonaki-10676 Athens, Greece. kpapamdoc@yahoo.gr
Telephone: +30-210-7201609 Fax: +30-210-7239716
Received: March 23, 2009 Revised: May 13, 2009
Accepted: May 20, 2009
Published online: June 14, 2009

Abstract

Helicobacter pylori (*H pylori*) infection is a leading world-wide infectious disease as it affects more than half of the world population and causes chronic gastritis, peptic ulcer disease and gastric malignancies. The infection elicits a chronic cellular inflammatory response in the gastric mucosa. However, the effects of this local inflammation may not be confined solely to the digestive tract but may spread to involve extra-intestinal tissues and/or organs. Indeed, *H pylori* infection has been epidemiologically linked to extra-digestive conditions and diseases. In this context, it has been speculated that *H pylori* infection may be responsible for various endocrine disorders, such as autoimmune thyroid diseases, diabetes mellitus, dyslipidemia, obesity, osteoporosis and primary hyperparathyroidism. This is a review of the relationship between *H pylori* infection and these endocrine disorders.

Key words: *Helicobacter pylori*; Hormones; Thyroid; Osteoporosis; Diabetes; Dyslipidemia

Peer reviewer: Dr. Katsunori lijima, Division of Gastroenterology, Tohoku University Graduate School of Medicine, 1-1 Seiryo-machi, Aobaku., Sendai 980-8574, Japan

Papamichael KX, Papaioannou G, Karga H, Roussos A, Mantzaris GJ. *Helicobacter pylori* infection and endocrine disorders: Is there a link? *World J Gastroenterol* 2009; 15(22): 2701-2707 Available from: URL: http://www.wjgnet.com/1007-9327/15/2701.asp DOI: http://dx.doi.org/10.3748/wjg.15.2701

INTRODUCTION

Helicobacter pylori (*H pylori*) is a gram-negative, spiral-shaped pathogenic bacterium that specifically colonizes the gastric epithelium and causes chronic gastritis, peptic ulcer disease and/or gastric malignancies[1,2]. The infection induces an acute polymorphonuclear infiltration in the gastric mucosa. If the infection is not effectively cleared, this acute cellular infiltrate is gradually replaced by an immunologically-mediated, chronic, predominantly mononuclear cellular infiltrate[3]. The latter is characterized by the local production and systemic diffusion of pro-inflammatory cytokines[4], which may exert their effect in remote tissues and organic systems[5]. As a result, *H pylori* infection has been epidemiologically linked to some extra-digestive conditions, including endocrine disorders (Table 1), although there are contradictory data regarding the relationship between *H pylori* infection and these diseases.

H pylori AND DIABETES MELLITUS

The relationship between diabetes mellitus (DM) and *H pylori* infection is controversial. According to some studies there is a high prevalence of *H pylori* infection in patients with either type I [6-9] or type II DM[10-13] which is correlated with the duration of DM[7,9], the presence of dyspeptic symptoms[13,14] and cardiovascular autonomic neuropathy[13,15], age[6,8], gender[16], body mass index (BMI)[16], blood pressure[16], fasting glucose[16] and the HbA1c levels[16]. In particular, the prevalence of *H pylori* infection was found to be higher in obese, female, middle-aged patients with a long standing DM, dyspeptic symptoms, cardiovascular autonomic neuropathy and increased blood pressure, fasting glucose levels and HbA1c values[6-9,13-16]. This could be related to a reduced gastric motility and peristaltic activity[10], various chemical changes in gastric mucosa following non-enzymatic glycosylation processes[10] and an impaired non-specific immunity observed in diabetic patients[11].

In contrast, other studies showed that *H pylori* infection is not associated with DM, as there is no

difference in the prevalence of *H pylori* infection between diabetics and non-diabetics[17], regardless of the type[8,17-22] and duration of DM[18,19,22] and/or severity of dyspeptic symptoms in patients with DM[22]. The presence of micro-angiopathy in patients with DM may be a negative factor for colonization by *H pylori*, because micro-vascular changes in the gastric mucosa may create an unfavourable environment for the establishment or survival of *H pylori*[16]. Interestingly, one study even showed a lower sero-prevalence of *H pylori* in patients with DM, in comparison with the healthy population[23], while another showed a significantly lower incidence of *H pylori* infection in diabetics with active duodenal ulceration, as compared with non-diabetics[24].

The relationship between gastrointestinal symptoms in DM and *H pylori* infection is also controversial. According to some studies, there is no difference between diabetics and non-diabetics concerning the prevalence of *H pylori*-related gastro-duodenal disorders[17]. Moreover, *H pylori* infection was not associated with either delayed gastric emptying[9,25] or upper gastrointestinal symptoms in DM[19,21,25]. On the other hand, a high prevalence of esophagitis and peptic ulcer was found in *H pylori*+ve patients with DM, with or without dyspepsia, especially those with cardiovascular autonomic neuropathy[13,15] suggesting that this population should be considered as "high risk" for *H pylori* infection and suitable candidates for treatment[12]. In addition, some data demonstrated a higher prevalence of *H pylori* infection in diabetic patients with dyspepsia[14,26], reactive gastritis[27] and chronic gastritis[26] compared to those with no signs or symptoms of gastrointestinal disease.

The relationship between DM complications and *H pylori* infection is another issue which is contentious and deserves further investigation, as only few data are available. According to some data there is no relationship between *H pylori* infection and diabetic complications, such as nephropathy[13], retinopathy[13], and/or micro-angiopathy[16] while other data shows that virulent strains of *H pylori*, such as cytotoxin-associated gene $CagA^+$, are associated with macro-angiopathy[16], neuropathy[16] and micro-albuminuria in type Ⅱ diabetic patients, maybe due to an immuno-mediated injury at the level of the endothelium, caused by a systemic immune response to the infection, leading to albumin leakage[28]. Additionally, some data indicate a possible association of *H pylori* infection and the development of coronary heart disease, thrombo-occlusive cerebral disease, or both, in diabetic patients[29].

One point on which all studies seem to converge is that the effectiveness of eradication regimens for *H pylori* infection is significantly lower in diabetics than in non-diabetics[20,30-32] whereas re-infection rates seem to be higher, especially in patients with type Ⅱ DM compared to the general population[20,31]. This may be due to changes in the gastric microvasculature leading to reduced absorption of antibiotics. Alternatively, frequent antibiotic use in diabetics may result in the development of resistant *H pylori* strains[30,32]. Moreover, type I diabetic patients achieve lower *H pylori* eradication rates on standard triple therapy than non-insulin-dependent diabetic subjects, regardless of the dosage and/or the duration of therapy[20,31,32], and higher re-infection rates one year after eradication of *H pylori* compared with control subjects[33]. Quadruple therapies seem to cure a large percentage of patients who fail first-line therapy, although this is accompanied by a greater incidence of minor side effects[20,31]. These data suggest that vaccine development seems to be the only effective long term treatment for patients with DM[20].

Noteworthy is the observation that children with type I DM and *H pylori* infection had an increased daily insulin requirement compared with their uninfected peers[34]. Finally, several issues, such as the role of *H pylori* in etiopathogenesis of DM and the influence of *H pylori* eradication on the control of DM, remain to be elucidated.

Table 1 Endocrine disorders in relationship with *H pylori* infection

Endocrine disorders
Autoimmune thyroid diseases
Autoimmune atrophic thyroiditis
Hashimoto's thyroiditis
Thyroid mucosal associated lymphocyte tissue (MALT) lymphoma
Diabetes mellitus
Dyslipidemia
Obesity
Osteoporosis
Primary hyperparathyroidism

H pylori AND OSTEOPOROSIS

There are limited data regarding the association between *H pylori* infection and osteoporosis. According to one study, *H pylori* infection was not accompanied by significant changes in levels of markers of bone metabolism in children, such as estradiol, parathyroid hormone (PTH), cross-linked collagen I carboxy terminal telopeptide, total alkaline phosphatase (ALP), bone-specific ALP, N-terminal cross-links of human pro-collagen type I , osteocalcin, calcium and phosphate[35]. In another study, infection by $CagA^+$ *H pylori* strains was more prevalent in men with osteoporosis compared to the general population, who showed reduced systemic levels of estrogens and increased bone turnover[36]. *H pylori* infection by $CagA^+$ strains may therefore be considered a risk factor for osteoporosis in men[36]. Further studies are required to clarify the relationship between *H pylori* infection and osteoporosis and whether *H pylori* infection causes time-dependent changes in bone turnover markers during the long course of this chronic inflammatory disease.

H pylori AND HYPERPARATHYROIDISM

There are only a few studies attempting to clarify the association between *H pylori* infection and hyperparathyroidism. In fact, only one study showed that *H pylori* infection was more prevalent amongst patients with primary hyperparathyroidism (PHPT) than in the

general population, suggesting that patients with PHPT, and especially those with dyspeptic symptoms, should be evaluated for *H pylori* infection and treated appropriately if positive[37]. Also, a case report described an association of PHPT with duodenal ulcer and *H pylori* infection[38]. On the other hand, another study claimed no significant relationship between parathyroid abnormalities and *H pylori* infection in haemodialysis patients and this study found that a longer period of dialysis therapy was related to a decreased ability of these patients to produce antibodies against *H pylori*[39].

H pylori AND OBESITY

The relationship between obesity and *H pylori* infection is controversial. According to some studies, the risk of *H pylori* infection does not increase in overweight young persons[40] and *H pylori* seropositivity or CagA antibody status are not associated with the BMI[41,42] or fasting serum leptin levels[41]. Furthermore, one study indicated an inverse relationship between morbid obesity and *H pylori* seropositivity, leading to the hypothesis that the absence of *H pylori* infection during childhood may enhance the risk of the development of morbid obesity[43]. In contrast, other studies showed that obesity[10] and/or an elevation of the BMI[44] may be associated with an increased incidence of *H pylori* colonization, probably as a result of reduced gastric motility[10]. In addition, the incidence of *H pylori* infection in patients undergoing Roux-en-Y gastric bypass surgery for morbid obesity was higher than that found in all patients undergoing endoscopies and biopsy, even though the incidence of infection was not higher in controls matched for age[45].

The relationship between obesity and *H pylori* eradication is also controversial. There are data which demonstrate that eradication of *H pylori* significantly increases the incidence of obesity in patients with peptic ulcer disease, since it increases the level of BMI[46,47], and/or enhances the appetite of asymptomatic patients, due to an elevation of plasma ghrelin[48] and a reduction of leptin levels[49,50]. In fact, *H pylori* infection caused a marked reduction in plasma levels of ghrelin[44,49,51-53], as a result of a negative effect of this infection on the density of gastric ghrelin-positive cells[51,54] and an increase in plasma levels of leptin and gastrin[49,55,56]. Since ghrelin exerts orexigenic and adipogenic effects in contrast to leptin which exerts anorexigenic effects[52], alterations in plasma levels of gastric originated appetite-controlling hormones in children and adults infected by *H pylori* may contribute to chronic dyspepsia and loss of appetite[49]. Consequently, *H pylori* can be a "protective" factor against the development of becoming overweight[50]. In contrast, other studies showed that there are no differences in plasma ghrelin levels between *H pylori*+ve and *H pylori*-ve patients matched for age and BMI[57] and that successful eradication of *H pylori* had no effect on plasma ghrelin levels[44,57].

H pylori AND THYROID DISEASES

There have been controversial reports linking *H pylori* infection to thyroid disorders including autoimmune thyroid disorders (ATD) such as autoimmune atrophic thyroiditis[58] and Hashimoto's thyroiditis[59], or thyroid mucosal associated lymphocyte tissue (MALT) lymphoma[60].

Thus, some studies have reported an increased prevalence of *H pylori* infection in adults[58,61,62] and children[63] with ATD and a relationship between *H pylori* infection and the presence of high titers of thyroid auto-antibodies, such as anti-thyroglobulin (anti-Tg) and anti-thyroperoxidase (anti-TPO) antibodies[58,61,62] resulting in abnormalities of gastric secretory function[58]. It has also been suggested that CagA$^+$ *H pylori* strains increase the risk for ATD, especially in women, and that they are involved in the pathogenesis of Hashimoto's thyroiditis. This is based on the detection of monoclonal antibodies against Cag-A$^+$ *H pylori* strains which cross-react with follicular cells of the thyroid gland and also on the fact that *H pylori* strains possessing the Cag-A pathogenicity island carry a gene encoding for an endogenous peroxidase[61]. Moreover, the strong correlation between IgG anti-*H pylori* antibodies and thyroid auto-antibodies, as well as the observation that eradication of *H pylori* infection is followed by a gradual decrease in the levels of thyroid auto-antibodies[64], suggest that *H pylori* antigens might be involved in the development of autoimmune atrophic thyroiditis or that autoimmune function in this disease may increase the likelihood of *H pylori* infection[58]. One study showed a significant decrease of Free-T_3 and Free-T_4 in *H pylori*+ve subjects compared to *H pylori*-ve controls[62].

On the contrary, other studies showed no differences in the serum levels of thyroid hormones or thyroid auto-antibodies in patients with and without *H pylori* infection[59,65] whereas *H pylori* infection seemed not to increase the risk of ATD in individuals with dyspeptic symptoms[65]. Taking these results into account, it was proposed that screening for ATD in patients with a positive urea breath test is not indicated[65]. Other studies have failed to show any correlation between *H pylori* infection and ATD in children[66]. Moreover, the similar prevalence of *H pylori* infection, with or without CagA$^+$ strains, in patients with Hashimoto's thyroiditis and controls argues against a true association between *H pylori* infection and Hashimoto's thyroiditis[59]. To further explore the relationship between ATD and *H pylori* infection more clinical trials are required.

Lymphoid follicles in the gastric mucosa are common in ATD, and *H pylori* infection plays a causative role[67]. When an autoimmune disease such as ATD coexists with *H pylori* infection[68], *H pylori* may be involved in the pathogenesis of extra-gastric MALT lymphomas, such as thyroid MALT lymphoma, as shown by a case report describing a primary thyroid MALT lymphoma which occurred in an *H pylori*+ve patient with gastric cancer and Hashimoto's thyroiditis[60]. In this case, after subtotal gastrectomy, the thyroid lymphoma became smaller transiently and when the patient was treated with *H pylori* eradication therapy, the lymphoma completely disappeared. Nevertheless, *H pylori* organisms were not detected in the thyroid lymphoma tissue by polymerase

chain reaction (PCR), questioning the role of *H pylori* in the development of extra-gastric MALT lymphoma in patients with an autoimmune disease[60]. In addition, one study suggested that patients with an autoimmune disease might not be optimal candidates for *H pylori* eradication, even in the case of an early stage gastric MALT lymphoma, since very few of these patients responded to an *H pylori* eradication therapy[68].

On the other hand, it is important to realize that patients with *H pylori*-related gastritis, atrophic gastritis, or both conditions required increased daily doses of T_4 than controls, suggesting that normal gastric acid secretion is necessary for effective absorption of oral T_4[69]. In addition, development of *H pylori* infection in patients treated with T_4 led to an increased serum level of thyrotropin (TSH), an effect that was nearly reversed after eradication of *H pylori* infection[69].

H pylori AND DYSLIPIDEMIA

H pylori infection may cause dyslipidemia, as it leads to elevated levels of total cholesterol[70,71], low-density lipoprotein cholesterol (LDL-c)[71,72], lipoprotein Lp(a)[71], apolipoprotein apo-B[73], triglyceride concentrations[72,74,75] and decreased levels of high-density lipoprotein cholesterol (HDL-c)[73-78] and apolipoprotein apoA-1 concentration in the blood[73,75]. In addition, plasma levels of cholesterol and LDL-c were significantly higher in *H pylori*+ve patients with ischemic stroke compared to *H pylori*-ve patients[70]. It was postulated that chronic *H pylori* infection may shift lipid profiles towards an atherogenic direction *via* the action of pro-inflammatory cytokines, such as interleukins 1 and 6 (IL-1 and IL-6), interferon-α (INF-α) and tumour necrosis factor-α (TNF-α). These cytokines are capable of affecting lipid metabolism in different ways, including activation of adipose tissue lipoprotein lipase, stimulation of hepatic fatty acid synthesis and influencing lipolysis[71,79]. This atherogenic modified lipid profile created by *H pylori* infection may increase the risk for cardiovascular and cerebrovascular diseases, by participating in the process of atherogenesis, especially when Cag-A^+ cytotoxic strains of *H pylori* are present[80,81], although other studies do not support this hypothesis[71,82,83].

According to other studies, *H pylori* infection did not cause any significant changes in plasma levels of total cholesterol[78,84], triglycerides[78,84], LDL-c[78,84] and Apo-B[78,85].

The relationship between dyslipidemia and *H pylori* eradication is also controversial. After one year of eradication of *H pylori* in patients with duodenal ulcers, a significant increase of HDL-c, apo-AI and apo-AII levels was observed in the study by Scharnagl *et al*[86]. Moreover, eradication of *H pylori* in healthy subjects seems to increase HDL-c and decrease LDL-c levels[78]. Also, 6 mo following successful eradication of *H pylori* infection the plasma levels of total cholesterol and LDL-c were found to be significantly lower than those in *H pylori*+ve controls and *H pylori*+ve patients with stroke[70].

In contrast, one study showed that eradication of *H pylori* is associated with minor lipid changes[84], while others showed a significant increase in the incidence of hyperlipidemia in patients with peptic ulcer disease, as serum total cholesterol and triglycerides were elevated in these patients after eradication of *H pylori*[46,47,87].

Table 2 Endocrine disorders and eradication of *H pylori*

Endocrine disorders	*H pylori* eradication
Autoimmune thyroid diseases	↓ of thyroid auto-antibodies[64] ↓ of thyrotropin in *H pylori*+ve patients treated with T4[69]
Diabetes mellitus	↓ in diabetics more than in non-diabetics[20,30-32] ↓ in type I diabetic patients on standard triple therapy more than non-insulin dependent diabetic subjects, regardless of the dosage and/or the duration of therapy[20,31,32]
Dyslipidemia	↑ of HDL-c, apo-AI and apo-AII levels in patients with duodenal ulcers, after 1 year[86] ↑ of HDL-c and ↓ LDL-c levels in healthy subjects[78] ↓ of total cholesterol and LDL-c after 6 mo in *H pylori*+ve controls and *H pylori*+ve patients with stroke[70] ↔ of lipids in patients submitted for endoscopy[84] ↑ of total cholesterol and triglycerides in patients with peptic ulcer disease[46,47] or without[87]
Obesity	↑ of BMI in patients with peptic ulcer disease[46,47] ↑ of the appetite of asymptomatic patients, due to ↑ of plasma ghrelin[48] and ↓ of leptin levels[49,50] ↔ of plasma ghrelin levels in subjects referred for upper gastrointestinal endoscopy[44,57]

BMI: Body mass index; HDL-c: High-density lipoprotein cholesterol; apo-AI: Apolipoprotein AI; apo-AII: Apolipoprotein AII; LDL-c: Low-density lipoprotein cholesterol; +ve: Positive.

CONCLUSION

Since the discovery of *H pylori*, a variety of studies, essentially epidemiological or therapeutic trials, case reports and others, have evaluated the potential direct or indirect involvement of this bacterium in the pathogenesis of various extra-gastric diseases or disorders, amongst them disorders of the endocrine system. A critical review of data published on these proposed associations suggests a strong link between dyslipidemia and *H pylori* infection, whereas increasing evidence emerges on the role of *H pylori* infection in thyroid autoimmune diseases. On the contrary, the association between *H pylori* infection and obesity, PHPT, DM and osteoporosis remains controversial, as evidence is hindered by the small numbers and methodological problems. Therefore, these associations should be interpreted cautiously. Although some evidence suggests that eradication of *H pylori* may lead to an improvement of many endocrine disorders, such as DM, dyslipidemia and autoimmune thyroid disease, excluding obesity (Table 2), more clinical trials are needed in order to confirm this beneficial effect. In conclusion, the causal association between *H pylori* infection and endocrine disorders is still controversial but worthy of further investigation since these diseases affect many people and have a great impact on human health and health economics[88].

REFERENCES

1 **Wotherspoon AC**, Ortiz-Hidalgo C, Falzon MR, Isaacson PG. Helicobacter pylori-associated gastritis and primary B-cell gastric lymphoma. *Lancet* 1991; **338**: 1175-1176
2 **Parsonnet J**. Helicobacter pylori and gastric cancer. *Gastroenterol Clin North Am* 1993; **22**: 89-104
3 **Graham DY**, Osato MS, Olson CA, Zhang J, Figura N. Effect of H. pylori infection and CagA status on leukocyte counts and liver function tests: extra-gastric manifestations of H. pylori infection. *Helicobacter* 1998; **3**: 174-178
4 **Perri F**, Clemente R, Festa V, De Ambrosio CC, Quitadamo M, Fusillo M, Grossi E, Andriulli A. Serum tumour necrosis factor-alpha is increased in patients with Helicobacter pylori infection and CagA antibodies. *Ital J Gastroenterol Hepatol* 1999; **31**: 290-294
5 **Patel P**, Mendall MA, Khulusi S, Northfield TC, Strachan DP. Helicobacter pylori infection in childhood: risk factors and effect on growth. *BMJ* 1994; **309**: 1119-1123
6 **Oldenburg B**, Diepersloot RJ, Hoekstra JB. High seroprevalence of Helicobacter pylori in diabetes mellitus patients. *Dig Dis Sci* 1996; **41**: 458-461
7 **Gasbarrini A**, Ojetti V, Pitocco D, De Luca A, Franceschi F, Candelli M, Sanz Torre E, Pola P, Ghirlanda G, Gasbarrini G. Helicobacter pylori infection in patients affected by insulin-dependent diabetes mellitus. *Eur J Gastroenterol Hepatol* 1998; **10**: 469-472
8 **Salardi S**, Cacciari E, Menegatti M, Landi F, Mazzanti L, Stella FA, Pirazzoli P, Vaira D. Helicobacter pylori and type 1 diabetes mellitus in children. *J Pediatr Gastroenterol Nutr* 1999; **28**: 307-309
9 **Arslan D**, Kendirci M, Kurtoglu S, Kula M. Helicobacter pylori infection in children with insulin dependent diabetes mellitus. *J Pediatr Endocrinol Metab* 2000; **13**: 553-556
10 **Perdichizzi G**, Bottari M, Pallio S, Fera MT, Carbone M, Barresi G. Gastric infection by Helicobacter pylori and antral gastritis in hyperglycemic obese and in diabetic subjects. *New Microbiol* 1996; **19**: 149-154
11 **Senturk O**, Canturk Z, Cetinarslan B, Ercin C, Hulagu S, Canturk NZ. Prevalence and comparisons of five different diagnostic methods for Helicobacter pylori in diabetic patients. *Endocr Res* 2001; **27**: 179-189
12 **Quatrini M**, Boarino V, Ghidoni A, Baldassarri AR, Bianchi PA, Bardella MT. Helicobacter pylori prevalence in patients with diabetes and its relationship to dyspeptic symptoms. *J Clin Gastroenterol* 2001; **32**: 215-217
13 **Gulcelik NE**, Kaya E, Demirbas B, Culha C, Koc G, Ozkaya M, Cakal E, Serter R, Aral Y. Helicobacter pylori prevalence in diabetic patients and its relationship with dyspepsia and autonomic neuropathy. *J Endocrinol Invest* 2005; **28**: 214-217
14 **Gentile S**, Turco S, Oliviero B, Torella R. The role of autonomic neuropathy as a risk factor of Helicobacter pylori infection in dyspeptic patients with type 2 diabetes mellitus. *Diabetes Res Clin Pract* 1998; **42**: 41-48
15 **Persico M**, Suozzo R, De Seta M, Montella F, Torella R, Gentile S. Non-ulcer dyspepsia and Helicobacter pylori in type 2 diabetic patients: association with autonomic neuropathy. *Diabetes Res Clin Pract* 1996; **31**: 87-92
16 **Quadri R**, Rossi C, Catalfamo E, Masoero G, Lombardo L, Della Monica P, Rovera L, Pera A, Cavello Perin P. Helicobacter pylori infection in type 2 diabetic patients. *Nutr Metab Cardiovasc Dis* 2000; **10**: 263-266
17 **Anastasios R**, Goritsas C, Papamihail C, Trigidou R, Garzonis P, Ferti A. Helicobacter pylori infection in diabetic patients: prevalence and endoscopic findings. *Eur J Intern Med* 2002; **13**: 376
18 **Kozak R**, Juhasz E, Horvat G, Harcsa E, Lovei L, Sike R, Szele K. [Helicobacter pylori infection in diabetic patients] *Orv Hetil* 1999; **140**: 993-995
19 **Ko GT**, Chan FK, Chan WB, Sung JJ, Tsoi CL, To KF, Lai CW, Cockram CS. Helicobacter pylori infection in Chinese subjects with type 2 diabetes. *Endocr Res* 2001; **27**: 171-177
20 **Ojetti V**, Pitocco D, Ghirlanda G, Gasbarrini G, Gasbarrini A. [Role of Helicobacter pylori infection in insulin-dependent diabetes mellitus] *Minerva Med* 2001; **92**: 137-144
21 **Xia HH**, Talley NJ, Kam EP, Young LJ, Hammer J, Horowitz M. Helicobacter pylori infection is not associated with diabetes mellitus, nor with upper gastrointestinal symptoms in diabetes mellitus. *Am J Gastroenterol* 2001; **96**: 1039-1046
22 **Stanciu OG**, Trifan A, Sfarti C, Cojocariu C, Stanciu C. Helicobacter pylori infection in patients with diabetes mellitus. *Rev Med Chir Soc Med Nat Iasi* 2003; **107**: 59-65
23 **Zelenkova J**, Souckova A, Kvapil M, Soucek A, Vejvalka J, Segethova J. [Helicobacter pylori and diabetes mellitus] *Cas Lek Cesk* 2002; **141**: 575-577
24 **Kojecky V**, Roubalik J, Bartonikova N. [Helicobacter pylori in patients with diabetes mellitus] *Vnitr Lek* 1993; **39**: 581-584
25 **Jones KL**, Wishart JM, Berry M, Russo A, Xia HH, Talley NJ, Horowitz M. Helicobacter pylori infection is not associated with delayed gastric emptying or upper gastrointestinal symptoms in diabetes mellitus. *Dig Dis Sci* 2002; **47**: 704-709
26 **Marrollo M**, Latella G, Melideo D, Storelli E, Iannarelli R, Stornelli P, Valenti M, Caprilli R. Increased prevalence of Helicobacter pylori in patients with diabetes mellitus. *Dig Liver Dis* 2001; **33**: 21-29
27 **Malecki M**, Bien AI, Galicka-Latala D, Klupa T, Stachura J, Sieradzki J. [Reactive gastritis in patients with diabetics with dyspeptic symptoms] *Przegl Lek* 1996; **53**: 540-543
28 **Pietroiusti A**, Giuliano M, Magrini A, Bergamaschi A, Galante A. Cytotoxin-associated gene A strains of Helicobacter pylori represent a risk factor for the development of microalbuminuria in type 2 diabetes. *Diabetes Care* 2006; **29**: 1399-1401
29 **de Luis DA**, Lahera M, Canton R, Boixeda D, San Roman AL, Aller R, de La Calle H. Association of Helicobacter pylori infection with cardiovascular and cerebrovascular disease in diabetic patients. *Diabetes Care* 1998; **21**: 1129-1132
30 **Gasbarrini A**, Ojetti V, Pitocco D, Franceschi F, Candelli M, Torre ES, Gabrielli M, Cammarota G, Armuzzi A, Pola R, Pola P, Ghirlanda G, Gasbarrini G. Insulin-dependent diabetes mellitus affects eradication rate of Helicobacter pylori infection. *Eur J Gastroenterol Hepatol* 1999; **11**: 713-716
31 **Gasbarrini A**, Ojetti V, Pitocco D, Armuzzi A, Silveri NG, Pola P, Ghirlanda G, Gasbarrini G. Efficacy of different Helicobacter pylori eradication regimens in patients affected by insulin-dependent diabetes mellitus. *Scand J Gastroenterol* 2000; **35**: 260-263
32 **Sargyn M**, Uygur-Bayramicli O, Sargyn H, Orbay E, Yavuzer D, Yayla A. Type 2 diabetes mellitus affects eradication rate of Helicobacter pylori. *World J Gastroenterol* 2003; **9**: 1126-1128
33 **Ojetti V**, Pitocco D, Bartolozzi F, Danese S, Migneco A, Lupascu A, Pola P, Ghirlanda G, Gasbarrini G, Gasbarrini A. High rate of helicobacter pylori re-infection in patients affected by type 1 diabetes. *Diabetes Care* 2002; **25**: 1485
34 **Begue RE**, Mirza A, Compton T, Gomez R, Vargas A. Helicobacter pylori infection and insulin requirement among children with type 1 diabetes mellitus. *Pediatrics* 1999; **103**: e83
35 **Ozdem S**, Akcam M, Yilmaz A, Gultekin M, Artan R. Biochemical markers of bone metabolism in children with Helicobacter pylori infection. *Dig Dis Sci* 2007; **52**: 967-972
36 **Figura N**, Gennari L, Merlotti D, Lenzi C, Campagna S, Franci B, Lucani B, Trabalzini L, Bianciardi L, Gonnelli C, Santucci A, Nut A. Prevalence of Helicobacter pylori infection in male patients with osteoporosis and controls. *Dig Dis Sci* 2005; **50**: 847-852
37 **Dokmetas HS**, Turkay C, Aydin C, Arici S. Prevalence of Helicobacter pylori in patients with primary hyperparathyroidism. *J Bone Miner Metab* 2001; **19**: 373-377
38 **Sato H**, Abe K, Oshima N, Kawashima K, Hamamoto N, Moritani M, Mak R, Ishihara S, Adachi K, Kawauchi H, Kinoshita Y. Primary hyperparathyroidism with duodenal ulcer and H. pylori infection. *Intern Med* 2002; **41**: 377-380

39 **Bednarek-Skublewska A**, Schabowski J, Majdan M, Baranowicz-Gaszczyk I, Ksiazek A. [Relationships between hyperparathyroidism and Helicobacter pylori infection in long-term hemodialysis patients] *Pol Arch Med Wewn* 2001; **105**: 191-196

40 **Kyriazanos ID**, Sfiniadakis I, Gizaris V, Hountis P, Hatziveis K, Dafnopoulou A, Datsakis K. The incidence of Helicobacter pylori infection is not increased among obese young individuals in Greece. *J Clin Gastroenterol* 2002; **34**: 541-546

41 **Ioannou GN**, Weiss NS, Kearney DJ. Is Helicobacter pylori seropositivity related to body mass index in the United States? *Aliment Pharmacol Ther* 2005; **21**: 765-772

42 **Cho I**, Blaser MJ, Francois F, Mathew JP, Ye XY, Goldberg JD, Bini EJ. Helicobacter pylori and overweight status in the United States: data from the Third National Health and Nutrition Examination Survey. *Am J Epidemiol* 2005; **162**: 579-584

43 **Wu MS**, Lee WJ, Wang HH, Huang SP, Lin JT. A case-control study of association of Helicobacter pylori infection with morbid obesity in Taiwan. *Arch Intern Med* 2005; **165**: 1552-1555

44 **Isomoto H**, Ueno H, Nishi Y, Wen CY, Nakazato M, Kohno S. Impact of Helicobacter pylori infection on ghrelin and various neuroendocrine hormones in plasma. *World J Gastroenterol* 2005; **11**: 1644-1648

45 **Renshaw AA**, Rabaza JR, Gonzalez AM, Verdeja JC. Helicobacter pylori infection in patients undergoing gastric bypass surgery for morbid obesity. *Obes Surg* 2001; **11**: 281-283

46 **Fujiwara Y**, Higuchi K, Arafa UA, Uchida T, Tominaga K, Watanabe T, Arakawa T. Long-term effect of Helicobacter pylori eradication on quality of life, body mass index, and newly developed diseases in Japanese patients with peptic ulcer disease. *Hepatogastroenterology* 2002; **49**: 1298-1302

47 **Kamada T**, Hata J, Kusunoki H, Ito M, Tanaka S, Kawamura Y, Chayama K, Haruma K. Eradication of Helicobacter pylori increases the incidence of hyperlipidaemia and obesity in peptic ulcer patients. *Dig Liver Dis* 2005; **37**: 39-43

48 **Nwokolo CU**, Freshwater DA, O'Hare P, Randeva HS. Plasma ghrelin following cure of Helicobacter pylori. *Gut* 2003; **52**: 637-640

49 **Konturek PC**, Czesnikiewicz-Guzik M, Bielanski W, Konturek SJ. Involvement of Helicobacter pylori infection in neuro-hormonal control of food intake. *J Physiol Pharmacol* 2006; **57** Suppl 5: 67-81

50 **Loffeld RJ**. Helicobacter pylori, obesity and gastro-oesophageal reflux disease. Is there a relation? A personal view. *Neth J Med* 2005; **63**: 344-347

51 **Tatsuguchi A**, Miyake K, Gudis K, Futagami S, Tsukui T, Wada K, Kishida T, Fukuda Y, Sugisaki Y, Sakamoto C. Effect of Helicobacter pylori infection on ghrelin expression in human gastric mucosa. *Am J Gastroenterol* 2004; **99**: 2121-2127

52 **Shiotani A**, Miyanishi T, Uedo N, Iishi H. Helicobacter pylori infection is associated with reduced circulating ghrelin levels independent of body mass index. *Helicobacter* 2005; **10**: 373-378

53 **Osawa H**, Nakazato M, Date Y, Kita H, Ohnishi H, Ueno H, Shiiya T, Satoh K, Ishino Y, Sugano K. Impaired production of gastric ghrelin in chronic gastritis associated with Helicobacter pylori. *J Clin Endocrinol Metab* 2005; **90**: 10-16

54 **Liew PL**, Lee WJ, Lee YC, Chen WY. Gastric ghrelin expression associated with Helicobacter pylori infection and chronic gastritis in obese patients. *Obes Surg* 2006; **16**: 612-619

55 **Azuma T**, Suto H, Ito Y, Ohtani M, Dojo M, Kuriyama M, Kato T. Gastric leptin and Helicobacter pylori infection. *Gut* 2001; **49**: 324-329

56 **Nishi Y**, Isomoto H, Uotani S, Wen CY, Shikuwa S, Ohnita K, Mizuta Y, Kawaguchi A, Inoue K, Kohno S. Enhanced production of leptin in gastric fundic mucosa with Helicobacter pylori infection. *World J Gastroenterol* 2005; **11**: 695-699

57 **Gokcel A**, Gumurdulu Y, Kayaselcuk F, Serin E, Ozer B, Ozsahin AK, Guvener N. Helicobacter pylori has no effect on plasma ghrelin levels. *Eur J Endocrinol* 2003; **148**: 423-426

58 **de Luis DA**, Varela C, de La Calle H, Canton R, de Argila CM, San Roman AL, Boixeda D. Helicobacter pylori infection is markedly increased in patients with autoimmune atrophic thyroiditis. *J Clin Gastroenterol* 1998; **26**: 259-263

59 **Franceschi F**, Satta MA, Mentella MC, Penland R, Candelli M, Grillo RL, Leo D, Fini L, Nista EC, Cazzato IA, Lupascu A, Pola P, Pontecorvi A, Gasbarrini G, Genta RM, Gasbarrini A. Helicobacter pylori infection in patients with Hashimoto's thyroiditis. *Helicobacter* 2004; **9**: 369

60 **Arima N**, Tsudo M. Extragastric mucosa-associated lymphoid tissue lymphoma showing the regression by Helicobacter pylori eradication therapy. *Br J Haematol* 2003; **120**: 790-792

61 **Figura N**, Di Cairano G, Lore F, Guarino E, Gragnoli A, Cataldo D, Giannace R, Vaira D, Bianciardi L, Kristodhullu S, Lenzi C, Torricelli V, Orlandini G, Gennari C. The infection by Helicobacter pylori strains expressing CagA is highly prevalent in women with autoimmune thyroid disorders. *J Physiol Pharmacol* 1999; **50**: 817-826

62 **Triantafillidis JK**, Georgakopoulos D, Gikas A, Merikas E, Peros G, Sofroniadou K, Cheracakis P, Sklavaina M, Tzanidis G, Konstantellou E. Relation between Helicobacter pylori infection, thyroid hormone levels and cardiovascular risk factors on blood donors. *Hepatogastroenterology* 2003; **50** Suppl 2: cccxviii-ccccccxx

63 **Larizza D**, Calcaterra V, Martinetti M, Negrini R, De Silvestri A, Cisternino M, Iannone AM, Solcia E. Helicobacter pylori infection and autoimmune thyroid disease in young patients: the disadvantage of carrying the human leukocyte antigen-DRB1*0301 allele. *J Clin Endocrinol Metab* 2006; **91**: 176-179

64 **Bertalot G**, Montresor G, Tampieri M, Spasiano A, Pedroni M, Milanesi B, Favret M, Manca N, Negrini R. Decrease in thyroid autoantibodies after eradication of Helicobacter pylori infection. *Clin Endocrinol* (Oxf) 2004; **61**: 650-652

65 **Tomasi PA**, Dore MP, Fanciulli G, Sanciu F, Realdi G, Delitala G. Is there anything to the reported association between Helicobacter pylori infection and autoimmune thyroiditis? *Dig Dis Sci* 2005; **50**: 385-388

66 **Novikova VP**, Iur'ev VV, Tkachenko EI, Strukov EL, Liubimov IuA, Antonov PV. [Chronic gastritis in children with concomitant diseases of the thyroid gland] *Eksp Klin Gastroenterol* 2003; 40-43, 114

67 **Cammarota G**, De Marinis AT, Papa A, Valle D, Cuoco L, Cianci R, Fedeli G, Gasbarrini G. Gastric mucosa-associated lymphoid tissue in autoimmune thyroid diseases. *Scand J Gastroenterol* 1997; **32**: 869-872

68 **Raderer M**, Osterreicher C, Machold K, Formanek M, Fiebiger W, Penz M, Dragosics B, Chott A. Impaired response of gastric MALT-lymphoma to Helicobacter pylori eradication in patients with autoimmune disease. *Ann Oncol* 2001; **12**: 937-939

69 **Centanni M**, Gargano L, Canettieri G, Viceconti N, Franchi A, Delle Fave G, Annibale B. Thyroxine in goiter, Helicobacter pylori infection, and chronic gastritis. *N Engl J Med* 2006; **354**: 1787-1795

70 **Majka J**, Rog T, Konturek PC, Konturek SJ, Bielanski W, Kowalsky M, Szczudlik A. Influence of chronic Helicobacter pylori infection on ischemic cerebral stroke risk factors. *Med Sci Monit* 2002; **8**: CR675-CR684

71 **Chimienti G**, Russo F, Lamanuzzi BL, Nardulli M, Messa C, Di Leo A, Correale M, Giannuzzi V, Pepe G. Helicobacter pylori is associated with modified lipid profile: impact on Lipoprotein(a). *Clin Biochem* 2003; **36**: 359-365

72 **Laurila A**, Bloigu A, Nayha S, Hassi J, Leinonen M, Saikku P. Association of Helicobacter pylori infection with elevated serum lipids. *Atherosclerosis* 1999; **142**: 207-210

73 **Hoffmeister A**, Rothenbacher D, Bode G, Persson K, Marz W, Nauck MA, Brenner H, Hombach V, Koenig W. Current infection with Helicobacter pylori, but not seropositivity to Chlamydia pneumoniae or cytomegalovirus, is associated with an atherogenic, modified lipid profile. *Arterioscler Thromb Vasc Biol* 2001; **21**: 427-432

74 **Solcia E**, Fiocca R, Luinetti O, Villani L, Padovan L, Calistri D, Ranzani GN, Chiaravalli A, Capella C. Intestinal and diffuse gastric cancers arise in a different background of Helicobacter pylori gastritis through different gene involvement. *Am J Surg Pathol* 1996; **20** Suppl 1: S8-S22

75 **Niemela S**, Karttunen T, Korhonen T, Laara E, Karttunen R, Ikaheimo M, Kesaniemi YA. Could Helicobacter pylori infection increase the risk of coronary heart disease by modifying serum lipid concentrations? *Heart* 1996; **75**: 573-575

76 **Danesh J**, Peto R. Risk factors for coronary heart disease and infection with Helicobacter pylori: meta-analysis of 18 studies. *BMJ* 1998; **316**: 1130-1132

77 **Takashima T**, Adachi K, Kawamura A, Yuki M, Fujishiro H, Rumi MA, Ishihara S, Watanabe M, Kinoshita Y. Cardiovascular risk factors in subjects with Helicobacter pylori infection. *Helicobacter* 2002; **7**: 86-90

78 **Ando T**, Minami M, Ishiguro K, Maeda O, Watanabe O, Mizuno T, Fujita T, Takahashi H, Noshiro M, Goto H. Changes in biochemical parameters related to atherosclerosis after Helicobacter pylori eradication. *Aliment Pharmacol Ther* 2006; **24** Suppl 4: 58-64

79 **Feingold KR**, Grunfeld C. Role of cytokines in inducing hyperlipidemia. *Diabetes* 1992; **41** Suppl 2: 97-101

80 **Pieniazek P**, Karczewska E, Duda A, Tracz W, Pasowicz M, Konturek SJ. Association of Helicobacter pylori infection with coronary heart disease. *J Physiol Pharmacol* 1999; **50**: 743-751

81 **Kowalski M**. Helicobacter pylori (H. pylori) infection in coronary artery disease: influence of H. pylori eradication on coronary artery lumen after percutaneous transluminal coronary angioplasty. The detection of H. pylori specific DNA in human coronary atherosclerotic plaque. *J Physiol Pharmacol* 2001; **52**: 3-31

82 **Fraser AG**, Scragg RK, Cox B, Jackson RT. Helicobacter pylori, Chlamydia pneumoniae and myocardial infarction. *Intern Med J* 2003; **33**: 267-272

83 **Al-Nozha MM**, Khalil MZ, Al-Mofleh IA, Al-Ghamdi AS. Lack of association of coronary artery disease with H.pylori infection. *Saudi Med J* 2003; **24**: 1370-1373

84 **Elizalde JI**, Pique JM, Moreno V, Morillas JD, Elizalde I, Bujanda L, De Argila CM, Cosme A, Castiella A, Ros E. Influence of Helicobacter pylori infection and eradication on blood lipids and fibrinogen. *Aliment Pharmacol Ther* 2002; **16**: 577-586

85 **Adiloglu AK**, Can R, Kinay O, Aridogan BC. Infection with Chlamydia pneumoniae but not Helicobacter pylori is related to elevated apolipoprotein B levels. *Acta Cardiol* 2005; **60**: 599-604

86 **Scharnagl H**, Kist M, Grawitz AB, Koenig W, Wieland H, Marz W. Effect of Helicobacter pylori eradication on high-density lipoprotein cholesterol. *Am J Cardiol* 2004; **93**: 219-220

87 **Furuta T**, Shirai N, Xiao F, Takashima M, Hanai H. Effect of Helicobacter pylori infection and its eradication on nutrition. *Aliment Pharmacol Ther* 2002; **16**: 799-806

88 **Figura N**, Piomboni P, Ponzetto A, Gambera L, Lenzi C, Vaira D, Peris C, Lotano MR, Gennari L, Bianciardi L, Renieri T, Valensin PE, Capitani S, Moretti E, Colapinto R, Baccetti B, Gennari C. Helicobacter pylori infection and infertility. *Eur J Gastroenterol Hepatol* 2002; **14**: 663-669

S- Editor Tian L **L- Editor** Logan S **E- Editor** Ma WH

Online Submissions: wjg.wjgnet.com
wjg@wjgnet.com
doi:10.3748/wjg.15.2708

World J Gastroenterol 2009 June 14; 15(22): 2708-2713
World Journal of Gastroenterology ISSN 1007-9327

ORIGINAL ARTICLES

Size does not determine the grade of malignancy of early invasive colorectal cancer

Takahisa Matsuda, Yutaka Saito, Takahiro Fujii, Toshio Uraoka, Takeshi Nakajima, Nozomu Kobayashi, Fabian Emura, Akiko Ono, Tadakazu Shimoda, Hiroaki Ikematsu, Kuang-I Fu, Yasushi Sano, Takahiro Fujimori

Takahisa Matsuda, Yutaka Saito, Takahiro Fujii, Toshio Uraoka, Takeshi Nakajima, Nozomu Kobayashi, Fabian Emura, Akiko Ono, Endoscopy Division, National Cancer Center Hospital, Tokyo 104-0045, Japan
Tadakazu Shimoda, Clinical Laboratory Division, National Cancer Center Hospital, Tokyo 104-0045, Japan
Hiroaki Ikematsu, Kuang-I Fu, Yasushi Sano, Division of Digestive Endoscopy and Gastrointestinal Oncology, National Cancer Center Hospital East, Kashiwa 277-8577, Japan
Takahiro Fujimori, Department of Surgical and Molecular Pathology, Dokkyo University School of Medicine, Shimotsuga, Tochigi 321-0293, Japan
Author contributions: Matsuda T, Saito Y and Fujii T contributed equally to this work; Matsuda T, Uraoka T, Nakajima T and Kobayashi N designed the research; Matsuda T, Ikematsu H, Fu KI and Sano Y performed the research; Shimoda T and Fujimori T performed the histopathology; Matsuda T, Saito Y, Emura F and Ono A wrote the paper.
Correspondence to: Takahisa Matsuda, MD, Endoscopy Division, National Cancer Center Hospital, 5-1-1 Tsukiji, Chuo-ku, Tokyo 104-0045, Japan. tamatsud@ncc.go.jp
Telephone: +81-3-35422511 Fax: +81-3-35423815
Received: February 24, 2009 Revised: April 15, 2009
Accepted: April 22, 2009
Published online: June 14, 2009

Abstract

AIM: To clarify the clinicopathological characteristics of small and large early invasive colorectal cancers (EI-CRCs), and to determine whether malignancy grade depends on size.

METHODS: A total of 583 consecutive EI-CRCs treated by endoscopic mucosal resection or surgery at the National Cancer Center Hospital between 1980 and 2004 were enrolled in this study. Lesions were classified into two groups based on size: small (≤ 10 mm) and large (> 10 mm). Clinicopathological features, incidence of lymph node metastasis (LNM) and risk factors for LNM, such as depth of invasion, lymphovascular invasion (LVI) and poorly differentiated adenocarcinoma (PDA) were analyzed in all resected specimens.

RESULTS: There were 120 (21%) small and 463 (79%) large lesions. Histopathological analysis of the small lesion group revealed submucosal deep cancer (sm: ≥ 1000 μm) in 90 (75%) cases, LVI in 26 (22%) cases, and PDA in 12 (10%) cases. Similarly, the large lesion group exhibited submucosal deep cancer in 380 (82%) cases, LVI in 125 (27%) cases, and PDA in 79 (17%) cases. The rate of LNM was 11.2% and 12.1% in the small and large lesion groups, respectively.

CONCLUSION: Small EI-CRC demonstrated the same aggressiveness and malignant potential as large cancer.

Key words: Colorectal cancer; Submucosal invasion; Lymph node metastasis; Endoscopic mucosal resection

Peer reviewers: Peter L Lakatos, MD, PhD, Assistant Professor, 1st Department of Medicine, Semmelweis University, Koranyi S 2A, Budapest H1083, Hungary; Javier San Martín, Chief, Gastroenterology and Endoscopy, Sanatorio Cantegril, Av. Roosevelt y P 13, Punta del Este 20100, Uruguay

Matsuda T, Saito Y, Fujii T, Uraoka T, Nakajima T, Kobayashi N, Emura F, Ono A, Shimoda T, Ikematsu H, Fu KI, Sano Y, Fujimori T. Size does not determine the grade of malignancy of early invasive colorectal cancer. *World J Gastroenterol* 2009; 15(22): 2708-2713 Available from: URL: http://www.wjgnet.com/1007-9327/15/2708.asp DOI: http://dx.doi.org/10.3748/wjg.15.2708

INTRODUCTION

Colorectal cancer (CRC) is the third most important cause of cancer mortality in Japan, and its incidence is gradually increasing. To reduce CRC mortality, early detection and appropriate treatment are required. In general, small lesions are suspected of having a lower malignant potential than large ones, and hence are easy to remove endoscopically. Several authors have reported that the malignant potential of early invasive colorectal cancer (EI-CRC) increases with lesion size[1-3]. Therefore, lesion size is considered to be indicative of the depth of invasion and presence of lymph node metastasis (LNM). In contrast, flat, and in particular depressed lesions, are considered to have a tendency to invade rapidly the submucosal layer, even when small[4-6]. However, clinicopathological features of small EI-CRCs have still

not been studied extensively.

The aim of this retrospective study was to clarify the clinicopathological characteristics of small and large EI-CRCs and their implications for endoscopic treatment.

MATERIALS AND METHODS

Subjects

Five hundred and eighty-three patients (374 male and 209 female) with EI-CRC that had been resected surgically or endoscopically at the National Cancer Center Hospital, between January 1980 and January 2004, were examined retrospectively. In all of these patients, cancer cells invaded through the muscularis mucosa into the submucosal layer but did not extend deeply into the muscularis propria. Eligibility also required the lesions to be macroscopically non-pedunculated (sessile, flat and depressed). Patients with synchronous advanced CRC, multiple EI-CRCs, inflammatory bowel disease, hereditary non-polyposis colorectal cancer and familial adenomatous polyposis were excluded from the study.

Methods

All lesions were classified into two groups according to their endoscopic image size: small (≤ 10 mm) and large (> 10 mm). Furthermore, lesions were classified into three categories (sessile, 0- Ⅰs, Ⅰs+Ⅱa; flat, 0-Ⅱa; and depressed, 0-Ⅱc, Ⅱa+Ⅱc, Ⅰs+Ⅱc) according to the Paris classification[7]. Clinicopathological features, incidence of LNM and risk factors for LNM, such as depth of invasion, lymphovascular invasion (LVI) and poorly differentiated adenocarcinoma (PDA) were analyzed in all resected specimens.

Histopathology

Resected specimens were fixed in 10% formalin and examined histopathologically following hematoxylin and eosin staining. Histopathological diagnosis was based on the World Health Organization (WHO) criteria[8]. Submucosal invasion was measured from the muscularis mucosa to the deepest portion. When the muscularis mucosa could not be identified because of cancer invasion, the vertical length was measured from the surface of the lesion to the deepest portion according to Kitajima's classification[9]. Tumors with a vertical length of < 1000 μm in the submucosal layer were classified as submucosal superficial invasive cancers (sm-superficial), and lesions with a length ≥ 1000 μm were classified as submucosal deep invasive cancers (sm-deep). The tumor growth patterns were histopathologically divided into polypoid growth (PG) and non-polypoid growth (NPG) types. Shimoda *et al*[10] have reported polyp cancers with protrusions caused by intramucosal proliferation of the carcinoma or coexistent adenoma that behaved as PG type carcinoma, while flat/depressed type carcinoma without polypoid proliferation of intramucosal tumor behaved as NPG type carcinoma.

Statistical analysis

The significance of differences in proportions was assessed by the χ^2 test, Fisher's exact test and the Wilcoxon matched-pairs signed-ranks test using SPSS statistical software (SPSS for Windows , version 16.0J, Tokyo, Japan). Statistical significance was defined as $P < 0.05$.

RESULTS

A total of 583 EI-CRCs were retrospectively evaluated, with 120 (21%) small and 463 (79%) large lesions identified (Table 1). The gender ratio (male/female) was 2.4 and 1.7, and the mean age was 61.5 and 62.4 years in the small and large lesion groups, respectively. Mean size of the small and large lesions was 8.3 and 22.1 mm, respectively.

Macroscopic type, growth type and location

Macroscopic assessment of small lesions identified 51 cases as sessile (42%), 14 as flat (12%), and 55 as depressed (46%). Similarly, large lesion groups comprised 233 sessile (50%), 64 flat (14%), and 166 depressed (36%) type. PG types were identified in 32% (38/120) and 54% (250/463) of small and large lesions, respectively. In contrast, the prevalence of NPG type in the small lesion group was significantly higher than in the large lesion group (68% *vs* 46%, $P < 0.0001$). Regarding tumor location, there were 33 (27%) rectal, 56 (47%) distal colon and 31 (26%) proximal colon cancers in the small lesion group. In contrast, there were 213 (46%) rectal, 139 (30%) distal colon and 111 (24%) proximal cancers in the large lesion group. The incidence of rectal cancer in the large lesion group was significantly higher than in the small lesion group ($P = 0.02$).

LNM

Among the lesions treated surgically, the incidence of LNM was 11.2% (10/89) and 12.1% (46/381) in small and large lesion groups, respectively ($P = 0.85$) (Table 2).

Depth of invasion/LVI/PDA

Histopathological analysis of the small lesion group revealed sm-deep cancer in 90 (75%) cases, LVI in 26 (22%) and PDA in 12 (10%). Similarly, the large lesion group exhibited sm-deep cancer in 380 (82%) cases, LVI in 125 (27%), and PDA in 79 (17%). Therefore, in relation to depth of invasion, LVI and PDA, there were no significant differences between the groups.

Treatment strategy

Among the small lesion group, 62 (52%) cases were initially treated with endoscopic mucosal resection (EMR), while 58 (48%) cases were surgically resected. In contrast, among the large lesion group, 133 (29%) cases were initially treated with EMR, while 330 (71%) cases were surgically resected. Among all lesions treated by EMR, there were no differences in the rate of positive and unknown vertical and/or lateral cut margins in the small (18%, 11/62) and large lesion groups (20%, 26/133). Furthermore, among all positive cut margin cases in the small and large lesion groups, there were 11 (100%) and 18 (69%) positive vertical margin cases (Table 3, Figures 1 and 2).

Table 1 Comparison of clinicopathological and endoscopic characteristics for 583 study cases

	Small (≤ 10 mm)	Large (> 10 mm)	*P* value
No. of lesions, *n* (%)	120 (21)	463 (79)	
Gender (M/F)	85/35	289/174	0.09
Age (yr), mean (range)	61.5 (39-84)	62.4 (30-90)	0.86
Macroscopic type, *n* (%)			
Sessile (0-Ⅰs, Ⅰs+Ⅱa)	51 (42)	233 (50)	0.13
Flat (0-Ⅱa)	14 (12)	64 (14)	
Depressed (0-Ⅱc, Ⅱa+Ⅱc, Ⅰs+Ⅱc)	55 (46)	166 (36)	
Size (mm), mean ± SD	8.3 ± 1.6	22.1 ± 9.6	
Growth pattern (PG/NPG)	38/82	250/213	< 0.0001
Location, *n* (%)			
Rectum	33 (27)	213 (46)	0.02
Distal colon[1]	56 (47)	139 (30)	
Proximal colon[2]	31 (26)	111 (24)	

[1]Descending-sigmoid colon; [2]Cecum-transverse colon.

Table 3 Comparison of treatment strategy and positive rate of cut margin *n* (%)

	Small (≤ 10 mm)	Large (> 10 mm)	*P* value
Initial treatment			
EMR	62 (52)	133 (29)	< 0.0001
Surgery	58 (48)	330 (71)	
Positive rate of cut margin[1]	11 (18)	26 (20)	0.81
In EMR cases			
Lateral	0 (0)	8 (31)	0.08
Vertical	11 (100)	18 (69)	

[1]Positive and unknown cut margin. EMR: Endoscopic mucosal resection.

According to the initial treatment, there were 134 (69%) and 336 (87%) sm-deep cancers in the EMR and surgery groups, respectively. Furthermore, there were 33 (17%) and 118 (30%) LVI-positive, and 18 (9%) and 73 (19%) PDA-positive cases in the EMR and surgery groups, respectively. There were 37 (19%) positive cut margin cases, including 29 (78%) positive vertical margins in the EMR group. In contrast, there were no positive cut margin cases in the surgery group. In the EMR group, 82 (42%) patients underwent additional surgery with LN dissection after EMR within 6 mo. The incidence of LNM was 11.0% (9/82) and 12.1% (47/388) in the EMR and surgery groups, respectively ($P = 0.79$) (Table 4).

DISCUSSION

Several authors have reported a strong association between lesion size and submucosal invasion or risk of LNM when referring to the grade of malignancy of early CRC. Large lesion size has been considered an indicator of deep submucosal invasion and presence of LNM. However, in this large retrospective study, small EI-CRC demonstrated a similar aggressive behavior and malignant potential to those of large lesions, with a similar risk of LNM , LVI and PDA among both groups.

Intramucosal CRC is thought generally to have no potential for LNM. In contrast, it has been reported that

Table 2 Incidence of LNM and clinicopathological characteristics based on tumor size *n* (%)

	Small (≤ 10 mm)	Large (> 10 mm)	*P* value
LNM	10/89 (11.2)	46/381 (12.1)	0.85
Depth of invasion			
sm-superficial (< 1000 μm)	30 (25)	83 (18)	0.08
sm-deep (≥ 1000 μm)	90 (75)	380 (82)	
LVI	26 (22)	125 (27)	0.23
PDA	12 (10)	79 (17)	0.06

LVI: Lymphovascular invasion; PDA: Poorly differentiated adenocarcinoma; LNM: Lymph node metastasis.

Table 4 Comparison of clinicopathological characteristics and incidence of LNM based on the treatment strategy *n* (%)

	EMR (*n* = 195)	Surgery (*n* = 388)	*P* value
Depth of invasion			
sm-superficial (< 1000 μm)	61 (32)	52 (13)	< 0.0001
sm-deep (≥ 1000 μm)	134 (69)	336 (87)	
LVI	33 (17)	118 (30)	0.0006
PDA	18 (9)	73 (19)	0.0006
Positive rate of cut margin[1]	37 (19)	0 (0)	< 0.0001
Lateral	8 (22)	0 (0)	
Vertical	29 (78)	0 (0)	
Additional surgical operation	82 (42)	-	
LNM	9/82 (11.0)	47/388 (12.1)	0.79

[1]Positive and unknown cut margin.

LNM occurs in 6%-13% of patients with submucosal invasive CRC[11-15]. Therefore, radical surgery with LN dissection is recommended strongly in these cases. At present, EMR provides an endoscopic cure of early stage CRC when there is no risk of LNM. Advances in endoscopic instruments and techniques have increased the detection rates of early stage CRC and have expanded the indications for EMR[16].

In the past 20 years, many investigators have proposed the following histopathological criteria when considering additional surgery after EMR of submucosal cancers: massive submucosal invasion (≥ 1000 μm), and/or LVI, and/or PDA[17-22]. Among these factors, LVI and PDA are impossible to predict before resection. At this point, it is crucial to predict the vertical depth of invasion of submucosal cancers prior to EMR. In our center, we use routinely a magnifying colonoscope to decide on the adequate treatment of early stage CRC. Magnifying chromoendoscopy (MCE) is a standardized validated method that facilitates detailed analysis of the morphological architecture of colonic mucosal crypt orifices (pit pattern), in a simple and rapid manner. We have reported previously the efficacy of MCE to diagnose an invasive pattern as a typical finding of sm-deep cancers, and have demonstrated that it provides a good correlation between pit pattern and tumor depth in flat and depressed CRC[23-27].

Many authors have reported that depressed and/or NPG type lesions are considered to have a high malignant potential, compared to the polypoid type lesions of similar

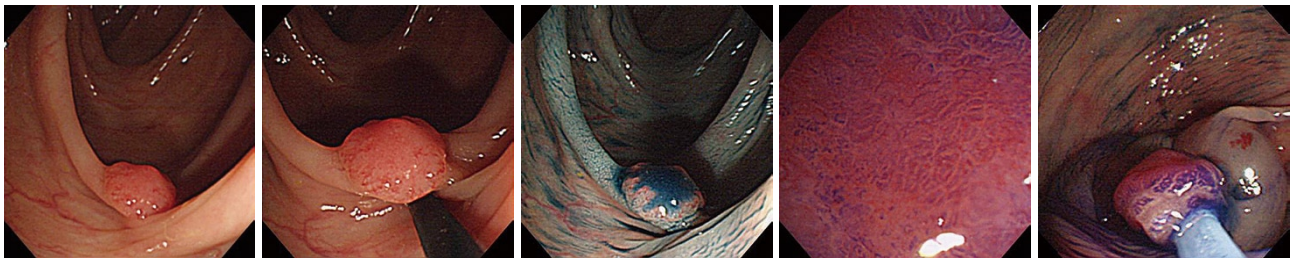

Figure 1 The lesion was located in the transverse colon. Endoscopic examination revealed a flat, elevated lesion with a central depression, which was macroscopically diagnosed as 0-Ⅱa+Ⅱc. The high-magnification view revealed a typical type Ⅵ pit (invasive) pattern on the depressed margin. The final endoscopic diagnosis was a 0-Ⅱa+Ⅱc type early colon cancer with submucosal deep invasion. However, patient strongly hoped EMR as an initial treatment. We performed EMR after injecting normal saline into the submucosa.

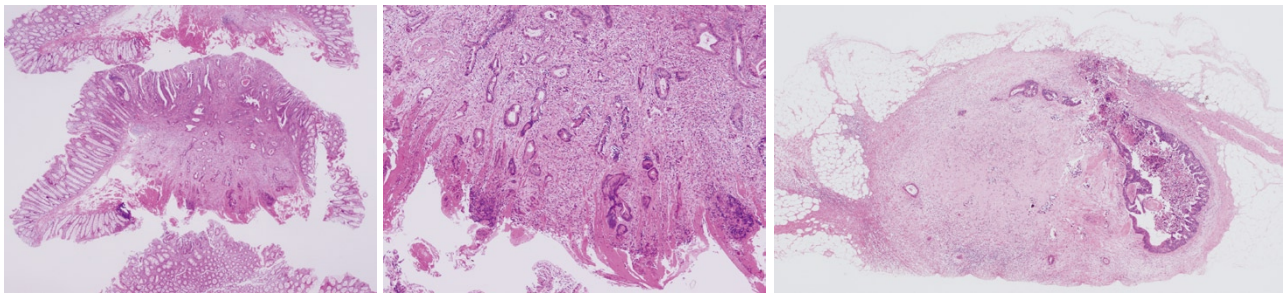

Figure 2 The final histopathological diagnosis was early invasive colon cancer, well-differentiated adenocarcinoma, sm-deep, NPG type, ly (-), v (-), cut end (+) (vertical margin positive). Since cancer was exposed in the vertical cut margin, additional surgical resection was performed and LNM was detected.

size[4,28-31]. Kurisu *et al*[20] have investigated the development and progression of EI-CRC. In that study, NPG lesions were significantly smaller in size (14.2 mm *vs* 24.2 mm) but showed deeper infiltration than PG types. They concluded that tumor development and the degree of invasion differed significantly between the two types of carcinoma. On the other hand, non-polypoid colorectal neoplasms (NP-CRNs) have been reported recently in the United States. Soetikno *et al*[31] have reported the prevalence of NP-CRNs in a veterans' hospital population. The overall prevalence of NP-CRNs and NP-CRNs with in situ or submucosal invasive carcinoma was 9.35% and 0.82%, respectively. They also concluded that NP-CRNs were more likely to contain carcinoma (OR: 9.78) than polypoid lesions, regardless of size. In the present study, small EI-CRCs ≤ 10 mm in diameter showed a significantly higher incidence of NPG type lesions than in the large lesion group ($P < 0.0001$). However, there was no significant difference in proportion of the macroscopic type between the groups ($P = 0.13$). Among the lesions diagnosed as Is type (sessile) in the small lesions group, 47% (14/30) were classified as NPG type histopathologically. From these results, we conclude that further investigation is required to confirm the growth pattern, especially for small sessile lesions diagnosed during colonoscopy.

In contrast, the rate of EMR as an initial treatment was 33% (195/583) in our study. In particular, it was significantly higher in the small lesion than the large lesion group (52% *vs* 29%, $P < 0.0001$). Among the 195 lesions removed by EMR as an initial treatment in both groups, 61 cases (32%) were sm-superficial cancers. On the other hand, there was no significant difference in the positive rate of cut margins between the small and large lesion groups (18% *vs* 20%). This result implies that EMR should not be performed readily for EI-CRC, from the viewpoint of no-touch isolation[32] and EMR complications. Intramucosal lesions (adenoma or intramucosal cancer) are usually well lifted by submucosal injection. In contrast, invasive cancer, especially sm-deep cancer, cannot be lifted because of the presence of submucosal fibrosis or desmoplastic reaction. Uno *et al*[33] have reported this phenomenon as the "non-lifting sign". Kobayashi *et al*[34] have reported, among 271 colorectal neoplastic lesions, that the non-lifting sign of deeper infiltration had a sensitivity of 61.5%, specificity of 98.4%, and accuracy of 94.8%. In contrast, endoscopic diagnosis had a sensitivity of 84.6%, specificity of 98.8%, and accuracy of 97.4%, with statistically significant differences in terms of sensitivity and accuracy. Furthermore, since submucosal injection varies depending on the expertise of the endoscopist, we consider that an endoscopic diagnosis is much more important and accurate when endoscopic resection is considered as the therapeutic option.

There are some limitations to this study. Firstly, this was a single-center study, and although the number of examined EI-CRCs was adequate, a multicenter analysis should be performed to clarify the clinical importance of small EI-CRCs. In addition, this study was carried out retrospectively between 1980 and 2004. In relation to endoscopic treatment for early CRC, endoscopic submucosal dissection (ESD) technique and Glycerol/Sodium hyaluronate as an injected solution during EMR has made progress recently[35,36]. In particular, ESD provides not only an *en bloc* large specimen but also

negative lateral and vertical cut margins.

In conclusion, with regard to the risk of LNM, small EI-CRCs demonstrate the same aggressiveness and malignant potential as large lesions. Moreover, from the perspective of the concept of no-touch isolation, therapeutic cost, and complications during EMR, special attention must be paid when treating even small early stage lesions, especially NPG type lesions.

COMMENTS

Background

In general, small colorectal lesions are suspected of having a lower malignant potential than large ones, and hence are easy to remove endoscopically. Several authors have reported that the malignant potential of early invasive colorectal cancer (EI-CRC) increases with lesion size.

Research frontiers

The aim of this retrospective study was to clarify the clinicopathological characteristics of small (≤ 10 mm) and large (> 10 mm) EI-CRCs.

Innovations and breakthroughs

A total of 583 EI-CRCs were evaluated retrospectively, with 120 (21%) small and 463 (79%) large lesions identified. With regard to the risk of lymph-node metastasis (LNM), small EI-CRCs demonstrate the same aggressiveness and malignant potential as large lesions.

Peer review

The authors examined retrospectively a large group of patients with EI-CRCs gathered over 20 years in a national cancer hospital, and demonstrated that small EI-CRCs (≤ 10 mm) had the same aggressiveness and malignant potential as large cancers. Special attention must be paid when treating even small lesions.

REFERENCES

1 **Tanaka S**, Yokota T, Saito D, Okamoto S, Oguro Y, Yoshida S. Clinicopathologic features of early rectal carcinoma and indications for endoscopic treatment. *Dis Colon Rectum* 1995; **38**: 959-963

2 **Saito Y**, Fujii T, Kondo H, Mukai H, Yokota T, Kozu T, Saito D. Endoscopic treatment for laterally spreading tumors in the colon. *Endoscopy* 2001; **33**: 682-686

3 **Uraoka T**, Saito Y, Matsuda T, Ikehara H, Gotoda T, Saito D, Fujii T. Endoscopic indications for endoscopic mucosal resection of laterally spreading tumours in the colorectum. *Gut* 2006; **55**: 1592-1597

4 **Kudo S**, Kashida H, Tamura T, Kogure E, Imai Y, Yamano H, Hart AR. Colonoscopic diagnosis and management of nonpolypoid early colorectal cancer. *World J Surg* 2000; **24**: 1081-1090

5 **Hurlstone DP**, Cross SS, Adam I, Shorthouse AJ, Brown S, Sanders DS, Lobo AJ. A prospective clinicopathological and endoscopic evaluation of flat and depressed colorectal lesions in the United Kingdom. *Am J Gastroenterol* 2003; **98**: 2543-2549

6 **Soetikno R**, Friedland S, Kaltenbach T, Chayama K, Tanaka S. Nonpolypoid (flat and depressed) colorectal neoplasms. *Gastroenterology* 2006; **130**: 566-576; quiz 588-589

7 The Paris endoscopic classification of superficial neoplastic lesions: esophagus, stomach, and colon: November 30 to December 1, 2002. *Gastrointest Endosc* 2003; **58**: S3-S43

8 **Hamilton SR**, Aaltonen LA, editors. World Health Organization classification of tumours: pathology and genetics of tumours of the digestive system. Lyon: IARC Press, 2000: 104-119

9 **Kitajima K**, Fujimori T, Fujii S, Takeda J, Ohkura Y, Kawamata H, Kumamoto T, Ishiguro S, Kato Y, Shimoda T, Iwashita A, Ajioka Y, Watanabe H, Watanabe T, Muto T, Nagasako K. Correlations between lymph node metastasis and depth of submucosal invasion in submucosal invasive colorectal carcinoma: a Japanese collaborative study. *J Gastroenterol* 2004; **39**: 534-543

10 **Shimoda T**, Ikegami M, Fujisaki J, Matsui T, Aizawa S, Ishikawa E. Early colorectal carcinoma with special reference to its development de novo. *Cancer* 1989; **64**: 1138-1146

11 **Kyzer S**, Bégin LR, Gordon PH, Mitmaker B. The care of patients with colorectal polyps that contain invasive adenocarcinoma. Endoscopic polypectomy or colectomy? *Cancer* 1992; **70**: 2044-2050

12 **Minamoto T**, Mai M, Ogino T, Sawaguchi K, Ohta T, Fujimoto T, Takahashi Y. Early invasive colorectal carcinomas metastatic to the lymph node with attention to their nonpolypoid development. *Am J Gastroenterol* 1993; **88**: 1035-1039

13 **Cooper HS**. Surgical pathology of endoscopically removed malignant polyps of the colon and rectum. *Am J Surg Pathol* 1983; **7**: 613-623

14 **Nusko G**, Mansmann U, Partzsch U, Altendorf-Hofmann A, Groitl H, Wittekind C, Ell C, Hahn EG. Invasive carcinoma in colorectal adenomas: multivariate analysis of patient and adenoma characteristics. *Endoscopy* 1997; **29**: 626-631

15 **Nascimbeni R**, Burgart LJ, Nivatvongs S, Larson DR. Risk of lymph node metastasis in T1 carcinoma of the colon and rectum. *Dis Colon Rectum* 2002; **45**: 200-206

16 **Tanaka S**, Haruma K, Teixeira CR, Tatsuta S, Ohtsu N, Hiraga Y, Yoshihara M, Sumii K, Kajiyama G, Shimamoto F. Endoscopic treatment of submucosal invasive colorectal carcinoma with special reference to risk factors for lymph node metastasis. *J Gastroenterol* 1995; **30**: 710-717

17 **Morson BC**, Whiteway JE, Jones EA, Macrae FA, Williams CB. Histopathology and prognosis of malignant colorectal polyps treated by endoscopic polypectomy. *Gut* 1984; **25**: 437-444

18 **Fujimori T**, Kawamata H, Kashida H. Precancerous lesions of the colorectum. *J Gastroenterol* 2001; **36**: 587-594

19 **Coverlizza S**, Risio M, Ferrari A, Fenoglio-Preiser CM, Rossini FP. Colorectal adenomas containing invasive carcinoma. Pathologic assessment of lymph node metastatic potential. *Cancer* 1989; **64**: 1937-1947

20 **Cranley JP**, Petras RE, Carey WD, Paradis K, Sivak MV. When is endoscopic polypectomy adequate therapy for colonic polyps containing invasive carcinoma? *Gastroenterology* 1986; **91**: 419-427

21 **Nivatvongs S**, Rojanasakul A, Reiman HM, Dozois RR, Wolff BG, Pemberton JH, Beart RW Jr, Jacques LF. The risk of lymph node metastasis in colorectal polyps with invasive adenocarcinoma. *Dis Colon Rectum* 1991; **34**: 323-328

22 **Netzer P**, Forster C, Biral R, Ruchti C, Neuweiler J, Stauffer E, Schönegg R, Maurer C, Hüsler J, Halter F, Schmassmann A. Risk factor assessment of endoscopically removed malignant colorectal polyps. *Gut* 1998; **43**: 669-674

23 **Fujii T**, Hasegawa RT, Saitoh Y, Fleischer D, Saito Y, Sano Y, Kato S. Chromoscopy during colonoscopy. *Endoscopy* 2001; **33**: 1036-1041

24 **Kato S**, Fujii T, Koba I, Sano Y, Fu KI, Parra-Blanco A, Tajiri H, Yoshida S, Rembacken B. Assessment of colorectal lesions using magnifying colonoscopy and mucosal dye spraying: can significant lesions be distinguished? *Endoscopy* 2001; **33**: 306-310

25 **Matsuda T**, Fujii T, Saito Y, Nakajima T, Uraoka T, Kobayashi N, Ikehara H, Ikematsu H, Fu KI, Emura F, Ono A, Sano Y, Shimoda T, Fujimori T. Efficacy of the invasive/non-invasive pattern by magnifying chromoendoscopy to estimate the depth of invasion of early colorectal neoplasms. *Am J Gastroenterol* 2008; **103**: 2700-2706

26 **Kato S**, Fu KI, Sano Y, Fujii T, Saito Y, Matsuda T, Koba I, Yoshida S, Fujimori T. Magnifying colonoscopy as a non-biopsy technique for differential diagnosis of non-neoplastic and neoplastic lesions. *World J Gastroenterol* 2006; **12**: 1416-1420

27 **Fu KI**, Kato S, Sano Y, Onuma EK, Saito Y, Matsuda T, Koba I, Yoshida S, Fujii T. Staging of early colorectal cancers: magnifying colonoscopy versus endoscopic ultrasonography for estimation of depth of invasion. *Dig Dis Sci* 2008; **53**:

1886-1892
28 **Kurisu Y**, Shimoda T, Ochiai A, Nakanishi Y, Hirata I, Katsu KI. Histologic and immunohistochemical analysis of early submucosal invasive carcinoma of the colon and rectum. *Pathol Int* 1999; **49**: 608-616
29 **Saitoh Y**, Waxman I, West AB, Popnikolov NK, Gatalica Z, Watari J, Obara T, Kohgo Y, Pasricha PJ. Prevalence and distinctive biologic features of flat colorectal adenomas in a North American population. *Gastroenterology* 2001; **120**: 1657-1665
30 **Tsuda S**, Veress B, Tóth E, Fork FT. Flat and depressed colorectal tumours in a southern Swedish population: a prospective chromoendoscopic and histopathological study. *Gut* 2002; **51**: 550-555
31 **Soetikno RM**, Kaltenbach T, Rouse RV, Park W, Maheshwari A, Sato T, Matsui S, Friedland S. Prevalence of nonpolypoid (flat and depressed) colorectal neoplasms in asymptomatic and symptomatic adults. *JAMA* 2008; **299**: 1027-1035
32 **Wiggers T**, Jeekel J, Arends JW, Brinkhorst AP, Kluck HM, Luyk CI, Munting JD, Povel JA, Rutten AP, Volovics A. No-touch isolation technique in colon cancer: a controlled prospective trial. *Br J Surg* 1988; **75**: 409-415
33 **Uno Y**, Munakata A. The non-lifting sign of invasive colon cancer. *Gastrointest Endosc* 1994; **40**: 485-489
34 **Kobayashi N**, Saito Y, Sano Y, Uragami N, Michita T, Nasu J, Matsuda T, Fu KI, Fujii T, Fujimori T, Ishikawa T, Saito D. Determining the treatment strategy for colorectal neoplastic lesions: endoscopic assessment or the non-lifting sign for diagnosing invasion depth? *Endoscopy* 2007; **39**: 701-705
35 **Saito Y**, Uraoka T, Matsuda T, Emura F, Ikehara H, Mashimo Y, Kikuchi T, Fu KI, Sano Y, Saito D. Endoscopic treatment of large superficial colorectal tumors: a case series of 200 endoscopic submucosal dissections (with video). *Gastrointest Endosc* 2007; **66**: 966-973
36 **Uraoka T**, Fujii T, Saito Y, Sumiyoshi T, Emura F, Bhandari P, Matsuda T, Fu KI, Saito D. Effectiveness of glycerol as a submucosal injection for EMR. *Gastrointest Endosc* 2005; **61**: 736-740

S- Editor Tian L **L- Editor** Kerr C **E- Editor** Lin YP

Online Submissions: wjg.wjgnet.com
wjg@wjgnet.com
doi:10.3748/wjg.15.2714

World J Gastroenterol 2009 June 14; 15(22): 2714-2722
World Journal of Gastroenterology ISSN 1007-9327

ORIGINAL ARTICLES

Higher CO_2-insufflation pressure inhibits the expression of adhesion molecules and the invasion potential of colon cancer cells

Jun-Jun Ma, Bo Feng, Yi Zhang, Jian-Wen Li, Ai-Guo Lu, Ming-Liang Wang, Yuan-Fei Peng, Wei-Guo Hu, Fei Yue, Min-Hua Zheng

Jun-Jun Ma, Bo Feng, Jian-Wen Li, Ai-Guo Lu, Ming-Liang Wang, Yuan-Fei Peng, Wei-Guo Hu, Fei Yue, Min-Hua Zheng, Department of General Surgery, Ruijin Hospital, Shanghai Jiao Tong University School of Medicine; Shanghai Minimally Invasive Surgery Center, Shanghai 200025, China
Jun-Jun Ma, Bo Feng, Yi Zhang, Yuan-Fei Peng, Fei Yue, Min-Hua Zheng, Shanghai Institute of Digestive Surgery, Shanghai 200025, China
Author contributions: Ma JJ carried out the Adhesion assays, drafted the manuscript and participated in the design of the study; Feng B carried out the molecular expression studies, and *in vitro* pneumoperitoneum establishment; Zhang Y carried out the cell invasive assay; Li JW participate in the induction of intra-abdominal tumors; Lu AG participated in the molecular expression studies; Wang ML performed the statistical analysis; Peng YF, Hu WG, Yue F participated in the cell invasive assay; Zheng MH conceived of the study, and participated in its design and coordination and helped to draft the manuscript.
Correspondence to: Min-Hua Zheng, Department of General Surgery, Ruijin Hospital, Shanghai Jiao Tong University School of Medicine; Shanghai Minimally Invasive Surgery Center, Shanghai 200025, China. marsnew790620@163.com
Telephone: +86-21-64458887 Fax: +86-21-64333548
Received: March 22, 2009 Revised: May 5, 2009
Accepted: May 12, 2009
Published online: June 14, 2009

Abstract

AIM: To investigate the influence of CO_2-insufflation pressure on adhesion, invasion and metastatic potential of colon cancer cells based on adhesion molecules expression.

METHODS: With an *in vitro* artificial pneumoperitoneum model, SW1116 human colon carcinoma cells were exposed to CO_2-insufflation in 5 different pressure groups: 6 mmHg, 9 mmHg, 12 mmHg, 15 mmHg and control group, respectively for 1 h. Expression of E-cadherin, ICAM-1, CD44 and E-selectin was measured at 0, 12, 24, 48 and 72 h after CO_2-insufflation using flow cytometry. The adhesion and invasion capacity of SW1116 cells before and after exposure to CO_2-insufflation was detected by cell adhesion/invasion assay *in vitro*. Each group of cells was injected intraperitoneally into 16 BALB/C mice. The number of visible abdominal cavity tumor nodules, visceral metastases and survival of the mice were recorded in each group.

RESULTS: The expression of E-cadherin, ICAM-1, CD44 and E-selectin in SW1116 cells were changed significantly following exposure to CO_2 insufflation at different pressures ($P < 0.05$). The expression of E-cadherin, CD44 and ICAM-1 decreased with increasing CO_2-insufflation pressure. The adhesive/invasive cells also decreased gradually with increasing pressure as determined by the adhesion/invasion assay. In animal experiments, the number of abdominal cavity tumor nodules in the 15 mmHg group was also significantly lower than that in the 6 mmHg group (29.7 ± 9.91 *vs* 41.7 ± 14.90, $P = 0.046$). However, the survival in each group was not statistically different.

CONCLUSION: CO_2-insufflation induced a temporary change in the adhesion and invasion capacity of cancer cells *in vitro*. Higher CO_2-insufflation pressure inhibited adhesion, invasion and metastatic potential *in vitro* and *in vivo*, which was associated with reduced expression of adhesion molecules.

Key words: Adhesion molecule; Colorectal cancer; Metastasis; Pneumoperitoneum; Artificial; Tumor invasion

Peer reviewer: Filip Braet, Associate Professor, Australian Key Centre for Microscopy and Microanalysis, Madsen Building (F09), The University of Sydney, Sydney NSW 2006, Australia

Ma JJ, Feng B, Zhang Y, Li JW, Lu AG, Wang ML, Peng YF, Hu WG, Yue F, Zheng MH. Higher CO_2-insufflation pressure inhibits the expression of adhesion molecules and the invasion potential of colon cancer cells. *World J Gastroenterol* 2009; 15(22): 2714-2722 Available from: URL: http://www.wjgnet.com/1007-9327/15/2714.asp DOI: http://dx.doi.org/10.3748/wjg.15.2714

INTRODUCTION

The laparoscopic approach is generally considered

to be less invasive and less immunosuppressive than conventional open surgery[1]. However, port site metastases and abdominal wall recurrences although rare nowadays, remain a problem with laparoscopic surgery for cancer[2]. Recently, several studies demonstrated that the five-year survival rates were similar after laparoscopically assisted colectomy and open colectomy for cancer patients, suggesting that the laparoscopic approach is an acceptable alternative to open surgery for colorectal cancer[3-5]. However, whether CO_2 insufflation, which is widely used in laparoscopic surgery, increases the metastatic potential of tumor cells is still the focus of related studies[6-8].

Adhesion molecules play an important role in cell-cell, cell-extracellular matrix (ECM) interactions at tumor metastasis[9,10]. ICAM-1, E-cadherin, and CD44 are representative molecules involved in the interaction not only between the adhesion of inflammatory cells but also between tumor cells and the endothelium. Previous studies have shown that reduced E-cadherin expression correlates with increased invasiveness in colorectal carcinoma cell lines[11]. The decrease or deletion of E-cadherin was reported to induce liver metastasis of colorectal tumors[12,13], and the increased expression of CD44 also induces tumor metastasis[14]. Recently it has been reported that CO_2 insufflation can effect the expression of adhesion molecules, such as E-cadherin, CD44 and ICAM-1, which are related to tumor metastasis[15-17]. However, there are few studies on the influence of CO_2-insufflation pressure on adhesion molecules and how CO_2 insufflation further impacts on metastatic potential following altered expression of these adhesion molecules.

In this study, we investigated whether expression of adhesion molecules are changed after CO_2 insufflation *in vitro*. We further investigated the influence of CO_2 pressure on the expression of these adhesion molecules, and how CO_2-insufflation influenced the adhesion and invasion potential of colon cancer cells *in vitro* and *in vivo*.

MATERIALS AND METHODS

Cell culture

The human colorectal adenocarcinoma cell line SW1116 (human, Caucasian, colon, adenocarcinoma, grade Ⅲ, CCL-233™) was cultured in RPMI 1640 medium (Hangzhou Genom Co. Cat. No. GNM31800.25) supplemented with 10% fetal calf serum (Life Technologies). The human colorectal adenocarcinoma cell line Lovo (human, colon, adenocarcinoma, grade IV, CCL-229™) used in the invasive assay was cultured in F12K medium (Hangzhou Genom Co. Cat. No. GNM21700.25) supplemented with 10% fetal calf serum. The monolayer cell culture was maintained in culture flasks under standard culture conditions at 37℃ in air with 5% CO_2.

Monoclonal antibodies

For flow cytometry, the following monoclonal antibodies (Mab) were used: anti-ICAM-1-PE-Cy5 (Clone HA58) and anti-E-selectin-PE (Clone 68-5H11). They were purchased from BD Biosciences (San Diego, CA, USA). Anti-CD44-FITC (Clone J.173) and unconjugated anti-E-cadherin (Clone 67A4) were purchased from Beckman Coulter™. Secondary goat anti-mouse IgG-PE, isotype control mouse IgG-PE-Cy5, and mouse IgG-PE were purchased from BD Biosciences. Mouse IgG FITC, and mouse IgG PE were purchased from Beckman Coulter™.

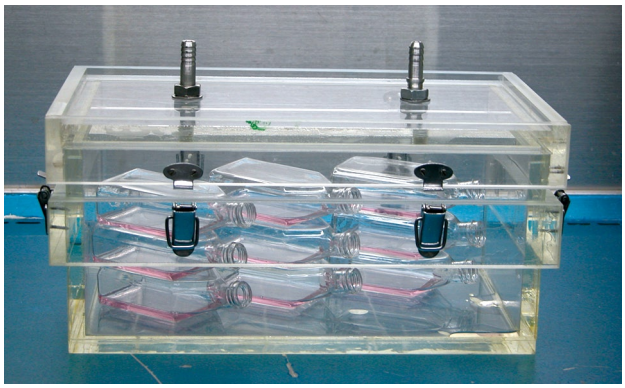

Figure 1 Five litres volume airtight Perspex box with two ventilating ports for pneumoperitoneum establishment *in vitro*.

Animals

Four to eight week-old male BALB/C mice (Chinese Academy of Sciences, Shanghai, China) were kept under standard laboratory conditions and fed a standard laboratory diet with access to water added *libitum* before and after injection.

In vitro pneumoperitoneum establishment

An *in vitro* pneumoperitoneum was established by connecting an electronic CO_2 insufflator (Stryker® Endoscopy) to a 5 L volume airtight Perspex box with two ventilating pits (Figure 1). Medical grade carbon dioxide at a concentration of 99.5% was used. To ensure exhaustion of air in the box, 10 L CO_2 were insufflated into the Perspex box before the tumor cells were placed into the box. The cells were divided into 5 groups with different insufflation pressures (6 mmHg, 9 mmHg, 12 mmHg, 15 mmHg, and room air as a control). The tumor cells and the boxes were transferred into an incubator at 37℃ and the *in vitro* pneumoperitoneum model was retained for 1 h at different insufflation pressures during a continuous CO_2 flow of 2.5 L/min.

Flow cytometry (FACScan)

At 0, 12, 24, 48, and 72 h after exposure, the cells were detached from the tissue culture flasks using ice-cold phosphate-buffered saline (PBS) containing 0.1% sodium azide and resuspended at 5×10^5 cells/mL. One milliliter of the cell suspension was incubated with the monoclonal antibodies (1:100). The cells (5×10^5/group) were incubated with anti-ICAM-1-PE-Cy5, 10 μL, anti-E-selectin-PE, 10 μL, anti-CD44-FITC, 20 μL and unconjugated anti-E-cadherin, 10 μL for 30 min at room

temperature. At the end of the incubation period, the cells were washed with PBS. After treatment with unconjugated anti-E-cadherin the cells were incubated with a secondary goat anti-mouse IgG-PE (3 μL/5 × 10^5 cells) for 30 min at room temperature. After washing with PBS, the cells were fixed with 0.5% formalin, and analyzed for surface receptor expression by flow cytometry (BD Calibur). The expression of 4 different cell adhesion molecules was measured at 5 time points (0, 12, 24, 48 and 72 h) after CO_2 insufflation. Expression of these adhesion molecules is given as mean fluorescence intensity of the cell population.

Adhesion assay

A cell adhesion assay (Cat. No. ECM 554, Chemicon International, USA) was used, in which the wells were coated with human fibronectin, one of the component proteins of the extracellular matrix (ECM). At 0 h and 72 h after exposure to CO_2 insufflation (at 6 mmHg, 9 mmHg, 12 mmHg, 15 mmHg and room air for 1 h, respectively), the cells were detached using 0.25% trypsin and washed with PBS. The wells were rehydrated with 200 μL of PBS per well for at least 15 min at room temperature before being plated at a concentration of 1 × 10^5 cells per well. After the plate was incubated at 37℃ in air with 5% CO_2 for 1 h, each well was washed gently 3 times with PBS. The cells which had adhered to the wells were then dyed with crystal violet and incubated for 5 min at room temperature. After the plate was gently washed 3 times with PBS, 100 μL of Solubilization Buffer (a 50/50 mixture of 0.1 mol/L NaH_2PO_4, pH 4.5 and 50% ethanol) was added to each well. The plate was shaken at room temperature gently to solubilize the cell-bound stain completely. Finally, a microplate reader was used to determine the absorbance at 570 nm as a measure of tumor cell adhesion on the ECM layer.

Cell invasive assay

The SW1116 cells were starved by incubation in serum-free RPMI 1640 for 18-24 h prior to assay. At 0 h and 72 h after CO_2 insufflation (6 mmHg, 9 mmHg, 12 mmHg, 15 mmHg and room air for 1 h, respectively), the cells were harvested by trypsinization, and resuspended in RPMI 1640 at 1 × 10^6 cells/mL. Twenty-four-well QCM™ Cell The Invasion Assay kit (Cat. No. ECM 101, Chemicon International, USA) was used. After rehydration of the ECM layer by adding 300 μL of pre-warmed serum-free medium to the interior of the inserts for 30 min at room temperature, 250 μL of the medium was removed from the inserts without disturbing the membrane. The prepared cell suspension (250 μL) as described previously was then added into each insert, and RPMI 1640 with 5% BSA was added to the lower chamber. After incubation for 24 h at 37℃ in the incubator with 5% CO_2, the medium and suspended cells were removed and the invasion chamber was placed into a clean well containing 225 μL of the cell detachment solution. The cells were then incubated at 37℃ for 30 min, and both lyses buffer and dye solution were added to each well containing the cell detachment solution with cells which had invaded the ECM coated membrane. Finally, the mixture was detected by a fluorescence plate reader using a 480/520 nm filter set. The fluorescence intensity was measured as an index of the quantity of invasive cells. Lovo cells underwent the same procedure in the invasive assay.

Induction of intra-abdominal tumors

To analyze the potential for abdominal cavity dissemination in each group of cells (exposed to CO_2 insufflation at 6 mmHg, 9 mmHg, 12 mmHg, 15 mmHg and room air), each group of cells was injected intraperitoneally into 16 BALB/C mice (1 × 10^6 cells/mouse). Fourteen days later, 10 mice in each group were sacrificed by cervical dislocation, and the number of visible abdominal cavity tumor nodules, reflecting the metastatic potential, was counted. The rate of viscera (liver, kidney, spleen, peritoneum or mesentery) metastasis was also recorded in each group. The remaining mice in each group were monitored for their survival.

Statistical analysis

For studies on the expression of adhesion molecules, each experiment was performed in triplicate. Cell adhesion and invasion assays were repeated five times. Data are expressed as mean ± SD. The repeated-measures ANOVA test, one-way ANOVA test and paired *t* test were used to compare the control mean with the various treatment means: adhesion molecules, cell adhesion and invasion assay *in vitro*, and abdominal cavity tumor metastasis *in vivo*. The rates of organ (liver, kidney, spleen, peritoneum or mesentery) metastasis were analyzed using Fisher's exact test. Statistical significance was set at the 5% level.

RESULTS

Effect of CO_2 insufflation on expression of adhesion molecules

Immediately after the 6 mmHg CO_2 insufflation, ICAM-1 (Figure 2A-C) and CD44 expression significantly increased compared to room air controls (F = 106.38, 297.73; $P < 0.01$), while the expression of ICAM-1 decreased at 48 h and 72 h after the 6 mmHg CO_2 insufflation (F = 17222.3, 385.61; $P < 0.01$) (Figure 2A-C). Immediately after the 9 mmHg CO_2 insufflation, E-selectin expression significantly increased compared to the controls (F = 147.75, P = 0.01), and CD44 expression increased significantly compared to controls (F = 39.20, P = 0.025); 24 h after 9 mmHg CO_2 insufflation, E-cadherin expression increased significantly compared to controls (F = 26.79, P = 0.035) (Figure 2D-F), while a significant reduction in E-selectin expression was observed (F = 33.43, P = 0.029). At 48 h after 9 mmHg CO_2 insufflation, a significant reduction in ICAM-1 expression was demonstrated (F = 282.94, $P < 0.01$). At 48 h after 12 mmHg CO_2 insufflation, CD44 expression increased significantly (F = 93.70, P = 0.011), while 72 h after 12 mmHg CO_2 insufflation, the expression of CD44

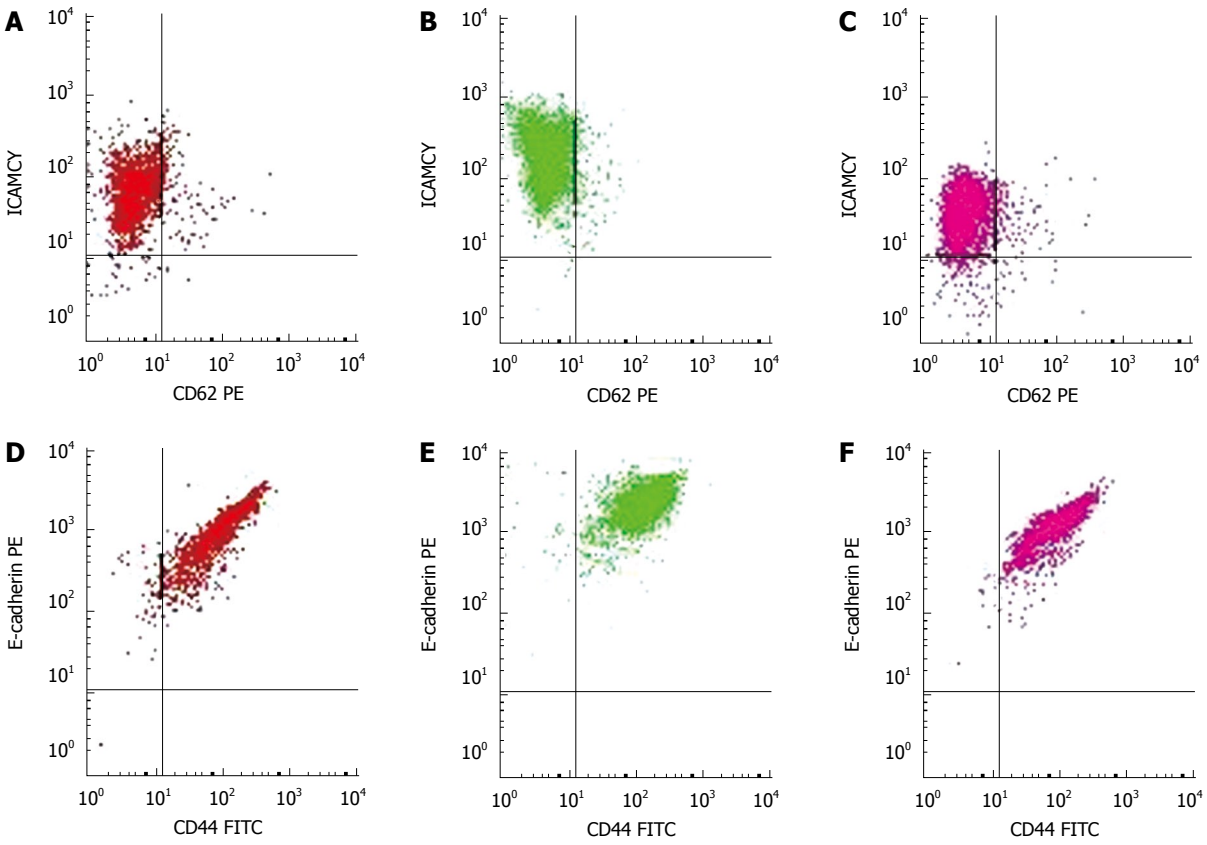

Figure 2 Flow cytometry analysis of ICAM-1 and E-cadherin expression in SW1116. A: ICAM-1 (Room air control); B: ICAM-1 (0 h after the 6 mmHg insufflation); C: ICAM-1 (72 h after the 6 mmHg insufflation); D: E-cadherin (Room air control); E: E-cadherin (24 h after the 9 mmHg insufflation); F: E-cadherin (72 h after the 9 mmHg insufflation). Immediately after the 6 mmHg CO_2 insufflation (B), ICAM-1 expression increased significantly compared to room air controls (A) (P = 0.009), while it was significantly less at 72 h after the 6 mmHg insufflation (C) than control group. Twenty four hours after 9 mmHg CO_2 insufflation (E), E-cadherin expression increased significantly compared to controls (D) (P = 0.035), but returned to the control value at 72 h after the 9 mmHg insufflation (F).

decreased significantly compared to the controls (F = 679.38, P < 0.01). Immediately after the 15 mmHg CO_2 insufflation, CD44 expression decreased significantly compared to the controls (F = 70.01, P = 0.014). At 12 h and 24 h after 15 mmHg CO_2 insufflation, an increased expression of E-cadherin was demonstrated (F = 53.53, 68.14, P = 0.018, 0.014). No significant differences in the expression of these adhesion molecules at other time points and pressures were observed.

Effect of rising insufflation pressure on expression of adhesion molecules

The expression of CD44, E-cadherin and ICAM-1 decreased with increasing CO_2-insufflation pressure. At the 0 h time point, the differences in CD44 expression between the 6 mmHg and the 9 mmHg group, the 9 mmHg and the 12 mmHg group, the 12 mmHg and the 15 mmHg group were significant (t = 4.4291, 4.5725, 7.3587, P < 0.01) (Figure 3A). At the same time point, E-cadherin expression in the 9 mmHg group was less than that in the 6 mmHg group (t = 7.1839, P < 0.01), while in the 12 mmHg and the 15 mmHg group, E-cadherin expression was significantly less than that in the 9 mmHg group (t = 4.5148, 4.4582, P < 0.01) (Figure 3B). ICAM-1 expression in the 9 mmHg, 12 mmHg and 15 mmHg groups was less than that in the 6 mmHg group, respectively (t = 3.3359, 2.3189, 2.7546, P < 0.01, P = 0.046, 0.022), and the expression at 15 mmHg was significantly less than that at 12 mmHg (t = 2.2912, P = 0.048) (Figure 3C).

Effect of CO_2 insufflation on adhesion potential of SW1116 in vitro

Immediately after exposure to increasing CO_2-insufflation pressure, cell adhesion decreased gradually. Cell adhesion in the 15 mmHg group was significantly less than that at 12 mmHg, 9 mmHg, 6 mmHg and the control (all P < 0.01), and cell adhesion in the 12 mmHg group was also less than that in the 9 mmHg, 6 mmHg and control groups (all P < 0.01). The cells exposed to 6 mmHg had more adhesion capacity than those exposed to 9 mmHg or the control group, however, the differences were not significant (P = 0.886, P = 0.058) (Figure 4A). At 72 h after CO_2 insufflation, the differences between the various insufflation pressure groups were not significant (Figure 4B).

Effect of CO2 insufflation on invasion potential of SW1116 and Lovo in vitro

Immediately after exposure to 15 mmHg CO_2 insufflation, the invasion of SW1116 cells decreased significantly compared to the cells before exposure (11.36 ± 0.861 *vs* 13.43 ± 1.113; P = 0.019), while immediately after exposure to 6 mmHg insufflation, invasive cells increased compared to

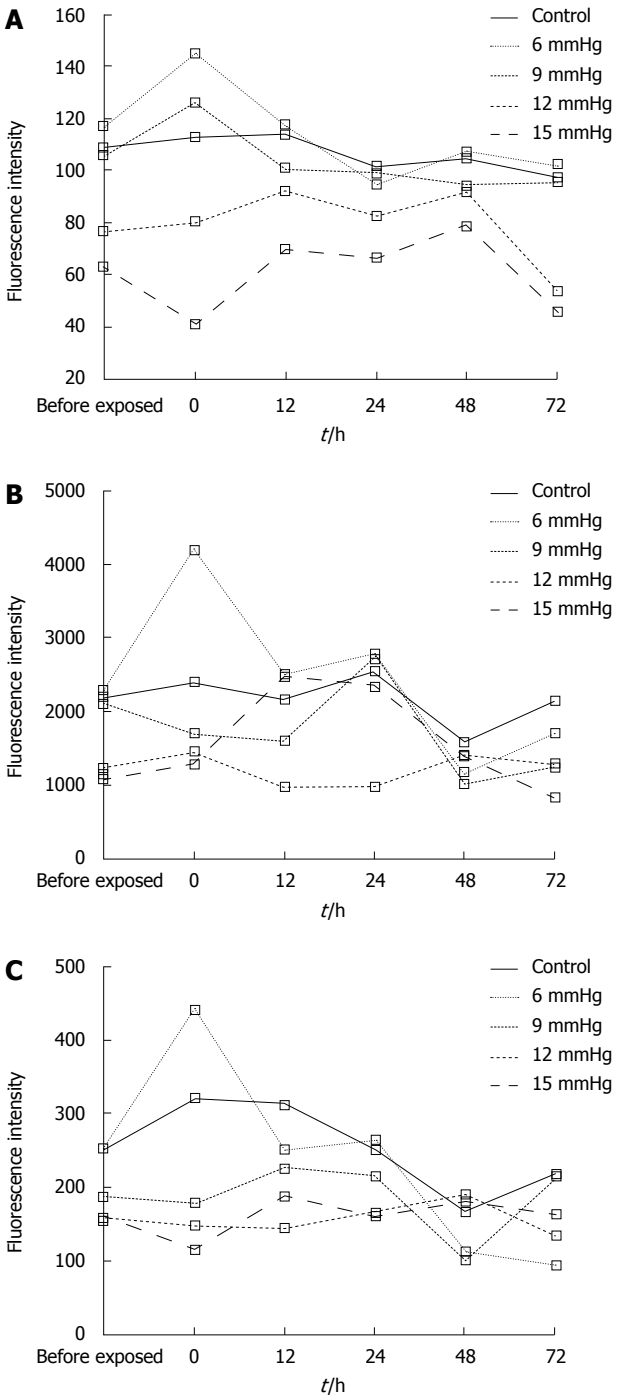

Figure 3 The effect of CO_2 insufflation pressure on expression of adhesion molecules. A: Expression of CD44; B: Expression of E-cadherin; C: Expression of ICAM-1. With increasing CO_2-insufflation pressure, the expression of CD44 (A), E-cadherin (B), and ICAM-1 (C) decreased at some time points, especially at the start (0 h) after CO_2-insufflation.

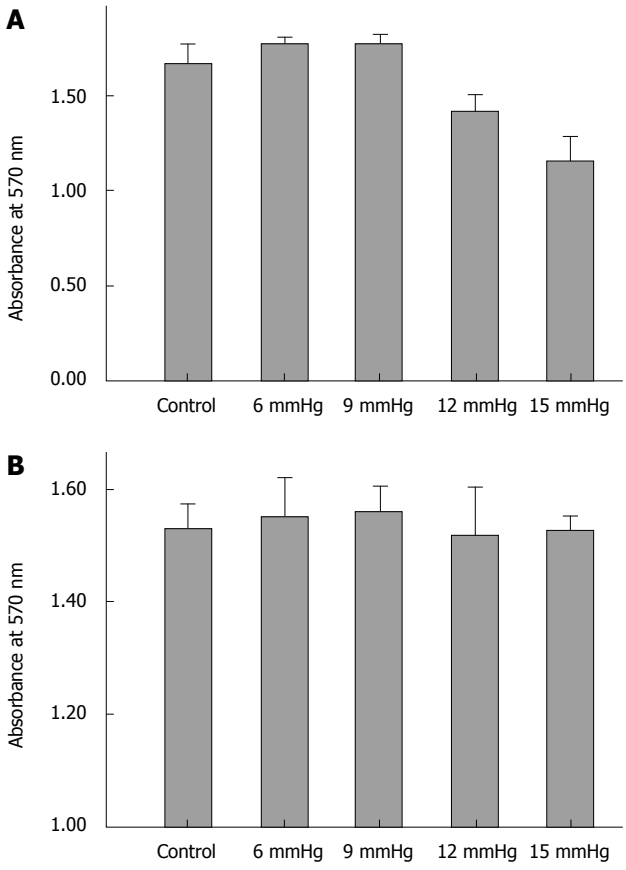

Figure 4 Results of adhesion assay. A: 0 h after CO_2 insufflation; B: 72 h after CO_2 insufflation. At 0 h after CO_2 insufflation (A), with increasing CO_2-insufflation pressure, the adhesion of the SW1116 cell line decreased gradually (12 mmHg *vs* control, $P < 0.001$; 15 mmHg *vs* 12 mmHg, $P < 0.001$). At 72 h after CO_2 insufflation (B), cell adhesion was similar among the different groups ($P > 0.05$).

before exposure (15.58 ± 1.015 *vs* 14.42 ± 1.491; $P = 0.056$), however, the difference was not significant (Figure 5A). At 72 h after CO_2 insufflation, cell invasion was similar to that for cells before exposure (Figure 5B).

The differences between various insufflation pressures were also compared. At the 0 h time point, the cells exposed to 15 mmHg were significantly less invasive than those exposed to the other insufflation pressures (*vs* 6 mmHg, $P < 0.01$; *vs* 9 mmHg, $P = 0.011$; *vs* 12 mmHg, $P = 0.016$; and *vs* room air, $P = 0.014$), and the cells exposed to 6 mmHg were more invasive than cells exposed to the other insufflation pressures (*vs* 9 mmHg, $P = 0.013$; *vs* 12 mmHg, $P < 0.01$; *vs* 15 mmHg $P < 0.01$; and *vs* room air, $P = 0.011$). However, these differences were not significant (Figure 5A). At 72 h after CO_2 insufflation, the differences between the various insufflation pressure groups were not significant (Figure 5B).

The human colon cancer cell line Lovo was also tested in the invasive assay, and a similar trend was observed (Figure 5C and D).

Effect of CO_2 insufflation on metastasis potential of SW1116 in vivo

The ratios of the number of mice which developed intra-abdominal tumors/the number of mice which received inoculation of SW1116 cells in the various groups were as follows: (1) control group, 10/10; (2) 6 mmHg group, 9/10; (3) 9 mmHg group, 9/10; (4) 12 mmHg group, 9/10; (5) 15 mmHg group, 10/10. The differences were not significant. The mean number of intra-abdominal tumor nodules in the various groups was as follows: (1) control group = 36.8 ± 15.32, (2) 6 mmHg group = 41.7 ± 14.90, (3) 9 mmHg group = 33.9 ± 10.29, (4) 12 mmHg group = 33.2 ± 11.72, (5) 15 mmHg = 29.7 ± 9.91. The difference between the 6 mmHg group and the 15 mmHg group was significant ($P = 0.046$) (Figure 6A-C), but the differences among

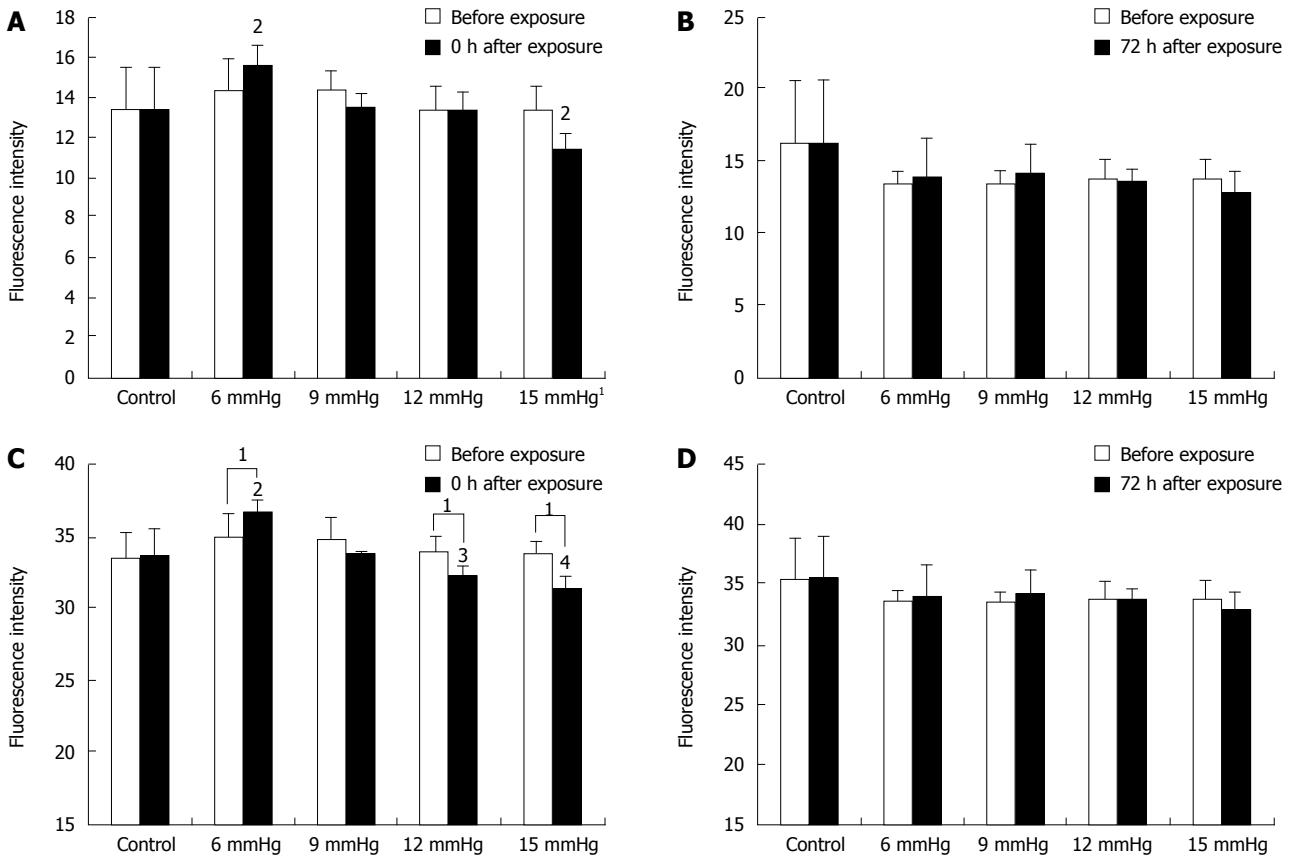

Figure 5 Results of invasion assay. A: SW1116, 0 h after exposure; B: SW1116, 72 h after exposure; C: Lovo, 0 h after exposure; D: Lovo, 72 h after exposure. A: [1]At 0 h after exposure to 15 mmHg CO_2 insufflation, invasive cells decreased significantly compared to the cells prior to exposure (P = 0.019); [2]At 0 h after exposure, invasion of the 6 mmHg or the 15 mmHg group was significantly different from the other pressure groups (P < 0.05). B: The invasion fluorescence intensities of SW1116 before and 72 h after exposure to CO_2 insufflation were not significantly different (P > 0.05). Seventy two hours after the CO_2 insufflation, there were no significant differences between the various insufflation pressure groups (P > 0.05); C: [1]At 0 h after exposure to 15 mmHg, 12 mmHg or 6 mmHg CO_2 insufflation, invasive cells of Lovo decreased significantly compared to the cells prior to exposure (P = 0.008, P = 0.0045, P = 0.043); [2]At 0 h after exposure, cell invasion at 6 mmHg was significantly different from the other pressure groups (P < 0.01); [3]At 0 h after exposure, cell invasion in the 12 mmHg group was significantly less than the 9 mmHg group (P < 0.05); [4]At 0 h after exposure, cell invasion in the 15 mmHg group was significantly less than the 6 and 9 mmHg groups (P < 0.01); D: The invasion fluorescence intensities of Lovo before and 72 h after exposure to CO_2 insufflation were not significantly different (P > 0.05). Seventy two hours after CO_2 insufflation, there were no significant differences between the various insufflation pressure groups (P > 0.05).

the other groups were not. The results of visceral (liver, kidney, spleen, peritoneum or mesentery) metastases (the number of mice with certain visceral metastasis/the number of mice with abdominal cavity metastasis after inoculation of SW1116 cells) are shown in Table 1. No significant differences in survival rate between the various groups were observed (P = 0.426). The overall survival curve is shown in Figure 7.

DISCUSSION

The use of minimal access techniques in the surgical management of colorectal cancer should be safe and feasible in terms of the oncologic effect on the tumor, as compared with conventional surgery. Recent clinical trials in Europe and America have demonstrated that the recurrence and 5-year survival of laparoscopic colorectal cancer surgery are identical to those obtained by open surgery[3-4]. Similar results have also been reported from Hong Kong[18]. However, the occurrence of port-site metastasis and peritoneal metastasis reported in early studies of laparoscopic surgery for cancer led to many studies investigating the biologic effects of positive pressure pneumoperitoneum on tumor growth and the development of trocar recurrences. Several experimental studies suggested that laparoscopic surgery can promote tumor growth[6,19]. Some animal studies have also shown that CO_2, especially at high insufflation pressures increased the incidence of distant metastases[20,21]. However, other researchers failed to confirm these experimental observations in similar animal models[22]. Thus, although the problem of port-site deposits in patients undergoing laparoscopic surgery for cancer has largely been resolved by improved oncological operative techniques, from a biological standpoint, the adverse effect of a sustained positive pressure CO_2 pneumoperitoneum is still debatable, and it is prudent to investigate the mechanism of tumor metastasis induced by CO_2 pneumoperitoneum.

Some adhesion molecules in cancer cells have been reported to play an important role in tumor metastasis. There is evidence that decreased expression of E-cadherin can initiate tumor invasion and metastasis because E-cadherin prevents detachment of tumor cells from

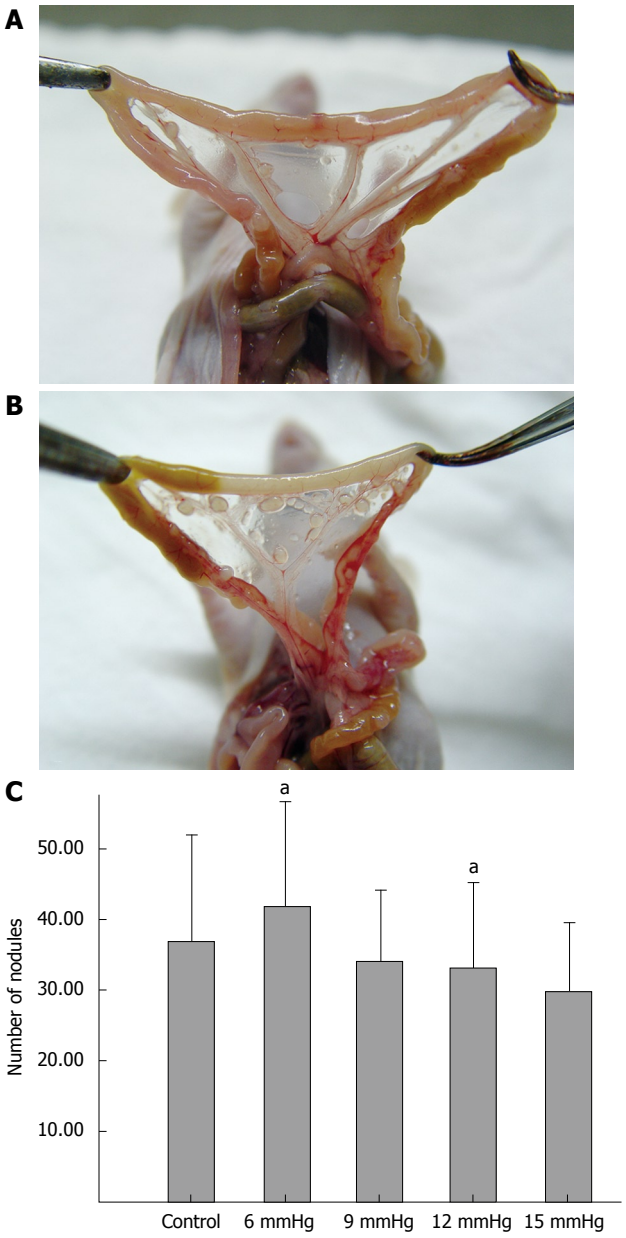

Figure 6 Results of intra-abdominal tumor nodules. A: Mesentery tumor nodules in the 15 mmHg group; B: Mesentery tumor nodules in the 6 mmHg group; C: Numbers of intra-abdominal tumor nodules in the various groups. The number of intra-abdominal tumor nodules in the 15 mmHg group (A) was significantly lower than those in 6 mmHg group (B) ($^aP = 0.046$). The mean numbers of abdominal cavity nodules formed by the cells in each group are described in (C).

the primary tumor[11,23,24]. ICAM-1 mediates the adhesion of circulating cells to the intravascular endothelium. ICAM-1 may also play a role in tumor cell adhesion to the mesothelium[25]. Changes in the expression of CD44 are reported to be related to increased tumor metastasis. The expression of E-selectin in primary colorectal cancer is significantly less than in secondary deposits from this tumor[26]. A number of recent studies have addressed the effects of the laparoscopic environment on these adhesion molecules in cancer cells. Kim *et al*[16] demonstrated a significant alteration in E-cadherin, ICAM-1 and CD44 expression in colon cancer cells after exposure to CO_2. Tahara *et al*[27] reported that CO_2 insufflation increased

Table 1 Distribution of visceral metastases (liver, kidney, spleen, peritoneum or mesentery)

	Liver (n1/n2)	Spleen (n1/n2)	Mesentery (n1/n2)	Kidney (n1/n2)	Peritoneum (n1/n2)
Control	10/10	4/10	10/10	5/10	4/10
6 mmHg	9/9	0/9	9/9	0/9	2/9
9 mmHg	9/9	1/9	9/9	2/9	1/9
12 mmHg	8/9	1/9	9/9	4/9	0/9
15 mmHg	10/10	1/10	10/10	4/10	1/10
P	> 0.05	> 0.05	> 0.05	> 0.05	> 0.05

n1: Number of mice with certain viscera metastasis; n2: Number of mice which developed intra-abdominal metastases after inoculation of SW1116 cells.

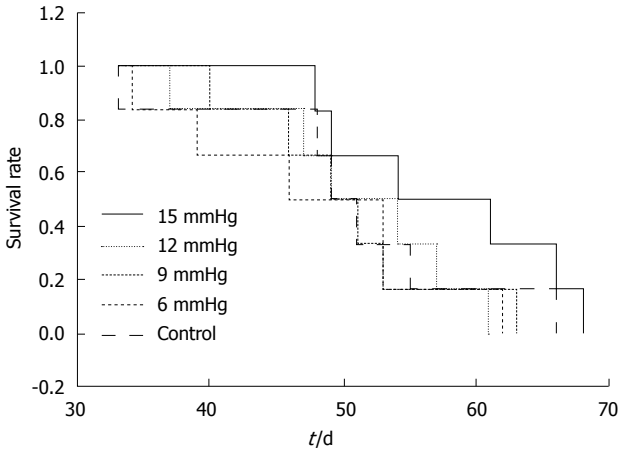

Figure 7 Survival time of the mice injected with SW1116 cells in the different groups ($P = 0.426$).

the expression of P-cadherin mRNA in the mouse peritoneum. However, neither of these two groups investigated how these CO_2-induced changes affected the invasive and metastatic potential of colon cancer cells.

In our study, we found that the expression of these adhesion molecules in the SW1116 cell line increased significantly 0-48 h after the cells were exposed to continuous CO_2-insufflation for 1 h ($P < 0.05$), and returned to the control level by 72 h. We found that these changes are temporary. At certain time points, ICAM-1, E-selectin, and CD44 were found to be even lower than the control levels ($P < 0.05$). In addition, contrary to the results reported by Kim *et al*[16], the expression of E-cadherin significantly increased, rather than decreased after exposure to CO_2-insufflation, although the effect was temporary. The important findings of the present study are that the changes in these adhesion molecules are bi-directional. Collectively increased expression of ICAM-1, E-selectin, and CD44 and decreased expression of E-cadherin signify increasing potential for tumor metastasis. However, the results of the present study also demonstrated the temporary and bi-directional nature of the changes in the expression of these adhesion molecules, indicating that CO_2-insufflation during laparoscopic surgery does not appear to increase the metastatic potential of solid

cancers. Our results document that with increasing CO_2-insufflation pressure, the expression of E-cadherin, CD44 and ICAM-1 decreased, especially at the start of CO_2-insufflation exposure ($P < 0.05$, Figure 3A-C). We believe that higher pressures of CO_2-insufflation could inhibit the expression of adhesion molecules.

We also investigated the effect of CO_2-insufflation on the adhesion and invasion potential of colon cancer cells *in vitro* and the effect on the metastatic capacity of the tumor cells *in vivo*. The cell invasion assays showed that CO_2-insufflation also changed the invasion potential of tumor cells (both the SW1116 and the Lovo cell line) temporarily but with increasing CO_2-insufflation pressures, invasion potential decreased. Similar results were obtained with the adhesion assays.

The *in vivo* animal studies with rising CO_2-insufflation pressure, showed a decrease in the number of tumor nodules when the data between the 15 mmHg and 6 mmHg groups were compared. This observation suggests that high CO_2-insufflation pressures could inhibit the adhesion, invasion and metastatic potential of colon cancer cells. Ziprin *et al*[28] reported that laparoscopic enhancement of tumor cell binding to the peritoneum is inhibited by anti-ICAM-1 monoclonal antibody. High CO_2-insufflation pressures could inhibit the adhesion, invasion or metastatic capacity of tumor cells *in vitro* and *in vivo* by inhibiting expression of the adhesion molecules ICAM-1 and CD44.

In the present study, the adhesion potential of the tumor cells from the CO_2-insufflation groups did not increase when compared to the control group. In addition, the numbers of tumor nodules in the four CO_2-insufflation groups were similar to the control group. Likewise, survival rates were not significantly different indicating that CO_2-insufflation did not increase the adhesion potential of colon cancer cells *in vitro* or the metastatic capacity *in vivo*. However, reaction of the host seems also to be highly important. Various host defence mechanisms in the organism are involved in tumouricidal killing processes. Some studies have reported that the mononuclear phagocytotic system, which largely consists of hepatic tissue macrophages (Kupffer cells), plays an important tumouricidal role. Previously, laparoscopic insufflation with CO_2 had been demonstrated to impair the activity of the mononuclear phagocyte system and was responsible for potential hepatic disadvantages[29]. In this study, only tumor cells treated with CO_2-insufflation *in vitro*, and the *in vivo* metastatic capacity of colon cancer cells treated with different CO_2-insufflation *in vitro* were the focus of this investigation. The reaction of the host after high pressure pneumoperitoneum, and the effect that the pneumoperitoneum may have on intraperitoneal cells was not considered. Further investigations are required.

In conclusion, this study has shown that the expression of adhesion molecules can be affected temporarily and bi-directionally by continuous CO_2-insufflation, which also induced a temporary change in the adhesion and invasion capacity of these cells *in vitro*. CO_2-insufflation at high pressures plays an important role in inhibiting the expression of adhesion molecules. In addition, high insufflation pressures inhibited the adhesion and invasion potential of colon cancer cells *in vitro* and inhibited metastatic potential *in vivo*, which was associated with inhibited expression of adhesion molecules. The results of our study do not provide any evidence that CO_2-insufflation increases the metastatic potential of colon cancer cells.

In conclusion, CO_2-insufflation induced a temporary change in the adhesion and invasion capacity of cancer cells *in vitro*. High pressures of CO_2-insufflation inhibited the adhesion, invasion and metastatic potential *in vitro* and *in vivo*, which was associated with reduced expression of adhesion molecules.

ACKNOWLEDGMENTS

We thank Dr. Yan-Yan Song of the Department of Public Health, Shanghai Jiao Tong University School of Medicine for assistance with the statistical analyses, and Dr. Bing-Ya Liu of the Department of Digestive Surgery, Shanghai Jiao Tong University School of Medicine for interpretation of data.

COMMENTS

Background

Laparoscopic CO_2-insufflation has been reported to correlate with growth and metastasis of colorectal cancer. However, few studies have addressed the influence of CO_2-insufflation pressure on the biological behaviour of colorectal cancer. The aim of this study is to investigate the influence of CO_2-insufflation pressure on adhesion, invasion and metastatic potential of colon cancer cells based on adhesion molecules expression.

Research frontiers

Recently, it has been reported that the CO_2 insufflation can effect the expression of some adhesion molecules, such as E-cadherin, CD44 and ICAM-1, which are related to the tumor metastasis. But few studies concerning the influence of the CO_2-insufflation pressure on the adhesion molecules and how CO_2 insufflation further impacts on the metastatic potential following altered expression of these adhesion molecules.

Innovations and breakthroughs

In this study, the authors found that CO_2-insufflation induced a temporary change in the adhesion and invasion capacity of cancer cells *in vitro*. High pressures of CO_2-insufflation inhibited the adhesion, invasion and metastatic potential *in vitro* and *in vivo*, which was associated with reduced expression of adhesion molecules.

Applications

The results of their study do not provide any evidence that CO_2-insufflation increases the metastatic potential of colon cancer cells. CO_2-insufflation may be used with oncological safety in laparoscopic surgery for colorectal cancer.

Peer review

The manuscript by Jun-Jun Ma and co-authors is well presented, and deals with a significant clinical issue when tumor tissue is resected. Indeed reoccurrences of tumor nodes stand central as a major post-operative complication. Furthermore, the authors applied an original approach to study this problem *in vitro* and *in situ*. This paper contains important information which might have significant translational medical implications.

REFERENCES

1 **Vittimberga FJ Jr**, Foley DP, Meyers WC, Callery MP. Laparoscopic surgery and the systemic immune response. *Ann Surg* 1998; **227**: 326-334

2 **Alexander RJ**, Jaques BC, Mitchell KG. Laparoscopically assisted colectomy and wound recurrence. *Lancet* 1993; **341**: 249-250

3 **Clinical Outcomes of Surgical Therapy Study Group**. A comparison of laparoscopically assisted and open colectomy for colon cancer. *N Engl J Med* 2004; **350**: 2050-2059

4 **Buunen M**, Veldkamp R, Hop WC, Kuhry E, Jeekel J, Haglind E, Pahlman L, Cuesta MA, Msika S, Morino M, Lacy A, Bonjer HJ. Survival after laparoscopic surgery versus open surgery for colon cancer: long-term outcome of a randomised clinical trial. *Lancet Oncol* 2009; **10**: 44-52

5 **Zheng MH**, Feng B, Lu AG, Li JW, Wang ML, Mao ZH, Hu YY, Dong F, Hu WG, Li DH, Zang L, Peng YF, Yu BM. Laparoscopic versus open right hemicolectomy with curative intent for colon carcinoma. *World J Gastroenterol* 2005; **11**: 323-326

6 **Lecuru F**, Agostini A, Camatte S, Robin F, Aggerbeck M, Jaes JP, Vilde F, Taurelle R. Impact of pneumoperitoneum on tumor growth. *Surg Endosc* 2002; **16**: 1170-1174

7 **Ishida H**, Idezuki Y, Yokoyama M, Nakada H, Odaka A, Murata N, Fujioka M, Hashimoto D. Liver metastasis following pneumoperitoneum with different gases in a mouse model. *Surg Endosc* 2001; **15**: 189-192

8 **Gutt CN**, Kim ZG, Hollander D, Bruttel T, Lorenz M. CO2 environment influences the growth of cultured human cancer cells dependent on insufflation pressure. *Surg Endosc* 2001; **15**: 314-318

9 **Haier J**, Nasralla M, Nicolson GL. Cell surface molecules and their prognostic values in assessing colorectal carcinomas. *Ann Surg* 2000; **231**: 11-24

10 **Jiang WG**. Cell adhesion molecules in the formation of liver metastasis. *J Hepatobiliary Pancreat Surg* 1998; **5**: 375-382

11 **Kinsella AR**, Lepts GC, Hill CL, Jones M. Reduced E-cadherin expression correlates with increased invasiveness in colorectal carcinoma cell lines. *Clin Exp Metastasis* 1994; **12**: 335-342

12 **Shimoyama Y**, Nagafuchi A, Fujita S, Gotoh M, Takeichi M, Tsukita S, Hirohashi S. Cadherin dysfunction in a human cancer cell line: possible involvement of loss of alpha-catenin expression in reduced cell-cell adhesiveness. *Cancer Res* 1992; **52**: 5770-5774

13 **Mohri Y**. Prognostic significance of E-cadherin expression in human colorectal cancer tissue. *Surg Today* 1997; **27**: 606-612

14 **Naor D**, Sionov RV, Ish-Shalom D. CD44: structure, function, and association with the malignant process. *Adv Cancer Res* 1997; **71**: 241-319

15 **Paraskeva PA**, Ridgway PF, Olsen S, Isacke C, Peck DH, Darzi AW. A surgically induced hypoxic environment causes changes in the metastatic behaviour of tumours in vitro. *Clin Exp Metastasis* 2006; **23**: 149-157

16 **Kim ZG**, Mehl C, Lorenz M, Gutt CN. Impact of laparoscopic CO2-insufflation on tumor-associated molecules in cultured colorectal cancer cells. *Surg Endosc* 2002; **16**: 1182-1186

17 **Cai KL**, Wang GB, Xiong LJ. Effects of carbon dioxide and nitrogen on adhesive growth and expressions of E-cadherin and VEGF of human colon cancer cell CCL-228. *World J Gastroenterol* 2003; **9**: 1594-1597

18 **Leung KL**, Kwok SP, Lam SC, Lee JF, Yiu RY, Ng SS, Lai PB, Lau WY. Laparoscopic resection of rectosigmoid carcinoma: prospective randomised trial. *Lancet* 2004; **363**: 1187-1192

19 **Gutt CN**, Kim ZG, Schmandra T, Paolucci V, Lorenz M. Carbon dioxide pneumoperitoneum is associated with increased liver metastases in a rat model. *Surgery* 2000; **127**: 566-570

20 **Ishida H**, Murata N, Idezuki Y. Increased insufflation pressure enhances the development of liver metastasis in a mouse laparoscopy model. *World J Surg* 2001; **25**: 1537-1541

21 **Ishida H**, Hashimoto D, Nakada H, Takeuchi I, Hoshino T, Murata N, Idezuki Y, Hosono M. Increased insufflation pressure enhances the development of liver metastasis in a mouse laparoscopy model: possible mechanisms. *Surg Endosc* 2002; **16**: 331-335

22 **Kuntz C**, Kienle P, Schmeding M, Benner A, Autschbach F, Schwalbach P. Comparison of laparoscopic versus conventional technique in colonic and liver resection in a tumor-bearing small animal model. *Surg Endosc* 2002; **16**: 1175-1181

23 **Shiozaki H**, Oka H, Inoue M, Tamura S, Monden M. E-cadherin mediated adhesion system in cancer cells. *Cancer* 1996; **77**: 1605-1613

24 **Jiang WG**. E-cadherin and its associated protein catenins, cancer invasion and metastasis. *Br J Surg* 1996; **83**: 437-446

25 **Nomura M**, Sugiura Y, Tatsumi Y, Miyamoto K. Adhesive interaction of highly malignant hepatoma AH66F cells with mesothelial cells. *Biol Pharm Bull* 1999; **22**: 738-740

26 **Ye C**, Kiriyama K, Mistuoka C, Kannagi R, Ito K, Watanabe T, Kondo K, Akiyama S, Takagi H. Expression of E-selectin on endothelial cells of small veins in human colorectal cancer. *Int J Cancer* 1995; **61**: 455-460

27 **Tahara K**, Fujii K, Yamaguchi K, Suematsu T, Shiraishi N, Kitano S. Increased expression of P-cadherin mRNA in the mouse peritoneum after carbon dioxide insufflation. *Surg Endosc* 2001; **15**: 946-949

28 **Ziprin P**, Ridgway PF, Peck DH, Darzi AW. Laparoscopic enhancement of tumour cell binding to the peritoneum is inhibited by anti-intercellular adhesion molecule-1 monoclonal antibody. *Surg Endosc* 2003; **17**: 1812-1817

29 **Gutt CN**, Gessmann T, Schemmer P, Mehrabi A, Schmandra T, Kim ZG. The impact of carbon dioxide and helium insufflation on experimental liver metastases, macrophages, and cell adhesion molecules. *Surg Endosc* 2003; **17**: 1628-1631

S- Editor Tian L **L- Editor** Webster JR **E- Editor** Ma WH

Online Submissions: wjg.wjgnet.com
wjg@wjgnet.com
doi:10.3748/wjg.15.2723

World J Gastroenterol 2009 June 14; 15(22): 2723-2730
World Journal of Gastroenterology ISSN 1007-9327

Biochemical metabolic changes assessed by ^{31}P magnetic resonance spectroscopy after radiation-induced hepatic injury in rabbits

Ri-Sheng Yu, Liang Hao, Fei Dong, Jian-Shan Mao, Jian-Zhong Sun, Ying Chen, Min Lin, Zhi-Kang Wang, Wen-Hong Ding

Ri-Sheng Yu, Liang Hao, Fei Dong, Jian-Zhong Sun, Ying Chen, Zhi-Kang Wang, Wen-Hong Ding, Department of Radiology, Second Affiliated Hospital, Zhejiang University School of Medicine, Hangzhou 310009, Zhejiang Province, China
Jian-Shan Mao, Department of Internal Medicine, Second Affiliated Hospital, Zhejiang University School of Medicine, Hangzhou 310009, Zhejiang Province, China
Min Lin, Department of Pathology, Second Affiliated Hospital, Zhejiang University School of Medicine, Hangzhou 310009, Zhejiang Province, China
Author contributions: Yu RS and Mao JS contributed equally to this work; Yu RS and Mao JS designed the research; Yu RS, Hao L, Dong F, Mao JS, Sun JZ, Chen Y, Lin M, Wang ZK and Ding WH performed the research; Yu RS, Mao JS, Hao L, Chen Y and Dong F analyzed the data; Yu RS, Dong F and Chen Y wrote the paper.
Supported by The National Natural Science Foundation of China, No. 30770626 and the Great Transversal Science Foundation of Zhejiang Province, China, No. 491020I20857
Correspondence to: Dr. Jian-Shan Mao, Department of Internal Medicine, the Second Affiliated Hospital, Zhejiang University School of Medicine, Hangzhou 310009, Zhejiang Province, China. jshmao@zju.edu.cn
Telephone: +86-571-87783859 Fax: +86-571-87784556
Received: February 28, 2009 Revised: April 7, 2009
Accepted: April 14, 2009
Published online: June 14, 2009

Abstract

AIM: To compare the features of biochemical metabolic changes detected by hepatic phosphorus-31 magnetic resonance spectroscopy (^{31}P MRS) with the liver damage score (LDS) and pathologic changes in rabbits and to investigate the diagnostic value of ^{31}P MRS in acute hepatic radiation injury.

METHODS: A total of 30 rabbits received different radiation doses (ranging 5-20 Gy) to establish acute hepatic injury models. Blood biochemical tests, ^{31}P MRS and pathological examinations were carried out 24 h after irradiation. The degree of injury was evaluated according to LDS and pathology. Ten healthy rabbits served as controls. The MR examination was performed on a 1.5 T imager using a ^{1}H/^{31}P surface coil by the 2D chemical shift imaging technique. The relative quantities of phosphomonoesters (PME), phosphodiesters (PDE), inorganic phosphate (Pi) and adenosine triphosphate (ATP) were measured. The data were statistically analyzed.

RESULTS: (1) Relative quantification of phosphorus metabolites: (a) ATP: there were significant differences (P < 0.05) (LDS-groups: control group *vs* mild group *vs* moderate group *vs* severe group, 1.83 ± 0.33 *vs* 1.55 ± 0.24 *vs* 1.27 ± 0.09 *vs* 0.98 ± 0.18; pathological groups: control group *vs* mild group *vs* moderate group *vs* severe group, 1.83 ± 0.33 *vs* 1.58 ± 0.25 *vs* 1.32 ± 0.07 *vs* 1.02 ± 0.18) of ATP relative quantification among control group, mild injured group, moderate injured group, and severe injured group according to both LDS grading and pathological grading, respectively, and it decreased progressively with the increased degree of injury (r = -0.723, P = 0.000). (b) PME and Pi; the relative quantification of PME and Pi decreased significantly in the severe injured group, and the difference between the control group and severe injured group was significant (P < 0.05) (PME: LDS-control group *vs* LDS-severe group, 0.86 ± 0.23 *vs* 0.58 ± 0.22, P = 0.031; pathological control group *vs* pathological severe group, 0.86 ± 0.23 *vs* 0.60 ± 0.21, P = 0.037; Pi: LDS-control group *vs* LDS-severe group, 0.74 ± 0.18 *vs* 0.43 ± 0.14, P = 0.013; pathological control group *vs* pathological severe group, 0.74 ± 0.18 *vs* 0.43 ± 0.14, P = 0.005) according to LDS grading and pathological grading, respectively. (c) PDE; there were no significant differences among groups according to LDS grading, and no significant differences between the control group and experimental groups according to pathological grading. (2) The ratio of relative quantification of phosphorus metabolites: significant differences (P < 0.05) (LDS-moderate group and LDS-severe group *vs* LDS-control group and LDS-mild group, 1.94 ± 0.50 and 1.96 ± 0.72 *vs* 1.43 ± 0.31 and 1.40 ± 0.38) were only found in PDE/ATP between the moderate injured group, the severe injured group and the control group, the mild injured group. No significant difference was found in other ratios of relative quantification of phosphorus metabolites.

CONCLUSION: ^{31}P MRS is a useful method to evaluate early acute hepatic radiation injury. The relative quantification of hepatic ATP levels, which can reflect the pathological severity of acute hepatic radiation injury, is correlated with LDS.

Key words: Liver; Magnetic resonance spectroscopy; Animal models; Pathology; Adenosine triphosphate

Peer reviewers: Dr. Cintia Siqueira, Institute of Molecular Medicine, Center of Gastroenterology, Av.Prof. Egas Moniz, Lisboa 1649-028, Portugal; Ezio Laconi, MD, PhD, Professor of General Pathology, Department of Sciences and Biomedical Technologies, Unit of Experimental Pathology, University of Cagliari, Via Porcell, 4-IV Piano, 09125 Cagliari, Italy

Yu RS, Hao L, Dong F, Mao JS, Sun JZ, Chen Y, Lin M, Wang ZK, Ding WH. Biochemical metabolic changes assessed by ^{31}P magnetic resonance spectroscopy after radiation-induced hepatic injury in rabbits. *World J Gastroenterol* 2009; 15(22): 2723-2730 Available from: URL: http://www.wjgnet.com/1007-9327/15/2723.asp DOI: http://dx.doi.org/10.3748/wjg.15.2723

INTRODUCTION

Acute hepatic radiation injury can lead to necrosis of hepatocytes, fatty degeneration and hepatic fibrosis. The current gold standard test is liver biopsy. This procedure is invasive, uncomfortable for the patient and sometimes leads to serious complications. These factors highlight the need for a noninvasive test to characterize diffuse liver disease. Already, it has been reported that phosphorus-31 magnetic resonance spectroscopy (^{31}P MRS) not only complements liver biopsy but also is a possible replacement and, furthermore, ^{31}P MRS has a particular value in assessing disease progression[1].

^{31}P MRS has been used to study liver metabolism *in vivo* for several years, including clinical liver disease[1-5] and experimental studies[6-8]. It enables the observation of energy metabolism through the signals of phosphomonoesters (PME), phosphodiesters (PDE), inorganic phosphate (Pi) and adenosine triphosphate (ATP). The PME and PDE signals are multi-component, with phosphorylcholine and phosphorylethanolamine the main contributors to PME as well as glycerophosphorylcholine and glycerophosphorylethanolamine which are the main contributors to PDE[1]. The final typical signal of ^{31}P MR spectra *in vivo* is phosphocreatine (PCr). Although it is a dominant signal in muscles, it is not readily observable in spectra of the liver because of its small contribution to hepatic metabolic processes. Its presence indicates some contribution of signals from abdominal wall muscles as a partial volume effect.

In this study, we investigated whether changes of ^{31}P MRS in the liver with early acute radiation injury were related to the liver damage score (LDS) and pathologic changes, we determined the value of ^{31}P MRS in detecting early acute hepatic radiation injury, and we identified the most valuable phosphorylated metabolite for detecting acute hepatic injury. This study set out to provide a rationale for clinical application of ^{31}P MRS in diffuse liver disease.

MATERIALS AND METHODS

Hepatic radiation injury model and experimental groups

This study was approved by the Animal Care Committee of Zhejiang University, School of Medicine. Forty healthy adult New Zealand white rabbits weighing 2.5-3.0 kg were used. These rabbits were randomly assigned into four groups of 10 rabbits. (1) Control group: without any treatment; (2) Group 1: the hepatic region of each rabbit received a single 5 Gy dose of radiation using an 8 MeV electron beam; (3) Group 2: the hepatic region of each rabbit received a single 10 Gy dose of radiation using an 8 MeV electron beam; (4) Group 3: the hepatic region of each rabbit received a single 20 Gy dose of radiation using an 8 MeV electron beam. The irradiation was confined to the whole liver by imaging-guidance. Blood biochemical tests and ^{31}P MRS were carried out 24 h after irradiation. Following each MRS examination, animals were sacrificed, and the liver samples were collected for pathological examination.

MRS examination and spectra evaluation

MRS examination was performed on a Siemens Sonata (Erlangen, Germany) whole-body MR imager operating at 1.5 Tesla equipped with a commercial dual ^{1}H/^{31}P surface coil. Prior to MR examination, animals were fasted overnight. A skin mark in the center of the hepatic region was used in each rabbit at first examination to reduce error. All MR examinations were performed between 8:00 am and 12:00 noon and animals were anesthetized with pentothal sodium (the depth of anesthesia kept well under control) and placed in a prone position with the liver centered on the surface coil.

The basic MR images in all orientations were obtained with true fast imaging with steady precession (true FISP) sequence for the localization of voxels. ^{31}P MR spectra were measured using a standard 2-dimensional chemical shift imaging (CSI) technique[9] in the transverse plane with the following parameters: TR = 440 ms, TE = 2.3 ms, matrix 8 × 8, viewing interpolation 16 × 16, field of view = 200 mm, mean number of times = 120, flip angle = 90 degrees, thickness = 4 cm, voxel volume 2.5 cm × 2.5 cm × 4 cm, acquisition time = 7.36 min. Respiration gating was not used.

Spectra were evaluated using Siemens syngo 2004B software. Briefly, the free induction decay underwent 10 kHz exponential line broadening prior to Fourier transformation, and the resulting spectra were processed with manual phase and baseline correction. Peaks were registered relative to α-ATP resonance (-7.5 ppm), which served as an internal chemical shift reference. Finally, peak integrals were calculated by Gaussian curve fitting with all signals treated as singlets. Signal intensities of PME, Pi, PDE and β-ATP (α-ATP and γ-ATP signals

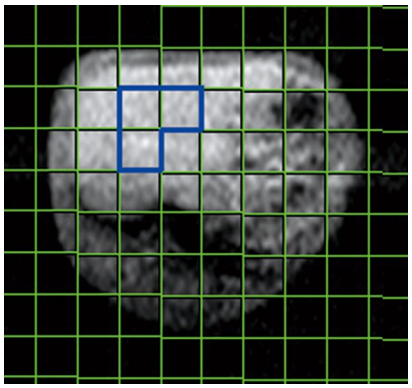

Figure 1 Orientation of CSI: the location of VOI of three voxels being selected in the largest section of rabbit liver on MRI with true FISP sequence.

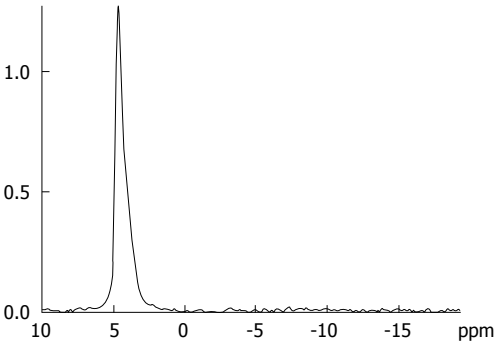

Figure 2 ^{31}P magnetic resonance spectrum from a 500 mL phosphate (NaH_2PO_4) solution phantom with 0.05 mol/L concentrations.

were not used for the evaluation because of overlap with signals of other compounds), which are derived from the integral values of peaks on the spectra, were used for the measurement of relative quantification of metabolites. Volume of interest (VOI) for quantitative evaluation was selected in the center of the liver and the mean integral value of peaks of three voxels on the spectra was used for quantification of metabolites for a rabbit to reduce error (Figure 1).

Phantom experiments were performed before the detection of relative quantification of hepatic metabolites in each rabbit to reduce error induced by the MR imager and environment factors[6,10]. A 500 mL phosphate (NaH_2PO_4) solution phantom with 0.05 mol/L concentration served as a phantom, on which identical MRS examinations were performed regularly throughout the experiment (Figure 2).

For the phantom, the relative quantification of phosphate was 16.6 ± 0.5, and the coefficient of variation was 3.03% (0.5/16.6). The ratio of relative quantification of phosphate between 2 d was conducted as the MRS correction factor (CF) of our MR imager, which was used to correct the relative quantification of hepatic metabolites in each rabbit. Therefore, all the relative quantification of phosphorus metabolites was corrected relative quantification. (corrected relative quantification = relative quantification × CF).

The corrected relative quantification might decrease the error made by the MR imager and the environmental factor in the room, and guarantee the comparability of various relative quantification of phosphorus metabolites.

Table 1 The criteria of liver damage score

Grade	Albumin (g/L)	γ-globulins (g/L)	AST (U/L)	Conjugated bilirubin (μmol/L)	Creatinine (μmol/L)
0	> 36.5	< 19.9	< 50	< 6	< 119
1	32.9-36.4	20-26	51-180	7-32	120-150
2	28.5-32.8	26.1-34.9	181-384	33-75	151-230
3	24.5-28.4	> 35	> 385	> 76	> 231
4	21.8-24.4				
5	< 21.7				

Evaluation of the degree of injury

This study adopted two methods to evaluate the degree of injury: LDS grading and pathological grading.

LDS grading: Sera were isolated from collected blood samples, and serum aspartate aminotransferase, alanine aminotransferase, alkaline phosphatase, r-glutamyl transpeptidase, albumin, globulin and albumin/globulin levels were measured by Olympus 2700 analyzer. Then the LDS was calculated for each rabbit according to Krastev's standard (Table 1)[11]. The degree of injury of the liver was divided into mild (LDS ⩽ 3 U), moderate (LDS 3-6 U) and severe (LDS > 6 U).

Pathological grading: The paraffin-section method and hematoxylin and eosin stain was applied to all liver samples, which were read by a single independent liver pathologist (Dr. Lin M) and assessed for swelling, degeneration, necrosis of hepatocytes, and hepatic hemorrhage. The pathologist was blinded to dose of radiation received and the results of ^{31}P MRS. (1) Normal group (control group): normal hepatocytes, integrity of structure of hepatic lobules and regular arrangement of hepatic cord (Figure 3A). (2) Mild group: mild cellular swelling, fatty degeneration and (or) hydropic degeneration, without cell necrosis or hepatic hemorrhage (Figure 3B). (3) Moderate group: moderate cellular swelling and fatty degeneration accompanied by punctal necrosis and stray bleeding points (Figure 3C). (4) Severe group: diffuse cellular swelling and fatty degeneration, with constriction or emphraxis of hepatic sinuses, with or without local cell necrosis and (or) hepatic hemorrhage (Figure 3D).

Statistical analysis

The data were expressed as mean ± SD. Analysis of variance with SNK tests (the Student-Newman-Keuls post-hoc tests) of one-way ANOVA with SPSS 11.0 was used to examine differences between groups. Using Pearson's correlation test, the correlation between relative quantification of ATP and LDS was examined. $P < 0.05$ were considered to indicate statistical significance.

RESULTS

Analysis of hepatic phosphorylated metabolite levels

For the control group, all rabbits had normal hepatic

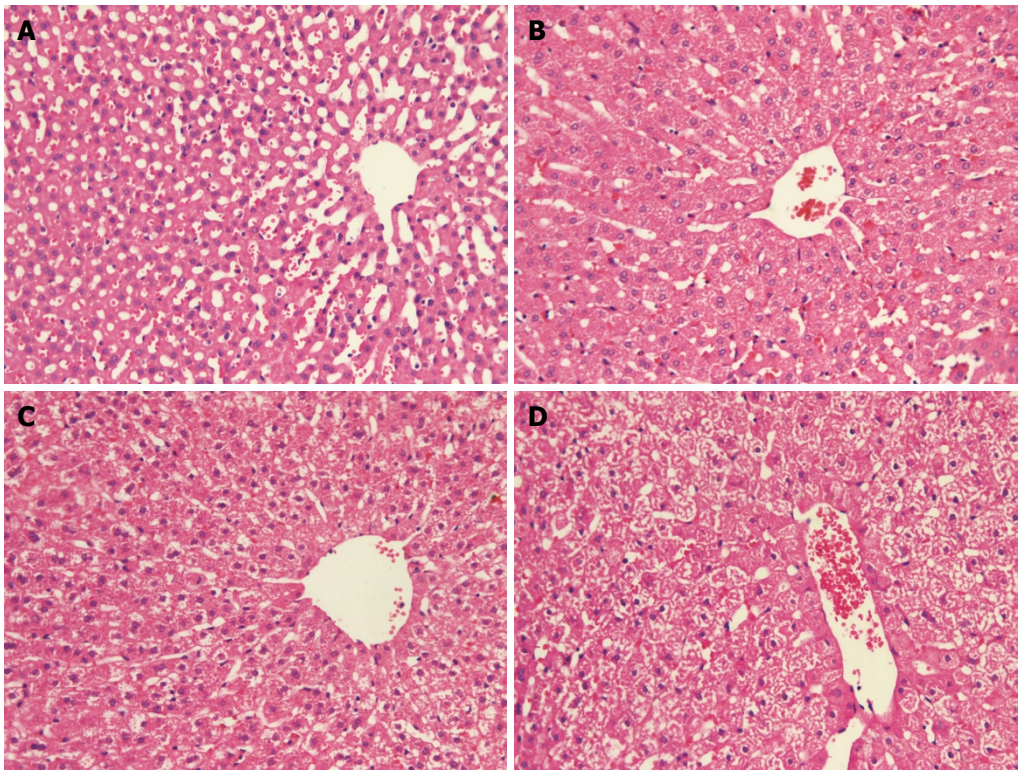

Figure 3 Hepatic ^{31}P MRS of the liver from a rabbit of the control group (A), mild injury group (B), moderate injury group (C) and severe injury group (D). A significant decrease in the ATP signal is seen in the ^{31}P MR spectra (C, D).

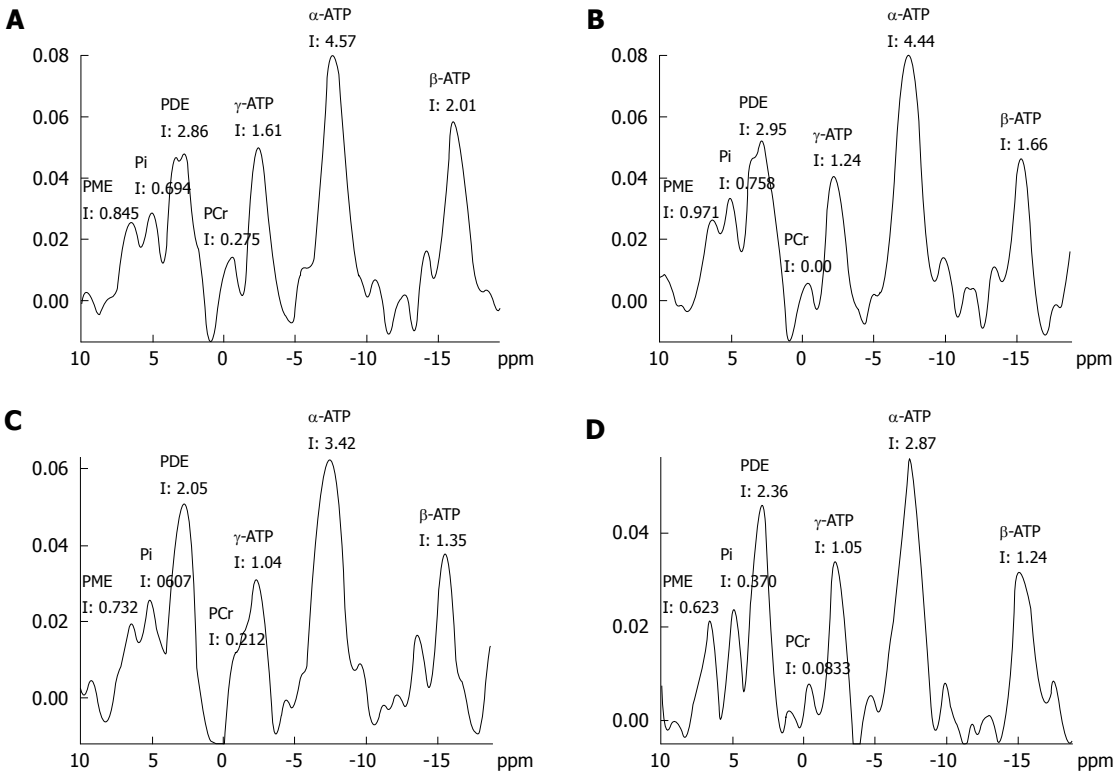

Figure 4 Representative histological section of the liver from a rabbit of the control group (A), mild injury group (B), moderate injury group (C) and severe injury group (D). I: Integral.

micro-structure and a LDS of zero, while rabbits in the experimental groups varied between each other in pathology and LDS, depending on the degree of injury. The spectroscopic data of rabbits in the control group and rabbits with acute hepatic radiation injury, grouped by LDS are summarized in Table 2. The spectroscopic data of rabbits in the control group and rabbits with acute hepatic radiation injury, grouped by pathology are summarized in Table 3. The relative quantification of phosphorus metabolites detected by MRS included PME, PDE, Pi and ATP (Figure 4).

The preceding two tables (Tables 2 and 3) showed

Table 2 Relative quantification of metabolites in rabbit liver using the LDS evaluation method (mean ± SD)

Metabolite	Control group (n = 10)	LDS-mild group (n = 13)	LDS-moderate group (n = 9)	LDS-severe group (n = 8)	F	P
PME	0.86 ± 0.23[j]	0.79 ± 0.33	0.80 ± 0.22	0.58 ± 0.22[a]	1.852	0.155
PDE	2.27 ± 0.62	2.14 ± 0.51	2.48 ± 0.63	1.99 ± 0.88	3.023	0.042
Pi	0.74 ± 0.18[j]	0.63 ± 0.28	0.62 ± 0.29	0.43 ± 0.14[a]	3.475	0.026
ATP	1.83 ± 0.33[e,i,l]	1.55 ± 0.24[b,h,l]	1.27 ± 0.09[c,e,j]	0.98 ± 0.18[c,f,g]	22.647	0.000
PME/PDE	0.36 ± 0.12	0.39 ± 0.18	0.35 ± 0.14	0.44 ± 0.54	0.462	0.710
PME/ATP	0.50 ± 0.11	0.50 ± 0.18	0.62 ± 0.15	0.61 ± 0.25	0.990	0.409
PDE/ATP	1.43 ± 0.31[g,j]	1.40 ± 0.38[g,j]	1.94 ± 0.50[a,d]	1.96 ± 0.72[a,d]	5.080	0.005
Pi /ATP	0.40 ± 0.09	0.41 ± 0.19	0.49 ± 0.24	0.46 ± 0.16	1.582	0.211
PME/Pi	1.47 ± 0.65	1.49 ± 0.92	1.76 ± 1.12	1.39 ± 0.58	0.081	0.970
PDE/Pi	3.46 ± 1.15	4.26 ± 2.58	4.91 ± 2.65	5.05 ± 3.18	0.902	0.450

[a]P < 0.05, [b]P < 0.01, [c]P < 0.005 *vs* control group; [d]P < 0.05, [e]P < 0.01, [f]P < 0.005 *vs* mild group; [g]P < 0.05, [h]P < 0.01, [i]P < 0.005 *vs* moderate group; [j]P < 0.05, [k]P < 0.01, [l]P < 0.005 *vs* severe group.

Table 3 Relative quantification of metabolites in rabbit liver with the pathological evaluation method

Metabolite	Control group (n = 10)	Pathological mild group (n = 12)	Pathological moderate group (n = 11)	Pathological severe group (n = 7)	F	P
PME	0.86 ± 0.23[j]	0.82 ± 0.35	0.79 ± 0.24	0.60 ± 0.21[a]	1.861	0.154
PDE	2.27 ± 0.62	2.08 ± 0.47[g]	2.67 ± 0.38[d,k]	1.92 ± 0.83[h]	1.118	0.355
Pi	0.74 ± 0.18[k]	0.61 ± 0.24	0.7 ± 0.33[j]	0.43 ± 0.14[b,g]	2.334	0.090
ATP	1.83 ± 0.33[d,i,l]	1.58 ± 0.25[a,g,l]	1.32 ± 0.07[c,d,k]	1.02 ± 0.18[c,f,h]	22.878	0.000
PME/PDE	0.36 ± 0.12	0.40 ± 0.18	0.31 ± 0.13	0.45 ± 0.48	0.189	0.903
PME/ATP	0.50 ± 0.11[h]	0.51 ± 0.19[i]	0.60 ± 0.18[b,f]	0.59 ± 0.22	1.412	0.255
PDE/ATP	1.43 ± 0.31[h]	1.34 ± 0.33[i,j]	2.04 ± 0.36[b,f]	1.83 ± 0.72[d]	4.082	0.014
Pi/ATP	0.40 ± 0.09	0.39 ± 0.15	0.54 ± 0.26	0.43 ± 0.16	0.601	0.619
PME/Pi	1.47 ± 0.65	1.57 ± 0.97	1.44 ± 1.03	1.61 ± 0.75	0.316	0.814
PDE/Pi	3.46 ± 1.15	4.12 ± 2.36	4.87 ± 2.63	5.09 ± 3.24	0.810	0.497

[a]P < 0.05, [b]P < 0.01, [c]P < 0.005 *vs* control group; [d]P < 0.05, [e]P < 0.01, [f]P < 0.005 *vs* mild group; [g]P < 0.05, [h]P < 0.01, [i]P < 0.005 *vs* moderate group; [j]P < 0.05, [k]P < 0.01, [l]P < 0.005 *vs* severe group.

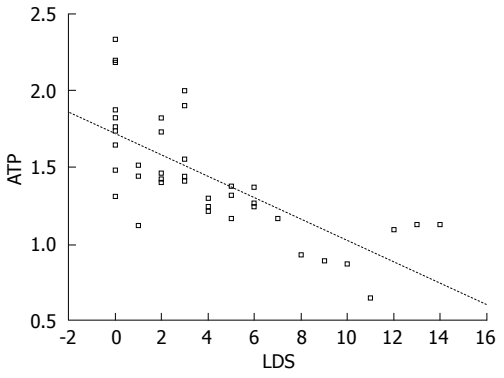

Figure 5 The graph shows the correlation between LDS and ATP, that is, the ATP relative quantification decreases progressively with the increase of LDS.

the relation between biochemical index and relative quantification of phosphorus metabolites, as well as the relation between pathology and relative quantification of phosphorus metabolites. However, the results evaluated with LDS and pathology were of perfect consistency. The analysis is detailed below.

Characteristics of relative quantification of hepatic phosphorus metabolites

ATP: There were significant differences in ATP relative quantification among the control group, mild group, moderate group, and severe group according to both LDS grading and pathological grading (LDS groups: mild group, moderate group, severe group *vs* control group had P = 0.007, 0.000, 0.000, respectively; moderate group, severe group *vs* mild group had P = 0.008, 0.000, respectively; severe group *vs* moderate group had P = 0.013. Pathological groups: mild group, moderate group, severe group *vs* control group had P = 0.017, 0.000, 0.000, respectively; moderate group, severe group *vs* mild group had P = 0.000, 0.000, respectively; severe group *vs* moderate group had P = 0.008); it decreased progressively with the increased degree of injury, which is visually displayed by the correlation graph of ATP and LDS (Figure 5). These data illustrated that the hepatic ATP level may be the most sensitive criterion for reflecting hepatic injury in rabbits.

PME and Pi: The relative quantification of PME and Pi decreased significantly in the severe injured group, and the difference was significant compared with the control group (PME: LDS-severe group *vs* LDS-control group had P = 0.031, pathological-severe group *vs* pathological-control group had P = 0.037. Pi: LDS-severe group *vs* LDS-control group had P = 0.013, pathological-severe group *vs* pathological-control group had P = 0.005). Also, from the ^{31}P MR spectra (Figure 4C and D), a significant decrease in the signal of phosphorylated metabolites could be seen. This indicated that if there was a significant

difference in PME and Pi between normal data and test data, the tested liver was likely to be severely injured.

PDE: The relative quantification of various hepatic PDE levels changed irregularly, which indicated that the relative quantification levels of PDE may not be applied solely to assess acute hepatic radiation injury.

The characteristics of the ratio of relative quantification of other phosphorus metabolites

There were significant changes in the PDE/ATP ratio between control group and moderate group; mild group and moderate, severe group; moderate group and control group, mild group (LDS-groups: moderate group, severe group *vs* control group had $P = 0.026$, 0.025, respectively; moderate group, severe group *vs* control group had $P = 0.014$, 0.014, respectively; pathological-groups: moderate group, severe group *vs* control group had $P = 0.076$, 0.064, respectively; moderate group, severe group *vs* control group had $P = 0.002$, 0.020, respectively). There were no significant changes in the PDE/Pi ratio among all groups. Compared with the control group, no significant changes of PME/PDE, Pi/ATP and PME/Pi ratio were found in other groups.

The above results illustrated that there were few characteristic differences in the ratios of relative quantification of various hepatic phosphorus metabolites in hepatic radiation injury. Therefore, the ratios of relative quantification may not be used to evaluate acute mild hepatic radiation injury.

DISCUSSION

Acute liver diseases can result from various causes which operate through different pathophysiological pathways and which elicit distinct patterns of hepatic injury. Diagnosis of acute liver diseases including hepatic radiation injury is mainly based on invasive methods such as liver biopsy, laparoscopy, various radiological examinations and other clinical tests. On the other hand, signals from ^{31}P MRS reflect *in vivo* intracellular and membrane metabolism non-invasively and they are objective parameters[2,12].

Evaluation method for ^{31}P MRS and its influencing factors

The evaluation of ^{31}P MRS in the liver includes absolute or relative quantification of metabolite levels. Nowadays, absolute quantification of metabolites in mmol/L is hampered by the use of too short TR values and other technical complications[13,14], but most studies with ^{31}P MRS deal with the relative signal intensity for quantification. Also, here we measured the relative quantification of metabolites, and the relative signal ratios of the metabolites. The relative quantification evaluation had to satisfy 3 conditions for decreasing detection errors: (1) phantom experiments before relative quantification of hepatic metabolites in each rabbit to reduce errors induced by the MR imager and environment factors, *etc*; (2) a VOI selected in the largest section of liver and a small PCr signal characterizing the presence of abdominal muscles; (3) moderate anesthesia of rabbits and keeping the rabbits in the same position in the bed of the MR imager.

The changes in hepatic ATP levels

Many published studies of ^{31}P MR spectra have shown that acute and chronic diffuse liver diseases are associated with a reduction in hepatic ATP levels[3,6,7], and some studies found that changes in hepatic ATP levels correlate with changes in liver histology[3,6]. Our findings, that the relative quantification of hepatic ATP levels displayed progressive reductions with increased hepatic injury, correspond to the results of a previous study[6], but we are the first to report that the changes in hepatic ATP levels correlate with the severity of acute hepatic radiation injury. Some reports have shown that, during the early phase of chronic diffuse liver diseases, only minor changes in hepatic ATP could be detected[15,16]. Our study showed that the relative quantification of hepatic ATP levels obviously decreased, because there were significant differences between the control group and both the pathological-mild group and LDS-mild group. We also found that the changes in levels of other hepatic metabolites were less sensitive than the changes in ATP levels in mild hepatic injury, and the relative quantification of hepatic ATP levels could be well correlated with LDS. Thus, we suggest that the hepatic ATP level may be the most reliable criterion for evaluating acute hepatic injury in rabbits. The reason is that the β-ATP peak is unique, and quite different from other phosphorylated metabolite peaks, which overlap with signals of other metabolites in the ^{31}P MRS map.

The mechanisms responsible for the decline in hepatic ATP levels include: gradual loss of viable hepatocytes, which is likely to be an important contributing factor-as the total amount of these cells per unit volume of liver decreases, MRS detectable signal from that volume will also decrease[6]; anoxemia of local liver tissue induced by injury of capillary vessels after hepatic radiation[17]; increased energy expenditure as liver disease progresses[18]. In addition, disturbed hepatic bioenergetics has also been ascribed to the capillarization of hepatic sinusoids during the development of cirrhosis[19].

The changes in levels and ratios of relative quantification of other phosphorus metabolites

PME, PDE and the correlation ratio: information about phospholipid membrane metabolism may also be obtained from the PME and PDE resonances in the ^{31}P MR spectrum. Both resonances are multicomponent peaks containing contributions from several metabolites[20]. The significance of the changes in PME and PDE levels is not clear. Some previous studies have reported that an increase in PME levels is accompanied by a decrease in PDE levels or increased ratios of hepatic PME/ATP and PME/PDE in acute and chronic diffuse liver diseases[1,2,21,22]. However, in other investigators, and our study, PME levels did not increase nor did PDE levels decrease in the same acute and chronic diffuse

liver diseases[6,8]. The main reason for these conflicting findings may be the broad, overlapping characteristics of these peaks along with the multiple signals contributing to these resonances hindering accurate quantification of the PME and PDE peaks[8]. Another explanation is that hepatic phospholipid membrane activity may differ in animal models of liver diseases versus liver diseases in humans[6]. Therefore, either the changes in PME and PDE levels or the ratio PME/PDE cannot accurately reflect the liver diseases.

Pi and the correlation ratio: Pi is another marker of tissue bioenergetics. Increases in Pi have been observed by ^{31}P MRS during high energy activities such as liver regeneration following partial hepatectomy[8,23]. The increase in hepatic Pi may result from the hydrolysis of high energy phosphate bonds which in turn liberates Pi species, increases hepatic uptake and accumulation of Pi due to enhanced metabolic activity and reduces recycling back to purine/pyrimidine moieties[8]. Some previous studies have reported a decrease or no difference in Pi levels in chronic diffuse liver diseases in humans and animals[1,6]. The reason for no changes in hepatic Pi is not clear, but the decrease in hepatic Pi may result from reduced hepatocyte mass[6]. In this study, significant decreases in Pi were only detected among the most seriously injured livers of the severe group. The lower levels of hepatic Pi likely result from reduced hepatocyte mass, as Corbin *et al*[6] reported. In addition, compared with the ATP peak, the Pi peak, which is located between the PME and PDE peaks, is more prone to being impacted by the overlapping characteristics of PME and PDE peaks, hindering accurate quantification of the Pi peak. However, some authors regarded the ratio ATP/Pi as the criterion of hepatic regenerative activity following partial hepatectomy, because the ATP levels decreased, the Pi levels increased, and the changes of the ratio were more sensitive than ATP or Pi alone[8]. However, the levels of ATP or Pi were decreased to different degrees after acute hepatic radiation injury in our study, so the ratio of ATP/Pi could not be used to evaluate acute hepatic radiation injury.

This study illustrated that ^{31}P MRS of clinical 1.5T MRS could detect various changes of phosphorylated metabolite levels in early acute hepatic injury. In addition, the study also showed that though there were many hepatic phosphorylated metabolites and correlated ratios, the measurement of levels of hepatic ATP may be the most reliable criterion for reflecting both pathological hepatic injury and LDS in rabbits.

COMMENTS

Background

Acute hepatic radiation injury can lead to necrosis of hepatocytes, fatty degeneration and hepatic fibrosis. The current gold standard test is liver biopsy. This procedure is invasive, uncomfortable for the patient and sometimes has serious complications. These factors highlight the need for a noninvasive test to characterize diffuse liver disease. Already, it has been reported that phosphorus-31 magnetic resonance spectroscopy (^{31}P MRS) not only complements liver biopsy but also is a possible replacement, and furthermore, ^{31}P MRS has particular value in assessing disease progression.

Research frontiers

^{31}P MRS has been used to study liver metabolism *in vivo* for several years, including clinical liver disease studies and experimental studies. The research focus is how to observe the energy metabolism or pathological changes through the signals of phosphorus metabolites.

Innovations and breakthroughs

In this study the authors carefully used two different methods [liver damage score (LDS), and pathology] to evaluate the degree of injury, and then they studied the correlation between MRS and the degree of injury. Furthermore, they report that the changes in hepatic adenosine triphosphate (ATP) levels correlate with the severity of acute hepatic radiation injury measured by LDS.

Applications

This study may be particularly useful for allowing clinical detection of early acute hepatic injury with ^{31}P MRS in the future.

Terminology

MRS: Spectroscopic method for measuring the magnetic moment of elementary particles such as atomic nuclei, protons or electrons. It is employed in clinical applications such as NMR Tomography (magnetic resonance imaging).

Peer review

^{31}P MRS is a very interesting method especially to replace the gold standard biopsy, particularly in assessing disease progression.

REFERENCES

1 **Lim AK**, Patel N, Hamilton G, Hajnal JV, Goldin RD, Taylor-Robinson SD. The relationship of in vivo 31P MR spectroscopy to histology in chronic hepatitis C. *Hepatology* 2003; **37**: 788-794

2 **Munakata T**, Griffiths RD, Martin PA, Jenkins SA, Shields R, Edwards RH. An in vivo 31P MRS study of patients with liver cirrhosis: progress towards a non-invasive assessment of disease severity. *NMR Biomed* 1993; **6**: 168-172

3 **Corbin IR**, Ryner LN, Singh H, Minuk GY. Quantitative hepatic phosphorus-31 magnetic resonance spectroscopy in compensated and decompensated cirrhosis. *Am J Physiol Gastrointest Liver Physiol* 2004; **287**: G379-G384

4 **Taylor-Robinson SD**. Applications of magnetic resonance spectroscopy to chronic liver disease. *Clin Med* 2001; **1**: 54-60

5 **Mann DV**, Lam WW, Hjelm NM, So NM, Yeung DK, Metreweli C, Lau WY. Human liver regeneration: hepatic energy economy is less efficient when the organ is diseased. *Hepatology* 2001; **34**: 557-565

6 **Corbin IR**, Buist R, Peeling J, Zhang M, Uhanova J, Minuk GY. Hepatic 31P MRS in rat models of chronic liver disease: assessing the extent and progression of disease. *Gut* 2003; **52**: 1046-1053

7 **Corbin IR**, Buist R, Peeling J, Zhang M, Uhanova J, Minuk GK. Utility of hepatic phosphorus-31 magnetic resonance spectroscopy in a rat model of acute liver failure. *J Investig Med* 2003; **51**: 42-49

8 **Corbin IR**, Buist R, Volotovskyy V, Peeling J, Zhang M, Minuk GY. Regenerative activity and liver function following partial hepatectomy in the rat using (31)P-MR spectroscopy. *Hepatology* 2002; **36**: 345-353

9 **Dezortova M**, Taimr P, Skoch A, Spicak J, Hajek M. Etiology and functional status of liver cirrhosis by 31P MR spectroscopy. *World J Gastroenterol* 2005; **11**: 6926-6931

10 **Meyerhoff DJ**, Karczmar GS, Matson GB, Boska MD, Weiner MW. Non-invasive quantitation of human liver metabolites using image-guided 31P magnetic resonance spectroscopy. *NMR Biomed* 1990; **3**: 17-22

11 **Krastev Z**. Liver damage score--a new index for evaluation of the severity of chronic liver diseases. *Hepatogastroenterology* 1998; **45**: 160-169

12 **Taylor-Robinson SD**, Sargentoni J, Bell JD, Saeed N, Changani KK, Davidson BR, Rolles K, Burroughs AK, Hodgson HJ, Foster CS, Cox IJ. In vivo and in vitro hepatic 31P magnetic resonance spectroscopy and electron microscopy of the cirrhotic liver. *Liver* 1997; **17**: 198-209

13 **Murphy-Boesch J**, Jiang H, Stoyanova R, Brown TR.

Quantification of phosphorus metabolites from chemical shift imaging spectra with corrections for point spread effects and B1 inhomogeneity. *Magn Reson Med* 1998; **39**: 429-438

14 **Sijens PE**, Dagnelie PC, Halfwerk S, van Dijk P, Wicklow K, Oudkerk M. Understanding the discrepancies between 31P MR spectroscopy assessed liver metabolite concentrations from different institutions. *Magn Reson Imaging* 1998; **16**: 205-211

15 **Kaita KD**, Pettigrew N, Minuk GY. Hepatic regeneration in humans with various liver disease as assessed by Ki-67 staining of formalin-fixed paraffin-embedded liver tissue. *Liver* 1997; **17**: 13-16

16 **Kawakita N**, Seki S, Yanai A, Sakaguchi H, Kuroki T, Mizoguchi Y, Kobayashi K, Monna T. Immunocytochemical identification of proliferative hepatocytes using monoclonal antibody to proliferating cell nuclear antigen (PCNA/cyclin). Comparison with immunocytochemical staining for DNA polymerase-alpha. *Am J Clin Pathol* 1992; **97**: S14-S20

17 **Yin J**, Gao Z, He Q, Zhou D, Guo Z, Ye J. Role of hypoxia in obesity-induced disorders of glucose and lipid metabolism in adipose tissue. *Am J Physiol Endocrinol Metab* 2009; **296**: E333-E342

18 **Schneeweiss B**, Graninger W, Ferenci P, Eichinger S, Grimm G, Schneider B, Laggner AN, Lenz K, Kleinberger G. Energy metabolism in patients with acute and chronic liver disease. *Hepatology* 1990; **11**: 387-393

19 **Harvey PJ**, Gready JE, Hickey HM, Le Couteur DG, McLean AJ. 31P and 1H NMR spectroscopic studies of liver extracts of carbon tetrachloride-treated rats. *NMR Biomed* 1999; **12**: 395-401

20 **Morikawa S**, Inubushi T, Kitoh K, Kido C, Nozaki M. Chemical assessment of phospholipid and phosphoenergetic metabolites in regenerating rat liver measured by in vivo and in vitro 31P-NMR. *Biochim Biophys Acta* 1992; **1117**: 251-257

21 **Schlemmer HP**, Sawatzki T, Sammet S, Dornacher I, Bachert P, van Kaick G, Waldherr R, Seitz HK. Hepatic phospholipids in alcoholic liver disease assessed by proton-decoupled 31P magnetic resonance spectroscopy. *J Hepatol* 2005; **42**: 752-759

22 **Menon DK**, Sargentoni J, Taylor-Robinson SD, Bell JD, Cox IJ, Bryant DJ, Coutts GA, Rolles K, Burroughs AK, Morgan MY. Effect of functional grade and etiology on in vivo hepatic phosphorus-31 magnetic resonance spectroscopy in cirrhosis: biochemical basis of spectral appearances. *Hepatology* 1995; **21**: 417-427

23 **Campbell KA**, Wu YP, Chacko VP, Sitzmann JV. In vivo 31P NMR spectroscopic changes during liver regeneration. *J Surg Res* 1990; **49**: 244-247

S- Editor Tian L **L- Editor** Cant MR **E- Editor** Zheng XM

Online Submissions: wjg.wjgnet.com
wjg@wjgnet.com
doi:10.3748/wjg.15.2731

World J Gastroenterol 2009 June 14; 15(22): 2731-2738
World Journal of Gastroenterology ISSN 1007-9327

Anti-*Helicobacter pylori* therapy followed by celecoxib on progression of gastric precancerous lesions

Li-Jing Zhang, Shi-Yan Wang, Xiao-Hui Huo, Zhen-Long Zhu, Jian-Kun Chu, Jin-Cheng Ma, Dong-Sheng Cui, Ping Gu, Zeng-Ren Zhao, Ming-Wei Wang, Jun Yu

Li-Jing Zhang, Xiao-Hui Huo, Jian-Kun Chu, Jin-Cheng Ma, Jun Yu, Department of Gastroenterology, the First Affiliated Hospital of Hebei Medical University, Shijiazhuang 050051, Hebei Province, China
Shi-Yan Wang, Jun Yu, Department of Medicine and Therapeutics, the Prince of Wales Hospital, the Chinese University of Hong Kong, Hong Kong, China
Zhen-Long Zhu, Department of Pathology, the First Affiliated Hospital of Hebei Medical University, Shijiazhuang 050051, Hebei Province, China
Dong-Sheng Cui, Ping Gu, Ming-Wei Wang, Department of Neurology, the First Affiliated Hospital of Hebei Medical University, Shijiazhuang 050051, Hebei Province, China
Zeng-Ren Zhao, Department of Surgery, the First Affiliated Hospital of Hebei Medical University, Shijiazhuang 050051, Hebei Province, China
Author contributions: Zhang LJ and Wang SY contributed equally to this work; Yu J, Ma JC and Wang MW designed the research; Zhang LJ, Huo XH, Zhu ZL, Chu JK, Ma JC, Cui DS, Gu P, Zhao ZR and Yu J performed the research; Zhang LJ, Wang SY and Yu J analyzed the data; Zhang LJ, Wang SY and Yu J wrote the paper.
Support by The National Natural Science Foundation of China, No. 30370637
Correspondence to: Jun Yu, MD, PhD, Department of Medicine and Therapeutics, Prince of Wales Hospital, Shatin, NT, Hong Kong, China. junyu@cuhk.edu.hk
Telephone: +852-26321195 Fax: +852-26321194
Received: March 8, 2009 Revised: April 14, 2009
Accepted: April 21, 2009
Published online: June 14, 2009

Abstract

AIM: To evaluate whether celecoxib, a selective cyclooxygenase 2 (COX-2) inhibitor, could reduce the severity of gastric precancerous lesions following *Helicobacter pylori* (*H pylori*) eradication.

METHODS: *H pylori*-eradicated patients with gastric precancerous lesions randomly received either celecoxib (n = 30) or placebo (n = 30) for up to 3 mo. COX-2 expression and activity was determined by immunostaining and prostaglandin E_2 (PGE_2) assay, cell proliferation by Ki-67 immunostaining, apoptosis by TUNEL staining and angiogenesis by microvascular density (MVD) assay using CD31 staining.

RESULTS: COX-2 protein expression was significantly increased in gastric precancerous lesions (atrophy, intestinal metaplasia and dysplasia, respectively) compared with chronic gastritis, and was concomitant with an increase in cell proliferation and angiogenesis. A significant improvement in precancerous lesions was observed in patients who received celecoxib compared with those who received placebo (P < 0.001). Of these three changes, 84.6% of sites with dysplasia regressed in patients treated with celecoxib (P = 0.002) compared with 60% in the placebo group, suggesting that celecoxib was effective on the regression of dysplasia. COX-2 protein expression (P < 0.001) and COX-2 activity (P < 0.001) in the gastric tissues were consistently lower in celecoxib-treated patients compared with the placebo-treated subjects. Moreover, it was also shown that celecoxib suppressed cell proliferation (P < 0.01), induced cell apoptosis (P < 0.01) and inhibited angiogenesis with decreased MVD (P < 0.001). However, all of these effects were not seen in placebo-treated subjects. Furthermore, COX-2 inhibition resulted in the up-regulation of PPARγ expression, a protective molecule with anti-neoplastic effects.

CONCLUSION: *H pylori* eradication therapy followed by celecoxib treatment improves gastric precancerous lesions by inhibiting COX-2 activity, inducing apoptosis, and suppressing cell proliferation and angiogenesis.

Key words: Apoptosis; Cyclooxygenase 2; Gastric precancerous lesions; *Helicobacter pylori*; Microvessel density; Proliferation

Peer reviewers: Reza Malekzadeh, Professor, Director, Digestive Disease Research Center, Tehran University of Medical Sciences, Shariati Hospital, Kargar Shomali Avenue, 19119 Tehran, Iran; Fabio Farinati, MD, Surgical and Gastroenterological Sciences, University of Padua, Via Giustiniani 2, Padua 35128, Italy

Zhang LJ, Wang SY, Huo XH, Zhu ZL, Chu JK, Ma JC, Cui DS, Gu P, Zhao ZR, Wang MW, Yu J. Anti-*Helicobacter pylori* therapy followed by celecoxib on progression of gastric precancerous lesions. *World J Gastroenterol* 2009; 15(22): 2731-2738 Available from: URL: http://www.wjgnet.com/1007-9327/15/2731.asp DOI: http://dx.doi.org/10.3748/wjg.15.2731

INTRODUCTION

Gastric cancer is the second leading cause of cancer deaths worldwide[1] and its 5-year survival rate is only 10%-15% in individuals with advanced disease[2]. *Helicobacter pylori* (*H pylori*) has been classified as a type I carcinogen by the WHO and is recognized as an important pathogen in gastric tumorigenesis[3]. *H pylori* infection initiates the inflammatory and atrophic changes in gastric mucosa accompanied by enhanced expression of some protumorigenic factors such as cyclooxygenase 2 (COX-2) and anti-apoptosis proteins, resulting in uncontrolled proliferation of mutated atrophic cells, suppression of apoptosis, excessive angiogenesis and finally the formation of adenocarcinoma[4].

In cancer prevention, the targeting of precancerous lesions has been recognized as the most promising method. However, progress has been achieved only in the chemoprevention of colorectal neoplasia[5]. There is no effective therapy for reversing gastric premalignant lesions. Although *H pylori* infection is a critical initiator and mediator in gastric premalignant changes and gastric carcinogenesis, eradication of *H pylori* alone failed to improve these precancerous lesions[6-8]. The failure of *H pylori* eradication may be explained by the fact that the expression of COX-2, an important mediator in *H pylori*-induced premalignant changes, remained high or only modestly reduced after *H pylori* eradication[6-8]. It has been widely accepted that COX-2 plays an important role in gastric carcinogenesis[9]. COX-2 over-expression has been found in *H pylori*-induced inflammation, precancerous lesions and gastric tumors[9]. Inhibition of COX-2 by non-steroidal anti-inflammatory drugs (NSAIDs) has been proven to be effective in preventing gastric carcinogenesis as evidenced in animal models and epidemiological studies[2,9,10]. Since eradication of *H pylori* alone is not sufficient to reverse gastric carcinogenesis due to failure of the inhibition of *H pylori*-induced protumorigenic factors such as COX-2, it would be reasonable to combine additional treatments such as COX-2 inhibition following *H pylori* eradication.

In the present study, we examined whether treatment with the selective COX-2 inhibitor celecoxib could reduce the severity of gastric precancerous lesions after *H pylori* eradication. The mechanisms of its action were also investigated.

MATERIALS AND METHODS

Patients and study design

We enrolled 233 patients who had upper-gastrointestinal symptoms such as anorexia, early satiety, stomach pain, abdominal distention and epigastric discomfort between January 2005 and July 2006 from the First Affiliated Hospital of Hebei Medical University, Shijiazhuang, China. Eligible subjects were between 30 and 70 years of age, and had no history of drug allergies. Subjects were ineligible if they were under 30 or older than 70 years old; pregnant or lactating; had peptic ulcer; gastric cancer or other cancers; upper gastrointestinal bleeding; liver cirrhosis; serious cardiovascular diseases, renal or lung diseases; hypersensitive to COX-2 inhibitors, NSAIDs, salicylates, or sulfonamides; used NSAIDs; and those unwilling to undergo repeat endoscopy after treatment.

H pylori infected patients who were defined both by the presence of the bacterium on histology as well as a positive C^{14} urea breath test were treated with a 1-wk course of eradication therapy (omeprazole, 20 mg; amoxicillin, 1000 mg; furaltadone, 100 mg; twice daily). Five weeks post-treatment, patients were recalled to hospital for repeat endoscopy and C^{14} urea breath test. *H pylori* eradication was confirmed by a negative C^{14} urea breath test and a negative *H pylori* histology examination from biopsies. Only patients with confirmed *H pylori* eradication were recruited into this study. During each endoscopy, a total of eight gastric biopsies were taken from the antrum (two from the greater curvature and two from the lesser curvature) and the corpus of the stomach (two from the greater curvature and two from the lesser curvature) for molecular experiments and histological examination. One of the two biopsy specimens from each site was immediately stored at -80℃ for RNA/protein extraction. The other specimens were fixed in 10% neutral buffered formalin and embedded in paraffin for histological examination and immunostaining. The severity of gastric histology including gastritis and precancerous lesions [gastric atrophy, intestinal metaplasia (IM) and low-grade dysplasia] was scored based on the following standards: absent (0), mild (1), moderate (2) and marked (3)[11]. Patients with high-grade dysplasia were excluded from the study. All gastric biopsies were interpreted by two pathologists who were unaware of the treatment assignments.

One hundred and thirty six eligible subjects who were histologically confirmed to have gastric precancerous lesions and negative tests for *H pylori* were randomly assigned to receive either celecoxib 200 mg twice daily or an identical-looking placebo at a 1:1 ratio for 3 mo. During the treatment period, 10 subjects were withdrawn due to adverse events and 66 were lost to follow-up. Some patients lost to follow-up migrated to other cities, some were non-compliant and failed to follow through with our treatment protocol, and some refused to undergo a second endoscopy. At the end of the 3-mo treatment period, 30 patients in the celecoxib group (16 males with an average age of 50.33 ± 10.39 years; 14 females with an average age of 57.36 ± 9.25 years) and 30 patients in the placebo group (14 males with an average age of 48 ± 10.43 years; 16 females with an average age of 50 ± 9.98 years) returned for endoscopic examination. The same protocols for obtaining gastric biopsy and histological examination were used as previously mentioned in the baseline endoscopy. The study protocol was approved by the Clinical Research Ethics Committee and all participants gave written informed consent.

Immunohistochemistry

The paraffin-embedded gastric sections were

Table 1 Primer sequences used for amplification of mRNA by semi-quantitative PCR

mRNA	Forward primer (5′-3′)	Reverse primer (5′-3′)	Size (bp)
PCNA	CTTTTCTGTCACCAAATTTGTACC	AACTGCATTTAGAGTCAAGACCC	206
Fas	CTGCCAAGAAGGGAAGGAGT	GGTGCAAGGGTCACAGTGTT	189
PPARγ	AGCCTCATGAAGAGCCTTCCA	ACCCTTGCATCCTTCACAAGC	89
β-actin	GTCTTCCCCTCCATCGTG	GGGTGAGGATGCCTCTCTT	251

deparaffinized and rehydrated in graded ethanol. The activity of endogenous peroxidase was blocked by methanol containing 3% H_2O_2 for 10 min and washed with PBS. After blocking with 10% nonimmunized goat serum at 37℃ for 20 min, sections were incubated with the primary antibody for COX-2 (1:500, Santa Cruz Biotechnology, Santa Cruz, CA, USA), Ki-67 (1:200, Chemicon International Inc., Temecula, CA, USA), peroxisome proliferator-activated receptor γ (PPARγ) (1:100, Santa Cruz) overnight at 4℃. Peroxidase activity was visualized by applying diaminobenzidine to the sections, which were then counter-stained with hematoxylin. Analysis of the immunostained sections was independently performed by two pathologists in a blinded fashion.

Microvessel density (MVD) was performed on paraffin-embedded gastric tissue sections stained with CD31 (1:150, DAKO, Glostrup, Denmark) as an indicator. For the determination of MVD in each case, five of the most highly vascularized areas within a section were selected and counted under a light microscope. The average numbers of microvessels in the selected fields were recorded as the MVD for each case.

cDNA synthesis and RT-PCR

Gastric tissue specimens were homogenized with a homogenizer. Total RNA was extracted using TRIzol reagent (Invitrogen, USA). Five micrograms of total RNA from each sample was reverse transcribed into cDNA using the AMV Reverse Transcription system (Promega, San Luis Obispo, CA, USA). Semi-quantitative PCR was performed. The primer sequences of proliferation cell nuclear antigen (PCNA), factor associated suicide (FAS), PPARγ and β-actin are listed in Table 1. A DNA free template control (containing water) was included and each sample was added in duplicate. PCR products were separated by 15% agarose gel electrophoresis and quantified by the Gel Imaging System after ethidium bromide (10 mg/L) staining. The mRNA expression level of the target gene was defined by the densitometry ratio of target gene to β-actin.

PGE_2 assay

PGE_2 levels were measured in snap frozen tissue specimens using a radioimmunoassay-based assay. Briefly, about 20 mg of snap frozen tissues were homogenized in 10 volumes of sodium chloride by a ground glass homogenizer on ice. The mixture was incubated at 37℃ for 15 min and then centrifuged for 20 min at 3000 r/min. The supernatant was then applied to the pre-primed immunoassay reaction mixture and reacted with the antibody overnight. PGE_2 was precipitated with 0.7 mL volumes of 25% polyethylene glycol. The quantity of PGE_2 in the supernatants was determined using RIA.

Determination of cell proliferation

Proliferation was assayed by immunoperoxidase staining for Ki-67 as described previously[12]. The immunochemistry method for staining the sections with Ki-67 antibody has been specified above. The proliferation index (PI) was defined as a percentage of the ratio of Ki-67-positive nuclei to the total nuclei counted.

Terminal deoxynucleotidyl transferase-mediated nick end labeling (TUNEL)

Apoptosis was determined *in situ* from paraffin-embedded tissue sections by the TUNEL assay using the *in situ* Cell Death Detection kit (Roche Applied Science, Indianapolis, IN, USA). Briefly, paraffin-embedded slides were deparaffinized, hydrated and incubated with proteinase K (20 mg/mL in 10 mmol/L Tris-HCl) for 20 min. After labeling with the TUNEL reaction mixture, slides were developed by converter-POD and DAB substrate. PBS replaced the primary antibodies as a negative control. The results of staining were analyzed and evaluated by three individuals independently. At least 1000 cells were counted in five random fields. Apoptosis index (AI) was represented as the percentage of positive cells with TUNEL staining to the total cells.

Statistical analysis

Data were analyzed by SPSS 12.0 software and are shown in a default form of mean ± SD. The association between COX-2 expression and the progression of precancerous lesions was analyzed by χ^2 test. The correlation between COX-2 expression and MVD/PI was analyzed using Pearson's Correlation Coefficient. The difference between the groups was compared by *t* test. The paired *t* test was used to determine the difference between pre-treatment and after-treatment within each treatment group. $P < 0.05$ was considered statistically significant.

RESULTS

Association between COX-2 expression and progression of precancerous lesions

The percentage of COX-2 positive cells in gastric tissues was increased with the progression of chronic gastritis

(33.3%), atrophy (51.6%), IM (53.3%), and dysplasia (79.3%) as determined by immunostaining. COX-2 expression in dysplasia (79.3%) was significantly higher than in any other type of lesion ($P < 0.05$). COX-2 expression was significantly elevated in atrophy and IM compared with chronic gastritis ($P < 0.05$). However, there was no significant difference between gastric atrophy and IM ($P > 0.05$).

COX-2 expression correlated with cell proliferation

Cell proliferation was determined by Ki-67 staining. A significant positive correlation between COX-2 expression and PI ($\chi^2 = 10.5$, $P = 0.001$) was observed by Pearson's Correlation Coefficient analysis, indicating COX-2 expression correlated with cell proliferation.

COX-2 expression correlated with angiogenesis

We also evaluated the correlation between COX-2 expression and angiogenesis as determined by CD31 immunostaining. The mean MVD was significantly higher in COX-2-positive tissues ($n = 47$, 23.85 ± 7.44) than in COX-2-negative tissues ($n = 27$, 18.47 ± 6.02) ($P < 0.001$), indicating a positive correlation between COX-2 expression and MVD. Thus COX-2 also played an important role in angiogenesis.

Effect of celecoxib on the improvement in histology of gastric precancerous lesions

After three months treatment, a significant improvement in precancerous lesions was observed in 66.7% (20/30) of patients ($P < 0.001$) who were treated with celecoxib. However, only 16.1% of cases who received placebo showed improved histology ($P > 0.05$). Of these three changes, 84.6% of sites with dysplasia regressed in patients treated with celecoxib ($P = 0.002$) compared with 60% in the placebo group, suggesting that celecoxib was effective on the regression of dysplasia (Table 2). However, differences in pathological improvement of atrophy and intestinal metaplasia were not observed between the celecoxib and placebo groups (Table 2). With regard to the mixed pathological sites with both atrophy and intestinal metaplasia, we did not have sufficient sample size to make an accurate conclusion.

Effect of celecoxib on COX-2 protein expression and COX-2 activity

COX-2 protein expression as determined by the percentage of COX-2 positive cells in the gastric tissues was significantly lower after treatment with celecoxib (pre-treatment: 40.93% ± 11.96% *vs* after-treatment: 27.88% ± 4.94%, $P < 0.001$) (Figure 1A-C). COX-2 protein expression was reduced in 73%, remained the same in 13% and increased in 13% of patients treated with celecoxib. However, COX-2 expression was reduced in only 48% of patients in the placebo group (Table 3). PGE_2 level, an indicator of COX-2 activity, was concomitantly reduced in patients treated with celecoxib (pre-treatment: 358.9 ± 59.3 *vs* after-treatment: 143.6 ± 24.2, $P < 0.001$). However, these differences in COX-2 expression and COX-2 activity were not seen in patients treated with placebo (Figure 1D).

Table 2 Effect of celecoxib on the histological improvement of gastric precancerous lesions

Precancerous lesions	Regression site *n* (%)		*P*-value
	Celecoxib group	Placebo group	
Atrophy	11/13 (84.6)	7/13 (53.8)	0.202
Metaplasia	9/14 (64.3)	9/18 (50)	0.419
Atrophy + metaplasia[1]	3/4 (75)	3/6 (50)	0.895
Dysplasia	35/39 (89.7)	24/40 (60)	0.002

[1]Indicates that both atrophy and metaplasia were regressed in one site.

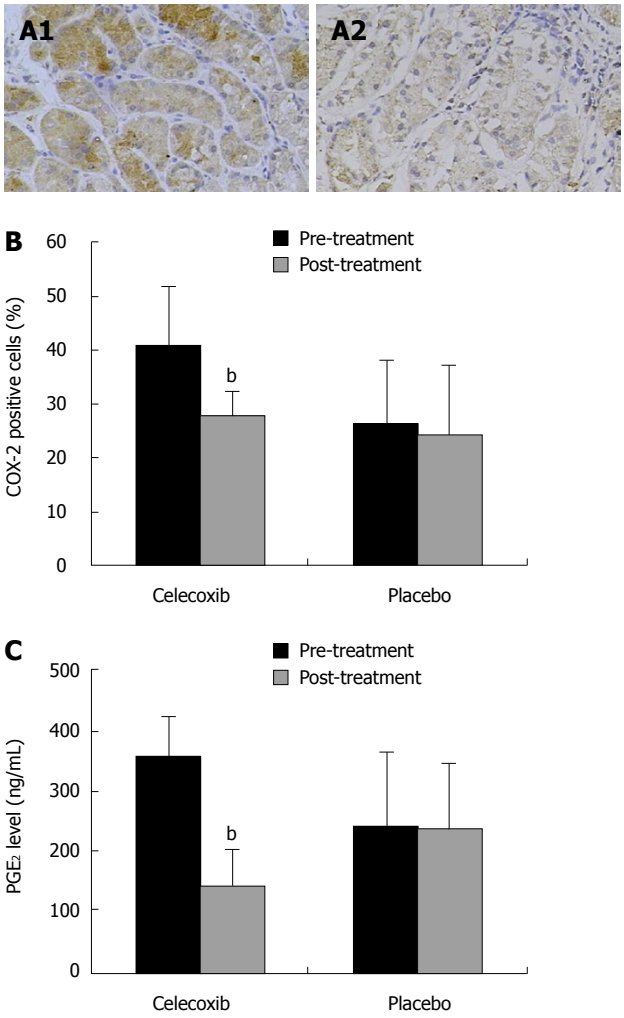

Figure 1 Effects of celecoxib on COX-2 expression and PGE_2 levels. A: Representative image of COX-2 protein expression as determined by immunostaining in paraffin-embedded gastric tissue sections: (A1) pre-treatment, and (A2) post-treatment with celecoxib; B: Percentage of COX-2 positive cells in gastric mucosa; C: PGE_2 levels. Data are mean ± SD. $^bP < 0.001$.

Effect of celecoxib on cell proliferation

Cell proliferation was significantly reduced in the celecoxib group after 3 mo of treatment (pre-treatment: 27.46% ± 6.77% *vs* after-treatment: 20.18% ± 4.05%, $P < 0.01$) (Figure 2A and B). However, this difference was not observed in patients treated with placebo (Figure 2B). Seventy percent of patients in the celecoxib

Table 3 Effect of celecoxib on COX-2 expression and other parameters

	Celecoxib group *n* (%)			Placebo group *n* (%)		
	Reduction	Same	Worse	Reduction	Same	Worse
COX-2 expression	22 (73)	4 (13)	4 (13)	15 (48)	3 (10)	13 (43)
Cell proliferation	23 (77)	2 (7)	5 (17)	11 (37)	3 (10)	16 (53)
Cell apoptosis	8 (53)	4 (27)	3 (20)	4 (27)	5 (17)	6 (40)
Angiogenesis	22 (73)	4 (13)	4 (13)	12 (39)	10 (32)	9 (29)
PPARγ expression	15 (50)	5 (17)	10 (33)	9 (29)	5 (16)	17 (55)

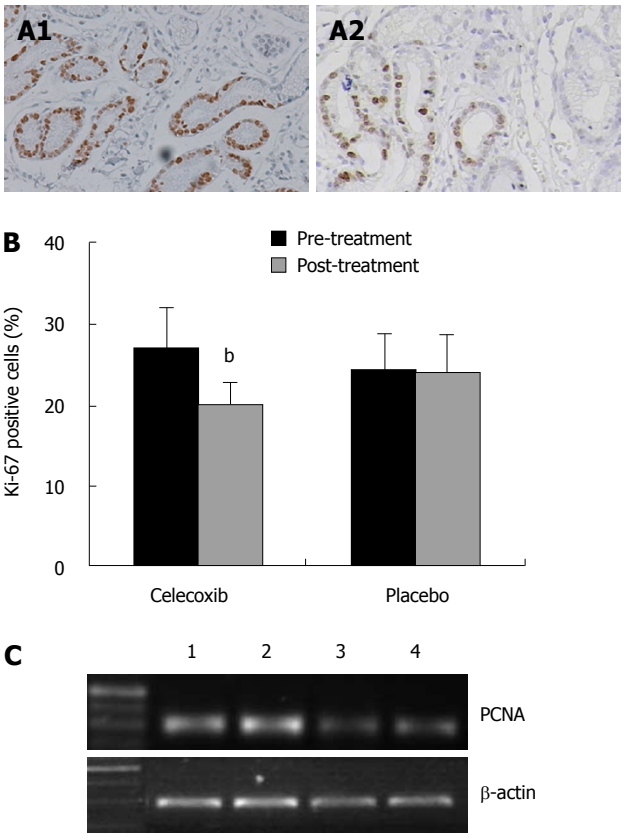

Figure 2 Effects of celecoxib on cell proliferation. A: Representative Ki-67 staining of gastric mucosa before (A1) and after treatment (A2) with celecoxib; B: Celecoxib led to a significant reduction in proliferation index (PI); C: Celecoxib down-regulated mRNA expression of proliferation cell nuclear antigen (PCNA). 1 and 2: Plecebo; 3 and 4: Celecoxib. Data are mean ± SD. $^{b}P < 0.01$.

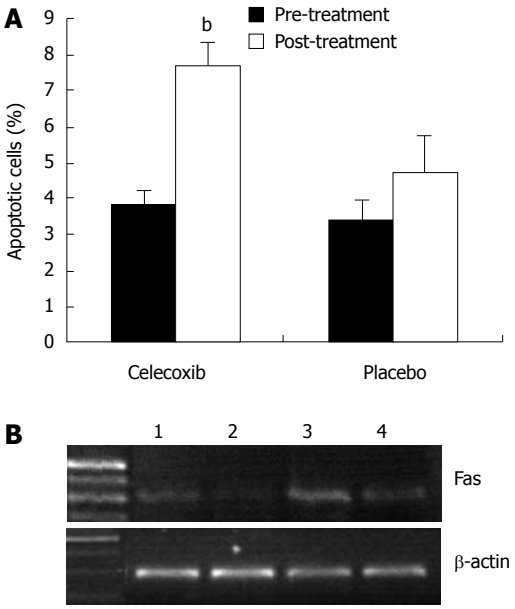

Figure 3 Effects of celecoxib on cell apoptosis. A: Celecoxib induced the apoptosis index (AI) in gastric mucosa; B: Celecoxib up-regulated mRNA expression of Fas, a pro-apoptosis gene. 1 and 2: Plecebo; 3 and 4: Celecoxib. Data are mean ± SD. $^{b}P < 0.01$.

group had reduced PCNA protein expression while a reduction in PCNA expression was observed in only 37% of patients in the placebo group (Table 3). In addition, mRNA expression of PCNA was markedly down-regulated by celecoxib treatment (Figure 2C).

Effect of celecoxib on cell apoptosis

Treatment with celecoxib significantly induced cell apoptosis as assayed by TUNEL staining (pre-treatment: 3.86% ± 0.44% *vs* after-treatment: 7.72% ± 0.64%, $P < 0.01$) (Figure 3A, Table 3). In keeping with this, mRNA expression of the pro-apoptotic gene *fas* was also enhanced (Figure 3B), suggesting that celecoxib-induced apoptosis was *via* up-regulation of *fas* expression.

Effect of celecoxib on angiogenesis

Angiogenesis was evaluated by the MVD assay using CD31 staining. MVD was significantly lower after celecoxib treatment ($P < 0.001$) (Figure 4, Table 3), indicating a suppressive effect on angiogenesis by celecoxib. However, this difference was not seen in the placebo group.

Effect of celecoxib on PPARγ expression

Celecoxib treatment led to an increase in the number of PPARγ positive cells as determined by immunostaining (pre-treatment: 18% ± 4.33% *vs* after-treatment: 22.6% ± 4.3%, $P < 0.05$) (Figure 5, Table 3). Thus, celecoxib resulted in up-regulation of PPARγ expression.

DISCUSSION

We report here that COX-2 is markedly up-regulated in gastric tissues with inflammation and was more prominent during progression in precancerous lesions in *H pylori*-eradicated patients. Moreover, the induction of COX-2 appeared to coincide with increased cell proliferation and angiogenesis. These results suggested that COX-2 was induced by *H pylori* infection and mediated by *H pylori*-associated premalignant gastric lesions. Our observation on the profile of COX-2 expression is supported by previous studies[7,8,13-16],

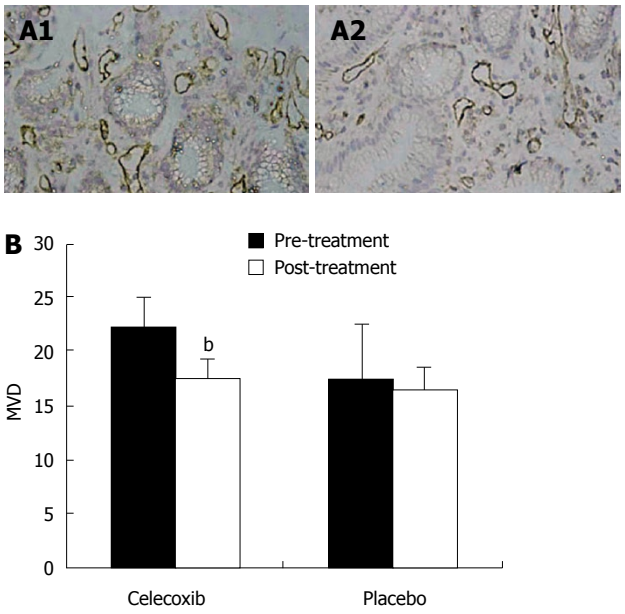

Figure 4 Effects of celecoxib on angiogenesis. A: Representative microvessel image of paraffin-embedded gastric tissue sections stained with CD31. (A1) pre-treatment, and (A2) post-treatment with celecoxib; B: Celecoxib suppressed microvessel density (MVD). Data are mean ± SD. $^{b}P < 0.001$.

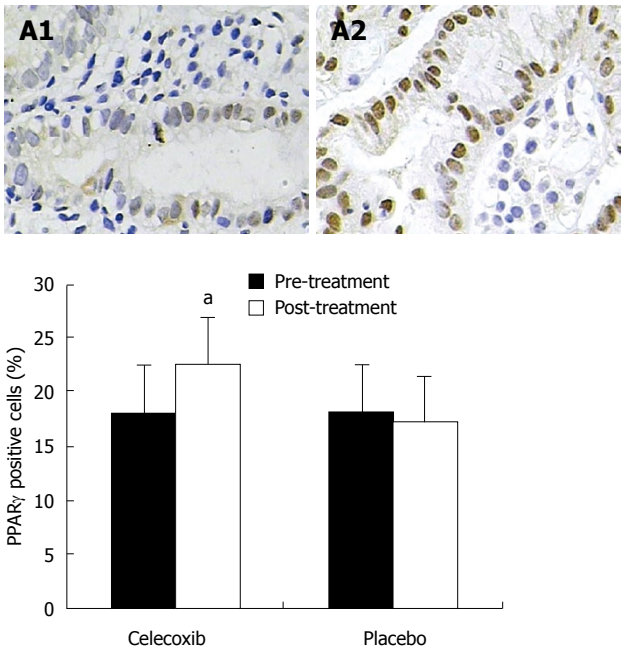

Figure 5 Effects of celecoxib on PPARγ protein expression. Representative PPARγ expression in paraffin-embedded gastric tissue sections by immunostaining. (A1) pre-treatment, and (A2) post-treatment with celecoxib. Nuclear staining of PPARγ was markedly increased post-treatment with celecoxib. $^{a}P < 0.05$.

suggesting that COX-2 is a relatively early event and plays an important role during gastric carcinogenesis.

To evaluate whether progression of precancerous lesions could be reduced or reversed, we conducted a 3-mo intervention of celecoxib in patients with precancerous lesions after *H pylori* eradication. Our results showed that the histology of precancerous lesions was improved in 66.7% of patients treated with celecoxib, which was significantly higher than the placebo group (16.1%) ($P < 0.001$). Of the three precancerous changes (atrophy, intestinal metaplasia and dysplasia), celecoxib was effective on the regression of dysplasia. However, the evidence for chemopreventive effects on gastric precancerous lesions by NSAIDs has only been limited to animal experiments[13,17-22]. In the animal model of carcinogenesis induced by co-treatment with *H pylori* and N-methyl-N-nitrosourea (MNU), mice underwent *H pylori*-induced gastritis with multifocal atrophy and intestinal metaplasia, and finally gastric adenocarcinoma. Long term co-administration with a COX-2 inhibitor, either celecoxib or nimesulide not only reduced the development of intestinal metaplasia, but also adenocarcinoma[20-22]. In human studies, a recent report showed that treatment with NSAIDs for more than 3 mo reversed *H pylori*-induced harmful effects in gastric epithelial cells[23]. On the other hand, large-scale clinical trials have shown that NSAIDs were effective in the chemoprevention of colorectal neoplasia[5]. NSAIDs (celecoxib and sulindac) promoted regression in both number and size in high risk individuals with familial adenomatous polyposis[5]. In the more common sporadic setting, refecoxib and celecoxib reduced the occurrence of human colorectal adenomas[5]. Collectively, these results suggest that the protective effects of NSAIDs such as celecoxib could effectively prevent or reverse the precancerous lesions of gastric cancer.

We further evaluated the underlying mechanisms for the anti-tumorigenic effects of the COX-2 inhibitor. On the basis of the cell proliferation and apoptosis analyses, improvements in precancerous lesions caused by celecoxib were most likely associated with the suppression of cell proliferation and induction of cell apoptosis. In keeping with this, in an animal experiment, celecoxib but not indomethacin suppressed gastric cancer formation by inducing cell apoptosis and suppressing cell proliferation[24,25] in a dose dependent manner. A recent report also indicated that NSAIDs induced apoptosis through activation of extrinsic and intrinsic pathways of apoptosis[26]. However, the pro-apoptotic efficacy of various NSAIDs differed greatly[27,28]. That may explain why the anti-tumor effects of NSAIDs varied in different experiments.

In the present work, we showed that, in addition to inhibition of cell proliferation and induction of apoptosis, the regression of precancerous lesions in the stomach by celecoxib was also related to inhibition of angiogenesis. It is well-established that the inducible enzyme COX-2 is an important mediator of angiogenesis during tumor growth[29]. COX-2 expression significantly correlated with MVD[30] and vascular endothelial growth factor (VEGF) in human gastric adenomas and carcinomas[31]. The pro-angiogenic effects of COX-2 are mediated primarily by the metabolites of arachidonic acid, resulting in increased production of VEGF, enhanced survival of endothelial cells, induction of matrix metalloproteinases, promotion of vascular sprouting and migration and activation of epidermal growth factor receptor-mediated angiogenesis[29]. In this regard, we showed in this study that induction of

COX-2 is parallel with the induced angiogenesis in precancerous lesions. Treatment with celecoxib inhibited angiogenesis with a concomitant histological regression of precancerous lesions. Others have also reported that NSAIDs including celecoxib inhibited angiogenesis and decreased tumor growth in gastric cancer and other cancers both *in vitro* and *in vivo* in animal models[13, 32-34]. Our study provided the first clinical evidence that treatment with celecoxib effectively suppressed angiogenesis and lowered MVD in *H pylori*-eradicated patients with gastric precancerous lesions.

The expression of PPARγ, a protective anti-neoplastic molecule[35], was enhanced by the COX-2 inhibitor rofecoxib in human gastric cancer with a concomitant induction of apoptosis and attenuation of proinflammatory cytokines production[36]. We also observed the up-regulation of PPARγ in patients treated with celecoxib. The up-regulation of PPARγ by NSAIDs was reported either *via* the COX-2 independent pathway or the COX-2 dependent pathway[37-39]. Activation of PPARγ was shown by us and others to prevent mammary carcinogenesis in experimental animals[40-42] through suppression of COX-2 expression[40]. In mice treated with MNU and *H pylori*, nimesulide administration substantially reduced *H pylori*-associated gastric tumorigenesis along with substantial activation of PPARγ and induction of apoptosis[21]. Collectively, these findings raise the possibility that up-regulation of PPARγ by celecoxib contributed to the histological improvement in precancerous lesions.

In conclusion, COX-2 expression was induced in gastric epithelium with the progression of precancerous lesions. Eradication of *H pylori* combined with a 3-mo intervention of celecoxib was effective in improving the severity of precancerous lesions mainly by inducing apoptosis, and inhibiting cell proliferation and angiogenesis. Thus COX-2 is a promising target in reversing gastric precancerous lesions and celecoxib showed efficacy in the chemoprevention of these lesions.

COMMENTS

Background

Epidemiologic studies have shown that cyclooxygenase 2 (COX-2) inhibitor could reduce the risk of gastric cancer. The authors aim to evaluate whether celecoxib, a selective COX-2 inhibitor, could reduce the severity of gastric precancerous lesions following *Helicobacter pylori* (*H pylori*) eradication.

Research frontiers

Gastric cancer is the most common cancer and the leading cause of cancer-related death in China, with an overall 5-year survival rate of only 10%-20%. There is a compelling need to explore the novel targets that contribute to gastric carcinogenesis for effective treatment. The development of gastric cancer is generally believed to be a multi-step progression from chronic gastritis to atrophy, intestinal metaplasia (IM), dysplasia and cancer, that is triggered by *H pylori* infection. Eradication of *H pylori* alone is not efficient in preventing the progression of gastric IM. The authors hypothesized in addition to eradicate *H pylori*, inhibition of COX-2, a potential oncogene gene that was induced in the early stage of gastric carcinogenesis, by selective COX-2 inhibitor (celecoxib) may regress the premalignant changes in the stomach by suppressing COX-2. Herein, they tested the effect of a specific COX-2 inhibitor in patients with confirmed gastric atrophy and/or IM after *H pylori* eradication. The present study was a prospective, randomized, and placebo-controlled study.

Innovations and breakthroughs

The authors have demonstrated in this study that *H pylori* eradication therapy followed by celecoxib treatment improves and dampens the progression of gastric precancerous lesions. The anti-neoplastic properties of celecoxib were due to its ability of inhibiting COX-2 activity, inducing apoptosis, suppressing cell proliferation and angiogenesis.

Applications

COX-2 was a promising target in reversing gastric precancerous lesions and celecoxib showed efficacy in this chemoprevention. This finding may provide clinical implication.

Peer review

The authors report interesting data on the effect of celecoxib administration in patients with gastric precancerous lesions following *H pylori* eradicated. This is a well designed study with interesting results.

REFERENCES

1 **Parkin DM**, Bray F, Ferlay J, Pisani P. Estimating the world cancer burden: Globocan 2000. *Int J Cancer* 2001; **94**: 153-156

2 **Wang WH**, Huang JQ, Zheng GF, Lam SK, Karlberg J, Wong BC. Non-steroidal anti-inflammatory drug use and the risk of gastric cancer: a systematic review and meta-analysis. *J Natl Cancer Inst* 2003; **95**: 1784-1791

3 **Asaka M**, Takeda H, Sugiyama T, Kato M. What role does Helicobacter pylori play in gastric cancer? *Gastroenterology* 1997; **113**: S56-S60

4 **Konturek PC**, Konturek SJ, Brzozowski T. Gastric cancer and Helicobacter pylori infection. *J Physiol Pharmacol* 2006; **57** Suppl 3: 51-65

5 **Arber N**, Levin B. Chemoprevention of colorectal neoplasia: the potential for personalized medicine. *Gastroenterology* 2008; **134**: 1224-1237

6 **McCarthy CJ**, Crofford LJ, Greenson J, Scheiman JM. Cyclooxygenase-2 expression in gastric antral mucosa before and after eradication of Helicobacter pylori infection. *Am J Gastroenterol* 1999; **94**: 1218-1223

7 **Sung JJ**, Leung WK, Go MY, To KF, Cheng AS, Ng EK, Chan FK. Cyclooxygenase-2 expression in Helicobacter pylori-associated premalignant and malignant gastric lesions. *Am J Pathol* 2000; **157**: 729-735

8 **Sheu BS**, Yang HB, Sheu SM, Huang AH, Wu JJ. Higher gastric cycloxygenase-2 expression and precancerous change in Helicobacter pylori-infected relatives of gastric cancer patients. *Clin Cancer Res* 2003; **9**: 5245-5251

9 **Nardone G**, Rocco A. Chemoprevention of gastric cancer: role of COX-2 inhibitors and other agents. *Dig Dis* 2004; **22**: 320-326

10 **Dai Y**, Wang WH. Non-steroidal anti-inflammatory drugs in prevention of gastric cancer. *World J Gastroenterol* 2006; **12**: 2884-2889

11 **Dixon MF**, Genta RM, Yardley JH, Correa P. Classification and grading of gastritis. The updated Sydney System. International Workshop on the Histopathology of Gastritis, Houston 1994. *Am J Surg Pathol* 1996; **20**: 1161-1181

12 **Yu J**, Hui AY, Chu ES, Cheng AS, Go MY, Chan HL, Leung WK, Cheung KF, Ching AK, Chui YL, Chan KK, Sung JJ. Expression of a cyclo-oxygenase-2 transgene in murine liver causes hepatitis. *Gut* 2007; **56**: 991-999

13 **Saukkonen K**, Rintahaka J, Sivula A, Buskens CJ, Van Rees BP, Rio MC, Haglund C, Van Lanschot JJ, Offerhaus GJ, Ristimaki A. Cyclooxygenase-2 and gastric carcinogenesis. *APMIS* 2003; **111**: 915-925

14 **Saukkonen K**, Nieminen O, van Rees B, Vilkki S, Härkönen M, Juhola M, Mecklin JP, Sipponen P, Ristimäki A. Expression of cyclooxygenase-2 in dysplasia of the stomach and in intestinal-type gastric adenocarcinoma. *Clin Cancer Res* 2001; **7**: 1923-1931

15 **Rocco A**, Caruso R, Toracchio S, Rigoli L, Verginelli F, Catalano T, Neri M, Curia MC, Ottini L, Agnese V, Bazan V, Russo A, Pantuso G, Colucci G, Mariani-Costantini

R, Nardone G. Gastric adenomas: relationship between clinicopathological findings, Helicobacter pylori infection, APC mutations and COX-2 expression. *Ann Oncol* 2006; **17** Suppl 7: vii103-vii108

16 **van Rees BP**, Saukkonen K, Ristimäki A, Polkowski W, Tytgat GN, Drillenburg P, Offerhaus GJ. Cyclooxygenase-2 expression during carcinogenesis in the human stomach. *J Pathol* 2002; **196**: 171-179

17 **Xiao F**, Furuta T, Takashima M, Shirai N, Hanai H. Involvement of cyclooxygenase-2 in hyperplastic gastritis induced by Helicobacter pylori infection in C57BL/6 mice. *Aliment Pharmacol Ther* 2001; **15**: 875-886

18 **Kim TI**, Lee YC, Lee KH, Han JH, Chon CY, Moon YM, Kang JK, Park IS. Effects of nonsteroidal anti-inflammatory drugs on Helicobacter pylori-infected gastric mucosae of mice: apoptosis, cell proliferation, and inflammatory activity. *Infect Immun* 2001; **69**: 5056-5063

19 **Saukkonen K**, Tomasetto C, Narko K, Rio MC, Ristimäki A. Cyclooxygenase-2 expression and effect of celecoxib in gastric adenomas of trefoil factor 1-deficient mice. *Cancer Res* 2003; **63**: 3032-3036

20 **Hahm KB**, Song YJ, Oh TY, Lee JS, Surh YJ, Kim YB, Yoo BM, Kim JH, Han SU, Nahm KT, Kim MW, Kim DY, Cho SW. Chemoprevention of Helicobacter pylori-associated gastric carcinogenesis in a mouse model: is it possible? *J Biochem Mol Biol* 2003; **36**: 82-94

21 **Nam KT**, Hahm KB, Oh SY, Yeo M, Han SU, Ahn B, Kim YB, Kang JS, Jang DD, Yang KH, Kim DY. The selective cyclooxygenase-2 inhibitor nimesulide prevents Helicobacter pylori-associated gastric cancer development in a mouse model. *Clin Cancer Res* 2004; **10**: 8105-8113

22 **Futagami S**, Suzuki K, Hiratsuka T, Shindo T, Hamamoto T, Tatsuguchi A, Ueki N, Shinji Y, Kusunoki M, Wada K, Miyake K, Gudis K, Tsukui T, Sakamoto C. Celecoxib inhibits Cdx2 expression and prevents gastric cancer in Helicobacter pylori-infected Mongolian gerbils. *Digestion* 2006; **74**: 187-198

23 **Zhu GH**, Yang XL, Lai KC, Ching CK, Wong BC, Yuen ST, Ho J, Lam SK. Nonsteroidal antiinflammatory drugs could reverse Helicobacter pylori-induced apoptosis and proliferation in gastric epithelial cells. *Dig Dis Sci* 1998; **43**: 1957-1963

24 **Hu PJ**, Yu J, Zeng ZR, Leung WK, Lin HL, Tang BD, Bai AH, Sung JJ. Chemoprevention of gastric cancer by celecoxib in rats. *Gut* 2004; **53**: 195-200

25 **Yu J**, Tang BD, Leung WK, To KF, Bai AH, Zeng ZR, Ma PK, Go MY, Hu PJ, Sung JJ. Different cell kinetic changes in rat stomach cancer after treatment with celecoxib or indomethacin: implications on chemoprevention. *World J Gastroenterol* 2005; **11**: 41-45

26 **Jana NR**. NSAIDs and apoptosis. *Cell Mol Life Sci* 2008; **65**: 1295-1301

27 **Andrews J**, Djakiew D, Krygier S, Andrews P. Superior effectiveness of ibuprofen compared with other NSAIDs for reducing the survival of human prostate cancer cells. *Cancer Chemother Pharmacol* 2002; **50**: 277-284

28 **Takada Y**, Bhardwaj A, Potdar P, Aggarwal BB. Nonsteroidal anti-inflammatory agents differ in their ability to suppress NF-kappaB activation, inhibition of expression of cyclooxygenase-2 and cyclin D1, and abrogation of tumor cell proliferation. *Oncogene* 2004; **23**: 9247-9258

29 **Iñiguez MA**, Rodríguez A, Volpert OV, Fresno M, Redondo JM. Cyclooxygenase-2: a therapeutic target in angiogenesis. *Trends Mol Med* 2003; **9**: 73-78

30 **Honjo S**, Kase S, Osaki M, Ardyanto TD, Kaibara N, Ito H. Cyclooxygenase-2 expression in human gastric tubular adenomas and carcinomas; correlation with intratumoral microvessel density and apoptotic index. *Anticancer Res* 2004; **24**: 1439-1444

31 **Tatsuguchi A**, Matsui K, Shinji Y, Gudis K, Tsukui T, Kishida T, Fukuda Y, Sugisaki Y, Tokunaga A, Tajiri T, Sakamoto C. Cyclooxygenase-2 expression correlates with angiogenesis and apoptosis in gastric cancer tissue. *Hum Pathol* 2004; **35**: 488-495

32 **Grösch S**, Maier TJ, Schiffmann S, Geisslinger G. Cyclooxygenase-2 (COX-2)-independent anticarcinogenic effects of selective COX-2 inhibitors. *J Natl Cancer Inst* 2006; **98**: 736-747

33 **Sawaoka H**, Tsuji S, Tsujii M, Gunawan ES, Sasaki Y, Kawano S, Hori M. Cyclooxygenase inhibitors suppress angiogenesis and reduce tumor growth in vivo. *Lab Invest* 1999; **79**: 1469-1477

34 **Wu YL**, Fu SL, Zhang YP, Qiao MM, Chen Y. Cyclooxygenase-2 inhibitors suppress angiogenesis and growth of gastric cancer xenografts. *Biomed Pharmacother* 2005; **59** Suppl 2: S289-S292

35 **Han S**, Roman J. Peroxisome proliferator-activated receptor gamma: a novel target for cancer therapeutics? *Anticancer Drugs* 2007; **18**: 237-244

36 **Konturek PC**, Konturek SJ, Bielanski W, Kania J, Zuchowicz M, Hartwich A, Rehfeld JF, Hahn EG. COX-2 inhibition by rofecoxib on serum and tumor progastrin and gastrin levels and expression of PPARgamma and apoptosis-related proteins in gastric cancer patients. *Dig Dis Sci* 2003; **48**: 2005-2017

37 **Lehmann JM**, Lenhard JM, Oliver BB, Ringold GM, Kliewer SA. Peroxisome proliferator-activated receptors alpha and gamma are activated by indomethacin and other non-steroidal anti-inflammatory drugs. *J Biol Chem* 1997; **272**: 3406-3410

38 **Pawliczak R**, Han C, Huang XL, Demetris AJ, Shelhamer JH, Wu T. 85-kDa cytosolic phospholipase A2 mediates peroxisome proliferator-activated receptor gamma activation in human lung epithelial cells. *J Biol Chem* 2002; **277**: 33153-33163

39 **Shappell SB**, Gupta RA, Manning S, Whitehead R, Boeglin WE, Schneider C, Case T, Price J, Jack GS, Wheeler TM, Matusik RJ, Brash AR, Dubois RN. 15S-Hydroxyeicosate traenoic acid activates peroxisome proliferator-activated receptor gamma and inhibits proliferation in PC3 prostate carcinoma cells. *Cancer Res* 2001; **61**: 497-503

40 **Yu J**, Qiao L, Zimmermann L, Ebert MP, Zhang H, Lin W, Röcken C, Malfertheiner P, Farrell GC. Troglitazone inhibits tumor growth in hepatocellular carcinoma in vitro and in vivo. *Hepatology* 2006; **43**: 134-143

41 **Shaik MS**, Chatterjee A, Singh M. Effect of a selective cyclooxygenase-2 inhibitor, nimesulide, on the growth of lung tumors and their expression of cyclooxygenase-2 and peroxisome proliferator- activated receptor-gamma. *Clin Cancer Res* 2004; **10**: 1521-1529

42 **Shaik MS**, Chatterjee A, Jackson T, Singh M. Enhancement of antitumor activity of docetaxel by celecoxib in lung tumors. *Int J Cancer* 2006; **118**: 396-404

S- Editor Cheng JX **L- Editor** Webster JR **E- Editor** Yin DH

Online Submissions: wjg.wjgnet.com
wjg@wjgnet.com
doi:10.3748/wjg.15.2739

World J Gastroenterol 2009 June 14; 15(22): 2739-2747
World Journal of Gastroenterology ISSN 1007-9327

Predictive value of multi-detector computed tomography for accurate diagnosis of serous cystadenoma: Radiologic-pathologic correlation

Anjuli A Shah, Nisha I Sainani, Avinash Kambadakone Ramesh, Zarine K Shah, Vikram Deshpande, Peter F Hahn, Dushyant V Sahani

Anjuli A Shah, Nisha I Sainani, Avinash Kambadakone Ramesh, Zarine K Shah, Peter F Hahn, Dushyant V Sahani, Department of Radiology, Division of Abdominal Imaging and Interventional Radiology, White Bldg. 270, Massachusetts General Hospital, 55 Fruit St., Boston MA 02114, United States
Vikram Deshpande, Department of Pathology, Massachusetts General Hospital, 55 Fruit St., Boston MA 02114, United States
Author contributions: Shah AA, Sainani NI, Kambadakone AR, Shah ZK, Deshpande V, Hahn PF and Sahani DV contributed equally to this work; Sahani DV designed research and intellectual content; Shah AA, Sainani NI, Kambadakone AR, Shah ZK, Deshpande V and Sahani DV performed research; Shah AA, Kambadakone AR, Sainani NI, Deshpande V, Hahn PF and Sahani DV analyzed the data; Shah AA, Kambadakone AR, Deshpande V, Hahn PF and Sahani DV contributed to preparing the manuscript, editing and final approval.
Correspondence to: Dushyant V Sahani, MD, Director of CT, Division of Abdominal Imaging and Interventional Radiology, Massachusetts General Hospital, 55 Fruit street, White 270, Boston MA 02114, United States. dsahani@partners.org
Telephone: +1-617-7268396 Fax: +1-617-7264891
Received: July 1, 2008 Revised: August 26, 2008
Accepted: September 3, 2008
Published online: June 14, 2009

Abstract

AIM: To identify multi-detector computed tomography (MDCT) features most predictive of serous cystadenomas (SCAs), correlating with histopathology, and to study the impact of cyst size and MDCT technique on reader performance.

METHODS: The MDCT scans of 164 patients with surgically verified pancreatic cystic lesions were reviewed by two readers to study the predictive value of various morphological features for establishing a diagnosis of SCAs. Accuracy in lesion characterization and reader confidence were correlated with lesion size ($\leqslant$ 3 cm or $\geqslant$ 3 cm) and scanning protocols (dedicated *vs* routine).

RESULTS: 28/164 cysts (mean size, 39 mm; range, 8-92 mm) were diagnosed as SCA on pathology. The MDCT features predictive of diagnosis of SCA were microcystic appearance (22/28, 78.6%), surface lobulations (25/28, 89.3%) and central scar (9/28, 32.4%). Stepwise logistic regression analysis showed that only microcystic appearance was significant for CT diagnosis of SCA (P = 0.0001). The sensitivity, specificity and PPV of central scar and of combined microcystic appearance and lobulations were 32.4%/100%/100% and 68%/100%/100%, respectively. The reader confidence was higher for lesions > 3 cm (P = 0.02) and for MDCT scans performed using thin collimation (1.25-2.5 mm) compared to routine 5 mm collimation exams (P > 0.05).

CONCLUSION: Central scar on MDCT is diagnostic of SCA but is seen in only one third of SCAs. Microcystic morphology is the most significant CT feature in diagnosis of SCA. A combination of microcystic appearance and surface lobulations offers accuracy comparable to central scar with higher sensitivity.

Key words: Pancreas; Serous cystadenoma; Multi-detector computed tomography; Central scar; Lobulations; Microcystic

Peer reviewer: Dr. Aydin Karabacakoglu, Assistant Professor, Department of Radiology, Meram Medical Faculty, Selcuk University, Konya 42080, Turkey

Shah AA, Sainani NI, Kambadakone AR, Shah ZK, Deshpande V, Hahn PF, Sahani DV. Predictive value of multi-detector computed tomography for accurate diagnosis of serous cystadenoma: Radiologic-pathologic correlation. *World J Gastroenterol* 2009; 15(22): 2739-2747 Available from: URL: http://www.wjgnet.com/1007-9327/15/2739.asp DOI: http://dx.doi.org/10.3748/wjg.15.2739

INTRODUCTION

Pancreatic serous cystadenomas (SCAs) are rare lesions that are almost always benign and usually asymptomatic[1]. SCAs comprise 1%-2% of pancreatic neoplasms and 10%-15% of cystic lesions[2]. While SCAs are relatively uncommon in comparison to pseudocysts and solid tumors of the pancreas, their clinical importance is

indisputable. Though generally regarded as benign, 3% of SCAs have malignant potential with local infiltration and distant metastases[1,3-5]. These are slow growing tumors; however the growth rate varies depending on tumor size. When the tumor is under 4 cm in diameter, the growth rate is only 0.12 cm/year whereas when the tumors ⩾ 4 cm in diameter they can grow at a remarkable 1.98 cm/year[6]. Due to the benign nature and the morbidity associated with pancreatic surgery, a follow up imaging for surveillance is recommended for these tumors[3,7]. Complete resection is considered curative, and is recommended when the lesion is symptomatic, when it increases in size upon follow-up, and when confident non-invasive differentiation from a more aggressive lesion is impossible[6]. Tumors that are resected have a good prognosis, with no requirement for postoperative surveillance[3,6].

Due to increased utilization of high-resolution imaging such as multi-detector computed tomography (MDCT), magnetic resonance imaging (MRI) and MR cholangiopancreatography (MRCP), SCAs are now more frequently identified, and often incidentally[8,9]. This high rate of detection of incidental pancreatic cystic lesions has generated great interest regarding the appropriate management of these lesions[6]. However, there is some overlap in imaging appearance among cystic pancreatic lesions, and it can be difficult to differentiate SCAs from other types of pancreatic cysts, such as pseudocysts, mucinous cystic neoplasms (MCNs) and intraductal papillary mucinous neoplasms (IPMNs). Thus the diagnosis of serous cystadenomas assumes particular significance because they need to be differentiated from other cystic neoplasms like MCNs, which are known to be premalignant or malignant[10]. The differentiation is vital to avoid unnecessary pancreatic surgery, which although increasingly safe in experienced hands continues to cause significant postoperative morbidity[6]. Thus accurate preoperative lesion characterization is crucial in determining appropriate action.

MDCT is the initial imaging modality of choice for evaluation of cystic lesions of the pancreas. Although the imaging features of SCAs on MDCT have been described before, few studies have compared the accuracy of various CT features for distinguishing SCAs from other lesions. With this purpose in mind, we undertook this study to examine the different features of SCAs on MDCT and identify the common and uncommon imaging features of SCAs that enable a confident diagnosis. Other commonly occurring cystic lesions were also studied from a large cohort of cystic lesions to identify the specific features that characterize SCAs.

MATERIALS AND METHODS

Study design

This is a retrospective study that was approved by the Institutional Review Board and follows the Health Insurance Portability and Accountability Act regulations. Informed patient consent forms were waived. We searched the electronic database of hospital medical records for patients who had pancreatic surgery for cystic lesions from January 1999 to August 2007. The inclusion criteria required the patients to have had the MDCT exam prior to surgical resection. Out of a total of 180 patients with MDCT studies prior to surgical resection, 16 patients who had clinical and laboratory evidence of acute pancreatitis were excluded from the study. Criteria for diagnosis of pancreatitis were elevated serum amylase or lipase levels and/or imaging evidence of pancreatic inflammation. The process resulted in an initial cohort of 164 patients. These patients were evaluated for clinical presentation, imaging features, and pathological and surgical findings. Of the group of 164 patients, a subset consisting of 28 patients (17 women, 11 men; age range, 29-90 years; mean age, 62 years) with pathologically verified SCAs were studied to analyze their characteristic imaging features and constituted the main population for the present study. However, data from the other 136 patients in the cohort of 164 was also analyzed to study the accuracy of each imaging feature studied.

MDCT technique

All patients had undergone CT examinations on MDCT (GE Health Care, Milwaukee, WI) with four, eight or 16 detector rows. The acquisition protocol for the CT exam was either dedicated pancreatic protocol CT (91/164, 14 SCAs) or a routine contrast enhanced CT study (73/164, 14 SCAs). The initial scan was a non-enhanced CT acquisition of 5 mm thickness through the liver and pancreas. For routine abdominal CT scanning, 120-150 mL of nonionic contrast material (300-370 mg/mL) was injected at a rate of 3.0 mL/s, and 5 mm thick images were acquired after a 65-70 s delay.

Pancreatic protocol consisted of two phase acquisition after administration of 120-150 mL of nonionic contrast material (370 mg of iodine per milliliter) at a rate of 4-5 mL/s. Pancreatic phase imaging was performed 45 s after starting contrast material injection by obtaining 1.25-mm/2.5-mm targeted reconstructed sections through the pancreas. Portal venous phase imaging followed at 65-70 s after contrast material injection with 5-mm-thick sections. For pancreatic phase imaging, the field of view was 28 cm; for the other phases, the field of view was adjusted according to the size of the patient.

Post processing

Coronal reformatted images of 2.5-3 mm thickness were obtained in all of the patients. Additional reformatting techniques used included oblique coronal multiplanar reformations (MPRs, 5 mm) parallel to the pancreatic head or tail, 1-2 curved planar reformations along the course of the pancreatic duct (1.25 mm) and thin slab (5 mm) coronal maximum intensity projections (MIP) to display vessel involvement. These reformations were performed by one of the trained technologists on a work station (ADW 4.0, GE).

Data analysis

The CT images were retrospectively reviewed by consensus by two radiologists with 14 and 7 years of experience, respectively, who were kept blinded to patients' clinical details and histopathology of the cystic lesion. The analysis was done on picture archiving and communication system (PACS version 4.0, Agfa, Richmond, VA). For the image analysis, a template was created to evaluate features of a pancreatic cyst. The following features were assessed: cyst size, presence or absence of septations, lesion margins, solid components, lobulations, central scar, calcification, pancreatic duct communication, duct obstruction, lymphadenopathy and vascular involvement. The pancreas was evaluated for presence or absence of duct dilatation, parenchymal/ductal calcification and parenchymal atrophy.

The largest dimensions of the cyst were measured on axial scans and mean size calculated. The septations were evaluated for thickness and enhancement. The margins of the lesion were considered either well defined or ill defined. The shape of the cysts was defined as either smooth, simple lobulated or complex lobulated. Simple lobulation was defined as the shape of a simple closed curve with bosselated surface whose borders could not be described within the same circle[10]. A complex lobulated shape was defined as one containing a conglomeration of two or more cysts either round, oval or tubular (pleomorphic in shape)[10]. Central scar was defined as a central stellate area of soft tissue density with or without calcification and with or without radiating surrounding linear strands. Attenuation values were obtained for the cysts by placing a ROI (mean size, 20 mm^2) on the unenhanced scan. Care was taken to exclude septations, calcifications and solid component within the ROI. The attenuation values measured from the various types of lesions (SCA, MCN, *etc*) were then averaged for comparison. Cyst morphology was classified as unilocular, microcystic, macrocystic or oligocystic and cyst with solid component[8]. Simple unilocular cysts included pancreatic cysts without internal septa, a solid component or central-cyst wall calcification. Unilocular cysts with mural enhancement or calcification were categorized as complicated. Microcystic lesion was defined as consisting of collection of cysts (> 6) ranging in size from a few millimeters up to 2 cm in size[8]. Macrocystic or oligocystic lesions were defined as lesions with more than one but < 6 cysts with at least one of them > 2 cm in size.

Using these features, the cysts were categorized as a simple cyst/pseudocyst, SCA, mucinous cystadenoma (MCN) and intraductal papillary mucinous cystadenoma (IPMN) or else solid neoplasms with cystic degeneration (Adenocarcinoma, endocrine tumors and solid papillary epithelial neoplasm) on imaging. The criteria considered for diagnosis of SCAs included: lobulations, microcystic pattern, presence or absence of central scar, well defined margins and lack of enhancement. Readers' diagnostic confidence for the diagnosis of serous cystadenoma was rated on a 5-point scale (with 1 being least confident and 5 being most) along with confidence as to whether the lesion was benign or malignant using a similar 5-point scale. Cystic lesions which did not have any specific attributable features to the above categories or those with a reader confidence less than three were considered indeterminate.

Surgery and histopathologic correlation

The type of surgical procedure performed was recorded. Histopathological analysis had been performed by a single gastrointestinal pathologist with ten years of specialized experience in pancreatic pathology. The gross and microscopic descriptions of the resected specimens described in the pathology reports were reviewed. A predefined template for pathology was filled in. The gross specimens were reviewed for cyst morphology, which included lesion size, septations and intralesional solid components. The final histopathological diagnosis was recorded as: SCA, IPMN, MCN, adenocarcinoma, endocrine tumors or solid papillary epithelial neoplasm. Those cysts without specific identifiable features where a conclusive diagnosis was not rendered on histopathology were categorized as unclassified cysts. The features on MDCT were then correlated with pathological reports.

Statistical analysis

Sensitivity, specificity, positive predictive value (PPV), negative predictive value (NPV) and accuracy for the various MDCT findings of SCA were calculated in comparison to other cystic lesions by using histopathology as the gold standard. *T*-test was used to calculate the statistical significance for various values and $P < 0.05$ was considered to suggest statistically significant difference. Statistical significance between the size of SCA and the occurrence of scar was evaluated using two sided Fisher's exact test. Stepwise logistic regression was used to identify the significance of each CT feature for diagnosis of SCA using SAS software (SAS system release 8.2). The CT feature was considered significant for the diagnosis whenever a tail probability of $P < 0.05$ was reached.

RESULTS

CT findings

Of the 28 SCA (mean size, 39 mm; range, 8-92 mm), 11 lesions were located in the head, 11 in the body, 3 in the tail and 3 in body and tail (Table 1). 22/28 (78.6%) SCAs were observed to have microcystic morphology (Figure 1) and 6/28 (21.4%) of SCAs had macrocystic or oligocystic morphology (Figure 2). 25/28 (89.3%) of SCAs were lobulated whereas 3/28 (10.7%) presented with smooth wall. 9/28 (32.1%) SCAs showed central scar with calcification seen in 3 scars (Figure 3). 8/9 (88.9%) of SCAs with central scar measured at least 2 cm (mean size, 4.1 cm; range, 1.9-8.4 cm). This finding was statistically significant for lesion size and occurrence of central scar ($P = 0.02$, Fisher's exact test).

Of the 136 other cystic lesions included for comparison of the morphological features with SCAs,

Table 1 MDCT findings observed in the various pancreatic cystic lesions

	SCA (*n* = 28)	IPMN (*n* = 42)	MCN (*n* = 37)	Unclassified Cysts (*n* = 45)	Endocrine tumors (*n* = 6)	Adenocarcinoma (*n* = 4)	Lymphan-gioma (*n* = 1)	SPE (*n* = 1)
Size (cm) mean (range)	3.9 (0.8-9.2)	2.7 (0.9-5.2)	4.3 (2.2-11)	2.4 (0.5-7.4)	4.6 (1.6-8.9)	3 (1.4-5.2)	2.3	2.3
Location								
Head	11	26	12	20	2	2	1	
Body	11	7	7	8	0	1		1
Tail	3	7	17	12	4	1		
Body/Tail	3	3	1	5	0	0		
Lobulations (*n* = 35/164)	25	3	1	5	1	0	0	0
Microcystic (*n* = 25/164)	22	1	2	0	0	0	0	0
Central Scar (*n* = 9/164)	9[2]	0	0	0	0	0	0	0
L + M[1] (*n* = 19/164)	19	0	0	0	0	0	0	0
Septa	27	32	25	28	2	2	0	0
Wall								
Thin	28	40	30	31	0	2	1	1
Thick	0	2	7	14	6	2	0	0
Calcifications								
Wall	0	4	1	5	0	0	0	0
Septal	0	2	0	0	0	0	0	0
Parenchymal	1	0	0	0	0	0	0	0
Mural nodules	0	3	6	1	3	4	0	1
Dilatation of PD	3	14	11	2	0	3	0	0
Vascular involvement	0	0	1	2	0	2	0	0
Lymphadenopathy	0	3	6	3	0	2	0	0

MDCT: Multi-detector computed tomography; SCA: Serous cystadenoma; IPMN: Intraductal papillary mucinous neoplasm; MCN: Mucinous cystic neoplasm. [1]Combined presence of Lobulations and microcystic appearance; [2]3/9 showed calcifications within the central scar.

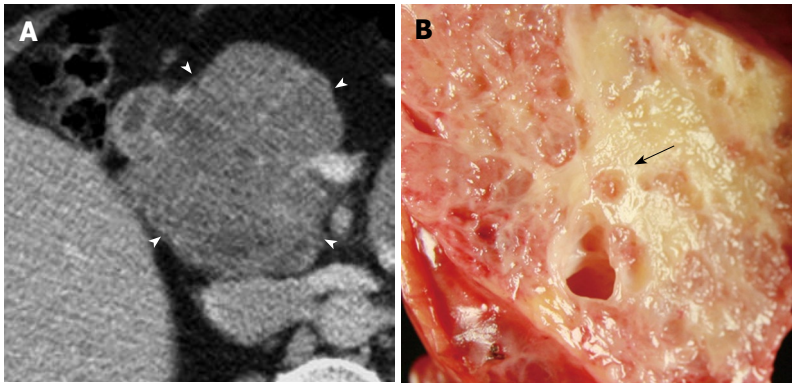

Figure 1 A 64-year-old woman who was incidentally found to have a mass in the head of the pancreas and subsequently underwent a Whipple procedure for removal. A: Lobulated (arrow heads) microcystic serous cystadenoma (SCA) with characteristic honeycomb appearance is seen on axial MDCT image (1.25 mm); B: Gross pathological specimen of the lesion reveals cluster of microcysts with a sponge pattern. A central scar is appreciated on the pathological image (black arrow), which is subtle and difficult to appreciate on the CT image.

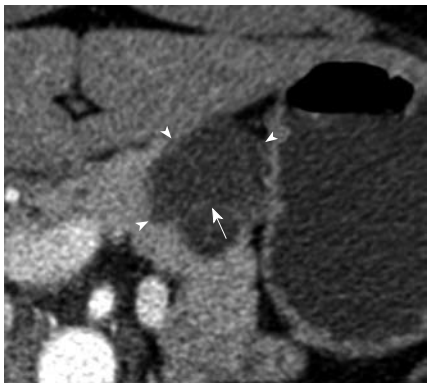

Figure 2 A 46-year-old woman who presented with abdominal pain was found to have a lesion in the body of the pancreas for which a partial pancreatectomy was performed. Axial MDCT image (1.25 mm) shows a lobulated (arrow heads) macrocystic SCA with septations (white arrow).

42 were IPMNs (mean size, 2.7 cm; range 0.9-5.2 cm), 37 were MCNs (mean size, 4.3; range, 2.2-11 cm), 45 were unclassified cysts (mean size, 2.4 cm; range 0.5-7.4 cm), 6 endocrine tumors (mean size, 4.6 cm; range, 1.6-8.9 cm), 4 adenocarcinomas (mean size, 3 cm; range, 1.4-5.2 cm), 1 was lymphangioma (2.3 cm) and 1 was solid papillary epithelial neoplasm (2.3 cm). Among these lesions microcystic pattern on CT was observed in 1 IPMN (2.3%) and 2 MCNs (5.4%) whereas the lobulated pattern was observed in 5 unclassified cysts (11.1%), 3 IPMNs (7.7%) and 1 MCN (3%). Central scar was not demonstrable in any of these lesions.

Upstream pancreatic ductal dilatation was observed in 3 patients. In one patient this was attributed to mass effect from a large SCA in the head of pancreas (Figure 4). However in two other patients with SCA,

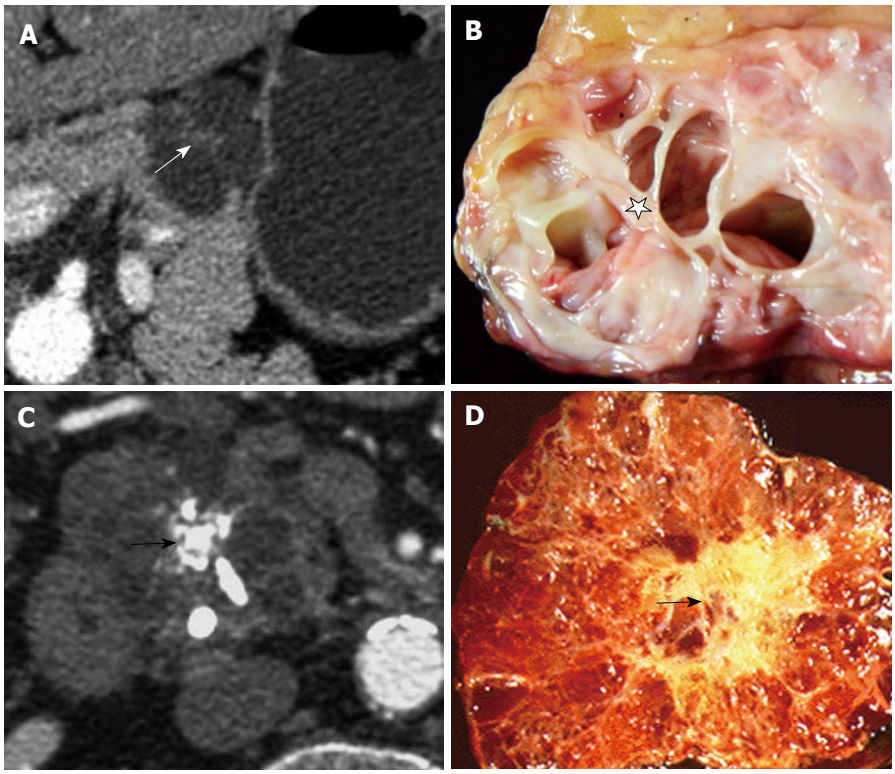

Figure 3 Images from 2 different patients with central scar. A: Axial MDCT image from a 46-year-old woman with a macrocystic SCA with a central scar (white arrow); B: Gross pathological specimen of the same patient also reveals the macrocystic pattern with the septa converging on a central scar (star); C: Axial MDCT image from a 66-year-old male who had a history of chronic pancreatitis, reveals a large lobulated microcystic lesion with central stellate calcification (black arrow). A Whipple procedure was done to remove a 4 cm mass from the head of the pancreas. Corresponding gross pathological image of the microcystic SCA with calcification (black arrow) in the central scar (D).

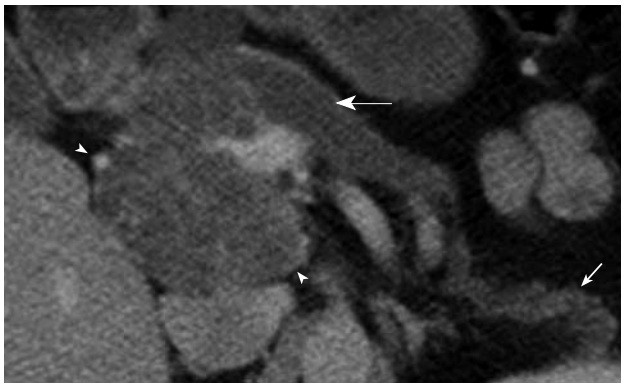

Figure 4 Axial MDCT image from a 64-year-old woman who had a large cyst in the pancreas detected incidentally. The patient underwent a Whipple procedure for removal of the large microcystic SCA (arrow heads) involving the head and uncinate process of the pancreas. The SCA caused upstream pancreatic duct dilatation (white arrow) and atrophy of the pancreatic body and tail (small white arrow).

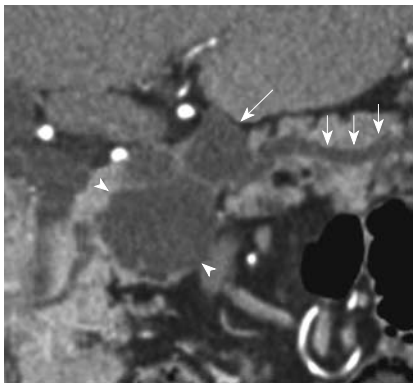

Figure 5 Coronal reformatted MDCT image from an asymptomatic 90-year-old woman, who had a 5 cm lesion in the head of the pancreas which was removed by Whipple procedure. The image shows an oligocystic SCA (arrow heads) in the head of pancreas which was mistaken for a mucinous lesion due to an associated side branch IPMN adjacent to it (white arrow). The two lesions were interpreted as a single multiloculated side branch mucinous lesion. There is mild upstream dilatation of the visualized pancreatic duct (small white arrows).

the pancreatic duct dilatation was considered due to background chronic pancreatitis changes in one and concurrent combined IPMN in another (Figure 5). Furthermore, five patients showed atrophy of the pancreatic parenchyma distal to the site of the lesion (Figures 4 and 6). None of the SCAs showed solid component, ductal communication or vascular encasement. The mean HU values for SCA were 19 ± 9 HU which was higher for microcystic variants (21 ± 8 HU) than the macrocystic variants (13 ± 4 HU). Though the average attenuation value for SCAs was higher than other types of cysts [mucinous lesions (MCNs and IPMNS): 10 ± 6 HU, pseudocysts: 12 ± 4 HU] it was not statistically significant ($P > 0.05$).

CT and histopathological correlation

Twenty four (85.7%) of the 28 SCAs were correctly characterized as such by CT. Of the four SCAs incorrectly identified on CT, two were classified as MCNs, one lesion as a possible IPMN, and one lesion was considered an indeterminate cystic lesion. The two classified as mucinous lesions had a macrocystic appearance and no central scar. One of these was classified as a benign mucinous lesion based on its macrocystic pattern and lack of central scar on CT. The second patient had two cysts, of which one was classified as mucinous and second as IPMN of side branch variety. However, histopathological analysis

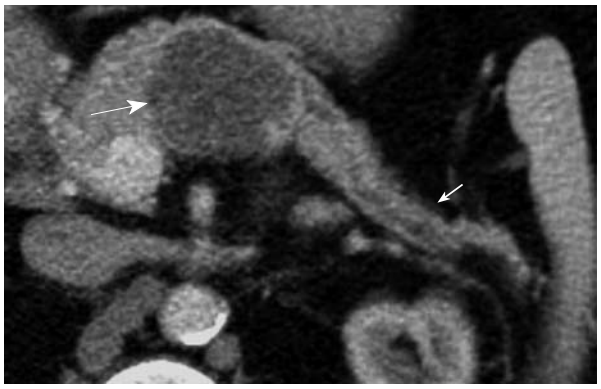

Figure 6 Axial MDCT image from a 64-year-old woman with an incidentally discovered cystic lesion in the body of the pancreas. A large serous cystadenoma (arrow) present in the body of pancreas displays microcystic morphology and fine lobulations with a central scar. Atrophy of the pancreatic parenchyma distal to the site of the lesion is also present (small arrow).

showed that the former was a SCA with a side branch IPMN in the vicinity (Figure 5). The lesion characterized as IPMN was microcystic, but confidence for diagnosis of SCA was low. The lesion classified as indeterminate cystic lesion was lobulated with thin septations and though the morphology was identified as macrocystic and benign, the reader confidence for diagnosis of SCA was less than 3.

When the imaging data of SCA were compared with pathological analysis, the majority of the observations remained constant (Table 2). MDCT features were consistent with the histological data for microcystic appearance (27/28, 96.4%) and surface lobulations (28/28, 100%). The 25 SCAs with pathologically confirmed lobulated morphology and the 3 with pathologically smooth morphology were correctly identified as such by CT. Of the 21 SCAs with pathologically confirmed microcystic morphology and 6 SCAs with pathologically confirmed macrocystic pattern, all were confidently identified as such on CT. One SCA which was characterized as microcystic on CT was found to be unilocular on pathology. This lesion measured 2 cm in diameter and there was substantial background noise on CT images.

Of the 10 central scars discovered on pathology, CT correctly identified them in 8 lesions. Central scars were missed on CT in 2, while in another SCA the central scar recorded on CT was found to represent converging septa on histopathology. In two lesions where CT failed to detect central scar, the SCA measured < 3 cm in size (average, 2.4 cm) and were evaluated using a routine protocol (5 mm). It is conceivable that these factors could have contributed to the reduced accuracy in depiction of SCA morphology.

For cyst characterization into benign and malignant, 27/28 lesions were confidently diagnosed as benign except for one lesion that was considered indeterminate on CT and was found to be benign on histopathology. This lesion measured 5.4 cm in diameter and presented with pancreatic duct dilatation and parenchymal atrophy, which raised the suspicion for an aggressive biology.

Table 2 Comparison of MDCT findings with pathological findings for SCA (n = 28)

	MDCT features	Pathology findings
Morphology		
Microcystic	22	21
Macrocystic/Oligocystic	6	6
Unilocular	-	1
Shape		
Lobulated	25	25
Smooth	3	3
Central scar	9	10
Wall		
Thin	28	28
Thick	0	0
Mural nodules	0	0
Septa	27	27

Morphological features in the diagnosis of SCA

The sensitivity, specificity, positive predictive value (PPV), negative predictive value (NPV) and accuracy of each of these features in the diagnosis of SCA are shown in Table 3. Based on pathologic verification, microcystic morphology on MDCT was demonstrated in 21/28 (75%) of SCAs. Microcystic pattern was also considered in other cystic lesions on MDCT that included 1 IPMN (n = 42) and 2 MCNs (n = 37), however on histopathology the CT appearance was not corroborated. The presence of microcystic morphology alone thus had a PPV of 88% and a specificity of 97.79% for the diagnosis of SCA. Lobulations were seen in 25/28 (89.3%) of SCAs, 5/45 unclassified cysts (11.1%), 3/42 IPMNs (7.1%) and 1/37 MCNs (2.7%). Lobulations had a PPV of 71.4% and specificity of 92.6% in the diagnosis of SCAs. When both lobulations and microcystic morphology were used for the identification of cystic lesions there was a PPV and specificity of 100% for identification of SCAs. It was found that central scar, microcystic pattern and combined presence of microcystic pattern and lobulations had the highest accuracy in the diagnosis of SCA. Stepwise logistic regression analysis showed that only microcystic appearance was significant for the CT diagnosis of SCA (P = 0.0001).

When comparing the diagnostic confidence for diagnosis of SCAs with reference to the lesion size, the confidence was higher for lesions ⩾ 3 cm (4.6) compared to lesions < 3 cm (3.9, P = 0.02). The CT pathologic concordance was better for lesions scanned with dedicated pancreatic protocol CT. The diagnostic confidence of readers in identifying the morphology of SCAs was better in those lesions scanned with dedicated pancreatic protocol (1.25-2.5 mm) compared to those scanned with routine abdomino-pelvic CT (5 mm) though this was not statistically significant (confidence level, 4.4 *vs* 4, P > 0.05).

DISCUSSION

High rate of incidental detection of cystic pancreatic lesions, including serous cystadenoma and the

Table 3 Sensitivity, specificity, predictive values and accuracy of morphological features in the diagnosis of SCA in comparison to other cystic lesions

	Lobulations (*n* = 35/164, %)	Microcystic (*n* = 25/164, %)	Central scar (*n* = 9/164, %)	L + M[1] (*n* = 19/164, %)
Sensitivity	89.30	78.50	32.40	67.85
Specificity	92.64	97.79	100.00	100.00
Positive predictive value	71.42	88.00	100.00	100.00
Negative Predictive value	97.67	95.70	87.74	93.80
Accuracy	92.00	94.50	88.40	94.50

[1]L + M: Lobulations and microcystic pattern.

overlapping imaging features of SCAs with other more aggressive cystic neoplasms makes management of these lesions challenging[7,9,11,12]. Accurate characterization is therefore imperative because of the low malignant potential of SCA and to determine the treatment options and to differentiate them from more aggressive lesions. Several studies have described the spectrum of imaging appearances of SCA on CT which include microcystic, macrocystic, unilocular and mixed morphologic patterns[7,9,11-14]. Microcystic pattern which is the most predominant pattern has been described in 70%-80% of SCAs[11,12,14]. Surface lobulations considered to be specific for the diagnosis of SCA have been studied with reference to oligocystic SCA (SOAs)[10,15,16]. Central scar which is considered pathognomonic for diagnosis of SCA has a low sensitivity and reliance on this imaging feature will not permit diagnosis of most SCAs[10,11,17]. The accuracy of CT in diagnosis of SCA in comparison to other cystic neoplasms has been reported in several previous studies which found accuracy ranging from 27%-93%[17-19]. More recent studies have compared SOAs with MCNs and IPMNs and have emphasized the importance of patient demographics, lesion location and shape of the cyst in characterization of the various lesions[4,10,15]. However, our study is unique as we have assessed the predictive value of specific features of SCA on MDCT in a large cohort of patients with surgically verified pancreatic cystic lesions and have evaluated how well the CT features correlate with pathology.

In our study, microcystic appearance was the only significant CT feature in the diagnosis of SCA. The combined presence of microcystic appearance and surface lobulations were also the strong predictors of SCA on CT with high PPV and specificity compared to other cystic lesions. Microcystic appearance was evident in 78% of SCAs in our study and this was concordant with other reports[11-14]. However, occasionally other cystic lesions when small in size can also appear microcystic on CT. In our study, small lesion size (< 2 cm) and background image noise potentially contributed to erroneous morphological depiction. Presence of surface lobulations within a cyst is a recognized feature of SCAs and can help to differentiate oligocystic SCAs from MCNs and IPMNs[10,15]. We observed lobulated contour in 89% of SCAs despite different morphologic appearances (microcystic, macrocystic and unilocular), a finding that has also been reported in other studies[10-11,15]. Although uncommon, surface lobulations can be encountered in a few MCNs (2.9%) and IPMNs (7.6%) as also reported by Kim *et al*[10].

The presence of a central scar is considered to be pathognomonic for SCAs, even when there is no distinct microcystic appearance[17]. Finding a central scar was highly specific of SCA in our study. It was not observed in any other cystic lesion but was encountered in only in 32% of SCAs. Other studies have observed it in anywhere from 30% to 45% of microcystic serous adenomas[17,20,21]. Eighty eight point nine percent of SCAs with central scar measured at least 2 cm indicating that larger the lesion size the more likelihood of occurrence of scar. Size of the lesion also determines the detectability of central scar since the two lesions in our study where the central scar was missed measured less than 3 cm in size.

The mean CT attenuation for all SCAs in our data set was higher than the values for other cystic lesions, more so for the microcystic variants though they were not statistically significant. The marginally elevated HU values could be accounted for by the presence of more stroma between the fluid filled sacs and the higher stroma: fluid ratio in SCA than other lesions. However, the attenuation values cannot be used as primary feature for differentiating between various pancreatic cystic lesions.

Lesion size itself can influence the reader confidence as the confidence for diagnosis of SCA was found to be higher for lesions ⩾ 3 cm compared to those with size < 3 cm. In addition to size of the cystic lesions, the MDCT scanning technique also influences the diagnostic accuracy and readers' confidence for lesion characterization.

Although the comparison of MDCT with MRI was not a part of this study, in our experience we have found that MRI might be beneficial when in doubt since the cyst morphology may be better appreciated on MRI. In our study, lesions which underwent dedicated pancreatic protocol examination with thin collimation (1.25-2.5 mm) had an improved reader confidence in the depiction of the morphological features compared to those which were scanned with routine protocol (5 mm). Two lesions where the central scars were missed on CT and the three cases of SCA which were misdiagnosed as mucinous lesions were evaluated by routine protocol, highlighting

the need to perform a dedicated pancreatic protocol CT for superior lesion characterization of cystic pancreatic lesions. We propose that all pancreatic cystic lesions should have at least one pancreatic protocol CT for better lesion characterization which will not only help avoid additional imaging follow up, but also prevent unnecessary surgical interventions.

This study had several limitations. Firstly, only surgically resected tumors were included for evaluation, which introduces a possible selection bias. However, since the majorities of SCAs are benign and are usually not resected, the comparison of MDCT findings with the histopathology findings in surgically resected SCAs adds to the value of the study. Secondly, not all patients had a dedicated pancreatic protocol CT exam. Though this could have affected the evaluation of diagnostic accuracy, it also provided us with an opportunity to study the effect of dedicated pancreatic protocol for evaluation of SCA compared to routine CT.

MDCT allows reliable assessment of the morphological features of SCA as depicted on gross histopathology. Central scar, although pathognomonic for SCA, is uncommonly seen. Microcystic morphology is the most significant CT feature in the diagnosis of SCA. Combined presence of microcystic morphology and surface lobulations offers high accuracy comparable to central scar but with higher sensitivity, thus allowing reliable diagnosis of SCA. Use of a dedicated pancreatic protocol with thin collimation improves the diagnostic accuracy of MDCT and enhances reader confidence.

COMMENTS

Background

Pancreatic serous cystadenomas (SCAs) are rare lesions that are almost always benign and usually asymptomatic. Though surgical resection results in complete cure, follow up surveillance is usually recommended due to their benign nature and the morbidity associated with pancreatic surgery. There is increased incidental detection of pancreatic cysts including SCAs with the use of multi-detector computed tomography (MDCT) and MRI. Accurate characterization of SCAs assumes importance due to their overlapping imaging features with other pancreatic cystic lesions particularly mucinous cystic neoplasms (MCNs) which have a malignant potential. Though several articles have described the imaging features of SCAs, few studies have compared the accuracy of these CT features in distinguishing between SCAs and other lesions. Therefore, this study was undertaken to evaluate the predictive values of various CT features of SCA that allow in its accurate characterization with pathological correlation.

Innovations and breakthroughs

One of the important innovations in the imaging evaluation of pancreatic cysts is the development of MDCT which allows excellent characterization of the morphology of pancreatic cyst. Though several authors have described the CT features of SCA, very few articles have discussed the predictive value of each imaging feature. This articles shows that microcystic appearance is the most significant imaging feature of SCA and the combination of microcystic appearance and surface lobulations is very specific for SCA in comparison to other cystic lesions.

Applications

The most important clinical application of this study is in the diagnosis and characterization of serous cystadenomas when incidentally detected on a CT scan. The finding of superiority of dedicated pancreatic protocol CT over routine protocol helps in the planning of CT examination when encountered with a incidental pancreatic cyst. This article emphasizes the effect of cyst size on lesion characterization and diagnostic accuracy. This calls for further studies for improve characterization of pancreatic cysts by furthering development of high resolution CT and MRI.

Peer review

The important part of the paper is that the study shows that microcystic appearance and lobulated pattern when present together are highly specific for diagnosis of SCA. This study highlights the value of performing a dedicated pancreatic protocol in the evaluation of pancreatic cystic lesions in improving diagnostic accuracy and reader confidence.

REFERENCES

1 **Strobel O**, Z'graggen K, Schmitz-Winnenthal FH, Friess H, Kappeler A, Zimmermann A, Uhl W, Büchler MW. Risk of malignancy in serous cystic neoplasms of the pancreas. *Digestion* 2003; **68**: 24-33

2 **Horvath KD**, Chabot JA. An aggressive resectional approach to cystic neoplasms of the pancreas. *Am J Surg* 1999; **178**: 269-274

3 **Galanis C**, Zamani A, Cameron JL, Campbell KA, Lillemoe KD, Caparrelli D, Chang D, Hruban RH, Yeo CJ. Resected serous cystic neoplasms of the pancreas: a review of 158 patients with recommendations for treatment. *J Gastrointest Surg* 2007; **11**: 820-826

4 **Goh BK**, Tan YM, Yap WM, Cheow PC, Chow PK, Chung YF, Wong WK, Ooi LL. Pancreatic serous oligocystic adenomas: clinicopathologic features and a comparison with serous microcystic adenomas and mucinous cystic neoplasms. *World J Surg* 2006; **30**: 1553-1559

5 **Le Borgne J**, de Calan L, Partensky C. Cystadenomas and cystadenocarcinomas of the pancreas: a multiinstitutional retrospective study of 398 cases. French Surgical Association. *Ann Surg* 1999; **230**: 152-161

6 **Tseng JF**, Warshaw AL, Sahani DV, Lauwers GY, Rattner DW, Fernandez-del Castillo C. Serous cystadenoma of the pancreas: tumor growth rates and recommendations for treatment. *Ann Surg* 2005; **242**: 413-419; discussion 419-421

7 **Bassi C**, Salvia R, Molinari E, Biasutti C, Falconi M, Pederzoli P. Management of 100 consecutive cases of pancreatic serous cystadenoma: wait for symptoms and see at imaging or vice versa? *World J Surg* 2003; **27**: 319-323

8 **Sahani DV**, Kadavigere R, Saokar A, Fernandez-del Castillo C, Brugge WR, Hahn PF. Cystic pancreatic lesions: a simple imaging-based classification system for guiding management. *Radiographics* 2005; **25**: 1471-1484

9 **Megibow AJ**, Lombardo FP, Guarise A, Carbognin G, Scholes J, Rofsky NM, Macari M, Balthazar EJ, Procacci C. Cystic pancreatic masses: cross-sectional imaging observations and serial follow-up. *Abdom Imaging* 2001; **26**: 640-647

10 **Kim SY**, Lee JM, Kim SH, Shin KS, Kim YJ, An SK, Han CJ, Han JK, Choi BI. Macrocystic neoplasms of the pancreas: CT differentiation of serous oligocystic adenoma from mucinous cystadenoma and intraductal papillary mucinous tumor. *AJR Am J Roentgenol* 2006; **187**: 1192-1198

11 **Procacci C**, Graziani R, Bicego E, Bergamo-Andreis IA, Guarise A, Valdo M, Bogina G, Solarino U, Pistolesi GF. Serous cystadenoma of the pancreas: report of 30 cases with emphasis on the imaging findings. *J Comput Assist Tomogr* 1997; **21**: 373-382

12 **Kim HJ**, Lee DH, Ko YT, Lim JW, Kim HC, Kim KW. CT of serous cystadenoma of the pancreas and mimicking masses. *AJR Am J Roentgenol* 2008; **190**: 406-412

13 **Procacci C**, Biasiutti C, Carbognin G, Accordini S, Bicego E, Guarise A, Spoto E, Andreis IA, De Marco R, Megibow AJ. Characterization of cystic tumors of the pancreas: CT accuracy. *J Comput Assist Tomogr* 1999; **23**: 906-912

14 **Chaudhari VV**, Raman SS, Vuong NL, Zimmerman P, Farrell J, Reber H, Sayre J, Lu DS. Pancreatic cystic lesions: discrimination accuracy based on clinical data and high resolution CT features. *J Comput Assist Tomogr* 2007; **31**: 860-867

15 **Cohen-Scali F**, Vilgrain V, Brancatelli G, Hammel P, Vullierme MP, Sauvanet A, Menu Y. Discrimination of unilocular macrocystic serous cystadenoma from pancreatic pseudocyst and mucinous cystadenoma with CT: initial observations. *Radiology* 2003; **228**: 727-733
16 **Khurana B**, Mortelé KJ, Glickman J, Silverman SG, Ros PR. Macrocystic serous adenoma of the pancreas: radiologic-pathologic correlation. *AJR Am J Roentgenol* 2003; **181**: 119-123
17 **Curry CA**, Eng J, Horton KM, Urban B, Siegelman S, Kuszyk BS, Fishman EK. CT of primary cystic pancreatic neoplasms: can CT be used for patient triage and treatment? *AJR Am J Roentgenol* 2000; **175**: 99-103
18 **Johnson CD**, Stephens DH, Charboneau JW, Carpenter HA, Welch TJ. Cystic pancreatic tumors: CT and sonographic assessment. *AJR Am J Roentgenol* 1988; **151**: 1133-1138
19 **Yuan D**, Yu W, Ren XB, Pan WD, Zhang LH. [Characterization and diagnostic accuracy of serous cystadenomas and mucinous neoplasms of the pancreas with multi-slice helical computed tomography] *Zhongguo Yi Xue Ke Xue Yuan Xue Bao* 2007; **29**: 232-237
20 **Yasuhara Y**, Sakaida N, Uemura Y, Senzaki H, Shikata N, Tsubura A. Serous microcystic adenoma (glycogen-rich cystadenoma) of the pancreas: study of 11 cases showing clinicopathological and immunohistochemical correlations. *Pathol Int* 2002; **52**: 307-312
21 **Box JC**, Douglas HO. Management of cystic neoplasms of the pancreas. *Am Surg* 2000; **66**: 495-501

S- Editor Zhong XY **L- Editor** Logan S **E- Editor** Yin DH

Online Submissions: wjg.wjgnet.com
wjg@wjgnet.com
doi:10.3748/wjg.15.2748

World J Gastroenterol 2009 June 14; 15(22): 2748-2753
World Journal of Gastroenterology ISSN 1007-9327

BRIEF ARTICLES

Pre-endoscopic screening for *Helicobacter pylori* and celiac disease in young anemic women

Lucy Vannella, Debora Gianni, Edith Lahner, Antonio Amato, Enzo Grossi, Gianfranco Delle Fave, Bruno Annibale

Lucy Vannella, Edith Lahner, Gianfranco Delle Fave, Bruno Annibale, Department of Digestive and Liver Disease, Hospital Sant'Andrea, II School of Medicine University Sapienza, 00189 Rome, Italy
Debora Gianni, Antonio Amato, Center for Thalassemic Disease of Rome, 00189 Rome, Italy
Enzo Grossi, Department of Medical Affair, Italian Diagnostic Center, 20100 Milan, Italy
Author contributions: Vannella L analyzed data and wrote the paper; Lahner E analyzed data; Delle Fave G and Amato A, Gianni D collected data; Grossi E and Delle Fave G revised the paper; Annibale B designed research and revised the paper.
Supported by (in part) Grants from the Italian Ministry for University and Research, MIUR, COFIN 2005 No. 0011222 and University Sapienza Roma and in part by a grant from Centro Diagnostico Italiano Milano, Italy
Correspondence to: Bruno Annibale, MD, Department of Digestive and Liver Disease, Sant'Andrea Hospital, 1035 Grottorossa Street, 00189 Rome, Italy. bruno.annibale@uniroma1.it
Telephone: +39-6-33775289 Fax: +39-6-4455292
Received: February 10, 2009 Revised: May 5, 2009
Accepted: May 12, 2009
Published online: June 14, 2009

Abstract

AIM: To evaluate the usefulness of pre-endoscopic serological screening for *Helicobacter pylori* (*H pylori*) infection and celiac disease in women aged < 50 years affected by iron-deficiency anemia (IDA).

METHODS: One hundred and fifteen women aged < 50 years with IDA were tested by human recombinant tissue transglutaminase IgA antibodies (tTG) and anti-*H pylori* IgG antibodies. tTG and *H pylori* IgG antibody were assessed using an enzyme-linked immunosorbent assay (ELISA). All women were invited to undergo upper GI endoscopy. During gastroscopy, biopsies were collected from antrum (n = 3), gastric body (n = 3) and duodenum (n = 4) in all patients, irrespective of test results. The assessment of gastritis was performed according to the Sydney system and celiac disease was classified by Marsh's System.

RESULTS: 45.2% women were test-positive: 41 patients positive for *H pylori* antibodies, 9 patients for tTG and 2 patients for both. The gastroscopy compliance rate of test-positive women was significantly increased with respect to those test-negative (65.4% *vs* 42.8%; Fisher test P = 0.0239). The serological results were confirmed by gastroscopy in 100% of those with positive *H pylori* antibodies, in 50% of those with positive tTG and in 81.5% of test-negative patient. Sensitivity and specificity were 84.8% and 100%, respectively for *H pylori* infection and, 80% and 92.8% for tTG. Twenty-eight patients had positive *H pylori* antibodies and in all the patients, an active *H pylori* infection was found. In particular, in 23 out of 28 (82%) patients with positive *H pylori* antibodies, a likely cause of IDA was found because of the active inflammation involving the gastric body.

CONCLUSION: Anti-*H pylori* IgG antibody and tTG IgA antibody testing is able to select women with IDA to submit for gastroscopy to identify *H pylori* pangastritis and/or celiac disease, likely causes of IDA.

Key words: Iron deficiency anemia; Women; Celiac disease; *Helicobacter pylori* gastritis

Peer reviewer: Wai-Man Wong, MD, Department of Medicine, University of Hong Kong, St Paul's Hospital, 2 Eastern Hospital Road, Causeway Bay, Hong Kong, China

Vannella L, Gianni D, Lahner E, Amato A, Grossi E, Delle Fave G, Annibale B. Pre-endoscopic screening for *Helicobacter pylori* and celiac disease in young anemic women. *World J Gastroenterol* 2009; 15(22): 2748-2753 Available from: URL: http://www.wjgnet.com/1007-9327/15/2748.asp DOI: http://dx.doi.org/10.3748/wjg.15.2748

INTRODUCTION

Iron-deficiency anemia (IDA) is common in women aged < 50 years with a prevalence of almost 5% in Western countries[1]. In this population, the balance of iron is often precarious due to menses, pregnancy and breastfeeding and an excessive menstrual flow is experienced by about 30% of women of reproductive age[2]. Menorrhagia is often considered the only cause of iron deficiency anemia, but some studies have shown the usefulness of a gastrointestinal (GI) tract

evaluation by endoscopy, thus indicating a role of the upper and/or lower GI tract as a likely cause of IDA[3-4]. The vast majority of IDA GI causes affect the upper GI tract and, in particular, there is a high prevalence of conditions associated with iron malabsorption such as *Helicobacter pylori* (*H pylori*) related-pangastritis, celiac disease and atrophic body gastritis in IDA premenopausal women[5-6]. On the contrary, as already reported in previous studies, bleeding lesions are infrequent in these patients and in particular in women aged < 50 years[5-8].

The diagnostic workflow in young women affected by IDA is not clearly established. The British Society of Gastroenterology recommends gastroscopy only in IDA women younger than 45 years presenting with GI symptoms[9]. However, the major issue of GI evaluation is that symptoms are often mild and aspecific in IDA women and that gastroscopy is an invasive procedure associated with a high number of refusals[10]. Furthermore, in our previous work on IDA premenopausal women, gastroscopy was performed as part of the diagnostic protocol in all patients, but was deemed unnecessary in almost 30% of the studied women because they were affected only by menorrhagia[5].

As shown in a previous study, non-invasive tests might be helpful in the selection of IDA women having a high probability of being affected by iron malabsorption GI diseases, in order to better address endoscopy and to increase the patients' compliance to the procedure[11].

The aim of the present study was to prospectively evaluate the usefulness of a pre-endoscopic serological screening for *H pylori* infection and celiac disease with the use of two tests (human recombinant tissue transglutaminase IgA antibodies and anti-*H pylori* IgG antibodies) in women aged < 50 affected by IDA in order to increase the compliance for gastroscopy.

MATERIALS AND METHODS

Patients

Between January and July 2006, 400 consecutive women (median age; 38 years) aged < 50 years with iron deficiency anemia were referred to the "Centro delle Microcitemie" of Rome, a public health institution specialized in the diagnosis of thalassemia. In these women the presence of an anemia emerged because they had previously undergone a complete blood count due to fatigue and/or for routine check-up, and were thus referred by their primary care physicians (60%), gynecologists (25.4%), hematologists (7.3%) or other physicians (7.3%) to the above mentioned center in order to exclude alpha- or beta-thalassemia minor, a frequent genetic disorder in the Italian population. In the "Centro delle Microcitemie", a complete blood count, serum iron and ferritin were repeated in all patients, and after the exclusion of α- and β-thalassemia, the presence of IDA was definitely diagnosed. IDA was defined as hemoglobin (Hb) < 12 g/dL with serum ferritin ≤ 20 μg/dL.

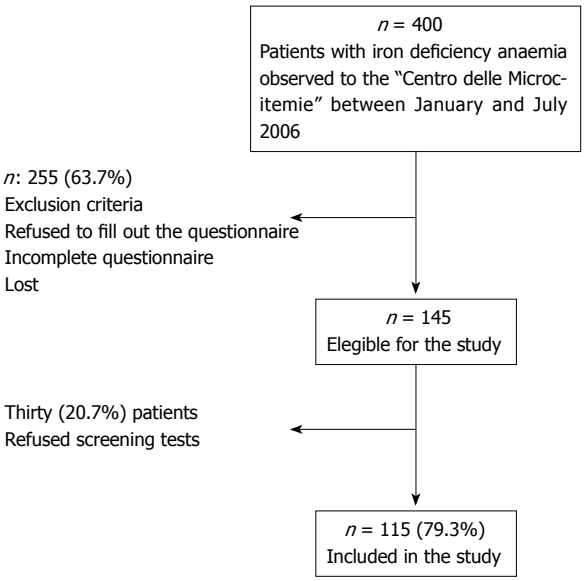

Figure 1 Study population. *n*: Numbers of patients.

IDA women were invited to answer a structured questionnaire to assess demographic data, previous iron supplementation, previous blood transfusion, previous hospitalization for anemia, obvious causes of blood loss, use of drugs (such as aspirin/NSAIDs, proton pump inhibitors, anticoagulants), 1st degree family history for colon or gastric cancer, peptic ulcer and celiac disease, type of diet, premenopausal status and GI symptoms. The duration of anemia was expressed as length of time from first diagnosis of IDA (mo) based on medical records. Upper GI symptoms included nausea, vomiting, dysphagia, heartburn, dyspepsia and upper abdominal pain. Lower GI symptoms included diarrhea, constipation, lower abdominal pain and hematochezia. The symptom was considered "present" if the patient referred to its presence at least once a week during the last three months[10]. Premenopausal status was defined as the patients' personal reports that within 3 mo prior to evaluation they were still menstruating[5].

The women were excluded from the study if they had: age > 50, obvious causes of GI bleeding, previous diagnosis of GI diseases probably responsible for IDA based on medical records, anorexia, vegetarian diet, pregnancy, breastfeeding, anemia of chronic diseases (for example chronic renal failure, cirrhosis and severe cardiopulmonary disease) and hematological diagnoses (e.g. aplastic anemia, myelodysplasia).

Study design

As shown in Figure 1, out of the initial 400 women with IDA, 145 women were considered eligible for the study (Figure 1). The diagnostic work-up included serological tests for the testing of anti-*H pylori* IgG antibodies to evaluate the presence of *H pylori* infection and tissue transglutaminase IgA antibodies to diagnose celiac disease. However, 30 women refused screening tests and thus, 115 women were included in the study and gave their informed consent.

Thus, 115 women were referred to University

Gastroenterology Department to pick up test results and were invited to undergo upper GI endoscopy to confirm test results. Patients with at least one of the 2 tests positive were defined as "test-positive" patients, those with all 2 tests negative were defined as "test-negative" patients.

Measurements

Serologic testing: Human recombinant tissue transglutaminase IgA antibodies were assessed using an enzyme-linked immunosorbent assay (ELISA) based on a commercially available kit (Bio-Rad Laboratories, Milan, Italy). A titre > 15 UI/mL was considered positive. *H pylori* IgG antibodies were assessed using an enzyme-linked immunosorbent assay (ELISA) based on a commercially available kit (Biohit, Helsinki, Finland). A titre > 1.1 UI/mL was considered positive.

Gastroscopy and histological evaluation: During gastroscopy, biopsies were collected from antrum (n = 3), gastric body (n = 3) and duodenum (n = 4) in all patients, irrespective of tests results. The assessment of gastritis was performed according to the Sydney system[12]. *Pangastritis* was defined as the presence of acute and chronic inflammatory infiltrate both in the gastric antrum and body as previously described[13]. If the sum of the inflammatory scores (acute and chronic) showed a two-grade difference between the antrum and corpus, the gastritis was considered as "*antrum-predominant*" or "*corpus-predominant*", respectively. *Antrum-restricted gastritis* was defined by the presence of acute and chronic inflammatory infiltrate exclusively in antrum according to the Sydney system[12]. Celiac disease was classified by Marsh's System[14]. The pathologist was unaware of the serological screening results.

Statistical analysis

Standard descriptive statistics was expressed as median and range and evaluated by appropriate statistical test (Mann-Whitney). Proportions were compared with the Fisher exact test. $P < 0.05$ was considered statistically significant.

RESULTS

Clinical features

The women included in the study had a median age of 38 years (range 21-50 years) and the median duration of IDA was 12 mo (range 1-408 mo). The value of median hemoglobin was 10.7 (range 7.3-11.9) g/dL, MCV was 72 (range 51-92) fL and ferritin was 10 (range 1-20) μg/L. Oral iron therapy was previously prescribed in 48 (41.7%) women. Only a small number of patients had previously needed blood transfusion (n = 3, 2.6%) or hospitalization for anemia (n = 8, 7%).

At least one symptom of the upper GI tract was present in 49.6% of patients (n = 57), while 57.4% of patients (n = 66) had a least one symptom of the lower GI tract. Reported GI symptoms were mainly non-specific, such as mild abdominal pain (24%) and bloating (46%). The vast majority of patients had a negative family history for GI diseases (80.8%): a family history for GI cancers or peptic ulcers was present only in 4.3% and 14% of patients, respectively. In 91.3% of women a premenopausal status was present.

Table 1 Clinical and biochemical features of the "test-positive" patients compared with "test-negative" patients

Patients, n = 115	Test-positive n = 52 (45.2%)	Test-negative n = 63 (54.8%)	P
Age (yr)	38 (23-50)	37.5 (21-50)	NS
Duration of Anemia (mo)	12 (1-408)	12 (1-312)	NS
Hb (g/dL)	10.6 (7.3-11.9)	10.9 (8-11.9)	NS
MCV (fl)	71 (51-90)	74 (58-92)	NS
Iron (μg/dL)	22 (6-65)	24.5 (9-52)	NS
Ferritin (μg/L)	10 (1-31)	10 (2-59)	NS
Smokers	10 (19%)	10 (16%)	NS
Previous therapy with iron	22 (41.5%)	26 (41.9%)	NS
Previous blood transfusion	2 (3.8%)	1 (1.8%)	NS
Previous therapy with vitamin B12	5 (9.4%)	9 (14.5%)	NS
Previous therapy with folic acid	18 (34%)	20 (32.2%)	NS
Hospitalization for anemia	3 (5.7%)	5 (9.4%)	NS
Upper GI symptoms	26 (49%)	31 (50%)	NS
Lower GI symptoms	29 (54.7%)	37 (59.7%)	NS
Premenopausal status	49 (94.2%)	56 (88.9%)	NS

Hb: Hemoglobin; MCV: Median corpuscular volume; GI: Gastrointestinal; NS: Not significant. All values are reported as median (range) unless otherwise indicated.

Serological tests

Fifty-two out of 115 patients (45.2%) were "test-positive". Of these, 41 (35.6%) patients had positivity for *H pylori* IgG antibodies, 9 (7.8%) patients for tissue transglutaminase IgA antibodies and 2 (1.7%) patients had positivity for both antibodies. As shown in Table 1, the group of patients with positive tests was not different from that with negative tests as far as clinical and biochemical features were concerned.

Gastroscopic/histological findings

"Test-Positive Patients": Four women did not undergo gastroscopy because they become pregnant after the start of the study. Of these, 3 patients had positive *H pylori* antibodies and 1 patient positive tissue transglutaminase IgA antibodies. Fourteen patients refused the invasive procedure, 12 out of these patients had positive *H pylori* antibodies and 2 patients had positive tissue transglutaminase IgA antibodies. Thus, 34 out of 52 (65.4%) "test-positive" patients consented to the upper GI endoscopy and the results are shown in Table 2.

Twenty-eight patients had positive *H pylori* antibodies, and in all these patients an active *H pylori* infection was found. Celiac disease was confirmed only in 4 out of 8 (50%) patients with positive tissue transglutaminase IgA antibodies, whereas in another patient who underwent gastroscopy for positive *H pylori* antibodies, celiac disease was also found. Of the 5 patients with celiac disease, 4 had Marsh 3 and 1 had Marsh 2.

In Table 3, the extent and the degree of *H pylori*-related gastritis is shown. Five IDA women with positive *H pylori* antibodies had exclusively *antrum-restricted gastritis*

Table 2 Gastroscopic/histological findings of patients according to diagnostic tests results

Patients	Test-positive $n = 34$			Test-negative $n = 27$
Gastroscopic/histological findings	*H pylori* antibodies $n = 26$	Tissue transglutaminase antibodies $n = 6$	*H pylori* & Tissue transglutaminase antibodies $n = 2$	
H pylori-related gastritis	26	-	2	5
Celiac disease	1	3	1	-
Normal	-	3	-	22
Total findings	27[1]	6	3[1]	27

[1]1 patient had both *H pylori*-related gastritis and celiac disease.

Table 3 Extent and degree of *H pylori*-related gastritis

Histological findings	Test-positive patients	Test-negative patients
Antrum-restricted gastritis	5	2
Pangastritis[1]	21	1
Antrum-predominant pangastritis	1	1
Corpus-predominant pangastritis	1	-
Atrophic body gastritis	-	1
Total	$n = 28$	$n = 5$

[1]Equal score of inflammatory infiltrate in antrum and corpus.

with active *H pylori* infection. In the remaining patients ($n = 23$), a pangastritis with active *H pylori* infection was present which in 91.3% of cases showed equal severity of the inflammatory score in antrum and corpus. Thus, in 23 out of 28 (82%) patients with positive *H pylori* antibodies, a likely cause of IDA was found because the active inflammation involved the gastric body.

"Test-Negative Patients": Three women could not undergo gastroscopy because they were pregnant, and 33 patients refused the procedure. Thus, 27 out of 63 (43%) "test-negative" patients underwent upper GI endoscopy. In 22 out of 27 (81.5%) patients, the negative serological tests results were confirmed because no gastroscopic/histological finding was revealed; instead in the remaining 5 patients *H pylori* gastritis was diagnosed (Table 2). In particular, 3 likely causes of IDA were misdiagnosed because 2 patients had "*antral-predominant*" chronic gastritis and 1 patient had atrophic body gastritis (Table 3).

The compliance rate of test-positive women (65.4%) was significantly higher than that of test-negative ones (42.8%) (Fisher test $P = 0.0239$). Patients undergoing gastroscopy were similar to the group of included patients in the study for demographic, clinical and biochemical data. Moreover, for these parameters, the group of dropped-out test-positive and test-negative patients was not different from those test-positive and test-negative patients who underwent gastroscopy (data not shown).

Diagnostic performance of tissue transglutaminase and anti-H pylori antibodies in IDA

On the basis of these results, the sensitivity, the specificity, and the positive and negative predictive values of tissue transglutaminase IgA antibodies for the diagnosis of celiac disease were 80%, 92.8%, 50% and 98.1%, respectively. The sensitivity, the specificity, and the positive and negative predictive values of anti-*H pylori* antibodies for the diagnosis of *H pylori* infection were 84.8%, 100%, 100% and 84.8%, respectively.

DISCUSSION

In the present study, 115 women aged < 50 years with unexplained IDA were tested by anti-*H pylori* IgG antibodies and human recombinant tissue transglutaminase IgA antibodies to diagnose *H pylori* infection and celiac disease. Almost half of the studied patients tested positive for at least one serological assay, and the suspicion of an upper GI disease as likely cause of IDA, raised by the serological result, was confirmed by gastroscopy in 100% of those with positive *H pylori* antibodies and in 50% of those with positive tissue transglutaminase IgA. On the other hand, in only 11% of test negative patients, gastroscopy with biopsies yielded a finding which may be interpreted as a likely cause of IDA (2 *H pylori*-related *antrum predominant* pangastritis and 1 atrophic body gastritis). Thus, these findings indicate that in women aged < 50 years with IDA, the dual-step approach e.g. serological tests and then invasive procedure, may be considered as a useful tool to optimize the use of gastroscopy, avoiding useless procedures, and to reduce the number of expensive histological examinations.

Previous studies have shown that the presence of GI symptoms or the severity of anemia were related to higher risk of GI causes of IDA[3,5-6]. In this study, no difference was found between test-positive and test-negative patients in terms of personal data, clinical and biochemical features including the frequency of upper GI symptoms and Hb values. Therefore, our results show that GI evaluation is of poor utility to target IDA patients for gastroscopy, strengthening the usefulness of the pre-endoscopic screening by serological tests.

H pylori infection was found in 35.6% of the investigated women, confirming the strong association between *H pylori* infection and IDA observed in previous epidemiological studies[15-16]. Since *H pylori* IgG antibodies do not discriminate between active or previous infection, they are not generally considered useful for diagnosing *H pylori* infection[17]; in this clinical setting of IDA women, *H pylori* antibody-positivity was always associated with active infection as shown by histological data (Table 3). Moreover, 82% of patients with *H pylori* antibody-positivity had gastritis involving the gastric body, while only five cases had an *antrum-restricted* gastritis. In fact, only when the inflammation involves the gastric body, the acid secretion is reduced and the iron absorption is impaired, is there a consequential IDA[13,18]. The presence of positive *H pylori* antibodies, in a patient at high risk for iron malabsorption diseases, supports the need of an accurate gastroscopic/histological evaluation with antral and corporal biopsies to define the extent of gastritis and

eventually its association with IDA. In our clinical setting, we observed 100% specificity and positive predictive value as well as a sensitivity of 85% for the *H pylori* antibodies assay. On the basis of this result, we believe that the assay of *H pylori* antibodies may be considered useful in the selection of IDA women aged < 50 years to submit for gastroscopy, also keeping in mind that this serological test is widely available and cheap and, for this reason, it may be used in the primary care.

Human recombinant tissue transglutaminase IgA antibodies were found to be positive in almost 7% of all patients. This antibody was chosen as screening test for celiac disease, because it is based on ELISA assay and is more accurate compared to the immunofluorescence method used for determining endomysial antibodies[19]. Our results showed a good sensitivity (80%), and specificity (93%) of the assay in keeping with a recent meta-analysis[20]. Our study confirmed also the poor positive predictive value (50%), which is a well known limit of this serological assay. Yet, this value is higher than the one (28%) reported in previous literature[21]. This difference may be explained by the fact that the women included in the present study were anemic and thus were at high risk for celiac disease[22]. Considering the occurrence of false positives of the tissue transglutaminase assay, even in this particular clinical setting, the need for a histological confirmation of celiac disease diagnosis is confirmed.

The main limitation of this work is the small size of the sample, in part due to the high percentage of patients who have refused to participate in the study and of those who, once included, refused gastroscopy. Thus, our findings suggest that the pre-selection of young women for gastroscopy by non-invasive serological testing is able to increase compliance for the invasive procedure. In fact, the compliance rate of test-positive women was significantly increased with respect to those test-negative (65.4% *vs* 42.8%; Fisher test $P = 0.0239$).

In conclusion, half of IDA women aged < 50 years tested positive to serological screening for *H pylori* infection and/or celiac disease, and gastroscopy with biopsies confirmed in the vast majority of them the presence of active *H pylori* gastritis involving gastric body, or celiac disease, as possible causes of IDA. Thus, two simple and widely available tests (tissue transglutaminase IgA antibodies and anti-*H pylori* IgG antibodies) are able to select women with IDA to submit for gastroscopy to identify IDA-related GI causes.

COMMENTS

Background

Iron-deficiency anemia (IDA) is common in women aged < 50 years. Menorrhagia is often considered the only cause of iron deficiency anemia, but some studies have shown the usefulness of a gastrointestinal (GI) tract evaluation. The vast majority of IDA GI causes affect the upper GI tract and there is a high prevalence of conditions associated with iron malabsorption such as *Helicobacter pylori* (*H pylori*) related-pangastritis, celiac disease and atrophic body gastritis in IDA premenopausal women.

Research frontiers

The diagnostic workflow in young women affected by IDA is not clearly established. The British Society of Gastroenterology recommends gastroscopy only in IDA women younger than 45 years presenting with GI symptoms. However, symptoms are often mild and aspecific in IDA women and the gastroscopy is an invasive procedure associated with a high number of refusals. In a previous work on IDA premenopausal women, gastroscopy was performed in all patients, later deemed unnecessary in almost 30% of the studied women because these were affected only by menorrhagia.

Innovations and breakthroughs

This study showed that two simple and widely available tests, ie those for tissue transglutaminase IgA antibodies and anti-*H pylori* IgG antibodies, are able to select women with IDA to submit for gastroscopy to identify IDA-related GI causes and to increase the compliance for the invasive procedure. Gastroscopy with biopsies confirmed in the vast majority of IDA women the presence of active *H pylori* pangastritis, atrophic gastric body, or celiac disease as possible causes of IDA.

Applications

This study showed that a pre-endoscopic serological screening for *H pylori* infection and celiac disease is useful to select IDA women having a high probability of being affected by iron malabsorption GI diseases and to increase the patients' compliance for the procedure.

Terminology

Pangastritis: *H pylori*-related gastritis involving the antrum and the body of the stomach. Malabsorptive diseases: diseases related to iron-malabsorption that include *H pylori*-pangastritis, atrophic body gastritis and celiac diseases.

Peer review

The paper is interesting to study the usefulness of non-invasive test to select women with IDA for gastroscopy. These findings may be not applicable to other countries if the prevalence of celiac disease or *H pylori* infection are low.

REFERENCES

1 **Looker AC**, Dallman PR, Carroll MD, Gunter EW, Johnson CL. Prevalence of iron deficiency in the United States. *JAMA* 1997; **277**: 973-976

2 **El-Hemaidi I**, Gharaibeh A, Shehata H. Menorrhagia and bleeding disorders. *Curr Opin Obstet Gynecol* 2007; **19**: 513-520

3 **Bini EJ**, Micale PL, Weinshel EH. Evaluation of the gastrointestinal tract in premenopausal women with iron deficiency anemia. *Am J Med* 1998; **105**: 281-286

4 **Fireman Z**, Zachlka R, Abu Mouch S, Kopelman Y. The role of endoscopy in the evaluation of iron deficiency anemia in premenopausal women. *Isr Med Assoc J* 2006; **8**: 88-90

5 **Vannella L**, Aloe Spiriti MA, Cozza G, Tardella L, Monarca B, Cuteri A, Moscarini M, Delle Fave G, Annibale B. Benefit of concomitant gastrointestinal and gynaecological evaluation in premenopausal women with iron deficiency anaemia. *Aliment Pharmacol Ther* 2008; **28**: 422-430

6 **Carter D**, Maor Y, Bar-Meir S, Avidan B. Prevalence and predictive signs for gastrointestinal lesions in premenopausal women with iron deficiency anemia. *Dig Dis Sci* 2008; **53**: 3138-3144

7 **Park DI**, Ryu SH, Oh SJ, Yoo TW, Kim HJ, Cho YK, Sung IK, Sohn CI, Jeon WK, Kim BI. Significance of endoscopy in asymptomatic premenopausal women with iron deficiency anemia. *Dig Dis Sci* 2006; **51**: 2372-2376

8 **Kepczyk T**, Cremins JE, Long BD, Bachinski MB, Smith LR, McNally PR. A prospective, multidisciplinary evaluation of premenopausal women with iron-deficiency anemia. *Am J Gastroenterol* 1999; **94**: 109-115

9 **Goddard AF**, McIntyre AS, Scott BB. Guidelines for the management of iron deficiency anaemia. British Society of Gastroenterology. *Gut* 2000; **46** Suppl 3-4: IV1-IV5

10 **Baccini F**, Spiriti MA, Vannella L, Monarca B, Delle Fave G, Annibale B. Unawareness of gastrointestinal symptomatology in adult coeliac patients with unexplained iron-deficiency anaemia presentation. *Aliment Pharmacol Ther* 2006; **23**: 915-921

11 **Annibale B**, Lahner E, Chistolini A, Gailucci C, Di Giulio E, Capurso G, Luana O, Monarca B, Delle Fave G. Endoscopic

evaluation of the upper gastrointestinal tract is worthwhile in premenopausal women with iron-deficiency anaemia irrespective of menstrual flow. *Scand J Gastroenterol* 2003; **38**: 239-245

12 **Dixon MF**, Genta RM, Yardley JH, Correa P. Classification and grading of gastritis. The updated Sydney System. International Workshop on the Histopathology of Gastritis, Houston 1994. *Am J Surg Pathol* 1996; **20**: 1161-1181

13 **Capurso G**, Lahner E, Marcheggiano A, Caruana P, Carnuccio A, Bordi C, Delle Fave G, Annibale B. Involvement of the corporal mucosa and related changes in gastric acid secretion characterize patients with iron deficiency anaemia associated with Helicobacter pylori infection. *Aliment Pharmacol Ther* 2001; **15**: 1753-1761

14 **Marsh MN**. Gluten, major histocompatibility complex, and the small intestine. A molecular and immunobiologic approach to the spectrum of gluten sensitivity ('celiac sprue'). *Gastroenterology* 1992; **102**: 330-354

15 **DuBois S**, Kearney DJ. Iron-deficiency anemia and Helicobacter pylori infection: a review of the evidence. *Am J Gastroenterol* 2005; **100**: 453-459

16 **Cardenas VM**, Mulla ZD, Ortiz M, Graham DY. Iron deficiency and Helicobacter pylori infection in the United States. *Am J Epidemiol* 2006; **163**: 127-134

17 **Cutler AF**, Prasad VM. Long-term follow-up of Helicobacter pylori serology after successful eradication. *Am J Gastroenterol* 1996; **91**: 85-88

18 **Annibale B**, Capurso G, Lahner E, Passi S, Ricci R, Maggio F, Delle Fave G. Concomitant alterations in intragastric pH and ascorbic acid concentration in patients with Helicobacter pylori gastritis and associated iron deficiency anaemia. *Gut* 2003; **52**: 496-501

19 **Lewis NR**, Scott BB. Systematic review: the use of serology to exclude or diagnose coeliac disease (a comparison of the endomysial and tissue transglutaminase antibody tests). *Aliment Pharmacol Ther* 2006; **24**: 47-54

20 **Zintzaras E**, Germenis AE. Performance of antibodies against tissue transglutaminase for the diagnosis of celiac disease: meta-analysis. *Clin Vaccine Immunol* 2006; **13**: 187-192

21 **Hopper AD**, Cross SS, Hurlstone DP, McAlindon ME, Lobo AJ, Hadjivassiliou M, Sloan ME, Dixon S, Sanders DS. Pre-endoscopy serological testing for coeliac disease: evaluation of a clinical decision tool. *BMJ* 2007; **334**: 729

22 **Rostom A**, Murray JA, Kagnoff MF. American Gastroenterological Association (AGA) Institute technical review on the diagnosis and management of celiac disease. *Gastroenterology* 2006; **131**: 1981-2002

S- Editor Tian L **L- Editor** Logan S **E- Editor** Yin DH

Online Submissions: wjg.wjgnet.com
wjg@wjgnet.com
doi:10.3748/wjg.15.2754

World J Gastroenterol 2009 June 14; 15(22): 2754-2762
World Journal of Gastroenterology ISSN 1007-9327

BRIEF ARTICLES

Ephrin A2 receptor targeting does not increase adenoviral pancreatic cancer transduction *in vivo*

Michael A van Geer, Conny T Bakker, Naoya Koizumi, Hiroyuki Mizuguchi, John G Wesseling, Ronald PJ Oude Elferink, Piter J Bosma

Michael A van Geer, Conny T Bakker, John G Wesseling, Ronald PJ Oude Elferink, Piter J Bosma, Liver Center of the Academic Medical Center of the University of Amsterdam, Meibergdreef 69/71, 1105BK Amsterdam, The Netherlands
Naoya Koizumi, Hiroyuki Mizuguchi, Laboratory of Gene Transfer and Regulation, National Institute of Biomedical Innovation, 7-6-8 Saito, Asagi, Ibaraki, Osaka 567-0085, Japan
Supported by Maurits en Anna de Kock fund to MA van Geer
Author contributions: van Geer MA and Bakker CT performed the majority of the experiments; Koizumi N and Mizuguchi H provided vital reagents and analytical tools; Wesseling JG provided financial support for this work; Oude Elferink RPJ and Bosma PJ designed the study and wrote the manuscript.
Correspondence to: Dr. Piter J Bosma, Liver Center AMC, University of Amsterdam, Meibergdreeg 69/71, 1105BK Amsterdam, The Netherlands. p.j.bosma@amc.uva.nl
Telephone: +31-20-5668850 Fax: +31-20-5669190
Received: February 6, 2009 Revised: April 29, 2009
Accepted: May 6, 2009
Published online: June 14, 2009

Abstract

AIM: To generate an adenoviral vector specifically targeting the EphA2 receptor (EphA2R) highly expressed on pancreatic cancer cells *in vivo*.

METHODS: YSA, a small peptide ligand that binds the EphA2R with high affinity, was inserted into the HI loop of the adenovirus serotype 5 fiber knob. To further increase the specificity of this vector, binding sites for native adenoviral receptors, the coxsackie and adenovirus receptor (CAR) and integrin, were ablated from the viral capsid. The ablated retargeted adenoviral vector was produced on 293T cells. Specific targeting of this novel adenoviral vector to pancreatic cancer was investigated on established human pancreatic cancer cell lines. Upon demonstrating specific *in vitro* targeting, *in vivo* targeting to subcutaneous growing human pancreatic cancer was tested by intravenous and intraperitoneal administration of the ablated adenoviral vector.

RESULTS: Ablation of native cellular binding sites reduced adenoviral transduction at least 100-fold. Insertion of the YSA peptide in the HI loop restored adenoviral transduction of EphA2R-expressing cells but not of cells lacking this receptor. YSA-mediated transduction was inhibited by addition of synthetic YSA peptide. The transduction specificity of the ablated retargeted vector towards human pancreatic cancer cells was enhanced almost 10-fold *in vitro*. In a subsequent *in vivo* study in a nude (*nu/nu*) mouse model however, no increased adenoviral targeting to subcutaneously growing human pancreas cancer nodules was seen upon injection into the tail vein, nor upon injection into the peritoneum.

CONCLUSION: Targeting the EphA2 receptor increases specificity of adenoviral transduction of human pancreatic cancer cells *in vitro* but fails to enhance pancreatic cancer transduction *in vivo*.

Key words: Pancreatic cancer; Adenoviruses; Ephrin A receptor; Targeting; Genetic transduction

Peer reviewer: Julia B Greer, MD, MPH, Department of Gastroenterology, Hepatology and Nutrition, University of Pittsburgh Medical Center, M2, Presbyterian University Hospital, 200 Lothrop Street, Pittsburgh, Pa 15213, United States

van Geer MA, Bakker CT, Koizumi N, Mizuguchi H, Wesseling JG, Oude Elferink RPJ, Bosma PJ. Ephrin A2 receptor targeting does not increase adenoviral pancreatic cancer transduction *in vivo*. *World J Gastroenterol* 2009; 15(22): 2754-2762 Available from: URL: http://www.wjgnet.com/1007-9327/15/2754.asp DOI: http://dx.doi.org/10.3748/wjg.15.2754

INTRODUCTION

Pancreatic cancer is a devastating disease with a very poor prognosis[1]. The lack of options for curative treatment for pancreatic cancer and other gastrointestinal malignancies warrants a search for novel targets and novel therapies including gene therapy[2,3]. Adenovirus has been used widely as a gene therapy vector to treat solid tumors. After initial negative results in clinical trials with non-replicating vectors, conditional replicating adenoviral vectors have been tested in clinical trials recently. However, these have also shown disappointing efficacy[4,5]. Poor transduction efficiency and specificity of adenoviral vectors appears to be a major problem.

This seems to be the result of low expression of the primary receptor involved in adenoviral transduction on the tumors, the coxsackie and adenovirus receptor (CAR). Development of targeted vectors to circumvent CAR-mediated entry therefore seem to be required to increase the therapeutic potential of this approach.

Incorporation of ligands that bind to receptors highly expressed on cancer cells in the fiber HI loop enhance adenoviral transduction efficiency[6]. We have shown that incorporation of an RGD peptide improved transduction in pancreatic cancer[7]. Tumor specificity of RGD, however, is limited. Therefore, we decided to introduce the YSA peptide (YSAYPDSVPMMS) in the HI loop (van Geer, in review). YSA is a ligand for the EphA2 receptor (EphA2R) that is highly expressed on pancreatic cancers[8] and other solid tumors[9-11]. Since the YSA peptide has a high affinity for this receptor, it can be used for *in vivo* delivery of agents to tissues and tumors expressing the EphA2R[12]. In addition, binding of YSA activates the EphA2R and induces its internalization which may enhance adenoviral uptake. Adenoviral HI loop insertion of the YSA peptide increased the transduction specificity and efficiency both in human pancreatic tumor cell lines and in pancreatic tumor resection specimens *in vitro* (van Geer, in preparation). *In vivo* however, the presence of the native binding sites in the adenoviral capsid will compromise specific targeting. Even *in vitro*, YSA-mediated entry could only be proven upon inhibition of CAR-mediated entry. As we aim to target pancreas cancer *in vivo* we decided to ablate the native adenoviral binding sites of the YSA-targeted vector.

A highly conserved cluster of amino acids on the adenovirus fiber trimer is involved in CAR binding[13]. Site-directed mutagenesis of amino acids in this region was used to identify mutations that affect CAR binding. Mutations in the AB loop[14,15], the DE loop[16], and the FG loop[17] of the fiber knob all abolished CAR binding *in vitro*.

In addition to CAR, binding to integrins can also mediate adenoviral transduction. The presence of integrins on virtually all normal cells will also limit specific transduction of tumor cells. Removal of the integrin-binding motif RGD from the adenoviral penton base indeed enhances tumor specific targeting of adenoviral vectors[18].

To generate an adenoviral vector that targeted pancreatic cancer *in vivo* we therefore decided to combine HI loop insertion of the YSA peptide with ablation of the binding sites for CAR and integrin. The specificity of this doubly-ablated retargeted vector (Ad/ΔF(FG)Δ P-YSA) was determined *in vitro* and subsequently *in vivo*.

MATERIALS AND METHODS

Materials

Anti-fiber monoclonal 4D2 antibody (NeoMarkers, Fremont, California, USA); anti-EphA2R clone D7 (Sigma, Saint Louis, USA), synthetic peptide YSA (Eurogentec, Seraing, Belgium), Basement Membrane Matrix (BD Biosciences, Bedford, MA); luciferase activity was determined using a commercial kit (Promega) and a Berthold luminometer.

Cells

HEK293 cells, the established PC cell lines Capan-1 and Hs766-T, the mouse pre-adipocyte cell line 3T3-L1 and the mouse hepatoma Hepa 1-6 cell lines were obtained from the American Type Culture Collection Rockville, Maryland; BxPC-3 and MIA PaCa-2 were obtained from Boehringer Ingelheim (Belgium). The pancreatic carcinoma cell lines (p6.3 and p10.5) were obtained from Dr. E Jaffee, Johns Hopkins University School of Medicine, Baltimore, MD, USA. Human umbilical vein endothelial cells (HUVECs, passage 1-3) were isolated as described[19] and cultured in Medium-199 (GIBCO-BRL, Paisley, Scotland), supplemented with 20% (v/v) fetal bovine serum, 50 μg/mL heparin (Sigma, St Louis, MO, USA), 6-25 μg/mL endothelial cell growth supplement (ECGS; Sigma), penicillin (100 IU/mL), streptomycin (100 mg/mL) (GIBCO-BRL). Human fibroblasts (passage < 10) were a gift from the department of Genetic and Metabolic diseases AMC, Amsterdam. Fiber-293 cells expressing adenovirus type 5 fiber protein were used as the packaging cell line as previously described. All cells were cultured in Dulbecco's minimal essential medium (DMEM) with 10% fetal bovine serum (heat inactivated); L-glutamine (2 mmol/L) and penicillin (100 IU/mL), streptomycin (100 mg/mL) all from Cambrex Bio Science, Walkersville. All cell lines were cultured at 37℃ in 10% CO_2 atmosphere.

Plasmids

The E1-, E3-deleted adenovirus vector AdHM43 was used for propagation of integrin- and CAR-binding mutated adenovirus[20]. The RGD-peptide coding sequence at the penton base was changed from MNDHAIRGDTFATRAE to MNDTSRAE and the FG-loop of the fiber was deleted (T489, A490, Y491, T492). The cytomegalovirus (CMV) immediate-early promoter controlled enhanced green fluorescent protein (eGFP) and the CMV-controlled luciferase gene were inserted between the PI-Sce and Ceu-I sites of the pAdHM43 plasmid (van Geer, in review). Insertion of the YSA peptide (YSAPDSVPMMS) into pAdHM43-CMV-GFP and CMV/Luc was performed by digestion with BstB1 and ligation with 2 annealed primers: YSA forward: CGAAGTACAGCGCCTACCCCGACGG-CGTGCCCATGATGT. YSA reverse: CGACATCAT-GGGCACGCTGTCGGGGTAGGCGCTGTACTT. Clones identified by restriction enzyme analysis and PCR were sequenced to exclude mutations.

Virus generation, propagation and analysis

Recombinant ablated adenoviral vectors were generated by transfection of HEK 293 adeno fiber-expressing cells with *Pac* I -linearized Ad-CMV-GFP/Luc-YSA. Normal HEK 293 cells were used for the last propagation round as previously described[20]. Adenovirus was purified and concentrated by performing 2 cesium chloride gradients

and dialyzing against PBS. Glycerol was added to a final concentration of 10% (v/v) and virus preparations were stored at -80℃.

Modification of viral genomes were verified by PCR and sequencing using the following primers: fiber-forward: CAAACGCTGTTGGATTTATG; fiber-reverse: GTGTAAGAGGATGTGGCAAAT; RGD forward: TTGGATGTGGACGCCTAC; RGD reverse: AGGTGTCGCCGCGAATGGC.

The anti-fiber monoclonal 4D2 antibody (NeoMarkers, Fremont, California) was used to confirm proper trimerization of the fiber[21]. The number of viral genomic copies (gc) was determined by qPCR as previously described[22].

EphA2 receptor expression

Expression of EphA2R was studied with Western blotting using a 1:1000 dilution of a monoclonal antibody (anti-EphA2R clone D7, Sigma, Saint Louis, USA) and a peroxidase-conjugated anti IgG secondary antibody (1:2500). Cell lysates were prepared in 25 mmol/L Tris HCl pH 7.6, 150 mmol/L NaCl, 1% NP-40, 1% sodium deoxycholate, 0.1% SDS containing a cocktail of protease inhibitors (1:250, Roche). The protein concentration was determined with a BCA assay kit (Sigma). Detection was performed using the Lumi-light plus Western Blotting Substrate Kit (Roche, Mannheim, Germany). For receptor localization studies pancreatic tumor cells were gown on cover slips and were fixated 2 d later and stained for EphA2R using a 1:500 of the monoclonal antibody and a 1:2500 peroxidase-conjugated IgG secondary antibody.

Adenoviral transduction

5.0×10^4 cells were plated in 48-well plates and allowed to adhere overnight at 37℃. The next day virus was added (500 or 1000 VP/cell) in 2% DMEM. Blocking was performed by pre-incubating the cells with blocking agents in PBS for 20 min at room temperature. EphA2R was blocked with the synthetic peptide YSA (Eurogentec, Seraing, Belgium). For the bi-specific antibody experiments, 500 gc of virus were incubated for 60 min with 2.5 μL scFv bi-specific antibody (a kind gift from Dr. VW van Beusechem[23]).

In vivo transduction

1.0×10^7 Capan-1 pancreatic cancer cells were 1:1 diluted with Basement Membrane Matrix (BD Biosciences, Bedford, MA) and injected subcutaneously in both flanks of 6-9 wk old female athymic NMRI *nu/nu* mice (Harlem). When the tumor nodule reached a diameter of 0.4 to 0.7 cm, mice were injected intravenously (i.v.) or intraperitoneally (i.p.) with 1.0×10^{11} gc of Ad-/ΔF(FG)ΔP or Ad-/ΔF(FG)ΔP-YSA in 100 μL PBS. Blood was sampled by orbital puncture at 10 min after *i.v.* injection or at 90 min after *i.p.* injection. Three days after injection, mice were sacrificed and organs were harvested, snap frozen and used to determine luciferase activity according to standard procedures (Promega), using a Berthold luminometer. Luciferase activity was normalized for protein content. Viral DNA in blood was purified as described previously[24] and gc were quantified by qPCR using the primers against the CMV promoter (forward: AATGGGCGGTAGGCGTGTA, reverse AGGCGATCTGACGGTTCACTA). Serum aspartate aminotransferase (ASAT) and alanine aminotransferase (ALAT) levels were determined using standard clinical chemistry methods.

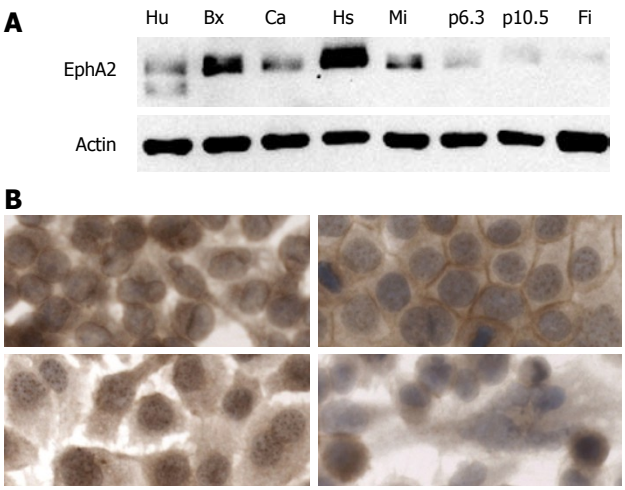

Figure 1 EphA-2 expression in human cell lines. A: Analysis of EphA2R expression by Western blotting in human umbilical vein endothelial cells (Hu), human pancreatic cancer cell lines BxPc-3 (Bx), Hs766-T (Hs), Capan-1 (Ca), MIA PaCa-2 (Mia), p6.3, p10.5 and human fibroblasts (Fi). EphA2R was detected using a monoclonal antibody and detection of actin levels was performed as a loading control; B: Immunolocalization of EphA2R in human pancreatic cancer cell lines BxPc-3 (left top), Capan-1 (right top), Hs766-T (bottom left), MiaPaca-2 (bottom right). Cells were fixated with methanol, acetone, and water, and a directed monoclonal antibody was used to detect EphA2R using a goat anti-mouse labeled with PO to perform DAB detection. Magnification (× 600), except for MiaPaca-2 (× 400).

RESULTS

Expression of the EphA2R on human pancreatic cancer cell lines and tissue specimens

The EphA2R is highly expressed on most solid tumors including pancreatic cancer. To investigate which cell lines are suitable as a model to study targeting, we determined its expression on a panel of established human pancreatic cancer cells and normal human cells such as fibroblasts and endothelial cells. The expression level of the EphA2R varied significantly in human pancreas cancer cell lines (Figure 1A). High expression was seen in Capan1, BxPc3, Hs766T and MIA PaCa-2, while expression in p6.3 and p10.5 was low. Of the normal cells, only human endothelial cells expressed EphA2R. Since this receptor is absent on normal human fibroblasts, we used these as negative control cells.

To investigate whether the EphA2R was accessible, we determined its localization in the cell lines highly expressing this receptor. The localization of this receptor differed between cell lines (Figure 1B). In Capan-1 and BxPc-3 cells, the EphA2R was detected on the membrane while in MIA PaCa-2, it was mostly seen in the cytoplasm. The signal seen in Hs766-T suggests

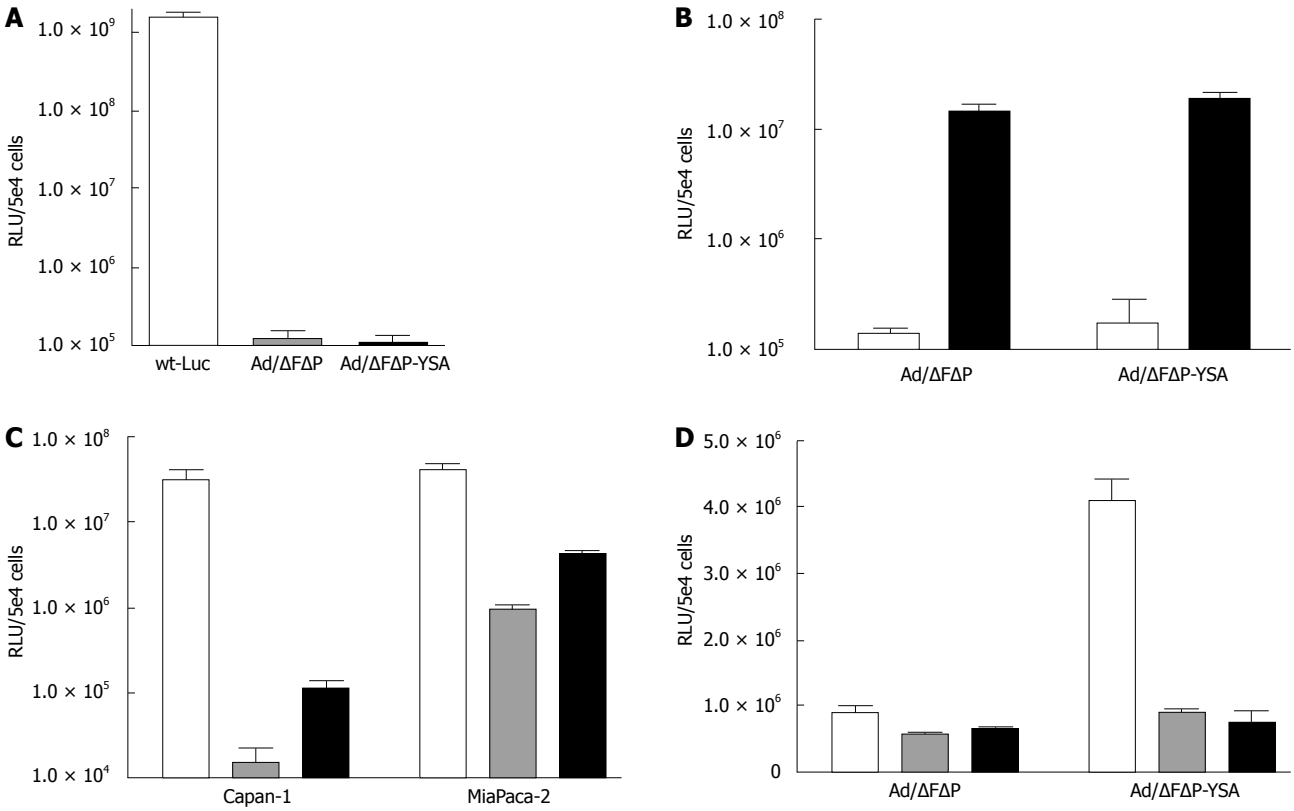

Figure 2 YSA redirects adenovirus to the EphA2 receptor. A: Transduction of CAR-expressing A549 cells with wild-type, ablated and YSA-retargeted adenoviral vectors with 1000 gc/cell: wt-Ad-Luc, Ad-Luc/ΔF(FG)ΔP and Ad-Luc/ΔF(FG)ΔP-YSA. Twenty four hours after infection cells were lysed to determine luciferase levels. Data are expressed as mean ± SD (n = 3). B: Incubation with bi-specific antibody restores infectivity of ablated adenoviral vectors in human fibroblasts. Cells were transduced with 500 gc/cell of Ad-/ΔF(FG)ΔP or Ad-/ΔF(FG)ΔP-YSA with (black bars) or without (white bars) EGF receptor targeted bi-specific scFV molecules. Luciferase activity was measured after 24 h and data are expressed as mean ± SD (n = 3). C: Insertion of YSA peptide in the HI loop of ablated adenoviral vector partially restores transduction of human pancreatic cancer cell lines Capan-1 and MiaPaca-2. Cells were transduced with 1000 gc/cell of wt-Ad-Luc (white bars), or Ad-Luc/ΔF(FG)ΔP (gray bars) or Ad-Luc/ΔF(FG)ΔP-YSA (black bars). Luciferase activity was measured after 24 h. Data are expressed as mean ± SD (n = 3). D: Pre-incubation with synthetic peptide blocks YSA-mediated targeting of human pancreatic cancer cell line MiaPaca-2. Cells were preincubated with 250 (grey bars) or 500 (black bars) μmol/L synthetic YSA peptide and transduced with 500 gc/cell of Ad-Luc/ΔF(FG)ΔP or Ad-Luc/ΔF(FG)ΔP-YSA. Luciferase was measured after 24 h. Data are expressed as mean ± SD (n = 3).

that, in this cell line, the EphA2R is present in nuclear granules. Since, in Capan-1 cells, the presence of the EphA2R on the membrane indicates that it is accessible for YSA binding, we chose to use this cell line for our subsequent studies.

Generation of ablated adenoviral vectors

We decided to use the FG loop mutation to ablate CAR binding because it has been well characterized[17,25]. By subsequent deletion of the RGD peptide from the penton base we obtained a doubly-ablated vector Ad-/ΔF(FG)ΔP which lacked both CAR and integrin binding. We inserted the YSA peptide in the HI loop of this doubly-ablated vector and generated Ad-/ΔF(FG)ΔP-YSA.

The lack of binding to native cellular receptors severely impairs the cellular entry of this doubly-ablated vector. Therefore, it can not be propagated on normal HEK 293 T cells. To overcome this, we used 293T cells that express the adenovirus type 5 fiber protein[20]. Incorporation of the normal fiber expressed in trans into the ablated vector allowed efficient cell entry and vector production. The last round of virus propagation was on normal 293T cells to generate the doubly-ablated vector. Because of impaired cell entry, the infectious particle (ip) titers of ablated vector stocks could not be preformed by standard procedures. To determine the functional titer of these vectors we therefore used a bi-specific antibody[23]. This antibody binds to the adenovirus knob and the epidermal growth factor receptor (EGFR). Upon binding to this antibody, the vector will enter the cells *via* the EGFR only. Therefore, this antibody allows direct comparison between the ip/gc ratio of the ablated and of the retargeted vectors.

To confirm the absence of CAR- and integrin-mediated entry, we compared the transduction efficiency of wild-type adenovirus type 5 with that of Ad-/ΔFΔP and Ad-/ΔFΔP-YSA on A549 cells that do express CAR but not EphA2R. The 3 to 4 log lower transduction by both ablated vectors confirmed efficient abolition of binding to the native receptors (Figure 2A). As expected, the transduction efficiency of both vectors on normal human fibroblasts that do not express the EphA2R was comparable but very low: 1.42×10^5 RLU for Ad-/ΔF(FG)ΔP and 1.77×10^5 RLU for Ad-/ΔF(FG)ΔP-YSA ($P = 0.06$) (Figure 2B). To confirm viability of the ablated vectors, we incubated both vectors with the bi-specific antibody, which resulted in a 2 log increase of

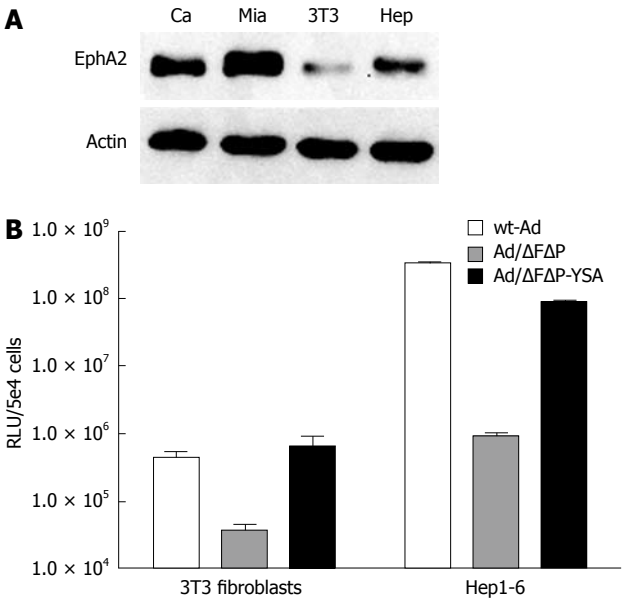

Figure 3 YSA targets adenovirus to cells expressing murine EphA2R. A: Western blotting demonstrates that mouse 3T3 and Hep1-6 cells, like human pancreatic cancer cell lines Capan-1 and MIA PaCa-2, express the EphA2R. EphA2R was detected using a monoclonal antibody and the housekeeping protein actin was used as a loading control. B: Efficient transduction of mouse 3T3 and Hep1-6 cells by YSA-retargeted adenoviral vector. Cells were transduced with 1000 gc/cell of wt-Ad-Luc (white bars), Ad-Luc/ΔF(FG)ΔP (gray bars) or Ad-Luc/ΔF(FG)ΔP-YSA (black bars). Luciferase was measured after 24 h. Data are expressed as mean ± SD (n = 3).

transduction efficiency for both vectors, Ad-/ΔF(FG)ΔP: 1.5×10^7 RLU and Ad-/ΔF(FG)ΔP-YSA: 1.9×10^7 RLU. The comparable transduction by both in the presence of the antibody indicated that both had a comparable ip/gc ratio ($P = 0.094$) and were viable.

To determine if insertion of the YSA peptide was functional, we tested transduction of both vectors on EphA2R-expressing Capan-1 and MiaPaca-2 cells. Although both cell lines do express integrins[7], ablation of native binding sites reduced their transduction by 3 to 1.5 logs. Insertion of the YSA peptide increased gene transfer to Capan-1 cells by 7.6-fold ($P = 0.0014$) and to MIA PaCa-2 cells by 4.5-fold ($P < 0.0001$). Insertion of the YSA peptide did not increase transduction in Hs766-T cells which only showed nuclear EphA2R staining (not shown). To confirm that entry of the retargeted vector was mediated by the YSA peptide, we performed competition experiments. As shown in Figure 2D, the 4-fold increased transduction efficiency of Ad-/ΔF(FG)ΔP-YSA compared to Ad-/ΔF(FG)ΔP was lost upon pre-incubation with synthetic YSA peptide. This indicated that the increased efficiency of the retargeted vectors was indeed mediated by the inserted YSA peptide. Thus, HI loop insertion of the YSA peptide in an adenovirus that lacks binding to CAR and integrins, resulted in cell entry *via* the EphA2R. Therefore, this vector appeared suitable for *in vivo* targeting of pancreatic cancer.

Targeting of the EphA2R by the YSA peptide has only been demonstrated in humans. Binding of the YSA peptide to the murine EphA2R has not been studied. Since binding to EphA2R expressed on activated (murine) endothelial cells will affect targeting of pancreatic cancer in a mouse model, we therefore decided to investigate the transduction efficiency of the YSA-retargeted adenoviral vector to mouse cells expressing the EphA2R. As shown in Figure 3A, mouse 3T3 fibroblasts and hepatoma cells (hepa1-6) both expressed the murine EphA2R, albeit at a lower level than in the human pancreatic cancer cell lines Capan-1 and MIA PaCa-2. Ablation of native cell binding sites reduced adenoviral transduction of these 2 mouse cell lines by 1 to 2 logs (Figure 3B). Insertion of the YSA peptide completely rescued cell entry of the ablated vector. Compared to the ablated vector, gene transfer of the YSA-retargeted vector was enhanced 17-fold in 3T3 cells and 95-fold in Hepa 1-6 cells. This efficient transduction of cells expressing the mouse EphA2R rendered the mouse a suitable model to study the efficiency of YSA-mediated targeting *in vivo*.

In vivo targeting in pancreatic cancer

To study *in vivo* targeting we used a *nu/nu* mouse model with subcutaneously growing human pancreatic tumor nodules. The virus was injected into mice which had nodules with a diameter of 0.4-0.7 cm, within 3 wk after injection of Capan-1 cells. We administered 1.0×10^{11} gc of ablated [Ad-/ΔF(FG)ΔP] or of the redirected vector Ad-/ΔF(FG)ΔP/-YSA, *via* the tail vein or i.p. Upon i.v. injection the clearance of both vectors was comparable. At 10 min after injection, $9.4 \times 10^8 \pm 6.3 \times 10^8$ gc/mL of Ad/ΔF(FG)ΔP and $1.1 \times 10^9 \pm 5.6 \times 10^8$ gc/mL of Ad/ΔF(FG)ΔP-YSA were present in blood. Since the total blood volume in a mouse is approximately 2.5 mL, the initial concentration of the virus was 4×10^{10} gc/mL. Thus 95% of the injected virus was cleared within 10 min. Based on the literature, we expected a slower clearance after i.p. injection, and determined the amount of virus in blood after 90 min. No significant difference was seen after 90 min between Ad-/ΔF(FG)ΔP-YSA ($1.4 \times 10^8 \pm 8.3 \times 10^7$ gc/mL) and Ad-/ΔF(FG)ΔP ($3.2 \times 10^8 \pm 4.3 \times 10^8$ gc/mL) ($P = 0.3$). Thus clearance for both vectors after *i.p.* injection was also comparable. Clearance of *i.p.*-injected virus was also efficient since less than 0.5% of the injected dose was present in blood after 90 min.

All mice were sacrificed 72 h after injection. Tissues were harvested and snap frozen in liquid nitrogen to determine adenoviral transduction by determining luciferase expression. After *i.v.* injection, expression of luciferase in the liver of Ad/ΔF(FG)ΔP-YSA treated mice was 6.7-fold lower ($P = 0.015$) than that in mice injected with Ad/ΔF(FG)ΔP (Figure 4B). Thus, the YSA peptide impaired liver transduction. No significant differences in expression were seen between both vectors in all other tissues. Surprisingly, the amount of luciferase expression in mice injected with Ad-/ΔF(FG)ΔP-YSA was only 15% of that in mice injected with Ad-/ΔF(FG)ΔP. This indicated that a large amount of the redirected vector was lost upon i.v. injection. The difference in luciferase expression between both vectors

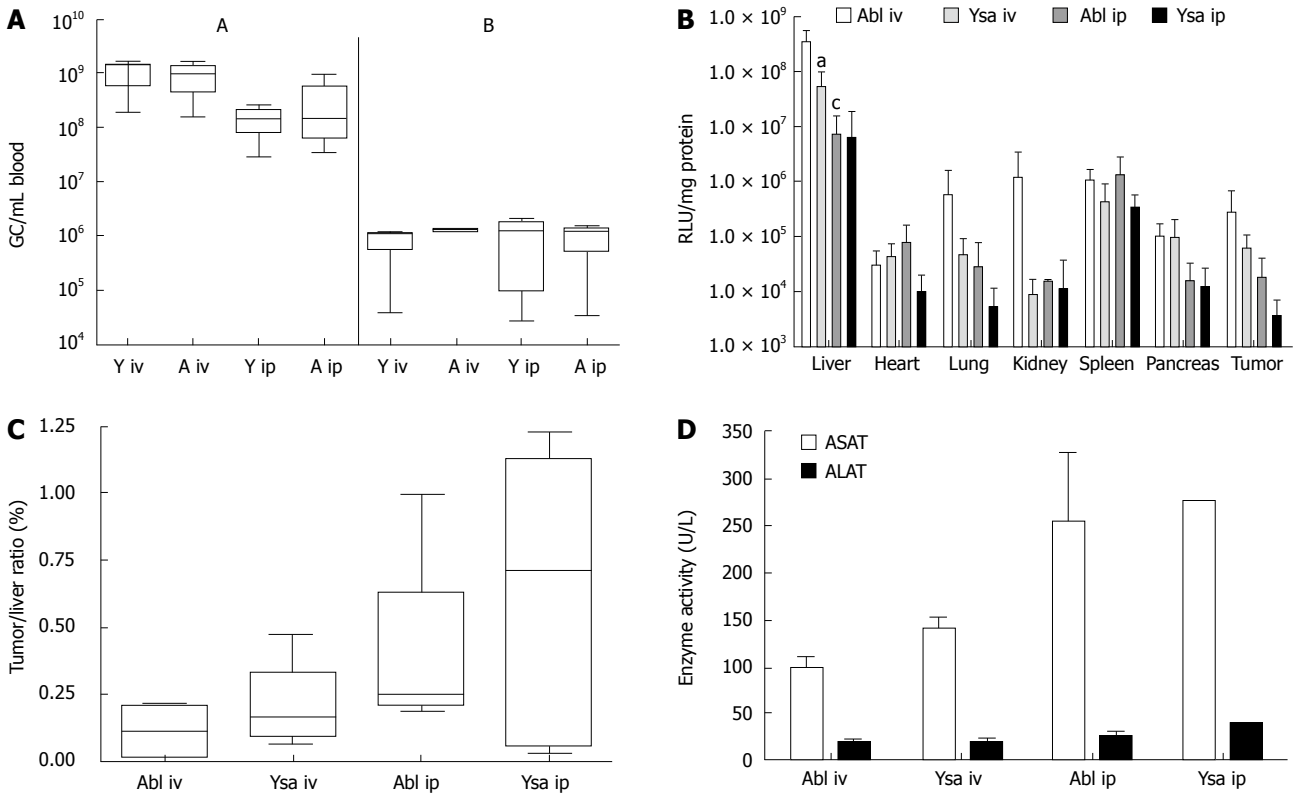

Figure 4 Lack of YSA specific targeting in nu/nu mice. A: 1 × 10^{11} gc of Ad/ΔF(FG)ΔP (ablated, A) or 1 × 10^{11} gc of Ad/ΔF(FG)ΔP-YSA (YSA; Y) are rapidly cleared from blood after intravenous (*i.v.*) and intraperitoneal (*i.p.*) administration into mice. At 10 min after *i.v.* or 90 min after *i.p.* injection and after 3 d (both), adenoviral genomic copies were determined in whole blood with real time PCR. B: Bio-distribution Ad/ΔF(FG)ΔP and Ad/ΔF(FG)ΔP-YSA injected *i.v.* or *i.p.* into *nu/nu* mice with a subcutaneous human pancreatic tumor. Animals were sacrificed 3 d after injection of 1 × 10^{11} gc of adenoviral vector. All organs were harvested and analyzed for luciferase expression/mg of protein. ($^{a}P < 0.05$ compared with Ad/ΔF(FG)ΔP after *i.v.* injection; $^{c}P < 0.05$ compared with Ad/ΔF(FG)ΔP after *i.v.* injection). C: The tumor/liver ratio of luciferase expression in each mouse demonstrates the lack of significant targeting of retargeted adenovirus to pancreatic cancer *in vivo*. D: Similar ASAT and ALAT levels in serum at 3 d after injection indicates comparable liver toxicity of ablated and retargeted adenoviral vectors in *nu/nu* mice. Data represent the mean ± SD of 4-7 mice.

was not seen after i.p. injection. This is due to the almost 50-fold lower luciferase expression in the liver after i.p. injection of Ad-/ΔF(FG)ΔP ($P = 0.0163$). For Ad/ΔF(FG)ΔP-YSA, the luciferase levels in the liver after *i.p.* injection were only reduced 9-fold and did not reach significance. The lower luciferase expression levels indicated that both vectors were cleared more efficiently without transduction after *i.p.* injection. To correct for the lower overall expression we chose to use the tumor liver ratio in each animal as an indication of retargeting efficiency. As shown in Figure 4C, no significant targeting of the tumor was seen with the YSA-redirected virus. Furthermore, the route of administration also did not affect tumor targeting.

Adenoviral vectors cause inflammation of the liver. Therefore we determined ALAT and ASAT levels 3 d after injection. Although we did see a 4 to 5-fold increase, no differences were seen between the 2 viral vectors (Figure 4D).

DISCUSSION

Conditional replicating adenovirus vectors are being developed to treating solid cancers[4,5]. However, these vectors have only been effective after direct injection into the tumors. As cancer is a systemic disease in virtually all fatal cases, this lack of systemic efficacy presents a major limitation to successful adenovirus-mediated gene therapy. Specific targeting therefore is a prerequisite for efficient eradication of solid cancer cells.

The aim of this study was to target the adenovirus to pancreatic cancers. Effective targeting *in vitro* to human cancer cells using HI loop insertion of peptide ligands has been reported by other groups. A well known example is the insertion of an integrin-binding RGD peptide that overcomes the poor transduction of human cancer caused by low expression of CAR[7,26,27]. Although integrins are highly expressed on cancer cells, the specificity of RGD targeting *in vivo* is questionable because of integrin expression in other tissues. Therefore more specific targeting peptides are needed. We compared binding of several ligands to receptors highly expressed on pancreatic cancers for their ability to target the adenovirus to pancreatic cancer cells (van Geer *et al*[12] in preparation). Of these ligands the YSA peptide appeared the most promising since it provided selective targeting *in vitro* to the EphA2R. Since YSA targets tissues expressing the EphA2R, we decided to test the specificity this retargeted vector *in vivo*.

Insertion of a peptide into the HI loop does not shield the native cell binding sites present in the adenoviral capsid. Binding of the retargeted vector

to these receptors present on liver cells for instance, will limit specific targeting[17]. Since ablation of these native binding reduces liver transduction and improves specific targeting *in vivo*[14], we combined YSA targeting with ablation of the native binding sites. We showed that ablation of CAR and integrin binding reduced adenoviral transduction by at least 2 logs *in vitro*. Insertion of the YSA peptide partly restored the transduction efficiency of the virus, but only on cells that expressed the EphA2R. Addition of synthetic YSA peptide blocked the increase in transduction efficiency. Together these data demonstrated that insertion of YSA enables EphA2R-mediated entry of ablated adenoviral vectors. Other groups have also reported that the loss of infectivity of ablated vectors can be restored by insertion of a targeting ligand in the HI loop[17,18,28]. However, not all retargeted vectors do provide efficient transduction. Insertion of RGD in a vector in which the CAR binding site was ablated in the KO1 mutation did not result in integrin-mediated uptake[29]. Apparently, in addition to preventing CAR binding, this mutation affected other essential steps such as internalization or trafficking of the adenovirus. In conclusion, our data and that of others show that HI loop insertion of a targeting peptide results in specific targeting of CAR/integrin-ablated adenoviral vectors *in vitro*.

Expression of the EphA2R is also enhanced in several normal tissues including tumor endothelium. Therefore, we investigated whether the YSA peptide also mediated adenoviral transduction *via* the mouse EphA2R. Since insertion of the YSA peptide increased the transduction of 2 mouse cell lines expressing the EphA2R by 1 to 2 logs, the YSA-retargeted vector was capable of targeting the mouse endothelium. The increase in transduction of mouse cells was stronger than in human pancreatic cancer cell lines while expression of the EphA2R in mouse cells was lower. This discrepancy seems to result from better accessibility of the EphA2R in mouse cells since, in human pancreatic cancer cells, most of the EphA2R was present in the cytosol (Figure 1A). Another possible explanation for this discrepancy is the expression of an inactive EphA2R in cancer cells. Since EphA2R activation impairs survival, cancer cells with an inactive receptor will have a growth advantage[11]. A third explanation could be a higher affinity of the Ad-/ΔF(FG)ΔP-YSA for the mouse EphA2R. Nevertheless, the efficient transduction of mouse cells expressing EphA2R renders the mouse a good model to study YSA-mediated targeting of pancreatic cancer *in vivo*.

After intravenous injection, luciferase expression in the liver of the YSA-retargeted vector Ad-/ΔF(FG)ΔP-YSA was lower than that by the ablated virus (Figure 4B). A decreased transduction of the liver was also reported in other studies in which the FG loop has been mutated. Thus, it seems that FG loop mutations lead to de-targeting of the hepatocytes[17]. In contrast, mutations in the AB loop did not decrease liver transduction[18,30]. These studies indicate that liver de-targeting occurred irrespective of the nature of the inserted peptide sequence. In our study, the decreased liver transduction due to YSA-retargeting was not accompanied by an increased transduction of any other tissue tested. Therefore, the increased loss of the redirected virus seems to result from degradation by tissue macrophages, which degrade more than 90% of injected adenoviruses. Since these cells do not express the EphA2R this would appear to be a non-specific effect.

In contrast to the receptor-mediated transduction of hepatocytes, uptake of adenovirus by macrophages depends on the binding of adenovirus fiber to blood factors. This induces uptake of adenovirus, for instance *via* the scavenger receptor[31,32]. Increased binding to blood factors of the mutated FG loop may cause the 10-fold greater loss of re-targeted adenovirus upon i.v. injection by increasing its degradation by macrophages. This may cause a lack of tumor targeting by Ad-/ΔF(FG)ΔP-YSA *in vivo*.

Akiyama *et al*[25] reported that after i.p. injection, a comparable ablated adenoviral vector efficiently entered the blood stream. Furthermore, they showed prolonged blood circulation and absence of hepatocyte transduction. Based on this, i.p. injection seemed a promising approach for systemic targeting. In our study, we could not repeat this observation. At 90 min after injection, less than 1% of the injected dose of vector was still present in the circulation while in contrast they still detected 20%. Increased uptake by macrophages may explain this discrepancy[33]. We used *nu/nu* mice to study retargeting of adenovirus while Akiyama *et al* reported a prolonged circulation time in normal mice. Several old studies have reported increased phagocytosis in *nu/nu* mice compared to normal mice to compensate for their immune defects[34,35]. A high dose of adenovirus can saturate the uptake by macrophages residing in the peritoneum and liver, and result in appearance of the virus in the circulation[36]. Apparently, the dose used in this study was too low to saturate the increased macrophage clearance capacity in *nu/nu* mice. The increased liver enzymes in serum after i.p. injection indicated increased macrophage uptake (Figure 4D). This increase was not observed for this ablated vector in normal mice. The increased uptake by macrophages in *nu/nu* mice rendered this model less suitable for adenoviral targeting studies[30]. Inhibition of phagocytosis therefore seems to be required to use this model for studying retargeting of ablated adenoviral vectors, e.g., by pre-injection of a small dose of virus[37].

For both administration routes, the luciferase expression in subcutaneously growing Capan-1 tumors was not significantly different between re-targeted and ablated vectors. The transduction of pancreatic cancer by our ablated vector suggests that adenoviral uptake can be mediated by other receptors. The role of additional receptors in Capan-1 cells is in accordance with Havenga *et al*[38]. They observed that gene transfer in these cells did not correlate with expression levels of CAR and/or integrins. In contrast, transduction by non-ablated adenoviral vectors was strongly impaired by loss

of CAR expression[7,39]. Apparently, removal of native cell binding sites is compensated by other low affinity binding sites, such as heparan sulphate proteoglycans[40]. The expression of the 2 most prominent proteoglycans, glypican-1 and syndecan-1, is indeed enhanced in pancreatic cancers. This may explain the efficient transduction of the tumor by the ablated vector[41,42]. Pancreatic cancer therefore seems susceptible to blood factor-mediated transduction by adenovirus as has been reported for herpes virus also[43]. Therefore, ablation of the sites in the fiber knob that bind to blood factors may be required to re-direct the adenovirus to cancer cells *in vivo*. Furthermore, studies to determine binding to (human) blood components of modified vectors are essential for predicting their *in vivo* efficacy. Binding to blood factors may explain why ablated vectors with a peptide insertion fail to target tumors following intravenous injection[6,44], while they do perform properly upon local injection[25,28,45].

In conclusion, we have generated a doubly-ablated virus that targets pancreatic cancer cells *via* the EphA2R. However, *in vivo* targeting remains inefficient as yet. Most likely, further modification of the Ad capsid is necessary to prevent binding to blood factors which lowers gene transfer to the liver[30,46].

COMMENTS

Background

The incidence of pancreatic adenocarcinoma is increasing in the Western world for unknown reasons. Due to its late diagnosis the prognosis for pancreatic cancer is very poor. Novel treatments such as adenovirus mediated gene therapy are needed to improve this.

Research frontiers

Adenoviral vector have been widely applied to treat solid tumors. Although the results in animal models were promising the results in subsequent clinical trials were disappointing due to limited transduction of the tumors. Poor transduction of cancer cells was mainly caused by their low expression of coxsackie and adenovirus receptor (CAR), the receptor that mediates adenoviral entry in to the cell.

Innovations and breakthroughs

Retargeting of adenoviral vectors can be used to circumvent CAR mediated entry and can improve the transduction of human cancer cells. In this study, the authors targeted adenoviral vectors to the EphA2 receptor that is highly expressed on pancreatic cancer cells *in vitro* and *in vivo*. To further improve specific targeting to cancer cells they removed the regions in the adenoviral capsid that mediate transduction of the liver. *In vitro*, this strategy indeed proved very specific. The results in a nude mouse model were however disappointing most likely due increased uptake of the retargeted vector by macrophages, a route that is enhanced in these mice due to a compensatory mechanism for loss of other immune responses.

Applications

The authors show that adenovirus can be targeted to the EphA2 receptor *in vitro*. However to allow application *in vivo* further ablation of endogenous adenobinding sites seem needed.

Terminology

EphA2 or ephrine A2 receptor is a receptor involved in embryogenesis and is upregulated in several solid tumors. Adenovirus has a icosahedral symmetry with 12 fibers spiking out at all corners. The adenofibers are trimeric proteins. At the end they form a knob with a peptide stretch exposed to the surface, the HI-loop.

Peer review

The goal of this study was to generate an adenoviral vector specifically targeting the EphA2 receptor, which is highly expressed on pancreatic cancer cells *in vivo* by first using an *in vitro* model. The methodology incorporated into this particular study was sound and that their findings were novel.

REFERENCES

1 **Boeck S**, Hinke A, Wilkowski R, Heinemann V. Importance of performance status for treatment outcome in advanced pancreatic cancer. *World J Gastroenterol* 2007; **13**: 224-227

2 **Ma WW**, Hidalgo M. Exploiting novel molecular targets in gastrointestinal cancers. *World J Gastroenterol* 2007; **13**: 5845-5856

3 **Tanaka T**, Kuroki M, Hamada H, Kato K, Kinugasa T, Shibaguchi H, Zhao J, Kuroki M. Cancer-targeting gene therapy using tropism-modified adenovirus. *Anticancer Res* 2007; **27**: 3679-3684

4 **Mulvihill S**, Warren R, Venook A, Adler A, Randlev B, Heise C, Kirn D. Safety and feasibility of injection with an E1B-55 kDa gene-deleted, replication-selective adenovirus (ONYX-015) into primary carcinomas of the pancreas: a phase I trial. *Gene Ther* 2001; **8**: 308-315

5 **Hecht JR**, Bedford R, Abbruzzese JL, Lahoti S, Reid TR, Soetikno RM, Kirn DH, Freeman SM. A phase I/II trial of intratumoral endoscopic ultrasound injection of ONYX-015 with intravenous gemcitabine in unresectable pancreatic carcinoma. *Clin Cancer Res* 2003; **9**: 555-561

6 **Rittner K**, Schreiber V, Erbs P, Lusky M. Targeting of adenovirus vectors carrying a tumor cell-specific peptide: in vitro and in vivo studies. *Cancer Gene Ther* 2007; **14**: 509-518

7 **Wesseling JG**, Bosma PJ, Krasnykh V, Kashentseva EA, Blackwell JL, Reynolds PN, Li H, Parameshwar M, Vickers SM, Jaffee EM, Huibregtse K, Curiel DT, Dmitriev I. Improved gene transfer efficiency to primary and established human pancreatic carcinoma target cells via epidermal growth factor receptor and integrin-targeted adenoviral vectors. *Gene Ther* 2001; **8**: 969-976

8 **Mudali SV**, Fu B, Lakkur SS, Luo M, Embuscado EE, Iacobuzio-Donahue CA. Patterns of EphA2 protein expression in primary and metastatic pancreatic carcinoma and correlation with genetic status. *Clin Exp Metastasis* 2006; **23**: 357-365

9 **Abraham S**, Knapp DW, Cheng L, Snyder PW, Mittal SK, Bangari DS, Kinch M, Wu L, Dhariwal J, Mohammed SI. Expression of EphA2 and Ephrin A-1 in carcinoma of the urinary bladder. *Clin Cancer Res* 2006; **12**: 353-360

10 **Miyazaki T**, Kato H, Fukuchi M, Nakajima M, Kuwano H. EphA2 overexpression correlates with poor prognosis in esophageal squamous cell carcinoma. *Int J Cancer* 2003; **103**: 657-663

11 **Zelinski DP**, Zantek ND, Stewart JC, Irizarry AR, Kinch MS. EphA2 overexpression causes tumorigenesis of mammary epithelial cells. *Cancer Res* 2001; **61**: 2301-2306

12 **Koolpe M**, Dail M, Pasquale EB. An ephrin mimetic peptide that selectively targets the EphA2 receptor. *J Biol Chem* 2002; **277**: 46974-46979

13 **Roelvink PW**, Mi Lee G, Einfeld DA, Kovesdi I, Wickham TJ. Identification of a conserved receptor-binding site on the fiber proteins of CAR-recognizing adenoviridae. *Science* 1999; **286**: 1568-1571

14 **Einfeld DA**, Schroeder R, Roelvink PW, Lizonova A, King CR, Kovesdi I, Wickham TJ. Reducing the native tropism of adenovirus vectors requires removal of both CAR and integrin interactions. *J Virol* 2001; **75**: 11284-11291

15 **Leissner P**, Legrand V, Schlesinger Y, Hadji DA, van Raaij M, Cusack S, Pavirani A, Mehtali M. Influence of adenoviral fiber mutations on viral encapsidation, infectivity and in vivo tropism. *Gene Ther* 2001; **8**: 49-57

16 **Alemany R**, Curiel DT. CAR-binding ablation does not change biodistribution and toxicity of adenoviral vectors. *Gene Ther* 2001; **8**: 1347-1353

17 **Mizuguchi H**, Koizumi N, Hosono T, Ishii-Watabe A, Uchida E, Utoguchi N, Watanabe Y, Hayakawa T. CAR- or alphav integrin-binding ablated adenovirus vectors, but not fiber-modified vectors containing RGD peptide, do not change the systemic gene transfer properties in mice. *Gene Ther* 2002; **9**: 769-776

18 **Martin K**, Brie A, Saulnier P, Perricaudet M, Yeh P, Vigne E. Simultaneous CAR- and alpha V integrin-binding ablation fails to reduce Ad5 liver tropism. *Mol Ther* 2003; **8**: 485-494

19 **Jaffe EA**, Nachman RL, Becker CG, Minick CR. Culture of human endothelial cells derived from umbilical veins. Identification by morphologic and immunologic criteria. *J Clin Invest* 1973; **52**: 2745-2756

20 **Koizumi N**, Mizuguchi H, Sakurai F, Yamaguchi T, Watanabe Y, Hayakawa T. Reduction of natural adenovirus tropism to mouse liver by fiber-shaft exchange in combination with both CAR- and alphav integrin-binding ablation. *J Virol* 2003; **77**: 13062-13072

21 **Von Seggern DJ**, Kehler J, Endo RI, Nemerow GR. Complementation of a fibre mutant adenovirus by packaging cell lines stably expressing the adenovirus type 5 fibre protein. *J Gen Virol* 1998; **79** (Pt 6): 1461-1468

22 **Ma L**, Bluyssen HA, De Raeymaeker M, Laurysens V, van der Beek N, Pavliska H, van Zonneveld AJ, Tomme P, van Es HH. Rapid determination of adenoviral vector titers by quantitative real-time PCR. *J Virol Methods* 2001; **93**: 181-188

23 **van Beusechem VW**, Mastenbroek DC, van den Doel PB, Lamfers ML, Grill J, Würdinger T, Haisma HJ, Pinedo HM, Gerritsen WR. Conditionally replicative adenovirus expressing a targeting adapter molecule exhibits enhanced oncolytic potency on CAR-deficient tumors. *Gene Ther* 2003; **10**: 1982-1991

24 **Boom R**, Sol CJ, Salimans MM, Jansen CL, Wertheim-van Dillen PM, van der Noordaa J. Rapid and simple method for purification of nucleic acids. *J Clin Microbiol* 1990; **28**: 495-503

25 **Akiyama M**, Thorne S, Kirn D, Roelvink PW, Einfeld DA, King CR, Wickham TJ. Ablating CAR and integrin binding in adenovirus vectors reduces nontarget organ transduction and permits sustained bloodstream persistence following intraperitoneal administration. *Mol Ther* 2004; **9**: 218-230

26 **Sandovici M**, Deelman LE, Smit-van Oosten A, van Goor H, Rots MG, de Zeeuw D, Henning RH. Enhanced transduction of fibroblasts in transplanted kidney with an adenovirus having an RGD motif in the HI loop. *Kidney Int* 2006; **69**: 45-52

27 **Dmitriev I**, Krasnykh V, Miller CR, Wang M, Kashentseva E, Mikheeva G, Belousova N, Curiel DT. An adenovirus vector with genetically modified fibers demonstrates expanded tropism via utilization of a coxsackievirus and adenovirus receptor-independent cell entry mechanism. *J Virol* 1998; **72**: 9706-9713

28 **Murugesan SR**, Akiyama M, Einfeld DA, Wickham TJ, King CR. Experimental treatment of ovarian cancers by adenovirus vectors combining receptor targeting and selective expression of tumor necrosis factor. *Int J Oncol* 2007; **31**: 813-822

29 **Kritz AB**, Nicol CG, Dishart KL, Nelson R, Holbeck S, Von Seggern DJ, Work LM, McVey JH, Nicklin SA, Baker AH. Adenovirus 5 fibers mutated at the putative HSPG-binding site show restricted retargeting with targeting peptides in the HI loop. *Mol Ther* 2007; **15**: 741-749

30 **Koizumi N**, Kawabata K, Sakurai F, Watanabe Y, Hayakawa T, Mizuguchi H. Modified adenoviral vectors ablated for coxsackievirus-adenovirus receptor, alphav integrin, and heparan sulfate binding reduce in vivo tissue transduction and toxicity. *Hum Gene Ther* 2006; **17**: 264-279

31 **Shayakhmetov DM**, Gaggar A, Ni S, Li ZY, Lieber A. Adenovirus binding to blood factors results in liver cell infection and hepatotoxicity. *J Virol* 2005; **79**: 7478-7491

32 **Xu Z**, Tian J, Smith JS, Byrnes AP. Clearance of adenovirus by Kupffer cells is mediated by scavenger receptors, natural antibodies, and complement. *J Virol* 2008; **82**: 11705-11713

33 **Lieber A**, He CY, Meuse L, Schowalter D, Kirillova I, Winther B, Kay MA. The role of Kupffer cell activation and viral gene expression in early liver toxicity after infusion of recombinant adenovirus vectors. *J Virol* 1997; **71**: 8798-8807

34 **Holub M**, Fornůsek L, Větvicka V, Chalupná J. Enhanced phagocytic activity of blood leukocytes in athymic nude mice. *J Leukoc Biol* 1984; **35**: 605-615

35 **Větvicka V**, Fornusek L, Holub M, Zídková J, Kopecek J. Macrophages of athymic nude mice: Fc receptors, C receptors, phagocytic and pinocytic activities. *Eur J Cell Biol* 1984; **35**: 35-40

36 **Tao N**, Gao GP, Parr M, Johnston J, Baradet T, Wilson JM, Barsoum J, Fawell SE. Sequestration of adenoviral vector by Kupffer cells leads to a nonlinear dose response of transduction in liver. *Mol Ther* 2001; **3**: 28-35

37 **Manickan E**, Smith JS, Tian J, Eggerman TL, Lozier JN, Muller J, Byrnes AP. Rapid Kupffer cell death after intravenous injection of adenovirus vectors. *Mol Ther* 2006; **13**: 108-117

38 **Havenga MJ**, Lemckert AA, Ophorst OJ, van Meijer M, Germeraad WT, Grimbergen J, van Den Doel MA, Vogels R, van Deutekom J, Janson AA, de Bruijn JD, Uytdehaag F, Quax PH, Logtenberg T, Mehtali M, Bout A. Exploiting the natural diversity in adenovirus tropism for therapy and prevention of disease. *J Virol* 2002; **76**: 4612-4620

39 **Yamamoto M**, Davydova J, Wang M, Siegal GP, Krasnykh V, Vickers SM, Curiel DT. Infectivity enhanced, cyclooxygenase-2 promoter-based conditionally replicative adenovirus for pancreatic cancer. *Gastroenterology* 2003; **125**: 1203-1218

40 **Vivès RR**, Lortat-Jacob H, Fender P. Heparan sulphate proteoglycans and viral vectors : ally or foe? *Curr Gene Ther* 2006; **6**: 35-44

41 **Conejo JR**, Kleeff J, Koliopanos A, Matsuda K, Zhu ZW, Goecke H, Bicheng N, Zimmermann A, Korc M, Friess H, Büchler MW. Syndecan-1 expression is up-regulated in pancreatic but not in other gastrointestinal cancers. *Int J Cancer* 2000; **88**: 12-20

42 **Kleeff J**, Ishiwata T, Kumbasar A, Friess H, Büchler MW, Lander AD, Korc M. The cell-surface heparan sulfate proteoglycan glypican-1 regulates growth factor action in pancreatic carcinoma cells and is overexpressed in human pancreatic cancer. *J Clin Invest* 1998; **102**: 1662-1673

43 **Liu J**, Shriver Z, Pope RM, Thorp SC, Duncan MB, Copeland RJ, Raska CS, Yoshida K, Eisenberg RJ, Cohen G, Linhardt RJ, Sasisekharan R. Characterization of a heparan sulfate octasaccharide that binds to herpes simplex virus type 1 glycoprotein D. *J Biol Chem* 2002; **277**: 33456-33467

44 **Bayo-Puxan N**, Cascallo M, Gros A, Huch M, Fillat C, Alemany R. Role of the putative heparan sulfate glycosaminoglycan-binding site of the adenovirus type 5 fiber shaft on liver detargeting and knob-mediated retargeting. *J Gen Virol* 2006; **87**: 2487-2495

45 **Miura Y**, Yoshida K, Nishimoto T, Hatanaka K, Ohnami S, Asaka M, Douglas JT, Curiel DT, Yoshida T, Aoki K. Direct selection of targeted adenovirus vectors by random peptide display on the fiber knob. *Gene Ther* 2007; **14**: 1448-1460

46 **Nicklin SA**, Wu E, Nemerow GR, Baker AH. The influence of adenovirus fiber structure and function on vector development for gene therapy. *Mol Ther* 2005; **12**: 384-393

S- Editor Li LF **L- Editor** Cant MR **E- Editor** Yin DH

Online Submissions: wjg.wjgnet.com
wjg@wjgnet.com
doi:10.3748/wjg.15.2763

World J Gastroenterol 2009 June 14; 15(22): 2763-2767
World Journal of Gastroenterology ISSN 1007-9327

Gallbladder function and dynamics of bile flow in asymptomatic gallstone disease

Sevim Süreyya Çerçi, Feride Meltem Özbek, Celal Çerçi, Bahattin Baykal, Hasan Erol Eroğlu, Zeynep Baykal, Mustafa Yıldız, Semahat Sağlam, Ahmet Yeşildağ

Sevim Süreyya Çerçi, Feride Meltem Özbek, Mustafa Yıldız, Semahat Sağlam, Nuclear Medicine, University of Suleyman Demirel Hospital, Isparta 32200, Turkey
Celal Çerçi, Hasan Erol Eroğlu, General Surgery, University of Suleyman Demirel Hospital, Isparta 32200, Turkey
Bahattin Baykal, Ahmet Yeşildağ, Radiology, University of Suleyman Demirel Hospital, Isparta 32200, Turkey
Zeynep Baykal, Internal Medicine, State Hospital Isparta, Isparta, 32040, Turkey
Author contributions: Çerçi SS, Çerçi C, Yıldız M designed research; Çerçi SS, Özbek FM, Baykal B, Baykal Z, Sağlam S, and Yeşildağ A performed research; Çerçi SS, Çerçi C, Eroğlu HE analyzed data and wrote the paper.
Correspondence to: Sevim Süreyya Çerçi, MD, Department of Nuclear Medicine, University of Suleyman Demirel Hospital, Isparta 32200, Turkey. sureyyacerci@hotmail.com
Telephone: +90-246-2112612 Fax: +90-246-2370240
Received: March 9, 2009 Revised: May 8, 2009
Accepted: May 15, 2009
Published online: June 14, 2009

Abstract

AIM: To investigate the effects of gallbladder stones on motor functions of the gallbladder and the dynamics of bile flow in asymptomatic gallstone disease.

METHODS: Quantitative hepatobiliary scintigraphy was performed to detect the parameters of gallbladder motor function [gallbladder ejection fraction (GBEF), gallbladder visualization time (GBVT), gallbladder time to peak activity (GBT_{max}), gallbladder half emptying time ($GBT_{1/2}$), and transit time of bile to duodenum (TTBD)] in 24 patients with asymptomatic cholelithiasis who were diagnosed incidentally during routine abdominal ultrasonographic examination and 20 healthy subjects with normal gallbladder.

RESULTS: Even though there was no significant difference in the clinical and laboratory parameters between the patient and control groups, all parameters of gallbladder function except TTBD were found to differ significantly between the two groups. GBEF in the patient group was decreased (P = 0.000) and GBVT, GBT_{max}, $GBT_{1/2}$ in the patient group were longer (P = 0.000, P = 0.015, P = 0.001, respectively).

CONCLUSION: Our results showed that even if there were not any clinical and laboratory findings, gallbladder filling and emptying could be impaired in patients with gallstone disease.

Key words: Asymptomatic gallstone disease; Hepatobiliary scintigraphy; Gallbladder function

Peer reviewer: Michele Cicala, Professor, Dipartimento di Malattie dell'Apparato Digerente, Università Campus Bio-Medico, Via Longoni, 8300155 Rome, Italy

Çerçi SS, Özbek FM, Çerçi C, Baykal B, Eroğlu HE, Baykal Z, Yıldız M, Sağlam S, Yeşildağ A. Gallbladder function and dynamics of bile flow in asymptomatic gallstone disease. *World J Gastroenterol* 2009; 15(22): 2763-2767 Available from: URL: http://www.wjgnet.com/1007-9327/15/2763.asp DOI: http://dx.doi.org/10.3748/wjg.15.2763

INTRODUCTION

Asymptomatic cholelithiasis is being diagnosed increasingly, mainly as a result of the widespread use of abdominal ultrasonography for the evaluation of patients for unrelated or vague abdominal complaints and in cases of routine checkup. Most studies have indicated that the progression of asymptomatic to symptomatic disease is relatively low[1-4]. Despite some controversy most authors agree that the vast majority of subjects should be managed by observation alone. The major concern when discussing the natural history of asymptomatic cholelithiasis is the possible development of a severe, potentially life-threatening complication, such as acute supurative cholangitis, severe pancreatitis, cholecystoenteric fistula, gallstone ileus or rarely gallbladder cancer. Unfortunately, it is impossible, using local (such as number, size, nature, alteration in wall thickness or gallbladder contractility) or general factors (such as age, gender, or associated comorbidity) to predict who among asymptomatic patients, will develop symptoms or complications and when[5].

Hepatobiliary scintigraphy is used to show both morphological and physiological changes in the gallbladder. Since physiological changes usually precede

morphological alterations by several weeks or months, there is great potential for early diagnosis by scintigraphy, before irreversible functional changes take place[6]. The main advantage of hepatobiliary scintigraphy is that the technique is noninvasive, quantitative, and reproducible and has a low interobserver error rate[7-11].

The current study aimed to investigate by quantitative hepatobiliary scintigraphy the effects of gallbladder stones on motor function of the gallbladder and the dynamics of bile flow in a group of patients with asymptomatic gallstone disease.

MATERIALS AND METHODS

The study design was approved by the local University ethical committee and was performed according to the Helsinki Declaration. Informed written consent was obtained from all participating subjects before their involvement in the study.

Subjects

The study was conducted from April 2006 to February 2008, and included 25 patients with asymptomatic cholelithiasis who had been diagnosed incidentally during routine abdominal ultrasonography. There were no gallstone-related symptoms, such as history of biliary pain (pain in the epigastrium or right upper abdominal quadrant that may radiate to the patient's back or to the right scapula) or gallstone related complications such as acute cholecystitis, cholangitis, or pancreatitis. The only one patient with nonvisualized gallbladder during hepatobiliary scintigraphy was excluded. Twenty-four patients, (10 male and 14 female; aged 54.66 ± 12.59 years) with asymptomatic gallbladder stones, and 20 control cases (12 male, 8 female; aged 50.30 ± 4.15 years) with normal gallbladder were enrolled in the study. None of the subjects had diabetes mellitus, or a history of disease or operation that affected gallbladder motility. None of the patients had received recent medication such as cholic acid, morphine, atropine, calcium channel blockers, octreotide, progesterone, indomethacin, theophyline, benzodiazepines, and histamine-2 receptor antagonists to influence gallbladder motor function. All patients in the study and control group had normal gallbladder wall thickness (no more than 2 mm), common bile duct upon ultrasound examination and liver function as shown by routine biochemical screening measures [aspartate amino transferase (AST), alanine aminotransferase (ALT), γ-glutamyltransferase (GGT), alkaline phosphatase (ALP) and total bilirubin levels].

Hepatobiliary scintigraphy

After the patients had fasted overnight, hepatobiliary scintigraphy was performed using 185 MBq (5 mCi) of 99m-Tc-mebrofenin (BRIDATEC, GIPHARMA S.r.I., Italy) intravenously. Two-phase dynamic images were taken from the right hypochondrium with the patient in the supine position, using a dual-head gamma camera (Siemens E-CAM, Illinois, USA) which included a low-energy high resolution collimator. Phase 1: 2 s × 60 frames (perfusion phase); phase 2: 60 s × 118 frames (hepatobiliary phase). In the mid-term of the second phase, a standard fatty meal (100 g milk chocolate) instead of cholecystokinin was given to the patients in order to stimulate gallbladder contraction. All of the dynamic images were evaluated with the raw data and cine projections from the computer.

We obtained the following parameters. (1) Gallbladder ejection fraction (GBEF) was calculated by determining count variation in the gallbladder during the filling and emptying period, using a computer program for GBEF. An E-CAM Siemens computer program calculated GBEF according to the time variation curves of these two phase (Figure 1). (2) Gallbladder visualization time (GBVT). (3) Gallbladder time to peak activity (GBT_{max}). (4) Gallbladder half emptying time ($GBT_{1/2}$). (5) Transit time of bile to duodenum (TTBD) were evaluated.

Table 1 Clinical and laboratory features of patient and control groups (mean ± SD)

	Patients (n = 24)	Controls (n = 20)	P
Number (M/F)	24 (10/14)	20 (12/8)	0.345
Age (yr)	54.66 ± 12.59	50.30 ± 4.15	0.267
AST (U/L)	30.62 ± 13.89	27.30 ± 9.99	0.547
ALT (U/L)	34.66 ± 27.86	21.60 ± 5.71	0.283
GGT (U/L)	48.20 ± 26.63	43.65 ± 10.80	0.915
ALP (U/L)	86.20 ± 23.68	86.10 ± 24.03	0.972
Total bilirubin (mg/dL)	0.74 ± 0.28	0.69 ± 0.27	0.579

Statistical analyses

The statistical analyses were done using SPSS 13 for Windows (Chicago, IL, USA). The data of the groups were given as mean ± SD and the Mann-Whitney U test was used as a non-parametric test to compare the means between the groups. $P < 0.05$ was considered as significant.

RESULTS

Table 1 shows the clinical and laboratory features of the patient and control groups (mean ± SD). There was no statistically difference in the clinical and laboratory parameters between the patient and control group ($P > 0.05$).

GBEF, GBVT, GBT_{max}, $GBT_{1/2}$, and TTBD of the patient and control groups are shown in Figure 2A-E. Mean GBEF in the patient group decreased when compared with that in the control group (49.79 ± 25.42 min *vs* 78.20 ± 11.23 min; $P = 0.000$). Mean GBVT (21.83 ± 8.51 min *vs* 12.20 ± 2.28 min; $P = 0.000$), GBT_{max} (59.41 ± 15.09 min *vs* 49.30 ± 6.74 min $P = 0.015$), $GBT_{1/2}$ (99.37 ± 22.95 min *vs* 74.40 ± 11.12 min $P = 0.001$) were longer in the patient group than in the control group. There was no significant difference in mean TTBD (22.58 ± 14.08 min *vs* 27.00 ± 15.36 min) between the two groups.

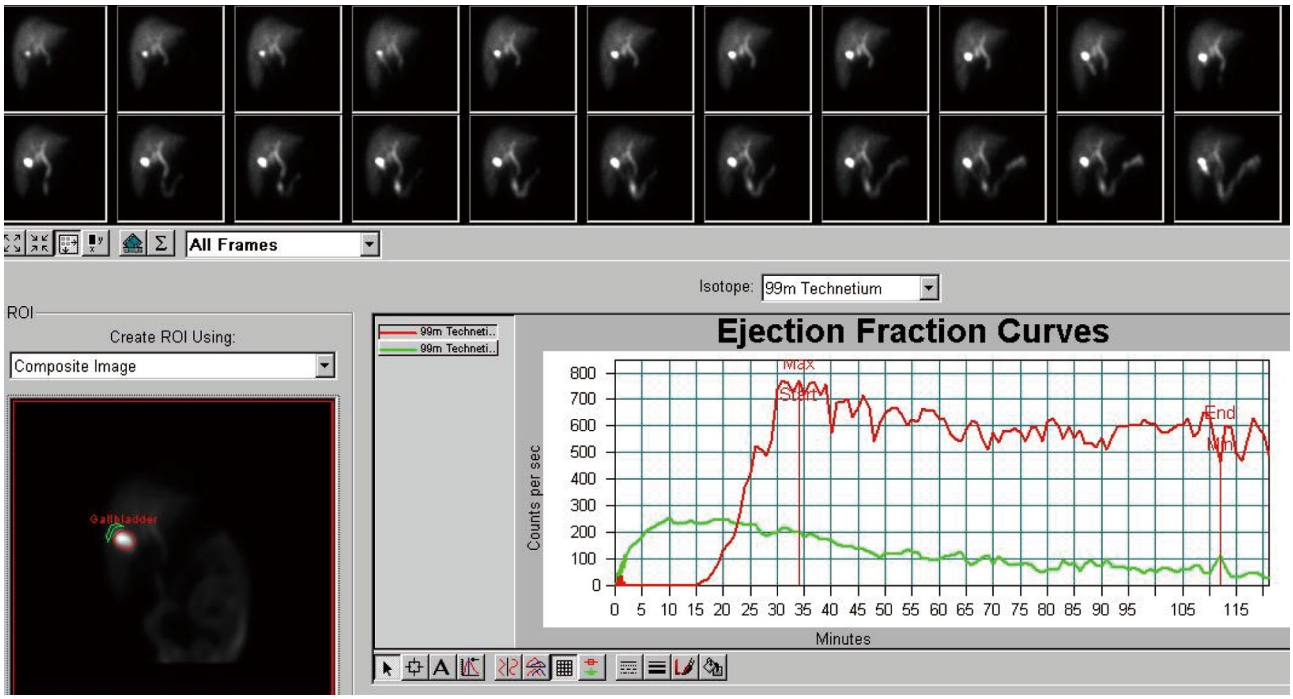

Figure 1 Image from Tc-99m mebrofenin cholescintigraphy and GBEF curve in a patient with asymptomatic cholelithiasis. Gallbladder emptying was slower and was not completed during the study.

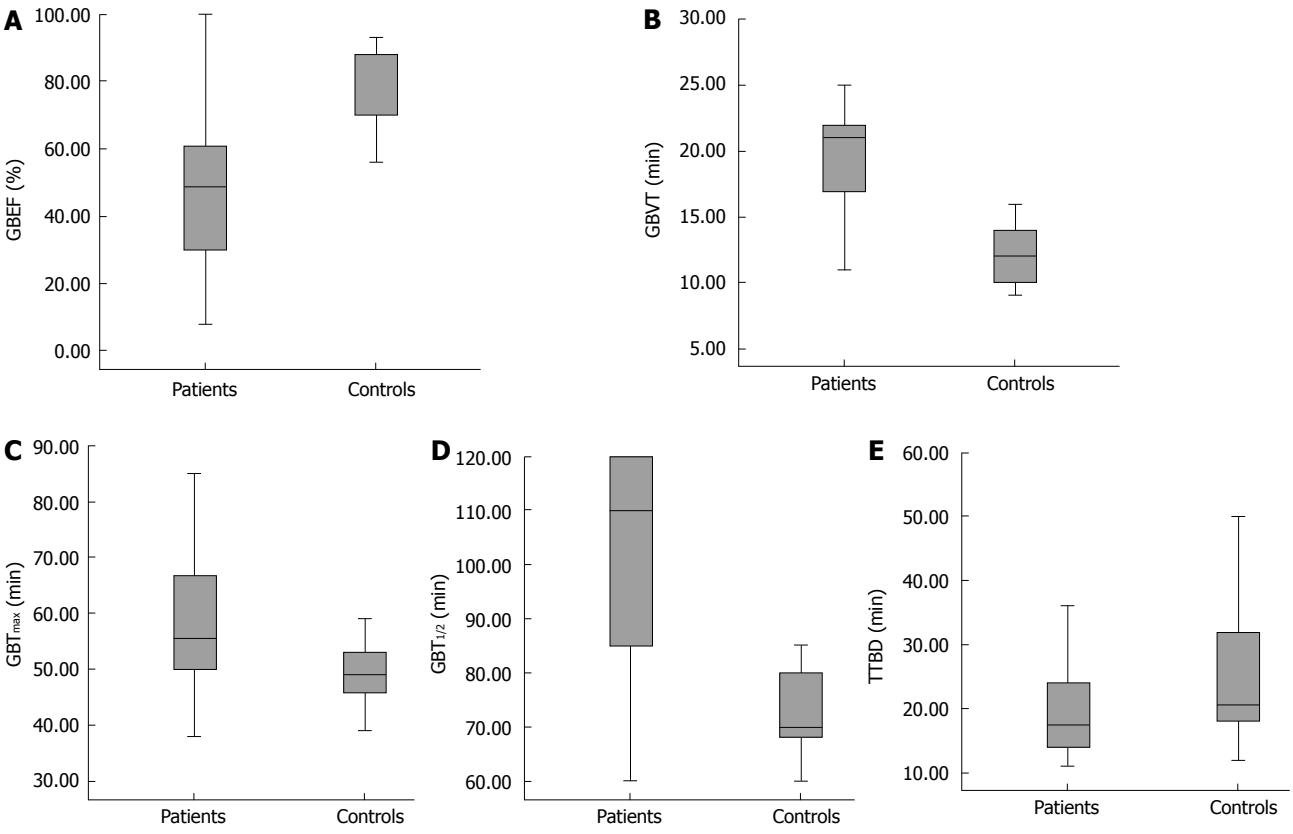

Figure 2 Parameters of gallbladder function. A: Mean GBEF of the patient group was significantly decreased when compared with the control group (P = 0.000); B: Mean GBVT was significantly longer in asymptomatic gallbladder patients than in the control group (P = 0.000); C: GBT_{max} was significantly longer in the patient group (P = 0.015); D: $GBT_{1/2}$ was significantly prolonged in the patient group (P = 0.001); E: There was no significant difference between TTBD in the two groups.

DISCUSSION

In the past, the majority of the literature has focused on the pathogenesis of gallstone formation rather than on the association of gallbladder motility and clinical symptoms[12]. Gallbladder stones may be asymptomatic in a considerable number of patients, and the pathogenesis of symptoms is not understood clearly.

Theoretically, gallbladder function may be an important predictor of outcome from either cholecystectomy or watchful waiting, because the symptoms traditionally are believed to arise from gallbladder contraction[13].

Several studies using different techniques and protocols have assessed gallbladder function in gallstone disease[8,14-16]. In these studies, patients groups were generally taken from symptomatic but uncomplicated patients.

Gallbladder emptying is under the control of neural and hormonal stimulation. For normal bile flow, Oddi sphincter relaxation should synchronize with gallbladder contraction. CCK, as a mediator, is responsible for relaxation of the sphincter of Oddi and gallbladder contraction. After a fatty meal is eaten, the gallbladder empties with active contraction, which is regulated mainly by the release of endogenous CCK, which simultaneously induces Oddi sphincter relaxation, therefore allowing maximal bile outflow from the common bile duct into the duodenum at the time of maximal gallbladder contraction[17].

In this manner, it is important to understand how symptoms occur and what the reason is. It is also important to know that, if we perform cholecystectomy the pathological bile flow will resolve. It is still controversial whether impaired gallbladder emptying/contraction is the cause or the result of bile stones[13].

Quantitative hepatobiliary scintigraphy is a well-established method that can be used in the evaluation of hepatocellular function and patency of the biliary system by tracing the production and flow of bile from the liver through the biliary system into the small intestine[18]. Of the quantitative parameters of hepatobiliary scintigraphy, time variables of the gallbladder (GBVT, GBT_{max}, $GBT_{1/2}$, and TTBD) and GBEF are regarded as sensitive parameters for diagnosing gallbladder motor function abnormalities.

In previous scintigraphic studies, GBEF and gallbladder emptying time were found to be different in patients with symptomatic gallbladder stones[14,15,19]. Most of these studies, agreed that, although gallbladder emptying was impaired, filling was unaffected. In our study, emptying time was significantly longer in patients with asymptomatic gallstones and GBEF was significantly reduced.

We found that gallbladder filling time was also prolonged compared with the controls and Kao *et al*[20] have reported that gallbladder stones may impair gallbladder function, especially the filling fraction. Abnormal gallbladder filling and emptying of bile in the gallbladder can result from mechanical obstruction to bile flow, such as altered cystic duct resistance or abnormal sphincter of Oddi tone, decreased gallbladder contractile force, or increased bile viscosity. Patients with organic obstruction at the cystic duct could not be visualized during hepatobiliary scintigraphy and therefore a patient who had a non-visualized gallbladder was excluded from the present study. Increased resistance to bile flow might occur either at the cystic duct or sphincter of Oddi. In our study, there was no difference in TTBD between the control group and asymptomatic gallstone group, thus increased resistance to bile flow in the sphincter of Oddi was not the cause of prolongation in emptying time. On the other hand, viscosity tends to be higher in gallbladder bile of patients with gallstones[21] and may be another cause abnormal gallbladder emptying or filling, but normal TTBD was probably the indicator of normal bile viscosity in our study group. The most likely explanation for the abnormal gallbladder filling in our patients was increased resistance to bile flow at the cystic duct. Similar to our findings Pitt *et al*[22] have reported increased cystic duct resistance in rodents with gallstones, but we have not been able to find any human study about cystic duct resistance in patients with gallbladder stones. Jazrawi *et al*[23] have combined ultrasonography with scintigraphy and have shown that turnover of bile is impaired during the refilling phase in patients with gallstones. Moreover Cicala *et al*[24] have demonstrated that there is decreased turnover of bile that may contribute to cholesterol crystal precipitation and stone growth, as shown by ultrasonographic measurements of gallbladder volume variation. From another point of view, in the patient group, abnormal gallbladder smooth muscle contraction was probably the cause of both impaired emptying time and reduced GBEF.

It is also known that, in patients with impaired emptying, the contractile defect may have developed at a very early stage of gallstone formation[25]. Furthermore, the symptoms in gallstone patients are believed traditionally to arise from gallbladder spasm and normal gallbladder contractility is thought to be a prerequisite for the development of symptoms[12]. The gallbladder motility defect is restricted apparently to asymptomatic patients and appears to protect from symptomatic disease[26].

In conclusion, our results showed that even if there were not any clinical and laboratory findings, gallbladder filling and emptying can be impaired in gallstone patients.

COMMENTS

Background

Asymptomatic cholelithiasis is being increasingly, diagnosed today, mainly as a result of the widespread use of abdominal ultrasonography. Hepatobiliary scintigraphy is a noninvasive, quantitative, and reproducible technique that can be used to show morphological and physiological changes in the gallbladder. The authors investigated by hepatobiliary scintigraphy the effects of gallbladder stones on motor function of the gallbladder and the dynamics of bile flow in asymptomatic gallstone disease.

Research frontiers

Cholelithiasis is a very common disease, and it is still controversial whether impaired gallbladder emptying/contraction are the cause or result of bile stones. Gallbladder stones may be asymptomatic in a considerable number of patients with gallstones, and the pathogenesis of symptoms is not understood clearly. In previous scintigraphic studies, motor function parameters of the gallbladder have been found to be different in patients with symptomatic gallbladder stones, however, no definitive data have been published in asymptomatic cholelithiasis.

Innovations and breakthroughs

The authors showed for the first time that, even in the absence of any clinical and laboratory findings, gallbladder motor functions such as filling and emptying time and ejection fraction, were impaired in asymptomatic gallstone patients.

Applications

Their study was designed to analyze the scintigraphic parameters of gallbladder motor function (gallbladder ejection fraction, gallbladder visualization time, gallbladder time to peak activity, gallbladder half emptying time, and transit time of bile to duodenum) in patients with asymptomatic cholelithiasis who had been diagnosed incidentally during routine abdominal ultrasonography.

Terminology

99m-Tc-mebrofenin is a radiopharmaceutical agent for hepatobiliary scintigraphy, Gallbladder ejection fraction describes gallbladder emptying function.

Peer review

This is a very interesting study. This paper reports on the results of an investigation aimed at assessing the effects of gallbladder stones on gallbladder motility and at assessing the dynamics of bile flow in asymptomatic gallstone disease patients. The authors report that, even in the absence of any clinical and laboratory findings, gallbladder filling and emptying can be impaired in this subgroup of gallstone patients.

REFERENCES

1 **Gracie WA**, Ransohoff DR. The silent stone requiescat in pace. In: Delaney JP, Varco RL, editors. Controversies in surgery II. Philadelphia: Saunders, 1983: 361-370
2 **McSherry CK**, Glenn F. The incidence and causes of death following surgery for nonmalignant biliary tract disease. *Ann Surg* 1980; **191**: 271-275
3 **Ransohoff DF**, Gracie WA, Wolfenson LB, Neuhauser D. Prophylactic cholecystectomy or expectant management for silent gallstones. A decision analysis to assess survival. *Ann Intern Med* 1983; **99**: 199-204
4 **Thistle JL**, Cleary PA, Lachin JM, Tyor MP, Hersh T. The natural history of cholelithiasis: the National Cooperative Gallstone Study. *Ann Intern Med* 1984; **101**: 171-175
5 **Meshikhes AW**. Asymptomatic gallstones in the laparoscopic era. *J R Coll Surg Edinb* 2002; **47**: 742-748
6 **Yaylali OT**, Yilmaz M, Kiraç FS, Değirmencioğlu S, Akbulut M. Scintigraphic evaluation of gallbladder motor functions in H pylori positive and negative patients in the stomach with dyspepsia. *World J Gastroenterol* 2008; **14**: 1406-1410
7 **Krishnamurthy S**, Krishnamurthy GT. Gallbladder ejection fraction: a decade of progress and future promise. *J Nucl Med* 1992; **33**: 542-544
8 **Krishnamurthy GT**, Bobba VR, McConnell D, Turner F, Mesgarzadeh M, Kingston E. Quantitative biliary dynamics: introduction of a new noninvasive scintigraphic technique. *J Nucl Med* 1983; **24**: 217-223
9 **Jazrawi RP**. Review article: measurement of gall-bladder motor function in health and disease. *Aliment Pharmacol Ther* 2000; **14** Suppl 2: 27-31
10 **Shaffer EA**. Review article: control of gall-bladder motor function. *Aliment Pharmacol Ther* 2000; **14** Suppl 2: 2-8
11 **Ryan J**, Cooper M, Loberg M, Harvey E, Sikorski S. Technetium-99m-labeled n-(2,6-dimethylphenylcarbamoylmethyl) iminodiacetic acid (tc-99m HIDA): a new radiopharmaceutical for hepatobiliary imaging studies. *J Nucl Med* 1977; **18**: 997-1004
12 **Chan DC**, Chang TM, Chen CJ, Chen TW, Yu JC, Liu YC. Gallbladder contractility and volume characteristics in gallstone dyspepsia. *World J Gastroenterol* 2004; **10**: 721-724
13 **Larsen TK**, Qvist N. The influence of gallbladder function on the symptomatology in gallstone patients, and the outcome after cholecystectomy or expectancy. *Dig Dis Sci* 2007; **52**: 760-763
14 **Fisher RS**, Stelzer F, Rock E, Malmud LS. Abnormal gallbladder emptying in patients with gallstones. *Dig Dis Sci* 1982; **27**: 1019-1024
15 **Northfield TC**, Kupfer RM, Maudgal DP, Zentler-Munro PL, Meller ST, Garvie NW, McCready R. Gall-bladder sensitivity to cholecystokinin in patients with gall stones. *Br Med J* 1980; **280**: 143-144
16 **Zhu J**, Han TQ, Chen S, Jiang Y, Zhang SD. Gallbladder motor function, plasma cholecystokinin and cholecystokinin receptor of gallbladder in cholesterol stone patients. *World J Gastroenterol* 2005; **11**: 1685-1689
17 **Funch-Jensen P**, Ebbehøj N. Sphincter of Oddi motility. *Scand J Gastroenterol Suppl* 1996; **216**: 46-51
18 **Balon HR**, Fink-Bennett DM, Brill DR, Fig LM, Freitas JE, Krishnamurthy GT, Klingensmith WC 3rd, Royal HD. Procedure guideline for hepatobiliary scintigraphy. Society of Nuclear Medicine. *J Nucl Med* 1997; **38**: 1654-1657
19 **Pomeranz IS**, Shaffer EA. Abnormal gallbladder emptying in a subgroup of patients with gallstones. *Gastroenterology* 1985; **88**: 787-791
20 **Kao CH**, Wang SJ, Chen GH, Yeh SH. Evaluation of gallbladder function by quantitative radionuclide cholescintigraphy in patients with gallbladder sludge or stones. *Nucl Med Commun* 1994; **15**: 742-745
21 **Bouchier IA**, Cooperband SR, el-Kodsi BM. Mucous substances and viscosity of normal and pathological human bile. *Gastroenterology* 1965; **49**: 343-353
22 **Pitt HA**, Roslyn JJ, Kuchenbecker SL, Doty JE, Denbesten L. The role of cystic duct resistance in the pathogenesis of cholesterol gallstones. *J Surg Res* 1981; **30**: 508-514
23 **Jazrawi RP**, Pazzi P, Petroni ML, Prandini N, Paul C, Adam JA, Gullini S, Northfield TC. Postprandial gallbladder motor function: refilling and turnover of bile in health and in cholelithiasis. *Gastroenterology* 1995; **109**: 582-591
24 **Cicala M**, Guarino MP, Vavassori P, Alloni R, Emerenziani S, Arullani A, Pallone F. Ultrasonographic assessment of gallbladder bile exchanges in healthy subjects and in gallstone patients. *Ultrasound Med Biol* 2001; **27**: 1445-1450
25 **Fridhandler TM**, Davison JS, Shaffer EA. Defective gallbladder contractility in the ground squirrel and prairie dog during the early stages of cholesterol gallstone formation. *Gastroenterology* 1983; **85**: 830-836
26 **Brand B**, Lerche L, Stange EF. Symptomatic or asymptomatic gallstone disease: is the gallbladder motility the clue? *Hepatogastroenterology* 2002; **49**: 1208-1212

S- Editor Tian L **L- Editor** Kerr C **E- Editor** Yin DH

Online Submissions: wjg.wjgnet.com
wjg@wjgnet.com
doi:10.3748/wjg.15.2768

World J Gastroenterol 2009 June 14; 15(22): 2768-2777
World Journal of Gastroenterology ISSN 1007-9327

BRIEF ARTICLES

Application of a biochemical and clinical model to predict individual survival in patients with end-stage liver disease

Eduardo Vilar Gomez, Luis Calzadilla Bertot, Bienvenido Gra Oramas, Enrique Arus Soler, Raimundo Llanio Navarro, Javier Diaz Elias, Oscar Villa Jiménez, Maria del Rosario Abreu Vazquez

Eduardo Vilar Gomez, Luis Calzadilla Bertot, Enrique Arus Soler, Department of Hepatology, National Institute of Gastroenterology, Havana 10400, Cuba
Bienvenido Gra Oramas, Department of Pathology, National Institute of Gastroenterology, Havana 10400, Cuba
Raimundo Llanio Navarro, Department of Gastroenterology, National Institute of Gastroenterology, Havana 10400, Cuba
Javier Diaz Elias, Deparment of Gastroenterology, The "Calixto Garcia" Hospital, Havana 10400, Cuba
Oscar Villa Jiménez, Department of Gastroenterology, National Institute of Gastroenterology, Havana 10400, Cuba
Maria del Rosario Abreu Vazquez, Department of Biostatistics, National Institute of Gastroenterology, Havana 10400, Cuba
Author contributions: Gomez EV and Bertot LC contributed equally to this work; They performed the study, acquisition of data, analysis and interpretation of data, drafting of the manuscript, critical revision of the manuscript and statistical analysis; Oramas BG, Soler EA, Elias JD, Jiménez OV performed the design, acquisition of data, and analysis and interpretation of data; Navarro RL performed critical revision of the manuscript; Abreu Vazquez MR performed the statistical analysis.
Correspondence to: Eduardo Vilar Gomez, National Institute of Gastroenterology, 25th Avenue, 503, Vedado, Havana 10400, Cuba. vilar@infomed.sld.cu
Telephone: +53-7-8325067 Fax: +53-7-8333253
Received: February 11, 2009 Revised: May 1, 2009
Accepted: May 8, 2009
Published online: June 14, 2009

Abstract

AIM: To investigate the capability of a biochemical and clinical model, BioCliM, in predicting the survival of cirrhotic patients.

METHODS: We prospectively evaluated the survival of 172 cirrhotic patients. The model was constructed using clinical (ascites, encephalopathy and variceal bleeding) and biochemical (serum creatinine and serum total bilirubin) variables that were selected from a Cox proportional hazards model. It was applied to estimate 12-, 52- and 104-wk survival. The model's calibration using the Hosmer-Lemeshow statistic was computed at 104 wk in a validation dataset. Finally, the model's validity was tested among an independent set of 85 patients who were stratified into 2 risk groups (low risk $\leqslant$ 8 and high risk > 8).

RESULTS: In the validation cohort, all measures of fit, discrimination and calibration were improved when the biochemical and clinical model was used. The proposed model had better predictive values (c-statistic: 0.90, 0.91, 0.91) than the Model for End-stage Liver Disease (MELD) and Child-Pugh (CP) scores for 12-, 52- and 104-wk mortality, respectively. In addition, the Hosmer-Lemeshow (H-L) statistic revealed that the biochemical and clinical model (H-L, 4.69) is better calibrated than MELD (H-L, 17.06) and CP (H-L, 14.23). There were no significant differences between the observed and expected survival curves in the stratified risk groups (low risk, $P = 0.61$; high risk, $P = 0.77$).

CONCLUSION: Our data suggest that the proposed model is able to accurately predict survival in cirrhotic patients.

Key words: Liver cirrhosis; Prognosis; Statistical models; Prognostic factors; Model for end-stage liver disease score; Child-Pugh score; Survival

Peer reviewer: Dr. Sheikh Mohammad Fazle Akbar, Assistant Professor, Third Department of Internal Medicine, Ehime University School of Medicine, Shigenobu-Cho, Ehime 791-0295, Japan

Gomez EV, Bertot LC, Oramas BG, Soler EA, Navarro RL, Elias JD, Jiménez OV, Abreu Vazquez MR. Application of a biochemical and clinical model to predict individual survival in patients with end-stage liver disease. *World J Gastroenterol* 2009; 15(22): 2768-2777 Available from: URL: http://www.wjgnet.com/1007-9327/15/2768.asp DOI: http://dx.doi.org/10.3748/wjg.15.2768

INTRODUCTION

The Model for End-stage Liver Disease (MELD) and Child-Pugh (CP) scores have been the most widely applied prognostic markers for organ allocation in liver transplantation, mainly due to their simplicity of use in daily clinical practice[1-5]. The MELD score has gained wide acceptance for predicting survival in patients undergoing liver transplantation. It has been suggested

that it provides more accurate prognosis than the Child-Pugh (CP) score in patients with decompensated cirrhosis and that it therefore improves the evaluation of priority for liver graft allocation[4,5]. It is not surprising, however, that the magnitude of superiority of the MELD score over the CP score is modest and is primarily limited to the population at the highest risk of renal failure[6]. Additionally, changes in some objective laboratory parameters of the MELD score may be directly related to the extensive use of diuretics, volume status, albumin infusion and the patient's nutritional status. Finally, clinical complications of portal hypertension such as ascites, encephalopathy, spontaneous bacterial peritonitis (SBP) and gastrointestinal bleeding are not considered in the MELD score, probably underestimating any direct association with the severity of liver disease[7]. However, the model has been shown to predict mortality independent of the occurrence of complications of portal hypertension[3,4]. The classification applied to the clinical complications of portal hypertension (ascites, encephalopathy, variceal bleeding and SBP) in the MELD score does not clearly reveal the different grades of severity of liver disease and its clinical response to medical treatment. Therefore, its utility as a prognostic model could be limited. In this regard, several recent studies have shown that clinical manifestations secondary to portal hypertension (encephalopathy, ascites) are good prognostic markers in cirrhotic patients[8,9]. According to the results of these studies, the use of clinical markers in prognostic models may be recommended.

The aim of this study was to evaluate the short-, medium- and long-term prognosis of a series of cirrhotic patients by means of the BioCliM score using biochemical (creatinine and bilirubin) and clinical (encephalopathy, bleeding esophageal varices and ascites) variables, to compare BioCliM with the MELD and CP scores, and to identify those variables with liver-related mortality. Our model was developed to improve accuracy in predicting survival and consequently improve the further evaluation of priority for liver graft allocation in cirrhotic patients.

MATERIALS AND METHODS

Study design, setting and participants

We prospectively evaluated 180 consecutive cirrhotic patients who were admitted at the National Institute of Gastroenterology of Havana during the period May 2003 to January 2006. Inclusion criteria were histological, laparoscopic or clinical diagnosis of cirrhosis and presence of compensated or decompensated disease (stages A, B or C according to the CP classification). Patients with hepatocellular carcinoma, severe infection, severe primary cardiopulmonary failure, alcohol use within one month before initial evaluation, and intrinsic kidney disease were excluded from the study. Among 180 patients who had complete medical profiles and an established diagnosis of hepatic cirrhosis, 172 patients fulfilled the above selection criteria.

The model validation was performed by applying it to an independent group of 85 patients who were evaluated at the "Calixto Garcia" Hospital of Havana from March 2005 to August 2007. The baseline characteristics of the patient population are summarized in Table 1.

Table 1 Baseline characteristics of the patient population

Variables	Derivation set *n* = 172	Validation set *n* = 85
Follow-up period	56 (4-104)	58 (8-104)
Age (yr)	56 (20-79)	59 (23-78)
Sex, *n* (%)		
Male	106 (62)	58 (68)
Female	66 (38)	27 (32)
Cause of cirrhosis, *n* (%)		
Alcohol	30 (17)	16 (19)
Alcohol plus viral infection	15 (9)	4 (5)
HBV	20 (12)	12 (14)
HCV	92 (53)	50 (59)
Viral co-infection (HBV/HCV)	1 (1)	1 (1)
Unknown	13 (7)	1 (1)
NAFL	1 (1)	1 (1)
Complications on admission, *n* (%)		
Ascites		
Absent or controlled	147 (85)	72 (85)
Uncontrolled	25 (15)	13 (15)
BEV		
Absent or present without relapses	167 (97)	79 (94)
Present with relapses	5 (3)	5 (6)
Encephalopathy		
Absent or controlled	160 (93)	79 (93)
Uncontrolled	12 (7)	6 (7)
SBP		
Absent or present without relapses	168 (98)	82 (96)
Present with relapses	4 (2)	3 (4)
Hepatorenal syndrome, *n* (%)	3 (2)	1 (1)
Prothrombin time (s)	19 (13-55)	17 (13-53)
Partial thromboplastin time (s)	38 (26-165)	39 (26-167)
INR for prothrombin time	1.7 (1-7.5)	1.5 (1-6.9)
Albumin (g/L)	37 (20-48)	36 (21-47)
Creatinine (mmol/L)[1]	100 (42-516)	98 (39-489)
Bilirubin (mmol/L)[2]	20 (8-130)	23 (12-137)
Cholesterol (mmol/L)	3.8 (1.9-10.2)	3.9 (2-9.6)
Child-Pugh score[3]	7 (5-14)	7 (5-14)
Child-Pugh A, *n* (%)	67 (39)	30 (35)
Child-Pugh B, *n* (%)	75 (44)	34 (40)
Child-Pugh C, *n* (%)	30 (17)	21 (25)
MELD score	17 (9-42)	18 (10-43)
BioCliM score	7.7 (6.1-13.6)	7.9 (6-13.8)

HBV: Hepatitis B virus; HCV: Hepatitis C virus; NAFL: Non-alcoholic fatty liver; BEV: Bleeding esophageal varices; SBP: Spontaneous bacterial peritonitis; INR: International normalized ratio; MELD: Model for End-stage Liver Disease; BioCliM: Biochemical and Clinical Model. All quantitative variables are expressed as median (ranges). [1]To convert mmol/L into mg/dL, multiply by 0.01131. [2]To convert mmol/L into mg/dL, multiply by 0.0585. [3]The Child-Pugh, MELD and BioCliM scores are measures of the severity of liver disease.

Variables of interest, measurement, follow-up and ethics

Detailed medical history, complete physical examination, and a battery of laboratory tests were performed in all patients on the day of admission. Biochemical evaluations were carried out by the same laboratory. Prothrombin time expressed as PT-ratio (patient-to-normal coagulation time) was converted to prothrombin time international normalized ratio (INR) using an internal laboratory standard and was assessed by a single

operator. The main clinical complications of portal hypertension were initially evaluated and classified by an experienced hepatologist depending on the clinical response to medical treatment. Bleeding esophageal varices (BEV) were diagnosed by clinical signs of hematemesis and endoscopic signs of active bleeding or adherent clots on EV[10]; they were classified as absent, present with relapses or rebleeding (2 or more bleeding episodes in the last 3 mo) or without relapses (one bleeding episode in the last 3 mo). Variceal bleeding relapse or rebleeding was defined as the occurrence of hematemesis/melena, aspiration of more than 100 mL of fresh blood in patients with a nasogastric tube and decrease of 3 g in Hb if no transfusion was given. Portosystemic encephalopathy was defined according to the West Haven criteria for grading from 0 (subclinical) to 4 (coma)[11]; it was classified as absent (no episode of encephalopathy in the last year), medically controlled (episodic hepatic encephalopathy developing over hours to days, but does not persist with adequate medical treatment) or uncontrolled (persistent hepatic encephalopathy that develops upon discontinuation of medication), irrespective of disease severity. Ascites was classified as absent (no clinical and ultrasound evidence of ascites and without therapeutic intervention), medically controlled (no clinical and ultrasound evidence of ascites in patients undergoing full therapeutic intervention) or uncontrolled (ascites that requires repeated paracentesis for control or a sodium-restricted diet and intensive diuretic therapy). Diagnostic paracentesis and ascitic fluid culture were performed in all admitted cirrhotic patients. Spontaneous bacterial peritonitis (SBP) was diagnosed when the ascites polymorphonuclear leukocyte (PMN) count was > 250/mm^3, with or without positive ascites bacterial culture[12]; it was coded as absent, present without relapses (one SBP episode in the last year) and present with relapses (2 or more episodes in the last year). Patients were followed up from their date of initial evaluation until death (related or unrelated to liver disease), liver transplantation, or study closure. Patients with death unrelated to liver disease were excluded from the analysis. Patients lost to follow-up were censored at the last date known to be alive and patients undergoing liver transplantation were censored at the transplant date.

The study was conducted in compliance with the Declaration of Helsinki and approved by the ethics committee and the institutional review board of the National Institute of Gastroenterology. All patients provided written informed consent for participation.

Analysis for survival and derivation of the novel risk score

The probable prognostic predictors, including age, sex, serum biochemistry and clinical complications of portal hypertension, were analyzed to determine prognostic ability. To lessen the influence of extreme laboratory values, quantitative variables were transformed to their natural logarithms.

Univariate and multivariate forward stepwise Cox proportional hazards models were used to determine variables associated with survival. Variables that were significant ($P < 0.05$) in univariate analysis were included in multivariate analysis. Stepwise probabilities for entry or removal were set at 0.05 and 0.10, respectively.

With each Cox model, a risk score for each patient was calculated as: $R = \beta_1 X_1 + \beta_2 X_2 + \ldots + \beta_k X_k$, where X_1, X_2,…, X_k are the values of prognostic factors and β_1, β_2, …, β_k are the corresponding regression coefficients. A higher risk score corresponds to poorer prognosis.

The forward stepwise selection procedures were used for variable selection, assessment for interactions, and model development. The likelihood ratio statistic tested the significance of the addition of each variable separately to a predictive model that included ascites only. Furthermore, the c-statistic was computed as a criterion for the selection of a group of variables to be used in the new predictive model. The final criterion for inclusion in the model was minimization of the Bayes Information Criterion (BIC)[13]. The BIC is a likelihood-based measure in which lower values indicate better fit and in which a penalty is paid for increasing the number of variables. Thus, the variables selected for inclusion should provide not only the best fit but also a parsimonious prediction model.

Predictive models for survival and discrimination

The CP and MELD scores were calculated on parameters obtained at referral. The MELD score was calculated according to the original formula proposed by the Mayo Clinic group as follows: [9.57 × $\log_e$ creatinine mg/dL + 3.78 × $\log_e$ bilirubin mg/dL + 11.20 × $\log_e$ INR + 6.43 (constant for liver disease etiology)]. To avoid negative scores, laboratory values less than 1 were rounded up to 1. The maximal value of creatinine was 4 mg/dL[3].

Once a new risk model was determined, it was prospectively tested in the validation dataset of 85 patients from "Calixto Garcia" Hospital. The discrimination ability of the different models was measured by means of the concordance statistic (c-statistic), a measure of discrimination also known as a natural extension of the receiving operator characteristic (ROC) curve area in survival analysis. *P* values for the comparison of the c-statistic were computed using the bootstrap method. A c-statistic between 0.8 and 0.9 indicates excellent accuracy, and a value over 0.7 should be considered clinically useful. The concordance c-statistic was assessed for 12-, 52-, and 104-wk survival. A time-to-event with the censored data version for survival analysis was performed to compute the c-statistic.

The concordance probability estimates (CPE) were computed[14], because the c-statistic seems to overestimate the true concordance probability, especially if the censoring proportion is high. Since the CPE is a consistent estimate, it is a better measure in the context of using predictions from Cox regression models.

Calibration and external validation of the new risk score

To assess model calibration (or how closely the predicted

probabilities reflect actual risk), the Hosmer-Lemeshow calibration statistic, as modified by D'Agostino *et al*[15], comparing observed and predicted risk was implemented.

In addition, the new risk model was validated in a cohort of 85 independent patients from "Calixto Garcia" Hospital who were stratified into 2 risk (R) groups: R $\leqslant$ 8 and R > 8. Within each risk group the survival was calculated using the Kaplan-Meier procedure and the observed-predicted survivals were compared using the log-rank test.

Analyses were performed with the use of SAS software, version 9.1 (SAS Institute).

RESULTS

A total of 180 patients were examined for eligibility, and 172 were included in the study. The reasons for non-participation were: 3 patients with HCC, 3 with repeated alcohol use, and 2 with severe infection disease. The period of recruitment lasted from May 2003 to February 2004. One hundred and forty one patients completed the follow-up period. Thirty one patients died during the study, 29 liver-related and 2 unrelated to liver disease (myocardial infarction). One hundred and seventy patients were included in the outcome analyses.

The patients' clinical and serological features are summarized in Table 1.

In the derivation data set, the median follow-up period was 56 wk (range, 4-104 wk). The CP median score was 7 (range, 5-14) with 61% of the patients being CP class B and C. The MELD and BioCliM median scores were 17 (range, 8-42) and 7.7 (range, 5.7-13.6), respectively. During follow-up, 29 patients (17%) died. The 4-, 12-, 24-, 52- and 104-wk survival rates were 98%, 98%, 90%, 89% and 83%, respectively.

The patients of the validation group were followed for a median of 58 wk (range, 8–104 wk) during which 13 died. The 4-, 12-, 24-, 52- and 104-wk survival rates were 96%, 95%, 88%, 84% and 83%, respectively. The CP median score was 7 (range, 5-14) with 65% of the patients being CP class B and C. The MELD and BioCliM median scores were 18 (range, 9-43) and 7.9 (range, 6-13.8), respectively.

None of the patients in the derivation or validation groups underwent liver transplantation during the follow-up period.

Overall survival according to single prognostic factors

Univariate analysis for 104-wk overall survival: Univariate analysis using Cox proportional hazards models showed that serum levels of creatinine, bilirubin, cholesterol, albumin, prothrombin time, partial thromboplastin time, ascites, spontaneous bacterial peritonitis, encephalopathy and bleeding esophageal varices were significantly associated with survival (Table 2).

Multivariate analysis for 104-wk overall survival: Multivariate Cox regression analysis included those variables independently related to survival resulting from univariate analysis. The selected variables were available in all patients that entered the forward stepwise model. Of the candidate variables, only ascites, encephalopathy, bleeding esophageal varices and serum creatinine were independently predictive of survival (Table 3).

Table 2 Association of baseline characteristics with mortality in 170 cirrhotic patients, results from univariate Cox proportional hazards models

Variables	*P*	Hazard ratio	95% CI for Hazard ratio
Age (yr)	0.68	0.56	0.36-1.06
Sex (male)	0.54	0.44	0.89-1.26
Etiology (viral)	0.66	0.58	0.40-1.11
ALT (IU/L) ($\log_n$ value)	0.85	0.84	0.34-1.12
AST (IU/L) ($\log_n$ value)	0.43	0.90	0.56-1.34
ALT/AST ratio	0.64	0.87	0.50-1.21
Platelet count ($\times 10^9$/L) ($\log_n$ value)	0.54	0.89	0.52-1.30
Prothrombin time (s)[1] ($\log_n$ value)	0.01	2.23	1.24-4.89
INR for prothrombin time ($\log_n$ value)	0.03	1.99	1.13-3.96
Partial thromboplastin time (s)[2] ($\log_n$ value)	0.04	1.78	1.10-3.23
Albumin (mg/dL) ($\log_n$ value)	0.001	3.12	1.89-5.23
Bilirubin (mmol/L) ($\log_n$ value)	< 0.001	3.89	2.12-6.14
Creatinine (mmol/L) ($\log_n$ value)	< 0.001	3.95	2.18-6.56
Cholesterol (mmol/L) ($\log_e$ value)	0.03	1.83	1.34-3,42
Ascites	< 0.001	4.05	2.27-6.33
Spontaneous bacterial peritonitis	0.001	3.05	2.10-5.07
Encephalopathy	< 0.001	4.50	2.90-6.50
Bleeding esophageal varices	< 0.001	4.78	3.11-7.11

CI: Confidence interval; ALT: Alanine aminotransferase; AST: Aspartate aminotransferase. Hazard ratios (95% CI) for quantitative variables are expressed for 1 relevant unit increase of log. INR: International normalized ratio. [1]Prothrombin time (s): Value in seconds. [2]Partial thromboplastin time (s): Value in seconds.

The estimated hazard risk for ascites suggested that the risk of death for uncontrolled ascites was 10.2 times greater than for those with absent or controlled ascites. The risk of death in those patients with relapsing bleeding and uncontrolled encephalopathy increased 3.25 times compared to those without bleeding or with non-relapsing bleeding, and 2.5 times compared to those with absent or controlled encephalopathy. In terms of impact in prognosis, the ascites (hazard ratio (HR), 10.2) and serum creatinine (HR, 3.99) were the most important prognostic factors.

Model derivation and development

In the model derivation cohort, 11 potential variables selected from the univariate analysis ($P < 0.05$) were calculated for model inclusion. Of these only 5 were included in the model. The likelihood ratio statistic showed the significance of the addition of each variable separately to a predictive model that included ascites only (Table 3). The χ^2 statistic was progressively increased with the addition of creatinine, bleeding esophageal varices, hepatic encephalopathy, and bilirubin. The c-statistic in the model that included only ascites was 0.76, based on the c-statistic for censored data. When creatinine, BEV, HE and bilirubin were added to the model, the c-statistic was improved to 0.83, 0.85, 0.89, and 0.90, respectively. In the same context,

Table 3 Contributions of different variables to survival prediction at 104 wk, results from multivariate Cox regression models[1]

Variable	Variable χ^2	Regression coefficient	Hazard ratio	95% CI for Hazard ratio		*P* value	c-statistic	BIC
Ascites	53.90	2.310	10.2	3.78	28.1	< 0.0001	0.76	2014.15
+ Ln (creatinine)	63.43	1.370	3.99	1.57	10.9	0.006	0.83	1988.15
+ BEV	65.71	1.195	3.25	1.01	9.77	0.048	0.85	1970.65
+ HE	68.91	0.909	2.50	0.915	6.88	0.070	0.89	1961.89
+ Ln (bilirubin)[2]	70.11	0.349	1.46	0.66	3.33	0.427	0.90	1951.77

[1]Estimated from Cox proportional hazards models. [2]Biochemical (bilirubin and creatinine) and Clinical (ascites, encephalopathy and bleeding esophageal varices) Model; BEV: Bleeding esophageal varices; HE: Hepatic encephalopathy; BIC: Bayesian Information Criterion. Ln was used to normalize distributions and improve the fit for individual predictors. Hazard ratio for quantitative variables are expressed for 1 relevant unit increase of log. + indicates the addition of each variable separately to the model with ascites only. χ^2 is the likelihood ratio statistic for each group of variables when added to the model. The risk prediction was based on data from the model derivation cohort (n = 170) at 104 wk follow-up.

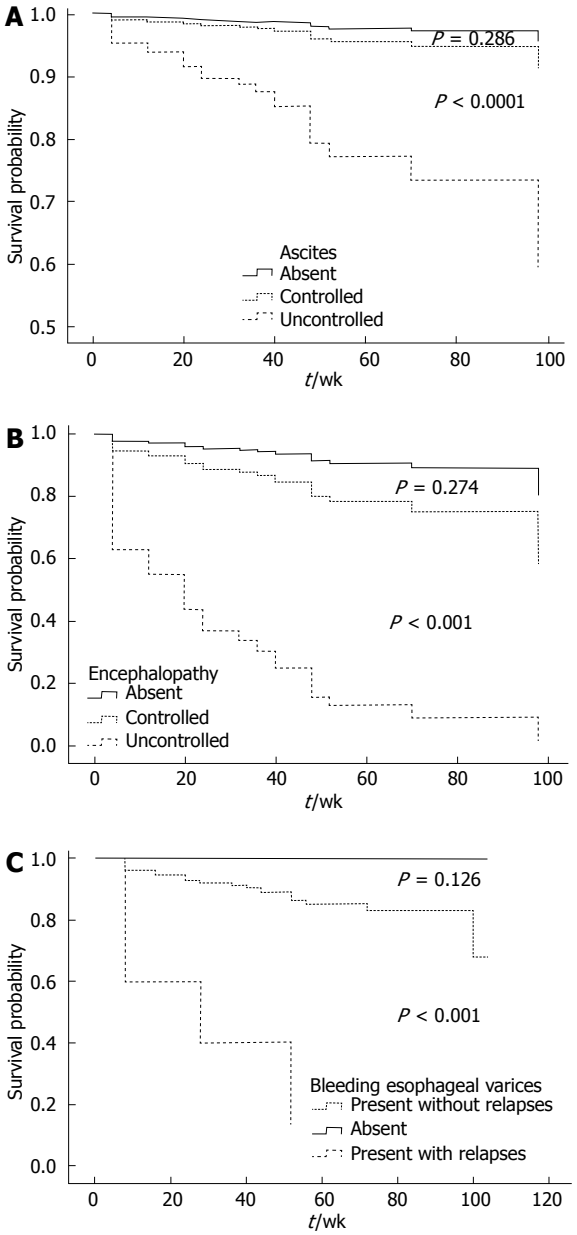

Figure 1 Kaplan-Meier estimated survival curves for clinical variables. A: Ascites; B: Encephalopathy; C: Bleeding esophageal varices.

the combination of ascites, creatinine, BEV, HE and bilirubin revealed the smallest BIC value (1951.77), thus, in the derivation set, the model with the combination of clinical and biochemical variables appeared to improve the risk prediction.

Computational formula for 104-wk risk using best-fitting model

The regression coefficients of the formula for calculating the new risk score (biochemical and clinical model) were selected from a Cox regression model[16] and are reported in Table 3.

The risk scores for individual patients were calculated using the following equation: [1.370 × $\log_e$ (creatinine mmol/L) + 0.349 × $\log_e$ (bilirubin mmol/L) + 2.310 × (ascites: 0 if absent or medically controlled and 1 if uncontrolled) + 0.909 × (encephalopathy: 0 if absent or medically controlled and 1 if uncontrolled) + 1.195 × (bleeding esophageal varices: 0 if absent or present without relapses and 1 if present with relapses). The clinical variables were coded depending on the clinical response to medical treatment. The variables grouped together as "absent or medically controlled" (ascites and encephalopathy) and "absent or present without relapses" (bleeding esophageal varices) have been so grouped because their survival was similar in each one of them (Figure 1). The missing values were imputed for survival modeling.

Survival probabilities were derived from the Cox proportional hazards model: $S(t) = S_0(t)^{\exp(R-R_o)}$. S(t) is the survival probability in wk, $S_0(t)$ the baseline survival function, R the individual risk score and R_0 the risk score of the average patient in the series. For example, the 12-wk survival probability is calculated as: $S_{(12\ wk)} = 0.981^{\exp(BioCliM\ score-7)}$, where 0.981 is the 12-wk baseline survival and 7 is the reference BioCliM score. To ease its use, the score was multiplied by 100.

Predictive models for 12-, 52- and 104-wk survival

Comparison of the c-statistic values among the CP, MELD and BioCliM scores was performed. All scoring systems were found to have diagnostic accuracy in predicting survival. The BioCliM score, however, showed to have better discriminative power in predicting short- (12 wk), intermediate- (52 wk) and long-term survival (104 wk) than the rest of the scores (Figure 2).

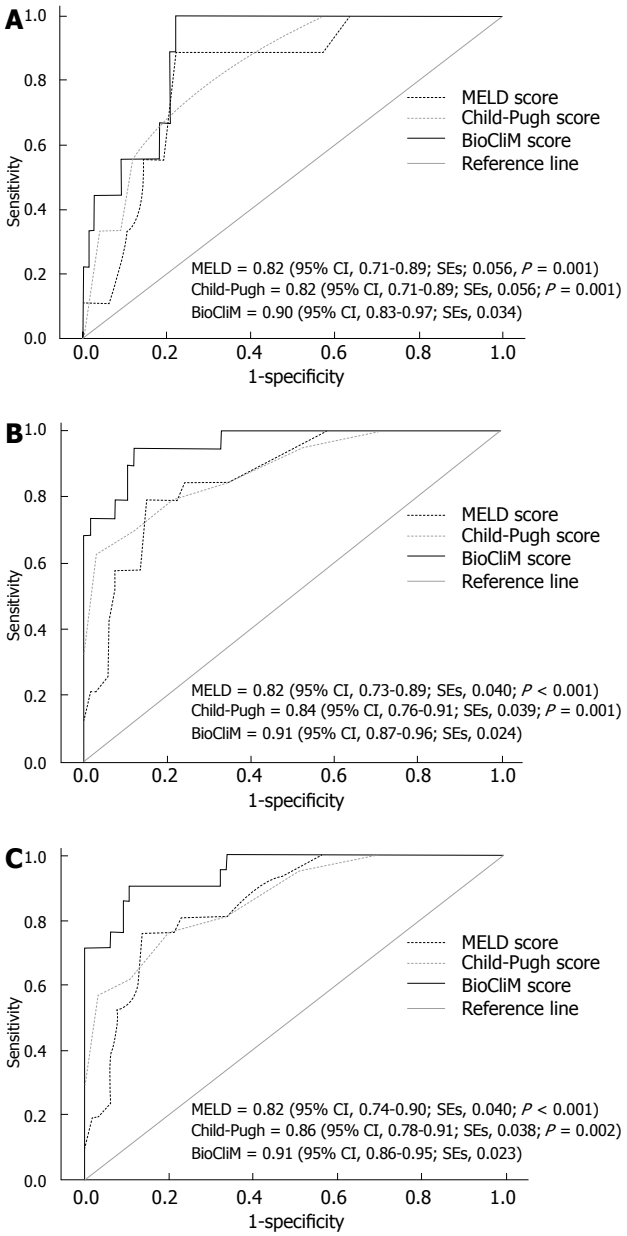

Figure 2 Comparison of the c-index values of the MELD, Child-Pugh and BioCliM scores for 12- (A), 52- (B) and 104-wk (C) survival. SE indicates standard errors. The different values were compared with BioCliM score using the bootstrap method.

The c-statistic for the CP and MELD scores were almost identical for 12-wk survival (0.82 and 0.82), and slightly higher for CP as compared with MELD for 52-wk (0.84 and 0.82) and 104-wk (0.86 and 0.82) survival.

We used an alternative way of computing the concordance probability for a censored outcome to estimate the true concordance probability in samples with a high censored proportion. The concordance probability estimates for the CP (CPE, 0.71; SE, 0.042), MELD (CPE, 0.74; SE, 0.043) and BioCliM (CPE, 0.78; SE, 0.050) models were lower at 12 wk in comparison with those obtained using the standard c-statistic value. Finally, the CPE at 12 wk was consistently higher for BioCliM as compared with CP and MELD scores.

Discrimination and model validation

The Hosmer-Lemeshow statistic (H-L) is a measure of the discrepancy between the observed and predicted risk. A better calibrated model would have a smaller discrepancy between the observed and predicted and thus a smaller H-L statistic.

A significant *P* value for the H-L statistic indicates a significant deviation between predicted and observed outcomes. Figure 3 compares the calibration of the BioCliM, MELD and CP scores in predicting the probability of death at 104 wk. The H-L statistic was 4.69 for the BioCliM score, 17.06 for the MELD score and 14.23 for the CP score, indicating a good calibration for all models; however, this analysis clearly shows that BioCliM is better calibrated.

Figure 4 illustrates the observed and expected Kaplan-Meier survival curves for each score in 2 patient subgroups divided according to risk score as low risk (R $\leqslant$ 8) and high risk (R > 8), selected from the "Calixto Garcia" Hospital. Using a cutoff value of 8 (risk score) to predict probability of survival within 104 wk, the sensitivity and specificity of the BioCliM score was 90% and 87%, respectively. Median survival was 104 wk and 47 wk for low- and high-risk groups, respectively. There were no significant differences between the observed and expected survival curves in the stratified risk groups (low risk, $P = 0.61$; high risk, $P = 0.77$). Thus, the BioCliM score allowed accurate prediction of survival in the cirrhotic patient validation group.

Survival according to the BioCliM score

The differences in the short-, intermediate- and long-term survival between patients with low risk ($\leqslant$ 8), and high risk (> 8) scores were compared (Figure 5).

Overall survival rates were significantly different between low-risk and high-risk patients ($P < 0.0001$). The 12-wk survival rates were 98% and 64% for low and high risk, respectively. For low and high risk, 1-year survival rates were 97% and 3%, and 2-year survival rates were 95% and 0%, respectively. Patients with a high risk score had the highest risk of mortality compared to patients with low values. Patients with a BioCliM score of $\geqslant$ 8 had a median survival of < 47 wk in comparison to patients with a median survival of 104 wk for patients with a BioCliM score of < 8.

DISCUSSION

The most widely used prognostic model to predict survival in cirrhotic patients has been the CP score. It is an important tool for the prognostic evaluation of cirrhotic patients and the current organ allocation policy. It has, however, several drawbacks such as the subjectivity of clinical parameters, limited discriminative capability and variability in the measurements of laboratory parameters[17,18]. Current CP score modifications by adding new variables or utilizing sophisticated measures did not improve its accuracy to predict survival[19-25]. A relatively new score, the MELD,

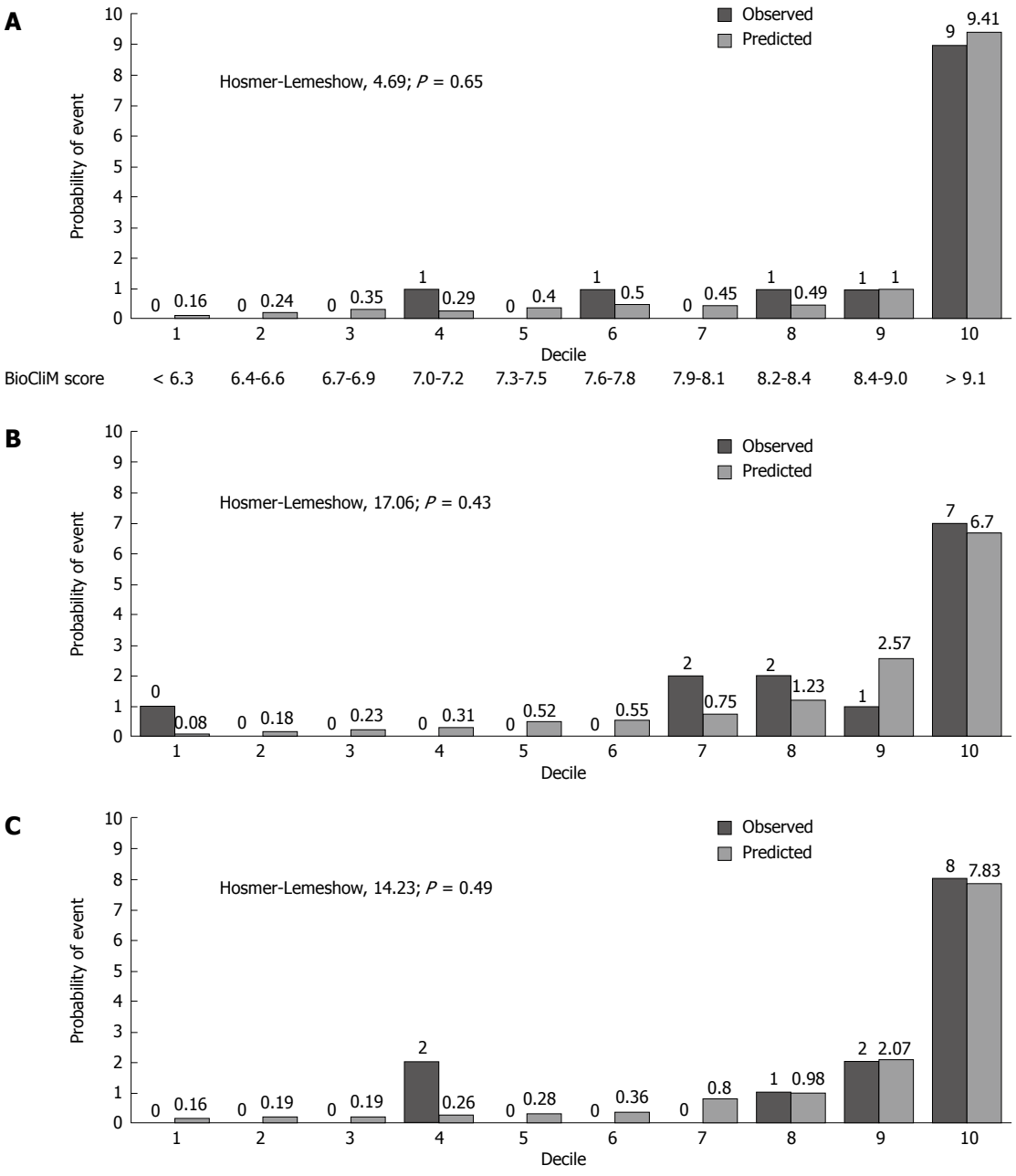

Figure 3 Observed and predicted probability of events at 104 wk. A, B and C shows the observed and predicted probability of death according to BioCliM, MELD and Child-Pugh scores in 10 groups (deciles) of patients, respectively. A significant *P*-value for the Hosmer-Lemeshow statistic indicates a significant deviation between predicted and observed outcomes.

has been instituted in patients with end-stage liver disease awaiting liver transplantation. MELD has shown an advantage over CP by using continuous objective variables that are not open to observer interpretation and are appropriately weighted according to their impact on prognosis[3,4,26]. Its ability to predict mortality, however, has been found to be similar or slightly superior to the traditional CP score[27-30]. These controversies suggest that a better predictive model is necessary to predict survival in cirrhotic patients.

In our study, the baseline characteristics were comparable with similar studies evaluating survival in cirrhotic patients[31-36]. Furthermore, all clinical and biochemical variables included in the CP and MELD scores were associated with survival in univariate analysis. Multivariate Cox proportional hazards analysis identified serum creatinine, ascites, encephalopathy and bleeding esophageal varices as independent prognostic factors for overall survival. The strongest predictors of mortality were ascites and serum creatinine. In our proposed model, ascites, encephalopathy and variceal bleeding were evaluated depending on medical treatment response, and the diagnosis and treatment of each of these was based on the most recent published guidelines[10-12,37]. The used nomenclature appeared to be more uniform and less subjective than the commonly applied classification into CP or MELD scores[2-4].

The major finding of this prospective study is that the BioCliM score, which is based on a combination of 3 clinical indices (ascites, encephalopathy and bleeding

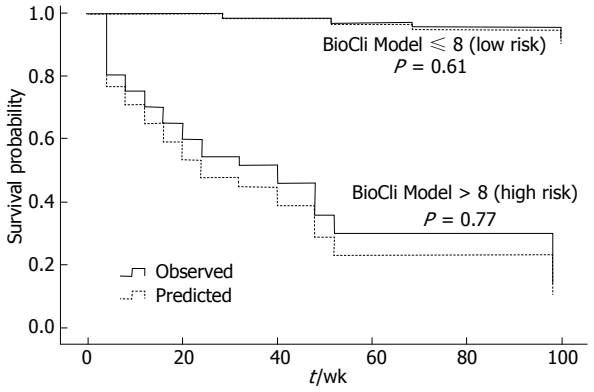

Figure 4 Observed and expected 104-wk survival curves for the BioCliM score. Survival of 85 independent patients from the "Calixto Garcia" Hospital who were stratified according to their risk score into two risk groups (low-risk ⩽ 8 and high-risk > 8). The observed and predicted BioCli Model survival curves were compared using log-rank test. The observed and expected survival was similar for the low- and high-risk groups.

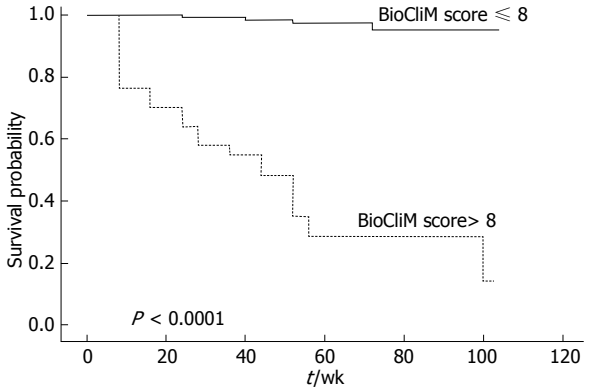

Figure 5 Kaplan-Meier estimated survival curves for the BioCli Model score.

esophageal varices) and 2 biochemical parameters (creatinine and bilirubin), is able to accurately predict short-term (12 wk), intermediate-term (52 wk) and long-term (104 wk) mortality in cirrhotic patients. Our results showed that the BioCliM score is superior to the CP and MELD scores in ranking patients according to their risk of death. In addition, the BioCliM score showed a sustained discriminative power to predict survival through the different evaluated periods (12-104 wk). Our data further support, as well as previous findings, that the MELD score is not significantly superior to the CP score in predicting survival in patients with hepatic cirrhosis[25,27-30]. Theoretically, the MELD score is undoubtedly more objective and robust than the CP score for the previously mentioned reasons; however, a major limitation of the MELD score is the poor discriminative power to predict survival among patients whose clinical course is often affected by other factors which are excluded by the model[38]. Recent studies have demonstrated that ascites, encephalopathy and hyponatremia are important independent predictors of early pretransplant mortality, especially for patients with low MELD scores[8,9,39,40], thus affecting the consideration for an expedited liver transplant under the "sickest first" model. In consequence, as the MELD score does not reflect the presence of ascites and encephalopathy, these patients need to be allocated separately for liver transplantation if MELD is used to prioritize organ allocation. By contrast, the BioCliM scale is able to accurately predict survival in patients with clinical complications of portal hypertension, thus the BioCliM score could be recommended in the individual management of these patients. Further studies are needed to validate its prognostic accuracy in patients undergoing liver transplantation.

Possibly the most important study limitations were the relatively small sample size, the poor geographic diversity of the patients included (single and tertiary center) and the major drawbacks of the MELD score related to wide variability of laboratory parameters such as serum creatinine and bilirubin[28,41,42].

In conclusion, both the CP and MELD scores can accurately predict short-term survival in cirrhotic patients, while the BioCliM score appears to have great discriminative power for short- (4 and 12 wk), intermediate- (24 and 52 wk) and long-term (104 wk) survival. In contrast to the MELD score, the use of the BioCliM score in patients with ascites, encephalopathy and variceal bleeding could significantly increase survival predictive values in patients with end-stage liver disease.

ACKNOWLEDGMENTS

We gratefully acknowledge the contributions of Dr. Frank E Harrell Jr. PhD, Professor and Chair of the Department of Biostatistics, Vanderbilt University, for critical review of the statistical analyses during the preparation of the manuscript.

COMMENTS

Background

The Child-Pugh and Model for End-stage Liver Disease (MELD) scores are important tools for the prognostic evaluation of cirrhotic patients and the current organ allocation policy. These have, however, several drawbacks such as the subjectivity of clinical parameters, limited discriminative capability and variability in the measurements of laboratory parameters. The current evidence suggests that a better predictive model is necessary to predict survival in cirrhotic patients.

Research frontiers

The clinical complications of portal hypertension such as ascites, encephalopathy, spontaneous bacterial peritonitis (SBP) and gastrointestinal bleeding are not considered in the MELD score, probably underestimating that they may have a direct association with the severity of liver disease. The classification applied to the clinical complications of portal hypertension (ascites, encephalopathy, variceal bleeding and SBP) in the MELD score does not clearly reveal the different grades of severity of liver disease and its clinical response to medical treatment. Therefore, its utility in the prognostic model could be limited. In this study, the authors have evaluated a new paradigm for clinical variables, depending on the severity and medical treatment response and how they have an influence, as prognostic factors, in the survival of cirrhotic patients.

Innovations and breakthroughs

Recent reports have demonstrated that ascites, encephalopathy and hyponatremia are important independent predictors of early pretransplant mortality, especially for patients with low MELD scores, thus affecting the consideration for an expedited liver transplantation under the "sickest first" model. In consequence, as the MELD score does not reflect the presence of

ascites and encephalopathy, these patients need to be allocated separately for liver transplantation if MELD is used to prioritize organ allocation. By contrast, the new biochemical and clinical model is able to accurately predict survival in patients with clinical complications of portal hypertension; thus the BioCliM score could be recommended in the individual management of these patients.

Applications

In contrast to the MELD score, BioCliM is able to accurately predict survival in patients with clinical complications of portal hypertension, thus the BioCliM score could be recommended in the individual management of these patients. Further studies are needed to validate its prognostic accuracy in patients undergoing liver transplantation.

Terminology

BioCliM is a new biochemical and clinical model that is able to accurately predict survival in patients with end-stage liver disease.

Peer review

The authors examined the prognostic value and predictive capability of a new prognostic model in patients with end-stage liver disease. A less subjective nomenclature to assess the clinical complications of portal hypertension was evaluated in combination with biochemical variables to determine their influence as prognostic factors of survival in cirrhotic patients. The biochemical and clinical model was shown to accurately predict survival in patients with clinical complications of portal hypertension and it appeared to have great discriminative power for short- (4 and 12 wk), intermediate- (24 and 52 wk) and long-term (104 wk) survival.

REFERENCES

1 **Child CG**, Turcotte JG. Surgery and portal hypertension. In: Child CG, editor. The Liver and Portal Hypertension. Philadelphia: W.B. Saunders Co, 1964: 1-85
2 **Pugh RN**, Murray-Lyon IM, Dawson JL, Pietroni MC, Williams R. Transection of the oesophagus for bleeding oesophageal varices. *Br J Surg* 1973; **60**: 646-649
3 **Kamath PS**, Wiesner RH, Malinchoc M, Kremers W, Therneau TM, Kosberg CL, D'Amico G, Dickson ER, Kim WR. A model to predict survival in patients with end-stage liver disease. *Hepatology* 2001; **33**: 464-470
4 **Wiesner R**, Edwards E, Freeman R, Harper A, Kim R, Kamath P, Kremers W, Lake J, Howard T, Merion RM, Wolfe RA, Krom R. Model for end-stage liver disease (MELD) and allocation of donor livers. *Gastroenterology* 2003; **124**: 91-96
5 **Freeman RB Jr**, Wiesner RH, Harper A, McDiarmid SV, Lake J, Edwards E, Merion R, Wolfe R, Turcotte J, Teperman L. The new liver allocation system: moving toward evidence-based transplantation policy. *Liver Transpl* 2002; **8**: 851-858
6 **Everson GT**. MELD: the answer or just more questions? *Gastroenterology* 2003; **124**: 251-254
7 **Reuben A**. Child comes of age. *Hepatology* 2002; **35**: 244-245
8 **Yoo HY**, Edwin D, Thuluvath PJ. Relationship of the model for end-stage liver disease (MELD) scale to hepatic encephalopathy, as defined by electroencephalography and neuropsychometric testing, and ascites. *Am J Gastroenterol* 2003; **98**: 1395-1399
9 **Heuman DM**, Abou-Assi SG, Habib A, Williams LM, Stravitz RT, Sanyal AJ, Fisher RA, Mihas AA. Persistent ascites and low serum sodium identify patients with cirrhosis and low MELD scores who are at high risk for early death. *Hepatology* 2004; **40**: 802-810
10 **D'Amico G**, De Franchis R. Upper digestive bleeding in cirrhosis. Post-therapeutic outcome and prognostic indicators. *Hepatology* 2003; **38**: 599-612
11 **Ferenci P**, Lockwood A, Mullen K, Tarter R, Weissenborn K, Blei AT. Hepatic encephalopathy--definition, nomenclature, diagnosis, and quantification: final report of the working party at the 11th World Congresses of Gastroenterology, Vienna, 1998. *Hepatology* 2002; **35**: 716-721
12 **Rimola A**, García-Tsao G, Navasa M, Piddock LJ, Planas R, Bernard B, Inadomi JM. Diagnosis, treatment and prophylaxis of spontaneous bacterial peritonitis: a consensus document. International Ascites Club. *J Hepatol* 2000; **32**: 142-153
13 **Harrell FE Jr**. Regression modeling strategies: with applications to linear models, logistic regression, and survival analysis. New York: Springer Verlag, 2001
14 **Gönen M**, Heller G. Concordance probability and discriminatory power in proportional hazards regression. *Biometrika* 2005; **92**: 965-970
15 **D'Agostino RB**, Nam BH. Evaluation of the performance of survival analysis models: discrimination and calibration measures. In: Balakrishnan N, Rao CR, editors. Advances in survival analysis. Amsterdan: Elsevier, 2004: 1-25
16 **Christensen E**. Multivariate survival analysis using Cox's regression model. *Hepatology* 1987; **7**: 1346-1358
17 **Forman LM**, Lucey MR. Predicting the prognosis of chronic liver disease: an evolution from child to MELD. Mayo End-stage Liver Disease. *Hepatology* 2001; **33**: 473-475
18 **Pagliaro L**. MELD: the end of Child-Pugh classification? *J Hepatol* 2002; **36**: 141-142
19 **Degré D**, Bourgeois N, Boon N, Le Moine O, Louis H, Donckier V, El Nakadi I, Closset J, Lingier P, Vereerstraeten P, Gelin M, Adler M. Aminopyrine breath test compared to the MELD and Child-Pugh scores for predicting mortality among cirrhotic patients awaiting liver transplantation. *Transpl Int* 2004; **17**: 31-38
20 **Adler M**, Verset D, Bouhdid H, Bourgeois N, Gulbis B, Le Moine O, Van de Stadt J, Gelin M, Thiry P. Prognostic evaluation of patients with parenchymal cirrhosis. Proposal of a new simple score. *J Hepatol* 1997; **26**: 642-649
21 **Merkel C**, Bolognesi M, Bellon S, Bianco S, Honisch B, Lampe H, Angeli P, Gatta A. Aminopyrine breath test in the prognostic evaluation of patients with cirrhosis. *Gut* 1992; **33**: 836-842
22 **Testa R**, Valente U, Risso D, Caglieris S, Giannini E, Fasoli A, Botta F, Dardano G, Lantieri PB, Celle G. Can the MEGX test and serum bile acids improve the prognostic ability of Child-Pugh's score in liver cirrhosis? *Eur J Gastroenterol Hepatol* 1999; **11**: 559-563
23 **Giannini E**, Botta F, Fumagalli A, Malfatti F, Testa E, Chiarbonello B, Polegato S, Bellotti M, Milazzo S, Borgonovo G, Testa R. Can inclusion of serum creatinine values improve the Child-Turcotte-Pugh score and challenge the prognostic yield of the model for end-stage liver disease score in the short-term prognostic assessment of cirrhotic patients? *Liver Int* 2004; **24**: 465-470
24 **Angermayr B**, Koening F, Cejna M, Karnel F, Gschwantler M, Ferenci P. Creatinine-modified Child-Pugh score (CPSP) compared with MELD-score to predict survival in patients undergoing TIPS. *Hepatology* 2002; **36**: 860A
25 **Papatheodoridis GV**, Cholongitas E, Dimitriadou E, Touloumi G, Sevastianos V, Archimandritis AJ. MELD vs Child-Pugh and creatinine-modified Child-Pugh score for predicting survival in patients with decompensated cirrhosis. *World J Gastroenterol* 2005; **11**: 3099-3104
26 **Malinchoc M**, Kamath PS, Gordon FD, Peine CJ, Rank J, ter Borg PC. A model to predict poor survival in patients undergoing transjugular intrahepatic portosystemic shunts. *Hepatology* 2000; **31**: 864-871
27 **Schepke M**, Roth F, Fimmers R, Brensing KA, Sudhop T, Schild HH, Sauerbruch T. Comparison of MELD, Child-Pugh, and Emory model for the prediction of survival in patients undergoing transjugular intrahepatic portosystemic shunting. *Am J Gastroenterol* 2003; **98**: 1167-1174
28 **Angermayr B**, Cejna M, Karnel F, Gschwantler M, Koenig F, Pidlich J, Mendel H, Pichler L, Wichlas M, Kreil A, Schmid M, Ferlitsch A, Lipinski E, Brunner H, Lammer J, Ferenci P, Gangl A, Peck-Radosavljevic M. Child-Pugh versus MELD score in predicting survival in patients undergoing transjugular intrahepatic portosystemic shunt. *Gut* 2003; **52**: 879-885
29 **Ferral H**, Gamboa P, Postoak DW, Albernaz VS, Young CR, Speeg KV, McMahan CA. Survival after elective transjugular intrahepatic portosystemic shunt creation: prediction with

model for end-stage liver disease score. *Radiology* 2004; **231**: 231-236

30 **Cholongitas E**, Papatheodoridis GV, Vangeli M, Terreni N, Patch D, Burroughs AK. Systematic review: The model for end-stage liver disease--should it replace Child-Pugh's classification for assessing prognosis in cirrhosis? *Aliment Pharmacol Ther* 2005; **22**: 1079-1089

31 **Ginés P**, Quintero E, Arroyo V, Terés J, Bruguera M, Rimola A, Caballería J, Rodés J, Rozman C. Compensated cirrhosis: natural history and prognostic factors. *Hepatology* 1987; **7**: 122-128

32 **Cooper GS**, Bellamy P, Dawson NV, Desbiens N, Fulkerson WJ Jr, Goldman L, Quinn LM, Speroff T, Landefeld CS. A prognostic model for patients with end-stage liver disease. *Gastroenterology* 1997; **113**: 1278-1288

33 **Christensen E**, Schlichting P, Fauerholdt L, Gluud C, Andersen PK, Juhl E, Poulsen H, Tygstrup N. Prognostic value of Child-Turcotte criteria in medically treated cirrhosis. *Hepatology* 1984; **4**: 430-435

34 **Infante-Rivard C**, Esnaola S, Villeneuve JP. Clinical and statistical validity of conventional prognostic factors in predicting short-term survival among cirrhotics. *Hepatology* 1987; **7**: 660-664

35 **Zoli M**, Cordiani MR, Marchesini G, Iervese T, Labate AM, Bonazzi C, Bianchi G, Pisi E. Prognostic indicators in compensated cirrhosis. *Am J Gastroenterol* 1991; **86**: 1508-1513

36 **Salerno F**, Borroni G, Moser P, Badalamenti S, Cassarà L, Maggi A, Fusini M, Cesana B. Survival and prognostic factors of cirrhotic patients with ascites: a study of 134 outpatients. *Am J Gastroenterol* 1993; **88**: 514-519

37 **Runyon BA**. Management of adult patients with ascites due to cirrhosis. *Hepatology* 2004; **39**: 841-856

38 **Cholongitas E**, Marelli L, Shusang V, Senzolo M, Rolles K, Patch D, Burroughs AK. A systematic review of the performance of the model for end-stage liver disease (MELD) in the setting of liver transplantation. *Liver Transpl* 2006; **12**: 1049-1061

39 **Said A**, Williams J, Holden J, Remington P, Gangnon R, Musat A, Lucey MR. Model for end stage liver disease score predicts mortality across a broad spectrum of liver disease. *J Hepatol* 2004; **40**: 897-903

40 **Huo TI**, Wu JC, Lin HC, Lee FY, Hou MC, Lee PC, Chang FY, Lee SD. Evaluation of the increase in model for end-stage liver disease (DeltaMELD) score over time as a prognostic predictor in patients with advanced cirrhosis: risk factor analysis and comparison with initial MELD and Child-Turcotte-Pugh score. *J Hepatol* 2005; **42**: 826-832

41 **Cholongitas E**, Marelli L, Kerry A, Senzolo M, Goodier DW, Nair D, Thomas M, Patch D, Burroughs AK. Different methods of creatinine measurement significantly affect MELD scores. *Liver Transpl* 2007; **13**: 523-529

42 **Trotter JF**, Brimhall B, Arjal R, Phillips C. Specific laboratory methodologies achieve higher model for endstage liver disease (MELD) scores for patients listed for liver transplantation. *Liver Transpl* 2004; **10**: 995-1000

S- Editor Li LF **L- Editor** Cant MR **E- Editor** Yin DH

Online Submissions: wjg.wjgnet.com
wjg@wjgnet.com
doi:10.3748/wjg.15.2778

World J Gastroenterol 2009 June 14; 15(22): 2778-2781
World Journal of Gastroenterology ISSN 1007-9327

BRIEF ARTICLES

Association of hepatitis C virus infection and diabetes in central Tunisia

Naoufel Kaabia, Elhem Ben Jazia, Ines Slim, Imen Fodha, Wissem Hachfi, Rafika Gaha, Mabrouk Khalifa, Aoutef Hadj Kilani, Halim Trabelsi, Ahmed Abdelaziz, Fethi Bahri, Amel Letaief

Naoufel Kaabia, Elhem Ben Jazia, Ines Slim, Wissem Hachfi, Mabrouk Khalifa, Fethi Bahri, Amel Letaief, Department of Internal Medicine and Infectious Disease, Unit of Research: 04/UR/08-21, University Hospital Farhat Hached, Sousse 4000, Tunisia
Imen Fodha, Halim Trabelsi, Microbiology Unit, University Hospital Sahloul, Sousse 4000, Tunisia
Rafika Gaha, Ahmed Abdelaziz, Epidemiology Unit, University Hospital Farhat Hached, Sousse 4000, Tunisia
Aoutef Hadj Kilani, Department of Medicine, Msaken hospital, Sousse 4000, Tunisia
Author contributions: Kaabia N, Ben Jazia E and Slim I contributed equally to this work; Hachfi W, Khalifa M, Hadj Kilani A, Bahri F and Letaief A designed the research; Fodha I and Trabelsi H performed microbiological assessment; Gaha R and Abdelaziz A analyzed statistical data.
Supported by Roch laboratory
Correspondence to: Dr. Elhem Ben Jazia, Department of Internal Medicine and Infectious Diseases, Unit of Research: 04/UR/08-21, University Hospital Farhat Hached, Sousse 4000, Tunisia. elhem.benjazia@rns.tn
Telephone: +216-73-211183 Fax: +216-73-211183
Received: November 21, 2008 Revised: April 29, 2009
Accepted: May 6, 2009
Published online: June 14, 2009

Abstract

AIM: To investigate hepatitis C virus (HCV) seroprevalence in Tunisian patients with diabetes mellitus and in a control group.

METHODS: A cross-sectional study was conducted to determine the HCV seroprevalence in 1269 patients with diabetes (452 male, 817 female) and 1315 non-diabetic patients, attending health centers in Sousse, Tunisia. HCV screening was performed in both groups using a fourth-generation enzyme immunoassay.

RESULTS: In the diabetic group, 17 (1.3%) were found to be HCV-infected compared with eight (0.6%) in the control group, although the difference was not significant (P = 0.057). Quantitative PCR was performed in 20 patients. Eleven patients were positive and showed HCV genotype 1b in all cases.

CONCLUSION: Frequency of HCV antibodies was low in patients with diabetes and in the control group in central Tunisia, with no significant difference between the groups.

Key words: Hepatitis C virus; Diabetes mellitus; Tunisia; Epidemiology; Autoantibodies; Hepatitis

Peer reviewer: Eva Herrmann, Professor, Department of Internal Medicine, Biomathematics, Saarland University, Faculty of Medicine, Kirrberger Str., 66421 Homburg/Saar, Germany

Kaabia N, Ben Jazia E, Slim I, Fodha I, Hachfi W, Gaha R, Khalifa M, Hadj Kilani A, Trabelsi H, Abdelaziz A, Bahri F, Letaief A. Association of hepatitis C virus infection and diabetes in central Tunisia. *World J Gastroenterol* 2009; 15(22): 2778-2781 Available from: URL: http://www.wjgnet.com/1007-9327/15/2778.asp DOI: http://dx.doi.org/10.3748/wjg.15.2778

INTRODUCTION

In recent years, a positive association between hepatitis C virus (HCV) infection and diabetes mellitus (DM) had been reported in a number of clinical studies[1-4]. It is now clear that hepatitis C conveys a risk for developing DM, in particular type 2[5-7]. Moreover, several studies have found a high prevalence of anti-HCV antibodies among patients with diabetes, especially those with type 2 DM[8-13]; however, some authors have not observed an association between HCV infection and diabetes[14-16]. Since effective therapy has become available for HCV, it may be worthwhile to determine virus prevalence in patients with and without diabetes, in order to decide whether a programme for screening should also focus on type 2 diabetes. The aim of the present study was to investigate HCV seroprevalence in Tunisian patients with DM and in a control group.

MATERIALS AND METHODS

Patients

During March 2003, we conducted a cross-sectional study of all consecutive patients with diabetes aged > 16 years who were attending the Departments of Internal Medicine, Infectious Diseases and Endocrinology of Farhat Hached Hospital, and primary health care centers in the region of Sousse, Tunisia. Sample size calculation was

based on a 2% HCV seroprevalence estimation with an 80% precision rate and a 95% confidence level. The formula for sample size determination yielded a total of 1223 patients with diabetes. Types 1 and 2 diabetes were defined on the basis of a history of therapy with oral hypoglycemic agents or insulin at the date of inclusion. Patients older than 40 years of age, and treated by oral hypoglycemic agents or switched from insulin were considered to have type 2 diabetes. A control group of non-diabetic patients were recruited from the same centers at the same time. Patients who had corticosteroid-induced diabetes were excluded. Informed consent was obtained from all participants, and the study was approved by Farhat Hached Hospital ethics committee.

Data collection

Data were recorded by using a questionnaire that collected information on demographic and clinical features of DM and risk factors for HCV infection. Blood samples were collected from all patients for HCV serology. Those who were positive for anti-HCV antibodies were called, and liver function tests, glucose blood level, HCV quantitative RNA and HCV genotyping were performed.

Laboratory methods

Serological testing for anti-HCV antibodies was performed by using a fourth-generation ELISA (Murex; Abbot Laboratories, France) according to the manufacturer's instructions. HCV RNA qualitative and quantitative testing (Amplicor; Roche Molecular Systems, Branchburg, NJ, USA) and HVC genotyping were performed at Pasteur Cerba Laboratoire, Cergy Pontoise, France). HVC genotyping was performed by RT-PCR on a segment from the core region and by hybridization of this fragment with oligonucleotide-specific probes. The assay was designed to recognize the 1a, 1b, 2a, 2b, 3, 4, 5 and 6 HCV genotypes.

Statistical analysis

Data were analyzed, using SPSS version 13.0 software (Chicago, IL, USA). A descriptive analysis was followed by bivariate analysis using the χ^2 test for comparison of the two groups, with a 5% statistical significance level. A multivariate analysis with logistic regression was used to determine predictive variables associated with seroprevalence among the significant factors found by bivariate analysis. ORs and 95% CI were calculated for these variables.

RESULTS

Our study included 1269 patients with diabetes and 1315 non-diabetic patients. In patients with diabetes, 1148 (90.5%) and 121 (9.5%) had type 2 and type 1 DM respectively; 284 (22.5%) were treated by insulin. The mean duration of DM was 8.4 years (1-35 years). Furthermore, history of surgery and hospitalization, and scarification were found to be more frequent in patients with diabetes. Patients in the control group were much younger than those with diabetes; the main demographic and clinical characteristics of both groups are shown in Table 1.

Table 1 Epidemiological features of the study population in patients with diabetes and control group *n* (%)

	Diabetes patients (*n* = 1269)	Control group (*n* = 1315)	*P*
Gender			
Female	817 (64.4)	890 (67.6)	0.06
Age			
Mean age (yr)	55.6	46.9	$< 10^{-3}$
Risk factors of HCV			
Transfusion	157 (12.5)	185 (14.2)	0.2
History of surgery	592 (46.8)	551 (42.1)	0.01
Drug addiction	2 (0.2)	7 (0.5)	0.17
Scarification	247 (19.8)	301 (23.1)	0.04
Endoscopic investigation	276 (21.9)	308(23.6)	0.30
Alcoholism	164 (13)	178 (13.6)	0.65
History of hospitalization	875 (69.3)	785 (59.9)	$< 10^{-3}$
Anti-HCV antibodies (+)	17 (1.3)	8 (0.6)	0.057

Table 2 Epidemiological features of the study population in type 2 DM patients and control group *n* (%)

	Type 2 DM patients (*n* = 1148)	Control group (*n* = 1315)	OR	*P*
Gender				
Female	739 (65.2)	890 (67.6)	0.8 (0.73-1.2)	0.06
Age				
Mean age (yr)	57 ± 10.4	46.9		$< 10^{-3}$
Risk factors of HCV				
Transfusion	136 (12.1)	185 (14.2)	0.83 (0.65-1.06)	0.2
History of surgery	528 (46.7)	551 (42.1)	1.18 (1.05-1.39)	0.01
Drug addiction	2 (0.2)	7 (0.5)	0.33 (0.05-1.78)	0.17
Scarification	222 (19.8)	301 (23.1)	0.81 (0.66-0.99)	0.04
Endoscopic investigation	248 (22)	308 (23.6)	0.90 (0.74-1.09)	0.30
Alcoholism	144 (12.8)	178 (13.6)	0.92 (0.78-1.17)	0.65
History of hospitalization	758 (67.1)	785 (59.9)	1.31 (1.11-1.55)	$< 10^{-3}$
Anti-HCV antibodies (+)	16 (1.4)	8 (0.6)	2.31 (1.01-5.90)	0.04

Antibodies against HCV were detected in 25 patients (1%) among the entire population studied (both diabetic and non-diabetic groups). In the diabetes group, 17 (1.3%) were found to be infected with HCV compared with eight (0.6%) control patients. No significant difference was found between DM patients and the control group ($P = 0.057$) (Table 1). Moreover, anti-HCV seropositivity was detected in 16 (1.4%) of the type 2 DM sub-group, which was significantly higher than that in the control group ($P = 0.04$) (Table 2). However, in multivariate analysis, this difference between seroprevalence of HCV in type2 DM and controls was not confirmed.

Quantitative PCR was performed in 20 patients: 13 with diabetes and seven without, was and a positive result

was obtained in eight and three patients, respectively. All patients were infected by genotype 1b HCV. All non-diabetic patients who were positive for HCV antibodies underwent liver function and blood glucose testing, but no new DM was discovered.

DISCUSSION

To the best of our knowledge, this is the first study in which HCV infection prevalence was evaluated in Tunisian patients with diabetes. Similar to blood donors in whom anti-HCV antibodies were low (0.5%-1.8%)[17-21], in our study HCV infection prevalence in the diabetes, type 2 DM, and control groups was 1.3%, 1.4% and 0.6%, respectively. Despite a high frequency of scarification, history of surgery and hospitalization in patients with diabetes and the type 2 DM subgroup, circumstances which increase risk of HCV infection, prevalence of anti-HCV antibodies was not significantly more frequent in the diabetes group ($P = 0.057$). Moreover, comparing type 2 DM patients to the control group, although a significant difference in HCV infection prevalence was observed in type 2 DM patients ($P = 0.04$), this was not confirmed by logistic regression analysis. Therefore, we cannot establish the diabetic population as a group at high risk for HCV infection. Our findings did not confirm other studies that have reported increased HCV seroprevalence in patients with diabetes[10,22-26]. In a case-control study conducted in the USA, 4.2% of 594 patients in a cohort with diabetes were found to be infected with HCV compared with 1.6% of control patients (377 patients with thyroid diseases)[27]. Other studies have reported an increased HCV seroprevalence, varying from 8% to 11% in European diabetic populations compared with 1%-2% HCV seroprevalence in the general population[10,28-30]. However, in a descriptive Greek study of patients with diabetes without a control group, HCV antibodies were detected in only seven cases, and this prevalence (1.65%) was similar to that in the general population[14].

In conclusion, our study confirms a low prevalence of anti-HCV antibodies in Tunisian patients with diabetes, and may argue against diabetes as a risk factor of HCV infection in this area. Further studies, possibly multicenter, prospective and case-control, are needed to establish the temporal relationship between HCV infection and DM.

COMMENTS

Background

Several studies have found a high prevalence of anti-hepatitis C virus (HCV) antibodies among patients with diabetes mellitus (DM), especially those with type 2 DM. However, some authors have not observed an association between HCV infection and diabetes. Since effective therapy has become available for HCV, it may be worthwhile to determine the prevalence of HCV in patients with and without diabetes, to decide whether a programme for screening should also focus on type 2 diabetes patients.

Research frontiers

The literature is still contradictory about high prevalence of HCV infection in type 2 DM. The prevalence of HCV infection is still unknown in Tunisia. In this study, the authors demonstrated that this prevalence was similar in the general population.

Innovations and breakthroughs

The study confirmed a low prevalence of anti-HCV antibodies in Tunisian patients with diabetes, and may disprove diabetes as a risk factor for HCV infection in this area.

Applications

The low prevalence of HCV infection in type 2 DM in this study argues against the systematic assessment of HCV antibodies in this population.

Peer review

The present manuscript describes a comparative analysis of HCV prevalence in diabetic and non-diabetic populations in central Tunisia. Although its findings are negative, they are interesting because of the relatively large sample size. This is an interesting small epidemiological study on the association between diabetes and HCV prevalence in central Tunisia.

REFERENCES

1 **Allison ME**, Wreghitt T, Palmer CR, Alexander GJ. Evidence for a link between hepatitis C virus infection and diabetes mellitus in a cirrhotic population. *J Hepatol* 1994; **21**: 1135-1139

2 **Fraser GM**, Harman I, Meller N, Niv Y, Porath A. Diabetes mellitus is associated with chronic hepatitis C but not chronic hepatitis B infection. *Isr J Med Sci* 1996; **32**: 526-530

3 **Tolman KG**, Fonseca V, Tan MH, Dalpiaz A. Narrative review: hepatobiliary disease in type 2 diabetes mellitus. *Ann Intern Med* 2004; **141**: 946-956

4 **Hadziyannis S**, Karamanos B. Diabetes mellitus and chronic hepatitis C virus infection. *Hepatology* 1999; **29**: 604-605

5 **Mehta SH**, Brancati FL, Sulkowski MS, Strathdee SA, Szklo M, Thomas DL. Prevalence of type 2 diabetes mellitus among persons with hepatitis C virus infection in the United States. *Ann Intern Med* 2000; **133**: 592-599

6 **Beymer CH**, Boyko EJ, Dominitz JA. The association of diabetes mellitus with hepatitis C virus infection in a seroprevalence survey of the general U.S. population 1988 to 1994 [Abstract]. *Hepatology* 2000; **32**: 313A

7 **Noto H**, Raskin P. Hepatitis C infection and diabetes. *J Diabetes Complications* 2006; **20**: 113-120

8 **Ozyilkan E**, Erbaş T, Simşek H, Telatar F, Kayhan B, Telatar H. Increased prevalence of hepatitis C virus antibodies in patients with diabetes mellitus. *J Intern Med* 1994; **235**: 283-284

9 **Caronia S**, Taylor K, Pagliaro L, Carr C, Palazzo U, Petrik J, O'Rahilly S, Shore S, Tom BD, Alexander GJ. Further evidence for an association between non-insulin-dependent diabetes mellitus and chronic hepatitis C virus infection. *Hepatology* 1999; **30**: 1059-1063

10 **Lonardo A**, Adinolfi LE, Loria P, Carulli N, Ruggiero G, Day CP. Steatosis and hepatitis C virus: mechanisms and significance for hepatic and extrahepatic disease. *Gastroenterology* 2004; **126**: 586-597

11 **Gray H**, Wreghitt T, Stratton IM, Alexander GJ, Turner RC, O'Rahilly S. High prevalence of hepatitis C infection in Afro-Caribbean patients with type 2 diabetes and abnormal liver function tests. *Diabet Med* 1995; **12**: 244-249

12 **Grimbert S**, Valensi P, Lévy-Marchal C, Perret G, Richardet JP, Raffoux C, Trinchet JC, Beaugrand M. High prevalence of diabetes mellitus in patients with chronic hepatitis C. A case-control study. *Gastroenterol Clin Biol* 1996; **20**: 544-548

13 **Ozyilkan E**, Arslan M. Increased prevalence of diabetes mellitus in patients with chronic hepatitis C virus infection. *Am J Gastroenterol* 1996; **91**: 1480-1481

14 **Sotiropoulos A**, Peppas TA, Skliros E, Apostolou O, Kotsini V, Pappas SI. Low prevalence of hepatitis C virus infection in Greek diabetic patients. *Diabet Med* 1999; **16**: 250-252

15 **Skliros EA**, Sotiropoulos A, Lionis C, Tassopoulos NC. Hepatitis B and C virus infection in patients with high serum transaminases. *Postgrad Med J* 1998; **74**: 511

16 **Mangia A**, Schiavone G, Lezzi G, Marmo R, Bruno F, Villani MR, Cascavilla I, Fantasia L, Andriulli A. HCV and diabetes mellitus: evidence for a negative association. *Am J Gastroenterol* 1998; **93**: 2363-2367
17 **Hatira SA**, Yacoub-Jemni S, Houissa B, Kaabi H, Zaeir M, Kortas M, Ghachem L. [Hepatitis C virus antibodies in 34130 blood donors in Tunisian Sahel] *Tunis Med* 2000; **78**: 101-105
18 **Triki H**, Said N, Ben Salah A, Arrouji A, Ben Ahmed F, Bouguerra A, Hmida S, Dhahri R, Dellagi K. Seroepidemiology of hepatitis B, C and delta viruses in Tunisia. *Trans R Soc Trop Med Hyg* 1997; **91**: 11-14
19 **Ben Alaya Bouafif N**, Triki H, Mejri S, Bahri O, Chlif S, Bettaib J, Héchmi S, Dellagi K, Ben Salah A. A case control study to assess risk factors for hepatitis C among a general population in a highly endemic area of northwest Tunisia. *Arch Inst Pasteur Tunis* 2007; **84**: 21-27
20 **Triki H**. [Epidemiology of hepatitis B virus, hepatitis C virus and Delta virus in the general population and in liver cirrhosis in Tunisia] *Arch Inst Pasteur Tunis* 1994; **71**: 403-406
21 **Sassi F**, Gorgi Y, Ayed K, Abdallah TB, Lamouchi A, Maiz HB. Hepatitis C virus antibodies in dialysis patients in Tunisia: a single center study. *Saudi J Kidney Dis Transpl* 2000; **11**: 218-222
22 **Chen HF**, Li CY, Chen P, See TT, Lee HY. Seroprevalence of hepatitis B and C in type 2 diabetic patients. *J Chin Med Assoc* 2006; **69**: 146-152
23 **Duong M**, Petit JM, Piroth L, Grappin M, Buisson M, Chavanet P, Hillon P, Portier H. Association between insulin resistance and hepatitis C virus chronic infection in HIV-hepatitis C virus-coinfected patients undergoing antiretroviral therapy. *J Acquir Immune Defic Syndr* 2001; **27**: 245-250
24 **Wilson C**. Hepatitis C infection and type 2 diabetes in American-Indian women. *Diabetes Care* 2004; **27**: 2116-2119
25 **Lecube A**, Hernández C, Genescà J, Esteban JI, Jardí R, Simó R. High prevalence of glucose abnormalities in patients with hepatitis C virus infection: a multivariate analysis considering the liver injury. *Diabetes Care* 2004; **27**: 1171-1175
26 **Soule JL**, Olyaei AJ, Boslaugh TA, Busch AM, Schwartz JM, Morehouse SH, Ham JM, Orloff SL. Hepatitis C infection increases the risk of new-onset diabetes after transplantation in liver allograft recipients. *Am J Surg* 2005; **189**: 552-557; discussion 557
27 **Mason AL**, Lau JY, Hoang N, Qian K, Alexander GJ, Xu L, Guo L, Jacob S, Regenstein FG, Zimmerman R, Everhart JE, Wasserfall C, Maclaren NK, Perrillo RP. Association of diabetes mellitus and chronic hepatitis C virus infection. *Hepatology* 1999; **29**: 328-333
28 **Simó R**, Hernández C, Genescà J, Jardí R, Mesa J. High prevalence of hepatitis C virus infection in diabetic patients. *Diabetes Care* 1996; **19**: 998-1000
29 **Antonelli A**, Ferri C, Fallahi P, Pampana A, Ferrari SM, Goglia F, Ferrannini E. Hepatitis C virus infection: evidence for an association with type 2 diabetes. *Diabetes Care* 2005; **28**: 2548-2550
30 **Skowroński M**, Zozulińska D, Juszczyk J, Wierusz-Wysocka B. Hepatitis C virus infection: evidence for an association with type 2 diabetes. *Diabetes Care* 2006; **29**: 750; author reply 751

S- Editor Tian L **L- Editor** Kerr C **E- Editor** Zheng XM

Online Submissions: wjg.wjgnet.com
wjg@wjgnet.com
doi:10.3748/wjg.15.2782

World J Gastroenterol 2009 June 14; 15(22): 2782-2786
World Journal of Gastroenterology ISSN 1007-9327

BRIEF ARTICLES

A dose-up of ursodeoxycholic acid decreases transaminases in hepatitis C patients

Shuichi Sato, Tatsuya Miyake, Hiroshi Tobita, Naoki Oshima, Junichi Ishine, Takuya Hanaoka, Yuji Amano, Yoshikazu Kinoshita

Shuichi Sato, Tatsuya Miyake, Hiroshi Tobita, Naoki Oshima, Junichi Ishine, Takuya Hanaoka, Yoshikazu Kinoshita, Department of Gastroenterology and Hepatology, Shimane University, School of Medicine, Izumo 693-8501, Japan
Yuji Amano, Division of Gastrointestinal Endoscopy, Shimane University Hospital, Izumo 693-8501, Japan
Author contributions: Sato S, Miyake T, Tobita H, Oshima N, Ishine J, Hanaoka T, Amano Y, and Kinoshita Y performed the majority of experiments and were also involved in editing the manuscript.
Correspondence to: Shuichi Sato, MD, PhD, Department of Gastroenterology and Hepatology, Shimane University, School of Medicine, 89-1, Enya-cho, Izumo, Shimane, Japan. bbsato@med.shimane-u.ac.jp
Telephone: +81-853-202190 Fax: +81-853-202187
Received: February 23, 2009 Revised: May 11, 2009
Accepted: May 18, 2009
Published online: June 14, 2009

Abstract

AIM: To examine whether a dose-up to 900 mg of ursodeoxycholic acid (UDCA) decreases transaminases in hepatitis C patients.

METHODS: From January to December 2007, patients with chronic hepatitis C or compensated liver cirrhosis with hepatitis C virus (HCV) (43-80 years old) showing positive serum HCV-RNA who had already taken 600 mg/d of UDCA were recruited into this study. Blood parameters were examined at 4, 8 and 24 wk after increasing the dose of oral UDCA from 600 to 900 mg/d.

RESULTS: Serum alanine aminotransferase (ALT), aspartate aminotransferase (AST), and gamma-glutamyl transpeptidase (GGT) levels were significantly decreased following the administration of 900 mg/d as compared to 600 mg/d. The decrease in ALT from immediately before the dose-up of UDCA to 8 wk after the dose-up was 14.3 IU/L, while that for AST was 10.5 IU/L and for GGT was 9.8 IU/L. Platelet count tended to increase after the dose-up of UDCA, although it did not show a statistically significant level (P = 0.05). Minor adverse events were observed in 3 cases, although no drop-outs from the study occurred.

CONCLUSION: Oral administration of 900 mg/d of UDCA was more effective than 600 mg/d for reducing ALT, AST, and GGT levels in patients with HCV-related chronic liver disease.

Key words: Chronic hepatitis; Hepatitis C virus; Liver fibrosis; Transaminase; Ursodeoxycholic acid

Peer reviewer: Paul Y Kwo, Professor, Gastroenterology and Hepatology Division, Indiana University School of Medicine, 975 West Walnut, IB 327, Indianapolis, Indiana 46202-5121, United States

Sato S, Miyake T, Tobita H, Oshima N, Ishine J, Hanaoka T, Amano Y, Kinoshita Y. A dose-up of ursodeoxycholic acid decreases transaminases in hepatitis C patients. *World J Gastroenterol* 2009; 15(22): 2782-2786 Available from: URL: http://www.wjgnet.com/1007-9327/15/2782.asp DOI: http://dx.doi.org/10.3748/wjg.15.2782

INTRODUCTION

Current treatment for chronic hepatitis C virus (HCV) infection is based on the administration of pegylated interferon (IFN) alone or in combination with other anti-viral agents such as ribavirin or protease inhibitors. However, these treatments are not completely effective in all patients with HCV genotype 1 and high viral load or in patients with liver cirrhosis[1-4]. Ursodeoxycholic acid (UDCA) was identified in 1902 from polar bear bile by Hammarsten and was isolated and crystallized by Shoda[5]. UDCA is used worldwide for the treatment of primary biliary cirrhosis (PBC) and chronic liver diseases[6-14]. Up to 2006, a dose of 150 mg/d of UDCA was approved as the standard treatment for hepatic protection in patients with chronic viral hepatitis by the public health insurance agency of Japan. However, this dosage is not effective for the treatment of chronic hepatitis[15]. A randomized, controlled-dose study of UDCA for chronic hepatitis C (CH-C) patients reported that UDCA administered at a dose of 600 or 900 mg/d resulted in greater decreases in the serum levels of alanine aminotransferase (ALT), aspartate aminotransferase (AST), and gamma-glutamyl

transpeptidase (GGT) compared to 150 mg/d, which was the dose recommended by the Japanese national health insurance policy at that time; however, the results with doses of 600 mg/d or 900 mg/d were similar. In contrast, 600 mg of UDCA, which is the maximum administration dose in PBC or other biliary system diseases such as gallstones, was used ambiguously in CH-C patients[16].

To determine the effect of 900 mg/d of UDCA for CH-C, the present study was conducted primarily as a dose-up trial from 600 mg/d to 900 mg/d in hepatitis C patients, with changes in ALT levels as the primary endpoint.

MATERIALS AND METHODS

Patients

From January to December in 2007, patients with CH-C or compensated liver cirrhosis with HCV (mean age 65.8, range 43 to 80 years) who tested positive for serum HCV-RNA were recruited into this study. All the enrolled patients had already received 600 mg/d of UDCA, and showed over 40 IU/L of ALT at the two points in the 4 wk prior to dose-up of UDCA. Patients were excluded from the study if they had received antiviral treatment with interferon with or without ribavirin or anticancer treatment for hepatocellular carcinoma (HCC). Patients with other malignancies diagnosed within 24 wk before the observation period or patients treated with corticosteroids and/or immunosuppressive drugs were also excluded. Patients with decompensated cirrhosis, hepatitis B, autoimmune liver disease, alcoholic or drug-induced liver injury, malignant tumors and biliary disorders were excluded. Patients receiving intravenous glycyrrhizin were enrolled in this study. However, when the dose or frequency of administration of glycyrrhizin was changed, this was defined as the study endpoint. Written informed consent was obtained from each patient before enrollment into the study.

Methods

After the 4-wk observation period, the dose of UDCA (Urso®, Mitsubishi Tanabe Pharma Corp., Osaka, Japan) was increased from 600 mg/d to 900 mg/d. Serum ALT was measured as a primary endpoint of liver function, and AST and GGT as secondary endpoints, using conventional methods. Blood samples were taken at the start of the observation period, at 0, 4, 8 and 24 wk after initiation of treatment, and at the final observation period. Serum concentrations of ALT, AST, GGT, albumin, total bilirubin and platelet counts were measured. CT and ultrasonography for HCC screening was carried out every 12 wk or 24 wk. Compliance with UDCA administration and adverse effects were determined by patient interview or confirmation of drug diaries.

Statistical analysis

Changes in AST, ALT, GGT, total bilirubin, albumin, and platelet count were analyzed by paired Student's *t*-test. $P < 0.05$ was considered significant.

Table 1 Patient characteristics before beginning the study (mean ± SE)

	Total (n = 32)
Mean age (range)	65.8 ± 2.6 (43-80)
Gender (male)	18 (56)
Liver cirrhosis (%)	7 (22)
Controlled hepatocellular carcinoma (%)	4 (12)
Glycyrrhizin administration (%)	6 (19)
AST (IU/L)	66.5 ± 4.1
ALT (IU/L)	57.1 ± 3.4
GGT (IU/L)	44.2 ± 2.1
Total bilirubin (mg/dL)	0.76 ± 0.5
Serum albumin (g/dL)	4.0 ± 0.1
Platelet count (× 1000/μL)	14.5 ± 1.0
HCVRNA (KIU/mL)	1309 ± 469
HCV genotype (1b/non 1b/not decided)	24/6/2

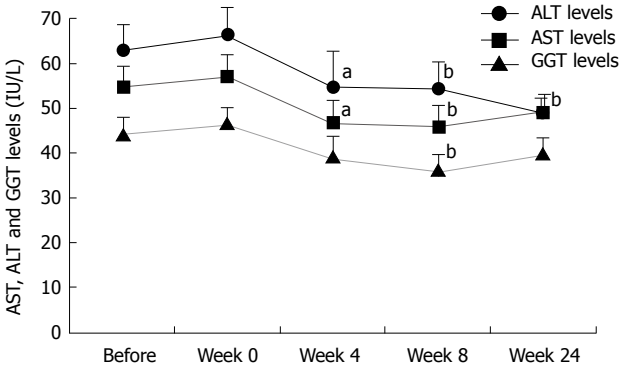

Figure 1 Changes in serum alanine aminotransferase (ALT) levels, serum aspartate aminotransferase (AST) levels and serum gamma-glutamyl transpeptidase (GGT) levels in patients before and during dose-up to 900 mg/d. Data are expressed as mean ± SD. $^aP < 0.05$, $^bP < 0.01$; paired *t*-test compared to week 0 in each parameter.

RESULTS

We enrolled 32 patients to this study. Patient characteristics are described in Table 1. In seven patients with liver cirrhosis, five patients were estimated as Child A and the others as Child B. Three patients with a history of HCC had been clinically diagnosed by dynamic computed tomography as having a complete response to trans-catheter arterial embolization and/or percutaneous radiofrequency ablation 24 wk or more before the start of the observation period. Compliance rate with UDCA administration was over 95%.

Changes in AST, ALT and GGT by dose-up of UDCA

Serum ALT, AST and GGT levels before and after the start of 900 mg of UDCA are shown in Figure 1. Serum ALT, AST and GGT levels were significantly decreased at 4, 8 and 24 wk after dose-up to 900 mg/d. The decrease (decreasing rate, %) in ALT levels before and 8 wk after dose-up to 900 mg of UDCA was 14.3 IU/L (22.1%) as shown in Figure 1. The decrease in AST and GGT were 10.5 IU/L (19.1%), and 9.8 IU/L (22.1%), respectively (Figure 1).

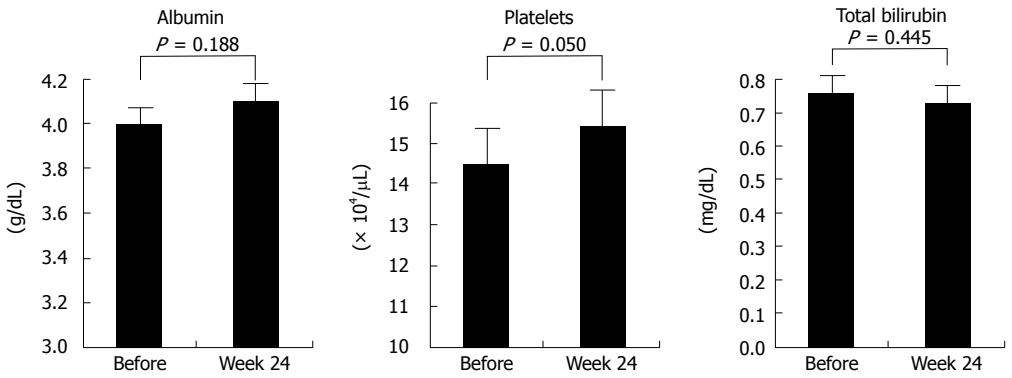

Figure 2 Changes in serum albumin, platelet count, and total bilirubin levels in chronic hepatitis C patients before and 24 wk after beginning the dose-up to 900 mg/d.

Changes in serum concentrations of albumin, total bilirubin and platelet count

Serum albumin level changed from 4.0 g/dL to 4.1 g/dL at 24 wk after the dose-up of UDCA. Platelet count changed from 145 000 to 154 000/μL, and total bilirubin changed from 0.76 to 0.73 mg/dL, although the difference did not reach a statistically significant level (P = 0.05, Figure 2). Serum HCV-RNA level did not change during the study period.

Safety

The number of adverse events during the administration of 900 mg UDCA, totaled three (9.4%), mild diarrhea in two patients and mouth discomfort in one patient. None of these adverse events influenced compliance with UDCA. Although HCC recurrence was detected in one patient at just 24 wk after dose-up of UDCA, this lesion was completely treated with percutaneous radiofrequency ablation.

DISCUSSION

The results of this study revealed that the dose-up trial of UDCA from 600 mg/d to 900 mg/d improved biochemical markers such as serum AST, ALT and GGT as early as the first or second dose-up week and continued to improve biochemical markers up to 24 wk after dose-up of UDCA was initiated. In addition, platelet count tended to increase following this dose-up therapy. These results suggested that 900 mg of UDCA can improve liver function tests in patients with chronic hepatitis C who have already received 600 mg of UDCA. In this study, the frequency of adverse events was lower than those in previous reports[15-18]. A possible reason for this is that patients enrolled in this study were not naïve to UDCA and may have quickly gotten used to the administration of UDCA.

In the natural course of CH-C, patients with normal serum aminotransferase levels show a slow fibrosis progression and a low incidence of HCC. Rino *et al*[19] demonstrated that the mode of reduction therapy and ALT levels were the most important factors, by multivariate analysis, to affect HCC development in patients with HCV-related cirrhosis of Child A classification followed for over 10 years. In addition, a previous study of postoperative patients with HCC found that recurrence was more frequent among patients with high serum ALT levels over 80 IU/L[20]. Moreover, using multivariate analysis in the Inhibition of Hepatocarcinogenesis by Interferon Therapy (IHIT) study, the risk of HCC after interferon treatment without virological response was strongly influenced by ALT levels, and the odds ratio of HCC in sustained virological responders was the same as that in sustained biochemical responders[21]. Therefore, high dose UDCA possibly reduced the occurrence and recurrence of HCC through the reduction of serum ALT level.

The anti-inflammatory mechanism of UDCA was considered to cause a reduction in the cytotoxicity of hydrophobic bile acids, stimulation of hepatobiliary secretion, suppression of NF-kB-dependent transcription by binding to the glucocorticoid receptor, and a decrease in proinflammatory cytokine-induced transcription of phospholipase A2[22-28].

The long-term effects of UDCA therapy in CH-C patients have not been fully elucidated[29]. Changes in liver histology following UDCA administration may not be clear from short-term observation periods. In this study, the dose-up treatment with 900 mg/d UDCA for 24 wk tended to increase serum platelet counts. In patients with hepatitis C virus-related chronic liver diseases, platelet counts reflect histological findings. When the platelet count is low in the patient, progression of liver fibrosis is suggested[30-33]. It is necessary to show histologically the morphological hepatic tissue changes in future studies.

In conclusion, oral administration of high dose 900 mg UDCA, despite the absence of an anti-viral effect, shows beneficial effects in reducing the activity of chronic hepatitis or cirrhosis.

COMMENTS

Background

Administration of pegylated interferon alone or in combination with anti-viral agents has improved the treatment for chronic hepatitis C, but is not very effective in some patients-especially those with hepatitis C virus (HCV) genotype 1 and high viral load or liver cirrhosis. Such patients may benefit from therapies which reduce liver inflammation and fibrosis.

Research frontiers

Researchers assessed the effect of ursodeoxycholic acid (UDCA) on serum liver enzyme levels in patients with chronic hepatitis C or compensated liver cirrhosis with HCV. Serum alanine aminotransferase (ALT), aspartate aminotransferase (AST), and gamma-glutamyl transpeptidase (GGT) levels were significantly decreased with 900 mg/d compared with 600 mg/d.

Innovations and breakthroughs

Increasing the oral UDCA dose to 900 mg/d was effective in reducing ALT, AST, and GGT levels. Adverse effects were reported in 3 cases (9.4%), but none of these adverse effects influenced UDCA compliance.

Applications

The study results suggest that patients with HCV genotype 1 and high viral load or liver cirrhosis may benefit from oral UDCA therapy.

Peer review

This manuscript demonstrates that raising the UDCA dose from 600 mg/d to 900 mg/d improves liver chemistries including AST, ALT, and GGT over a 6 mo period. The authors then suggest that this may lead to suppression of fibrosis in a HCV population. Also, this research suggests that UDCA is safe at this dose. This is novel in a Japanese HCV cohort and the methods are quite straightforward. While not particularly novel, it does suggest that higher dose UDCA can improve liver chemistries.

REFERENCES

1 **Sarrazin C**, Rouzier R, Wagner F, Forestier N, Larrey D, Gupta SK, Hussain M, Shah A, Cutler D, Zhang J, Zeuzem S. SCH 503034, a novel hepatitis C virus protease inhibitor, plus pegylated interferon alpha-2b for genotype 1 nonresponders. *Gastroenterology* 2007; **132**: 1270-1278

2 **Hadziyannis SJ**, Sette H Jr, Morgan TR, Balan V, Diago M, Marcellin P, Ramadori G, Bodenheimer H Jr, Bernstein D, Rizzetto M, Zeuzem S, Pockros PJ, Lin A, Ackrill AM. Peginterferon-alpha2a and ribavirin combination therapy in chronic hepatitis C: a randomized study of treatment duration and ribavirin dose. *Ann Intern Med* 2004; **140**: 346-355

3 **Kieffer TL**, Sarrazin C, Miller JS, Welker MW, Forestier N, Reesink HW, Kwong AD, Zeuzem S. Telaprevir and pegylated interferon-alpha-2a inhibit wild-type and resistant genotype 1 hepatitis C virus replication in patients. *Hepatology* 2007; **46**: 631-639

4 **Poynard T**, McHutchison J, Manns M, Trepo C, Lindsay K, Goodman Z, Ling MH, Albrecht J. Impact of pegylated interferon alfa-2b and ribavirin on liver fibrosis in patients with chronic hepatitis C. *Gastroenterology* 2002; **122**: 1303-1313

5 **Poupon R**, Serfaty L. Ursodeoxycholic acid in chronic hepatitis C. *Gut* 2007; **56**: 1652-1653

6 **Bateson MC**, Ross PE, Diffey BL. Ursodeoxycholic acid in primary biliary cirrhosis. *Lancet* 1989; **1**: 898-899

7 **Oka H**, Toda G, Ikeda Y, Hashimoto N, Hasumura Y, Kamimura T, Ohta Y, Tsuji T, Hattori N, Namihisa T. A multi-center double-blind controlled trial of ursodeoxycholic acid for primary biliary cirrhosis. *Gastroenterol Jpn* 1990; **25**: 774-780

8 **Crosignani A**, Podda M, Battezzati PM, Bertolini E, Zuin M, Watson D, Setchell KD. Changes in bile acid composition in patients with primary biliary cirrhosis induced by ursodeoxycholic acid administration. *Hepatology* 1991; **14**: 1000-1007

9 **Poupon RE**, Poupon R, Balkau B. Ursodiol for the long-term treatment of primary biliary cirrhosis. The UDCA-PBC Study Group. *N Engl J Med* 1994; **330**: 1342-1347

10 **Heathcote EJ**, Cauch-Dudek K, Walker V, Bailey RJ, Blendis LM, Ghent CN, Michieletti P, Minuk GY, Pappas SC, Scully LJ. The Canadian Multicenter Double-blind Randomized Controlled Trial of ursodeoxycholic acid in primary biliary cirrhosis. *Hepatology* 1994; **19**: 1149-1156

11 **Lindor KD**, Therneau TM, Jorgensen RA, Malinchoc M, Dickson ER. Effects of ursodeoxycholic acid on survival in patients with primary biliary cirrhosis. *Gastroenterology* 1996; **110**: 1515-1518

12 **Jackson H**, Solaymani-Dodaran M, Card TR, Aithal GP, Logan R, West J. Influence of ursodeoxycholic acid on the mortality and malignancy associated with primary biliary cirrhosis: a population-based cohort study. *Hepatology* 2007; **46**: 1131-1137

13 **Chazouillères O**, Poupon R, Capron JP, Metman EH, Dhumeaux D, Amouretti M, Couzigou P, Labayle D, Trinchet JC. Ursodeoxycholic acid for primary sclerosing cholangitis. *J Hepatol* 1990; **11**: 120-123

14 **Nakagawa S**, Makino I, Ishizaki T, Dohi I. Dissolution of cholesterol gallstones by ursodeoxycholic acid. *Lancet* 1977; **2**: 367-369

15 **Takano S**, Ito Y, Yokosuka O, Ohto M, Uchiumi K, Hirota K, Omata M. A multicenter randomized controlled dose study of ursodeoxycholic acid for chronic hepatitis C. *Hepatology* 1994; **20**: 558-564

16 **Omata M**, Yoshida H, Toyota J, Tomita E, Nishiguchi S, Hayashi N, Iino S, Makino I, Okita K, Toda G, Tanikawa K, Kumada H. A large-scale, multicentre, double-blind trial of ursodeoxycholic acid in patients with chronic hepatitis C. *Gut* 2007; **56**: 1747-1753

17 **Olsson R**, Boberg KM, de Muckadell OS, Lindgren S, Hultcrantz R, Folvik G, Bell H, Gangsøy-Kristiansen M, Matre J, Rydning A, Wikman O, Danielsson A, Sandberg-Gertzén H, Ung KA, Eriksson A, Lööf L, Prytz H, Marschall HU, Broomé U. High-dose ursodeoxycholic acid in primary sclerosing cholangitis: a 5-year multicenter, randomized, controlled study. *Gastroenterology* 2005; **129**: 1464-1472

18 **Lirussi F**, Beccarello A, Bortolato L, Morselli-Labate AM, Crovatto M, Ceselli S, Santini G, Crepaldi G. Long-term treatment of chronic hepatitis C with ursodeoxycholic acid: influence of HCV genotypes and severity of liver disease. *Liver* 1999; **19**: 381-388

19 **Rino Y**, Tarao K, Morinaga S, Ohkawa S, Miyakawa K, Hirokawa S, Masaki T, Tarao N, Yukawa N, Saeki H, Takanashi Y, Imada T. Reduction therapy of alanine aminotransferase levels prevent HCC development in patients with HCV-associated cirrhosis. *Anticancer Res* 2006; **26**: 2221-2226

20 **Tarao K**, Takemiya S, Tamai S, Sugimasa Y, Ohkawa S, Akaike M, Tanabe H, Shimizu A, Yoshida M, Kakita A. Relationship between the recurrence of hepatocellular carcinoma (HCC) and serum alanine aminotransferase levels in hepatectomized patients with hepatitis C virus-associated cirrhosis and HCC. *Cancer* 1997; **79**: 688-694

21 **Yoshida H**, Shiratori Y, Moriyama M, Arakawa Y, Ide T, Sata M, Inoue O, Yano M, Tanaka M, Fujiyama S, Nishiguchi S, Kuroki T, Imazeki F, Yokosuka O, Kinoyama S, Yamada G, Omata M. Interferon therapy reduces the risk for hepatocellular carcinoma: national surveillance program of cirrhotic and noncirrhotic patients with chronic hepatitis C in Japan. IHIT Study Group. Inhibition of Hepatocarcinogenesis by Interferon Therapy. *Ann Intern Med* 1999; **131**: 174-181

22 **Miura T**, Ouchida R, Yoshikawa N, Okamoto K, Makino Y, Nakamura T, Morimoto C, Makino I, Tanaka H. Functional modulation of the glucocorticoid receptor and suppression of NF-kappaB-dependent transcription by ursodeoxycholic acid. *J Biol Chem* 2001; **276**: 47371-47378

23 **Park IH**, Kim MK, Kim SU. Ursodeoxycholic acid prevents apoptosis of mouse sensory neurons induced by cisplatin by reducing P53 accumulation. *Biochem Biophys Res Commun* 2008; **377**: 1025-1030

24 **Rodrigues CM**, Fan G, Ma X, Kren BT, Steer CJ. A novel role for ursodeoxycholic acid in inhibiting apoptosis by modulating mitochondrial membrane perturbation. *J Clin Invest* 1998; **101**: 2790-2799

25 **Tanaka H**, Makino I. Ursodeoxycholic acid-dependent activation of the glucocorticoid receptor. *Biochem Biophys Res Commun* 1992; **188**: 942-948

26 **Ikegami T**, Matsuzaki Y, Fukushima S, Shoda J, Olivier JL, Bouscarel B, Tanaka N. Suppressive effect of ursodeoxycholic acid on type IIA phospholipase A2 expression in HepG2 cells. *Hepatology* 2005; **41**: 896-905

27 **Kano M**, Shoda J, Irimura T, Ueda T, Iwasaki R, Urasaki T, Kawauchi Y, Asano T, Matsuzaki Y, Tanaka N. Effects of long-term ursodeoxycholate administration on expression levels of secretory low-molecular-weight phospholipases A2 and mucin genes in gallbladders and biliary composition in patients with multiple cholesterol stones. *Hepatology* 1998; **28**: 302-313

28 **Yoshikawa M**, Tsujii T, Matsumura K, Yamao J, Matsumura Y, Kubo R, Fukui H, Ishizaka S. Immunomodulatory effects of ursodeoxycholic acid on immune responses. *Hepatology* 1992; **16**: 358-364

29 **Attili AF**, Rusticali A, Varriale M, Carli L, Repice AM, Callea F. The effect of ursodeoxycholic acid on serum enzymes and liver histology in patients with chronic active hepatitis. A 12-month double-blind, placebo-controlled trial. *J Hepatol* 1994; **20**: 315-320

30 **Shiratori Y**, Omata M. Predictors of the efficacy of interferon therapy for patients with chronic hepatitis C before and during therapy: how does this modify the treatment course? *J Gastroenterol Hepatol* 2000; **15** Suppl: E141-E151

31 **Giannini E**, Borro P, Botta F, Fumagalli A, Malfatti F, Podestà E, Romagnoli P, Testa E, Chiarbonello B, Polegato S, Mamone M, Testa R. Serum thrombopoietin levels are linked to liver function in untreated patients with hepatitis C virus-related chronic hepatitis. *J Hepatol* 2002; **37**: 572-577

32 **Macías J**, Girón-González JA, González-Serrano M, Merino D, Cano P, Mira JA, Arizcorreta-Yarza A, Ruíz-Morales J, Lomas-Cabeza JM, García-García JA, Corzo JE, Pineda JA. Prediction of liver fibrosis in human immunodeficiency virus/hepatitis C virus coinfected patients by simple non-invasive indexes. *Gut* 2006; **55**: 409-414

33 **Shaheen AA**, Myers RP. Diagnostic accuracy of the aspartate aminotransferase-to-platelet ratio index for the prediction of hepatitis C-related fibrosis: a systematic review. *Hepatology* 2007; **46**: 912-921

S- Editor Cheng JX **L- Editor** Webster JR **E- Editor** Yin DH

Online Submissions: wjg.wjgnet.com
wjg@wjgnet.com
doi:10.3748/wjg.15.2787

World J Gastroenterol 2009 June 14; 15(22): 2787-2793
World Journal of Gastroenterology ISSN 1007-9327

Spatial distribution patterns of anorectal atresia/stenosis in China: Use of two-dimensional graph-theoretical clustering

Ping Yuan, Liang Qiao, Li Dai, Yan-Ping Wang, Guang-Xuan Zhou, Ying Han, Xiao-Xia Liu, Xun Zhang, Yi Cao, Juan Liang, Jun Zhu

Ping Yuan, Liang Qiao, Ying Han, Xiao-Xia Liu, Xun Zhang, Yi Cao, Department of Epidemiology, West China School of Public Health, Sichuan University, Chengdu 610041, Sichuan Province, China
Li Dai, Yan-Ping Wang, Guang-Xuan Zhou, Juan Liang, Jun Zhu, National Center for Birth Defects Monitoring, West China Second University Hospital, Sichuan University, Chengdu 610041, Sichuan Province, China
Author contributions: Yuan P, Qiao L and Zhu J designed the research; Yuan P, Qiao L, Dai L, Wang YP, Zhou GX, Han Y, Liu XX, Zhang X, Cao Y, and Liang J performed the research; Qiao L performed the analysis; Yuan P, Qiao L and Zhu J wrote the paper.
Supported by The National Science & Technology Pillar Program during the Eleventh Five-year Plan Period, Grant No. 2006BAI05A01
Correspondence to: Jun Zhu, Professor, National Center for Birth Defects Monitoring, West China Second University Hospital, Sichuan University, Chengdu 610041, Sichuan Province, China. zhujun3@163.com
Telephone: +86-28-85503121 Fax: +86-28-85501386
Received: December 2, 2008 Revised: April 8, 2009
Accepted: April 15, 2009
Published online: June 14, 2009

Abstract

AIM: To investigate the spatial distribution patterns of anorectal atresia/stenosis in China.

METHODS: Data were collected from the Chinese Birth Defects Monitoring Network (CBDMN), a hospital-based congenital malformations registry system. All fetuses more than 28 wk of gestation and neonates up to 7 d of age in hospitals within the monitoring sites of the CBDMN were monitored from 2001 to 2005. Two-dimensional graph-theoretical clustering was used to divide monitoring sites of the CBDMN into different clusters according to the average incidences of anorectal atresia/stenosis in the different monitoring sites.

RESULTS: The overall average incidence of anorectal atresia/stenosis in China was 3.17 per 10000 from 2001 to 2005. The areas with the highest average incidences of anorectal atresia/stenosis were almost always focused in Eastern China. The monitoring sites were grouped into 6 clusters of areas. Cluster 1 comprised the monitoring sites in Heilongjiang Province, Jilin Province, and Liaoning Province; Cluster 2 was composed of those in Fujian Province, Guangdong Province, Hainan Province, Guangxi Zhuang Autonomous Region, south Hunan Province, and south Jiangxi Province; Cluster 3 consisted of those in Beijing Municipal City, Tianjin Municipal City, Hebei Province, Shandong Province, north Jiangsu Province, and north Anhui Province; Cluster 4 was made up of those in Zhejiang Province, Shanghai Municipal City, south Anhui Province, south Jiangsu Province, north Hunan Province, north Jiangxi Province, Hubei Province, Henan Province, Shanxi Province and Inner Mongolia Autonomous Region; Cluster 5 consisted of those in Ningxia Hui Autonomous Region, Gansu Province and Qinghai Province; and Cluster 6 included those in Shaanxi Province, Sichuan Province, Chongqing Municipal City, Yunnan Province, Guizhou Province, Xinjiang Uygur Autonomous Province and Tibet Autonomous Region.

CONCLUSION: The findings in this research allow the display of the spatial distribution patterns of anorectal atresia/stenosis in China. These will have important guiding significance for further analysis of relevant environmental factors regarding anorectal atresia/stenosis and for achieving regional monitoring for anorectal atresia/stenosis.

Key words: Spatial distribution; Anorectal atresia/stenosis; Two-dimensional graph-theoretical clustering; Incidence; Monitoring

Peer reviewer: Dr. Stephen E Roberts, Senior Lecturer in Epidemiology, School of Medicine, Swansea University, Honorary Research Fellow, Department of Public Health, University of Oxford, School of Medicine, Swansea University, Singleton Park, Swansea SA2 8PP, United Kingdom

Yuan P, Qiao L, Dai L, Wang YP, Zhou GX, Han Y, Liu XX, Zhang X, Cao Y, Liang J, Zhu J. Spatial distribution patterns of anorectal atresia/stenosis in China: Use of two-dimensional graph-theoretical clustering. *World J Gastroenterol* 2009; 15(22): 2787-2793 Available from: URL: http://www.wjgnet.com/1007-9327/15/2787.asp DOI: http://dx.doi.org/10.3748/wjg.15.2787

INTRODUCTION

Anorectal atresia/stenosis is a congenital malformation characterized by absence of continuity of the anorectal canal or of communication between rectum and anus, or narrowing of anal canal, with or without fistula, to neighboring organs[1]. Its incidence is rated high amongst gastrointestinal tract malformations. Incidence relates not only to genetic factors but also to environmental factors, especially spatial differences. There is, however, very little information available in literature about the spatial distribution patterns of anorectal atresia/stenosis in China.

Since 1986 China has been using the hospital-based Chinese Birth Defects Monitoring Network (CBDMN) to dynamically monitor severe congenital malformations such as anorectal atresia/stenosis[2]. We conducted this research to divide monitoring sites of the CBDMN into different clusters using two-dimensional graph-theoretical clustering analysis of the incidences of anorectal atresia/stenosis. Consideration was given to the similarities of the incidences of anorectal atresia/stenosis and the adjacent spatial relationships among different monitoring sites. This paper will present the spatial distribution patterns of anorectal atresia/stenosis and hopes to provide clues for research on its etiology.

MATERIALS AND METHODS

Objects

Research subjects were all perinatal fetal births more than 28 wk of gestation and neonates up to 7 d of age monitored in hospitals in the monitoring sites of the CBDMN from 2001 to 2005. They included live births, fetal deaths, stillbirths and those neonates who died within the first 7 d in these hospitals.

Monitoring hospitals

Using the hospital-based guidelines for monitoring birth defects in developing countries, as recommended by World Health Organization (WHO), the CBDMN gathered data from about 460 hospitals in this hospital-based network. These hospitals - all of them above the county level - were located in 138 cities (138 monitoring sites) of 31 different provinces, municipal cities, and autonomous regions in China. The selection of monitoring sites used the method of stratified sampling based on the combination of geographical location, economic development level and infant mortality rate. The spatial distribution of monitoring sites is in accordance with the distribution of nationwide births. The nationwide program covers approximately 450 000-500 000 births annually through all monitoring hospitals.

Information collection

The monitoring staff all received technical training on the case ascertainment of birth defects and the reporting of register forms. The monitoring hospitals collected the basic monthly information about the fetuses and neonates from units of delivery, pediatric and pathology quarterly reports and filled in the "Quarterly Form for Perinatal Births". The monitoring staff in these hospitals filled in the "Registration Card for Births with Congenital Malformations" regarding the cases of diagnosed anorectal atresia/stenosis. All the forms were required to be handed over to the provincial birth defects monitoring offices; these would be reported to the National Center for Birth Defects Monitoring after scrutiny. The specific monitoring methods and quality control measures complied with those in reference[3].

Inclusion and exclusion criteria

The perinatal births diagnosed as having anorectal atresia/stenosis with reference to criteria in Code Q42.1 and Code 42.3 in ICD-10 were included in this research. According to the criteria authorized by the International Clearing house for Birth Defects Surveillance and Research (ICBDSR), cases of mild stenosis which did not need correction and ectopic anus were excluded.

Spatial distribution analysis

The Excel Package was used to build the database of data of anorectal atresia/stenosis by monitoring sites. The ArcView GIS 3.2 was applied to spatially display the average incidences of anorectal atresia/stenosis in different provinces, municipal cities, and autonomous regions.

Two-dimensional graph-theoretical clustering: The graph is a set of vertices and edges that connect pairs of vertices in the space[4-6]. According to the basic requirements for clustering the two-dimensional ordinal samples, the similarities of the disease-related variables between members of the same cluster and their disparities between members of different clusters need to be maintained. The connectivity of the geographic units within the cluster also needs to be conserved. The weighted connected graph was supposed to be G = (V, E, D), in which (1) V represents the set of the locations of the geographic units (referred to monitoring sites in this research), (2) E represents the initial location connection matrix $B^{(0)}$ (Formula 1), the set of the adjacent relationships among different monitoring sites, and (3) D represents the initial disease-related distance matrix $D^{(0)}$ (Formula 2), the weights between different vertices in the tree algorithm in the graph theory. Based on the weighted connected graph G = (V, E, D), minimum spanning trees (MST) which were of biogeographic significance[7,8] were constructed by the Kruskal MST algorithm[9]. The two vertices with the minimum distance measures were selected and connected. One of the remaining vertices was selected and connected with the one of the two connected vertices to which it showed the minimum distance measured. The other remaining vertices were connected consecutively with those vertices already connected in the same manner until all the vertices were interconnected. The whole process was completed by the DPS7.05 software package[10].

$B^{(0)} = (b_{ik}^{(0)})_{n \times n}$; $i, k = 1, 2, ..., n$ (Formula 1)

$D^{(0)} = (d_{ik}^{(0)})_{n \times n}$; $i, k = 1, 2, ..., n$ (Formula 2)

Where $b_{ik}^{(0)}$ is the labeling of location connection between the monitoring site i and the monitoring site k. The value of $b_{ik}^{(0)}$ is 1 if the two monitoring sites are adjacent, while it is 0 when the two monitoring sites are not. $d_{ik}^{(0)}$ is the similarity distance between the incidence of the monitoring site i and that of the monitoring site k.

The MST was deconstructed by the method of "necks" in the graph theory[11]. Specific steps processed were as follows: (1) calculating the "branches": All n vertices were interconnected by (n-1) edges. Two of these vertices were connected only by one edge and the others were connected by at least two edges, which thus formed a chain without circuits, called the "branch". The branch with the most edges was called the main branch (or diameter) of the MST; (2) calculating the "subsidiary main branch". Starting from any vertex in the main branch of MST, the branch with the most edges, other than the main branch, was separated out and called the subsidiary main branch. The number of edges of the subsidiary main branch was called the "depth" of the vertex; (3) identifying "necks". The task was twofold: (Ⅰ) to appoint an integer "a" (that is > 1), and (Ⅱ) to find the subsidiary main branch of every vertex with a depth ≥ a in the main branch. The edges, which connected the vertices with the depth of 0 in the main shared parts of every subsidiary main branch, were called the "neck"; and (4) the necks were deleted in the graph to deconstruct the MST into parts so that the monitoring sites in the graph were divided into different clusters accordingly.

The layer of the deconstructed MST was added to the Administrative Boundary Layer of the 1:4M-scale Topographic Database of the National Fundamental Geographic Information System of China to formulate the two-dimensional MST-based cluster graph. The clustering results were used to make another cluster map for visual observation. This process was performed by the ArcView GIS 3.2 package software.

RESULTS

A total of 2670367 perinatal births were monitored from 2001 to 2005 all over China. Eight hundred and forty six cases of anorectal atresia/stenosis were found, equating to a total average incidence of 3.17 per 10000. See Table 1 for the average incidences of anorectal atresia/stenosis in different provinces, municipal cities or autonomous regions. The top five incidences appeared in Liaoning (4.89 per 10000 births), Zhejiang (4.83 per 10000 births), Guangdong (4.78 per 10000 births), Chongqing (4.59 per 10000 births) and Beijing (4.10 per 10000 births).

Spatial distribution

Regarding the geographic division standard for Eastern, Middle and Western China from the National Bureau of Statistics of China in 2003[12], the areas (provinces, autonomous regions, or municipal cities) with the highest average incidences of anorectal atresia/stenosis were concentrated in Eastern China, while the areas with the lowest average incidence of less than 1.99 per 10000 were mostly located in Western China (Figure 1).

Table 1 Average incidences of anorectal atresia/stenosis in different provinces, municipal cities or autonomous regions of China from 2001 to 2005

Province/Autonomous region/Municipal city	Perinatal births	Cases	Average incidence (per 10000)
Liaoning	79760	39	4.89
Zhejiang	111690	54	4.83
Guangdong	127648	61	4.78
Chongqing	60979	28	4.59
Beijing	114741	47	4.10
Guangxi	64444	26	4.03
Tianjin	62542	25	4.00
Anhui	100631	36	3.58
Fujian	95970	34	3.54
Ningxia	65064	23	3.53
Jiangsu	149984	52	3.47
Jilin	112606	38	3.37
Shanxi	76653	24	3.13
Henan	126082	39	3.09
Hubei	59964	18	3.00
Hebei	130441	39	2.99
Gansu	61629	18	2.92
Hunan	85919	25	2.91
Heilongjiang	71224	20	2.81
Hainan	54234	14	2.58
Shandong	164141	42	2.56
Guizhou	58695	15	2.56
Sichuan	88783	22	2.48
Shanghai	144361	34	2.36
Inner Mongolia	63061	14	2.22
Yunnan	85398	17	1.99
Jiangxi	84015	15	1.79
Xinjiang	56214	10	1.78
Shaanxi	64634	11	1.70
Qinghai	36666	6	1.64
Tibet	12194	0	0.00
Total	2670367	846	3.17

Results of the two-dimensional graph-theoretical clustering

The MST was constructed with consideration to the similarities of average incidences of anorectal atresia/stenosis and the spatial connectivity between different monitoring sites (Figure 2). According to the "neck" calculation method in the graph theory, when the integral constant, a, was designated as 2, the monitoring sites were divided into 6 clusters of different areas.

Regarding the average incidences of anorectal atresia/stenosis in different provinces, municipal cities and autonomous regions from 2001 to 2005, the monitoring sites were grouped into 6 clusters. Cluster 1 comprised the monitoring sites in Heilongjiang Province, Jilin Province, and Liaoning Province; Cluster 2 was composed of those in Fujian Province, Guangdong Province, Hainan Province, Guangxi Zhuang Autonomous Region, south Hunan Province,

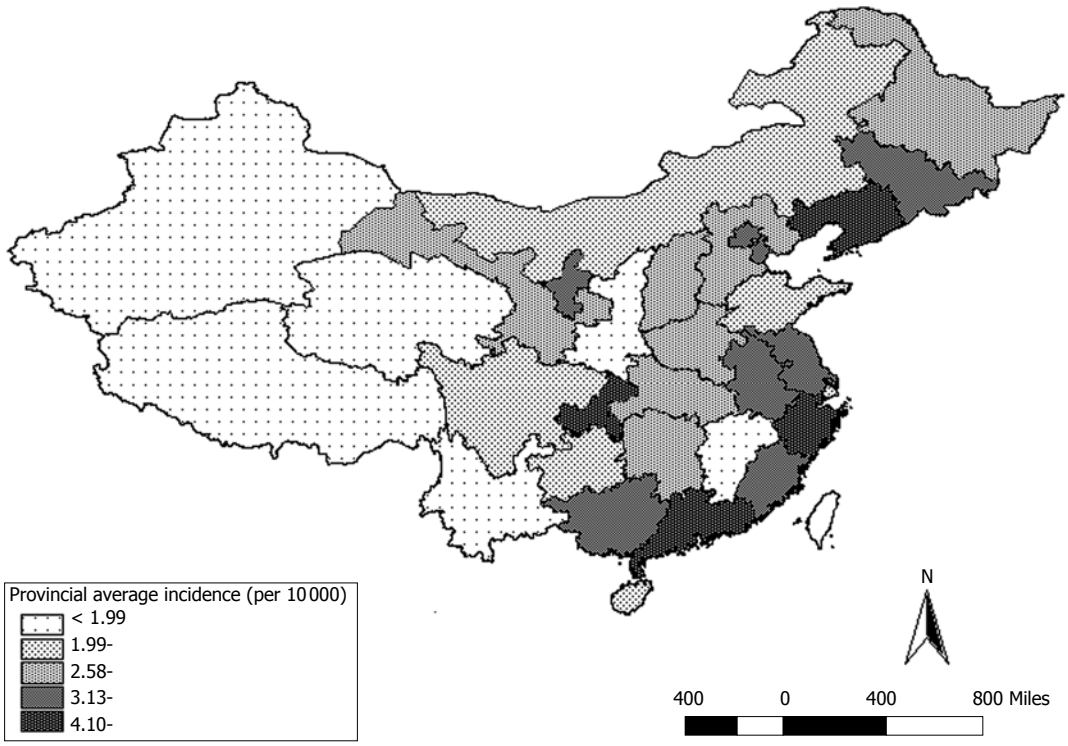

Figure 1 National distribution graph of average incidences of anorectal atresia/stenosis in different provinces, municipal cities and autonomous regions from 2001 to 2005.

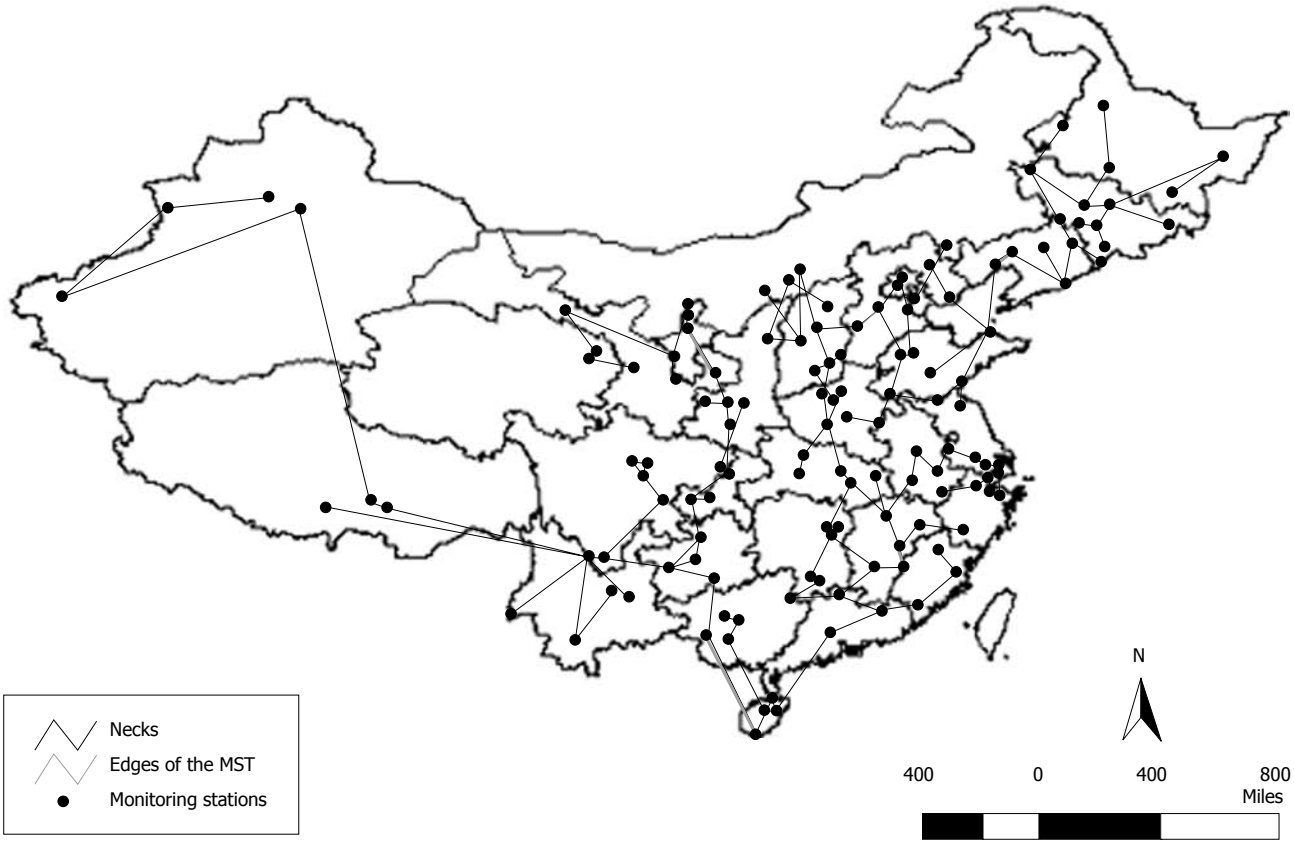

Figure 2 Two-dimensional MST-based cluster graph of monitoring sites in China from 2001 to 2005.

and south Jiangxi Province; Cluster 3 consisted of those in Beijing Municipal City, Tianjin Municipal City, Hebei Province, Shandong Province, north Jiangsu Province, and north Anhui Province; Cluster 4 was made up of those in Zhejiang Province, Shanghai Municipal City, south Anhui Province, south Jiangsu Province,

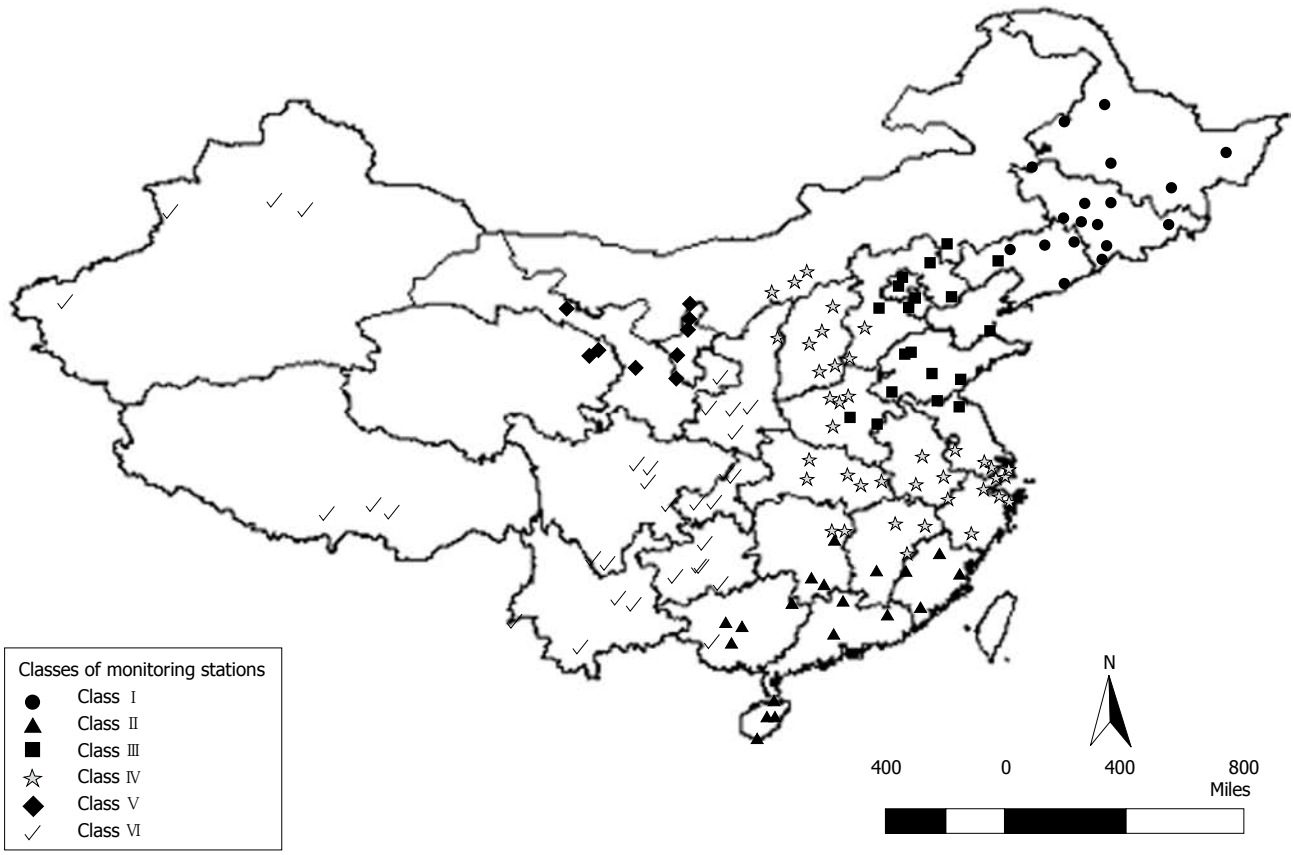

Figure 3 Cluster graph of monitoring sites in China from 2001 to 2005.

north Hunan Province, north Jiangxi Province, Hubei Province, Henan Province, Shanxi Province and Inner Mongolia Autonomous Region; Cluster 5 consisted of those in Ningxia Hui Autonomous Region, Gansu Province and Qinghai Province; and Cluster 6 included those in Shaanxi Province, Sichuan Province, Chongqing Municipal City, Yunnan Province, Guizhou Province, Xinjiang Uygur Autonomous Province and Tibet Autonomous Region (Figure 3).

DISCUSSION

Anorectal atresia/stenosis is one of the most common malformations in the gastrointestinal tract. Due to pathological changes in the anus and rectum, one-third of the perinatal births with anorectal atresia/stenosis suffer from defecation difficulties of varying degrees of severity following surgery. Most of these births need life-long treatment that severely compromises the quality of life and psychological development in particular. This situation is a burden not only to these babies, but also to their entire families and even to society as a whole in China[13-17]. Some researchers[18-22] suggested that mothers' contact (when they are pregnant) with environmental pollutants could increase their risk of giving birth to babies having congenital malformations. The current research found that the areas with the highest incidences of anorectal atresia/stenosis were concentrated in Eastern China, especially in Liaoning, Zhejiang and Guangdong. With a solid industrial and agricultural base, economic conditions in Eastern China flourish. Most manufacturing plants and industrial factories (including marine-aquatic industries) are located in Eastern China. It is known that these factories are responsible for water pollution and other industrial pollution at a level that is deemed severe. Perhaps mothers in Eastern China have babies with more congenital malformations because of the mothers' severe exposure to these physical and chemical pollutants when they are pregnant. In addition, the regional differences in awareness and uptake of available health care for pregnant woman, infrastructure of monitoring hospitals and diagnosis at a technical level were also factors likely to explain some of the observed geographical variation in anorectal atresia/stenosis. In Western China, limited at economic and cultural levels, most pregnant woman have weak awareness and uptake of health care, which means they do not actively seek antenatal care, so there is the probability of under-reporting of cases, resulting in the lower incidence. As to the health services, in the less developed western regions, the maternal and child healthcare facilities may lack necessary infrastructure, and the technical levels of monitoring staff may be limited, which may also result in the lower detection of congenital malformation.

Cluster analysis is an exploratory data analysis tool for solving classification problems. Assuming the samples as the vectorial points in hyperspace, the object of cluster analysis is to sort the samples into clusters so that the degree of association is strong between members of the same cluster and weak between members of different

clusters. It has widespread application because of its advantage of definite classification. In analysis of spatial distribution structures of disease, both the similarities and the adjacent relationships of geographic units of the same cluster are of interest to researchers[23]. The traditional cluster analysis cannot meet all the requirements. Nevertheless, the two-dimensional graph-theoretical clustering model systematically (1) combines the concept of the two-dimensional constrained spatial hierarchical clustering and the MST method in the graph theory; (2) utilizes the spatial analysis measures of Geographic Information System (GIS) in combination with the tree algorithm to divide the geographic units into clusters. This model allows researchers to consider the similarities as well as the spatial connectivity between different units in the same cluster. This is of significance in (1) analyzing the similarities of different geographic units, (2) demonstrating the spatial distribution of the disease, and (3) identifying the boundaries of the spatial heterogeneity of the disease. Luo *et al*[24] combined the principal component analysis and two-dimensional graph-theoretical clustering to identify the evaluation method for land consolidation priority. Cao *et al*[25] divided the national corn reserve regions based on the two-dimensional graph-theoretical clustering, providing references for application of regional corn reserve technology and for the formation of guidelines for macro-regional corn reserve technology. Few researchers, however, have reported on the use of two-dimensional graph-theoretical clustering as applied to study the spatial distribution of congenital malformations.

This research utilized the two-dimensional graph-theoretical clustering to divide monitoring sites of the CBDMN into different clusters of areas based on average incidences of anorectal atresia/stenosis. The findings in this research will have important guiding significance for further analysis of relevant environmental factors regarding anorectal atresia/stenosis and for allowing regional monitoring for anorectal atresia/stenosis. On the one hand, the congenital malformations relate not only to genetic factors, but also correspond with the influence of other conditions: geographic environment, climate, economic development and even cultural development[26-30]. The results from the two-dimensional graph-theoretical clustering will enable epidemiologists to determine which environmental factors affect the incidence of anorectal atresia/stenosis in each cluster of areas by considering their respective environmental characteristics. On the other hand, although these data showed high incidence of anorectal atresia/stenosis in Eastern China and low incidence in Western China, it is true that different areas within Eastern China and Western China have their own demographic, economic and environmental characteristics. Large-scale monitoring cannot obtain detailed influential factors of anorectal atresia/stenosis in any given region. The results in this research provide an approach for researchers to monitor relevant environmental influential factors for incidence of anorectal atresia/stenosis regionally. By dividing the monitoring sites of the CBDMN into different clusters, the detailed relevant environmental risk factors for anorectal atresia/stenosis in different geographic units can be collected within the same cluster to allow regional monitoring.

The current research took account of the adjacent relationship between different monitoring sites rather than different provinces, autonomous regions or municipal cities, which guaranteed the requirements for geographic divisions for this study. However, if different monitoring sites in the same province were incorporated into different clusters after two-dimensional graph-theoretical clustering, the monitoring work at the provincial level would be subjected to increased difficulties.

ACKNOWLEDGMENTS

We thank monitoring hospitals of the CNBDMN for data collection of anorectal atresia/stenosis. We also thank Mary Meyer and Steven Pan, who polished the paper with meticulous efforts.

COMMENTS

Background

The incidence of anorectal atresia/stenosis is high amongst gastrointestinal tract malformations. It relates not only to genetic factors but also to environmental factors, especially spatial differences. However, very little information available in literature about the spatial distribution patterns of anorectal atresia/stenosis in China.

Innovations and breakthroughs

This is the first study to report the spatial distribution of anorectal atresia/stenosis in China using two-dimensional graph-theoretical clustering considering simultaneously the similarities as well as the spatial connectivity between different units in the same cluster.

Applications

The findings will have important guiding significance for further analysis of relevant environmental factors of anorectal atresia/stenosis and for allowing regional monitoring for anorectal atresia/stenosis.

Terminology

Anorectal atresia/stenosis: a congenital malformation characterized by absence of continuity of the anorectal canal or of communication between rectum and anus, or narrowing of anal canal, with or without fistula to neighboring organs. Two-dimensional graph-theoretical clustering: a cluster method of combining the concept of the two-dimensional constrained spatial hierarchical clustering and the MST method in the graph theory, and utilizing the spatial analysis measures of geographic information system (GIS) in combination with the tree algorithm to divide the geographic units into clusters.

Peer review

The study is based on 460 hospitals from 138 cities across China, and is an interesting paper on the geographical distribution of anorectal atresia/stenosis across China.

REFERENCES

1 **International Clearinghouse for Birth Defects Surveillance and Research (ICBDSR)**. Annual Report 2006 with data for 2004. Roma: The International Centre on Birth Defects, 2006
2 **Zhu J**. Birth defect and its surveillance. *Zhongguo Shiyong Fuke Yu Chanke Zazhi* 2002; 18: 513-514
3 **Dai L**, Zhu J, Zhou G, Wang Y, Wu Y, Miao L, Liang J. [Dynamic monitoring of neural tube defects in China during 1996 to 2000] *Zhonghua Yu Fang Yi Xue Za Zhi* 2002; **36**: 402-405
4 **Douglas BW**. Introduction to Graph Theory. 2nd edition.

London: Prentice Hall College Div, 2001
5 **Wang SH**. Graph theory. Beijing: Science Press, 2004
6 **Xu JM**. Graph theory and its application. Hefei: University of Science and Technology of China Press, 2004
7 **Dunn G**, Everitt BS, Cannings C. An introduction to mathematical taxonomy. Cambridge: Cambridge University Press, 1982
8 **Page RDM**. Graphs and generalized tracks, quantifying Croizat's panbiogeography. *Systematic Zoology* 1987; **36**: 1-17
9 **Kruskal JB**. Multidimensional scaling by optimizing goodness of fit to a nonmetric hypothesis. *Psychometrika* 1964; **29**: 1-27
10 **Tang QY**, Feng MG. DPS Data Processing System for Practical Statistics. 1st edition. Beijing: Science Press, 2002: 265-267
11 **Fang KT**, Pan EP. Cluster analysis. Beijing: Geographic Publishing House, 1982: 116-119
12 How to divide Eastern, Middle and Western China. The Website of National Bureau of Statistics of China, 2003-08-12. Available from: URL: http://www.stats.gov.cn/tjzs/t20030812_402369584.htm
13 **Wang WL**. Basal and clinical research on congential malformations of the anus and rectum. *Jixu Yixue Jiaoyu* 2006; **20**: 22-24
14 **Bai YZ**, Wang WL, Wang HZ, Li Zheng. Preliminary long term follow up study on quality of life after anorectal malformation correction. *Zhonghua Xiaoer Waike Zazhi* 1999; 20: 263-266
15 **Rintala R**, Mildh L, Lindahl H. Fecal continence and quality of life in adult patients with an operated low anorectal malformation. *J Pediatr Surg* 1992; **27**: 902-5
16 **Rintala R**, Mildh L, Lindahl H. Fecal continence and quality of life for adult patients with an operated high or intermediate anorectal malformation. *J Pediatr Surg* 1994; **29**: 777-780
17 **Hassink EA**, Rieu PN, Brugman AT, Festen C. Quality of life after operatively corrected high anorectal malformation: a long-term follow-up study of patients aged 18 years and older. *J Pediatr Surg* 1994; **29**: 773-776
18 **Bai YN**, Qu Y, Hu XB, Pei HB, Zhao C, Li XF, Guo HJ, Wang XB, Cheng N. Multi-factor analysis of the birth defects. *Zhongguo Fuyou Baojian* 2004; **19**: 44-46
19 **Li ST**, Xiao X, Liu XX. Meta-analysis of the risk factors of perinatal birth defects in China. *Linchuang Erke Zazhi* 2008; **26**: 350-353
20 **Brender JD**, Zhan FB, Langlois PH, Suarez L, Scheuerle A. Residential proximity to waste sites and industrial facilities and chromosomal anomalies in offspring. *Int J Hyg Environ Health* 2008; **211**: 50-58
21 **Cordier S**, Bergeret A, Goujard J, Ha MC, Aymé S, Bianchi F, Calzolari E, De Walle HE, Knill-Jones R, Candela S, Dale I, Dananché B, de Vigan C, Fevotte J, Kiel G, Mandereau L. Congenital malformation and maternal occupational exposure to glycol ethers. Occupational Exposure and Congenital Malformations Working Group. *Epidemiology* 1997; **8**: 355-363
22 **Irgens A**, Krüger K, Skorve AH, Irgens LM. Reproductive outcome in offspring of parents occupationally exposed to lead in Norway. *Am J Ind Med* 1998; **34**: 431-437
23 **Shen Y**, Chen F. Conditional hierarchical clustering and its biomedical application. *Nantong Yixueyuan Xuebao* 2002; **22**: 112-114
24 **Luo GH**, Wu CF, Xu BG. Evaluation method for land consolidation priority and its application. *Zhejiang Daxue Xuebao Nongye Yu Shengming Kexue Ban* 2004; **30**: 347-352
25 **Cao Y**, Bian K, Chen CG, Fang L. Division of grain storage in China based on math clustering and map arithmetic. *Zhongguo Liangyou Xuebao* 2005; **20**: 122-124
26 **Song XM**, Wu JL, Chen G, Liu JF, Zhang L. Spatial analysis on geographical risk factors of birth defects. *Shichang Yu Renkou Fenxi* 2006; **12**: 47-53
27 **Zhang FL**, Wang BJ. A regression analysis model for the association between meteorological factors and birth defect. *Chengdu Qixiangxueyuan Xuebao* 1994; **28**: 58-63
28 **Wu ZY**, Yao XH, Wang YL. Relative factors analysis of 103 birth defects in Zunyi city. *Zunyi Yixueyuan Xuebao* 2001; **24**: 363-364
29 **Baron AM**, Donnerstein RL, Kanter E, Meaney FJ, Goldberg SJ. Congenital heart disease in the Medicaid population of Southern Arizona. *Am J Cardiol* 2001; **88**: 462-465
30 **Vrijheid M**, Dolk H, Stone D, Abramsky L, Alberman E, Scott JE. Socioeconomic inequalities in risk of congenital anomaly. *Arch Dis Child* 2000; **82**: 349-352

S- Editor Tian L **L- Editor** Logan S **E- Editor** Yin DH

Online Submissions: wjg.wjgnet.com
wjg@wjgnet.com
doi:10.3748/wjg.15.2794

World J Gastroenterol 2009 June 14; 15 (22): 2794-2799
World Journal of Gastroenterology ISSN 1007-9327

BRIEF ARTICLES

Effect of *p27mt* gene on apoptosis of the colorectal cancer cell line Lovo

Jun Chen, Wu-Hua Ding, Shao-Yong Xu, Jia-Ning Wang, Yong-Zhang Huang, Chang-Sheng Deng

Jun Chen, Shao-Yong Xu, Department of Gastroenterology, Affiliated People's Hospital of Yunyang Medical College, Shiyan 442000, Hubei Province, China
Wu-Hua Ding, Obstetrics and Gynecology Department, Affiliated Taihe Hospital of Yunyang Medical College, Shiyan 442000, Hubei Province, China
Jia-Ning Wang, Yong-Zhang Huang, Institute of Clinical Medical Science of Yunyang Medical College, Shiyan 442000, Hubei Province, China
Chang-Sheng Deng, Department of Gastroenterology, Affiliated Zhongnan Hospital of Wuhan University, Wuhan 430071, Hubei Province, China
Author contributions: Chen J designed the research; Chen J, Wang JN, Ding WH, Huang YZ performed the research and analyzed the data; Chen J wrote the paper; Xu SY and Deng CS supervised the whole study.
Supported by The Natural Science Foundation of Hubei Province, No. 2003ABA193; Bureau of Science and Technology of Shiyan City, No. 2005ZD036
Correspondence to: Jun Chen, MD, Associate Professor, Associate Chief Physician, Department of Gastroenterology, Affiliated People's Hospital of Yunyang Medical College, Shiyan 442000, Hubei Province, China. chenjun@medmail.com.cn
Telephone: +86-719-8637529 Fax: +86-719-8666352
Received: April 13, 2009 Revised: May 11, 2009
Accepted: May 18, 2009
Published online: June 14, 2009

Abstract

AIM: To construct *p27mt* recombinant adenovirus, transfect the colorectal cell line Lovo and observe the effects of *p27mt* on Lovo cell apoptosis and cell cycle inhibition.

METHODS: We constructed recombinant adenovirus containing *p27mt* by homologous recombination in bacteria. The colorectal cancer cell line Lovo was infected with recombinant replication-defective adenovirus Ad-p27mt, and expression of *p27mt* was determined by Western blotting; the inhibitory effect of *p27mt* on Lovo cells was detected by cytometry. Cell cycle was determined by flow cytometry. DNA fragment analysis identified the occurrence of apoptosis.

RESULTS: The recombinant adenovirus which already contained *p27mt* target gene was successfully constructed. When multiplicity of infection was $\geqslant$ 50, the infection efficiency was 100%. After transfection of Lovo cells with Ad-p27mt the cells had high *p27* expression which was identified by immunoblotting assay. PI staining and flow cytometry showed that 77.96% of colorectal cancer cells were inhibited in phase G_0/G_1, while in the Ad-LacZ group and blank control group, 27.57% and 25.29% cells were inhibited in the same phase, respectively. DNA fragment analysis, flow cytometry and TUNEL assay demonstrated that *p27mt* is able to induce apoptosis in colorectal cancer cells.

CONCLUSION: *p27mt* has an obvious blocking effect on colorectal cancer cell cycle, and most cells were inhibited in phase G_0/G_1. Therefore, *p27mt* can induce apoptosis in colorectal cells.

Key words: Apoptosis; Cell cycle; Colorectal cancer; *p27mt*; Recombinant adenovirus

Peer reviewer: Yoshiharu Motoo, MD, PhD, FACP, FACG, Professor and Chairman, Department of Medical Oncology, Kanazawa Medical University, 1-1 Daigaku, Uchinada, Ishikawa 920-0293, Japan

Chen J, Ding WH, Xu SY, Wang JN, Huang YZ, Deng CS. Effect of *p27mt* gene on apoptosis of the colorectal cancer cell line Lovo. *World J Gastroenterol* 2009; 15(22): 2794-2799 Available from: URL: http://www.wjgnet.com/1007-9327/15/2794.asp DOI: http://dx.doi.org/10.3748/wjg.15.2794

INTRODUCTION

p27Kip1 (*p27*) is a cyclin dependent kinase inhibitor (CDKI), whose specific late G_1 destruction allows progression of the cell across the G_1/S boundary. The protein was ubiquitinated by S-phase kinase-interacting protein-2 (Skp2) following its specific phosphorylation, and was subsequently degraded by the 26S proteasome[1]. There was a direct relationship between the low level of *p27* and rapid proliferation occurring in several benign states and in many malignancies. It has been reported that *p27* levels were markedly reduced in several malignancies, such as those of the skin[2], liver[3], bladder[4], thyroid[5], breast[6], prostate[7] and endometrium[8]. In some of the tumors studied, a strong correlation was found between the low level of *p27*, the aggressiveness of the disease and poor prognosis of the patients[6]. Interestingly, *p27* in all these tumors was of the wild-type species (*p27wt*), and its regulation has been attributed to phosphorylation of Thr-187 and subsequent

ubiquitination[9]. Overexpression of *p27 via* adenoviral gene transfer could suppress cancer cell growth regardless of *p27* mutation[10]. Montagnoli *et al*[11] showed that the ubiquitination of *p27* did not occur in *p27mt* with Thr-187 to Ala [p27 (T187A)]. Sheaff *et al*[12] showed that the transfection of p27 (T187A) plasmid caused a G_1 block, which was both resistant to and not modulated by cyclin E/Cdk2. On the basis of these observations of *p27* regulation and the nature of the *p27* tumor suppressor gene, we constructed Adenovirus expressing *p27mt* (Thr-187/Pro-188 to Met-187/Ile-188) to infect the colorectal cancer cell line Lovo, and then investigated its expression and functional significance in the cell proliferation and apoptosis of Lovo cells, by which we aimed to discuss novel methods of gene therapy in colorectal cancer.

MATERIALS AND METHODS

Main reagents

The restriction endonucleases such as *Age* I , *Nhe* I , *Kpn* I , *Pac* I and *Pme* I were purchased from New England Biolabs Co. *Hin*dⅢ, *Eco*RI, λDNA *Hin*dⅢ marker, 200 bp DNA ladder, dNTP, Tag enzyme and T4 DNA ligase were purchased from Huamei Biological Co. (China). The Western blotting kit was purchased from KPL Co. (USA). The rat anti-human *p27kip1* multi-antibody was purchased from Santa Cruz Co. (USA). The horseradish peroxidase (HRP) labeled sheep anti-rat IgG monoclonal antibody was purchase from Zhongshan Co. (China). The *p27mt* primer was designed and synthesized by Beijing Saibaisheng Biological Co. (China). The fetal bovine serum (FBS) was purchased from Hangzhou Sijiqing Biological Engineering Materials Co. (China). The liposome (polyfect) was purchased from Qiagen Co. (USA). Trypsin, DMEM culture medium, Hepes and Cscl were purchased from Sigma Co. (USA).

Plasmid, strain, adenovirus and cell lines

The pORF9-p27mt plasmid was purchased from Invivogen (USA). The pAdeasy-1 plasmid, pBluescript Ⅱsk (+), Ad293 cell, *E. coli* BJ5183 and XL10-gold were purchased from Stratagene (USA). The LacZ recombinant adenovirus (Ad-LacZ with titer 7.15×10^{15}/L)[13] and DH5α were gratefully provided by Doctor Wang Jianing, Clinical Research Institute, Yunyang Medical College. The Lovo cell line was purchased from Type Culture Collection Center, Wuhan University.

Main equipment

This equipment included a high speed freezing centrifuge (Universal 32R, Germany), the ultraspeed freezing centrifuge (Tokyo Cp80max, Japan), inverted phase contrast microscope (Nikon TE2000-u, Japan), CO_2 culture box (CB150#00-17611, wtb-binder), PCR machine (Biometra. Germany), ultraviolet spectrophotometer (Auriud CE2401, UK), Coulter Epics XL flow cytometer (Beckman Co., USA), high speed table-top centrifuge and a water bath shaking table (China).

Construction and identification of p27mt recombinant adenovirus

After pORF9-p27mt was digested by *Age* I and *Nhe* I enzymes, the 619 bp fragment was recycled and subcloned into pBluescript ⅡSK (+) which was digested by *Xma* I and *Xba* I enzymes, thus obtaining pBluescript-p27mt. Then pBluescript-p27mt was digested by *Not* I and *Kpn* I enzymes, and the 699 bp fragment was recycled and inserted into the shuttle plasmid vector pShuttle-CMV which was digested by the same enzymes, thus the transfer plasmid pShuttle-CMV-p27mt was obtained. The competent *E. coli* was transformed by the adenoviral framework plasmid pAdeasy-1. According to the ampicillin-resistant gene, the BJ5183 containing pAdeasy-1 was picked out and prepared into the ultra-competence BJ5183 containing pAdeasy-1. Then, the ultra-competence BJ5183 was transformed by transfer plasmid pShuttle-CMV-p27mt which was digested by *Pme* I enzyme and dephosphorylated by alkaline phosphatase. A little DNA from the transformed clone bacterial plasmid was taken out and the suspect DNA of the recombinant adenovirus plasmid was chosen according to the size of the plasmid in agarose electrophoresis. If the chosen DNA was identified as the correct DNA by digestion of *Pac* I enzyme, then the recombinant adenovirus plasmid pAdeasy-1-p27mt could be prepared. Recombinant adenovirus plasmid DNA was excised by *Pac* I , then transfected by Ad293 *via* liposome polyfect mediation, where the change in cells at different times after transfection was determined. When it appeared that 90% had cell lesions, scratch 293 cells from the culture bottle were vortexed three times at -80℃ to +37℃ to lyse the cells, then centrifuged and the supernatant containing the virus was collected, the 293 cells were reinfected with the above virus and proliferation of the virus occurred at a large scale. Purification of recombinant adenovirus was similar to the method of Cortin *et al*[14]. After purification the adenovirus underwent dialysis, test virus titers were detected using an ultraviolet spectrophotometer. Fifty microliter of purified adenovirus liquid, 100 g/L SDS 20 μL, PBS 430 μL, were assayed at absorbance values of A_{260} and A_{280}, then the granule numbers and purity of adenovirus were determined. If $A_{260} = 10^{15}$pfu/L and $A_{260}/A_{280} > 1.3$ this indicated that the purity was relatively high when virus titers (pfu/L) = $A_{260} \times$ dilution $\times 10^{15}$. PCR identification of recombinant adenovirus Ad-p27mt was carried out. Recombinant adenovirus genome DNA from the high titer virus storage liquid served as a template. Using primer toward the reporter gene *p27mt*, the PCR reaction parameters were: pre-denaturation at 95℃ for 5 min, denaturation at 94℃ for 20 s, annealing at 56℃ for 30 s, elongate at 72℃ for 30 s, 30 cycles, elongate at 72℃ for 10 min. Primer 1: 5'CCTAGAGGGCAAGTACGAGTG3'; Primer 2: 5'GAAGAATCGTCGGTTGCAGGTCGCT3'.

Detection of p27mt gene expression

Lovo cells were incubated in 100 mL/L FCS and RPMI-1640 culture medium at 37℃ in a 50 mL/L CO_2 culture box until the cells spread to 70%-80% of the area and were used in the following experiment.

Lovo cells taken from the 15 cm culture flask were infected with Ad-LacZ according to an Multiplicity of infection (MOI) of 20, 40, 50 and 100 and then incubated for another 48 h. The cells were then fixed by 5 mL/L glutaral for 15 min and washed three times with PBS,

X-gal staining solution (20:1) was added. The cells were then incubated at 37℃ in the 50 mL/L CO_2 culture box for 4-24 h. The blue-stained cells, i.e. the positive cells in which the LacZ gene was expressed, were observed under the microscope and the percentage of positive cells was calculated.

Lovo cells taken from the 75 cm culture flask were infected with Ad-p27mt (MOI 50) and Ad-LacZ (MOI 50), respectively. After incubation in the same conditions for 48 h, the cells were digested by 0.5 g/L trypsin, collected and washed twice with PBS. After lysis by 500 μL 1 × SDS-PAGE cell lysis solution and boiling for 5 min, the cells were centrifuged, the supernatant was collected and then detected by Western blotting.

Cycle detection and apoptosis of cells infected with Ad-p27mt by flow cytometry

Lovo cells cultured in the 75 cm culture flask were infected with Ad-p27mt (MOI 50). After incubation for 48 h, the cells were digested by 0.5 g/L trypsin, collected and then washed twice with PBS. The cell concentration was adjusted to 10^9/L with PBS. One hundred microliter of cell suspension was taken out and mixed with 200 μL DNA-PREP™ LPR and placed at room temperature in the dark for 3 min. The cell suspension was then mixed with 1000 μL DNA-PREP stain (PI staining). The cell cycle phase and apoptosis were detected by a Coulter Epics XL flow cytometer 15 min later. Ad-LacZ (MOI 50) group and normal controls (Lovo cells cultivated without adenovirus) were used as control groups.

Apoptosis by DNA fragment analysis

The cells in the three groups (Ad-p27mt and Ad-LacZ for 48 h and the normal control), were collected and centrifuged at 1000 r/min for 5 min. The supernatant was discarded, and 500 μL of cell lysis solution [1% Np40, 20 mmol/L EDTA, 50 mmol/L Tris-HCl (pH7.5)] and 10 μL protease K were added to the cell sediment. Following incubation in a water bath (56℃) for 1-2 h and extraction with phenol and chloroform, DNA was precipitated by dehydrated alcohol. After washing once with 700 mL/L alcohol, 200 μL TE was added to lyse the DNA. Then RNase (final concentration 50 μg/mL) was added and placed at 37℃ for one night. The DNA was electrophoresed in 10 g/L agarose gel and the results were observed under an ultraviolet lamp.

Detection of cell apoptosis by the TUNEL method

1×10^4 cell suspension was inoculated into a 60 mm dish with a cover glass (washed and high-pressure sterilized). Each of the Ad-p27mt group and the normal control were inoculated into 6 glasses and incubated for 24 h. The glasses were then taken out and washed twice with 1 × PBS and fixed with methanol and freezing acetic acid (3:1) for 30 min. The next procedure was carried out according to the kit instructions. One thousand cells were counted on each glass and the average number of apoptotic cells was determined. Then the apoptotic index (AI), i.e. the number of apoptotic cells in every 100 cancer cells, was calculated.

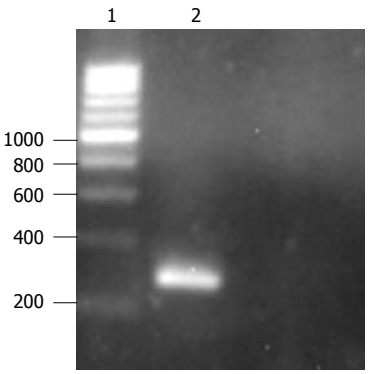

Figure 1 Identification of Ad-p27mt by PCR. 1: 200bp marker; 2: Ad-p27mt.

Statistical analysis

One way-ANOVA was used in processing the measured data, which were expressed as mean ± SD. χ^2 test was adopted in the calculation of enumeration data.

RESULTS

PCR identification of the recombinant adenovirus Ad-p27mt

The pathologically changed 293 cells and the culture fluid were collected, frozen and thawed three times and centrifuged. Five millilitre of the supernatant was taken out and added to 1 mg protease K, 2 mL 1% SDS, 10 mmol/L EDTA and 20 mmol/L Tris-HCl for 2 h. After centrifugation, the supernatant was extracted with phenol and chloroform. After precipitation with dehydrated alcohol, the viral DNA was collected. Then forward and reverse primers were added and the PCR reaction was carried out. The 275 bp target gene was amplified, which showed that the recombinant adenovirus already contained the *p27mt* target gene (Figure 1).

X-gal chemical staining

After Lovo cells were infected with Ad-LacZ, the adenovirus-mediated gene transfer rate was evaluated by X-gal staining. The results showed that the infection efficiency could reach 100% when MOI was larger than 50, which indicated that recombinant adenovirus could effectively transfer the gene to Lovo cells *in vitro* (Figure 2).

The expression of p27 protein was evaluated after Lovo cells were infected with human mutant p27 recombinant adenovirus in vitro

After Lovo cells were infected with Ad-p27mt (MOI 50) for 24 h, these cells were collected and lysed using 1 × SDS × PAGE cell lysis solution. After boiling at 100℃ for 5 min, the cells were centrifuged. The supernatant was collected and the protein was detected by the TMB system Western blotting kit (KPL, USA). After staining with TMB stain, a high expression of 27 KD protein was observed in the Ad-p27mt group while only slight expression (endogenous expression) was observed in the Ad-LacZ group and the normal control group. This showed that the *p27mt* recombinant adenovirus constructed in the present study could express *p27mt* gene in Lovo cells and the protein could also be expressed at a high level in Lovo cells (Figure 3).

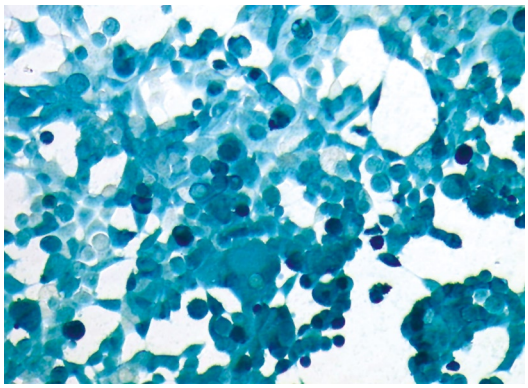

Figure 2 X-gal chemical staining detected the infection efficiency of Ad-p27mt (MOI 50).

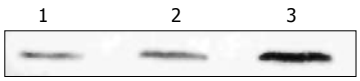

Figure 3 Western blotting of expressed p27 protein. 1: Non-infected Lovo cells; 2: Ad-lacZ infected Lovo cells; 3: Ad-p27mt infected Lovo cells.

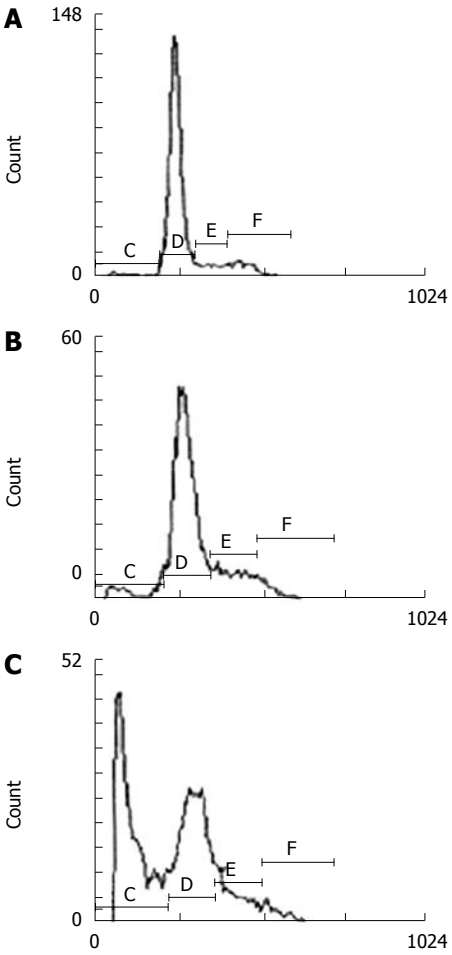

Figure 4 Determination of cell apoptosis by Flow cytometry. A: Non-infected Lovo cells; B: Ad-lacZ infected Lovo cells; C: Ad-p27mt infected Lovo cells.

Apoptosis of colorectal cancer cells induced by Ad-p27mt

After Lovo cells were treated with Ad-p27mt, Ad-LacZ and without virus for 24 h, apoptosis was observed by flow cytometry and was repeated six times. The average value of hypodiploid cells was: 41.0%, 4.67% and 1.96%, respectively. After statistical analysis, there was a significant difference among the three groups, ($P < 0.01$) (Figure 4).

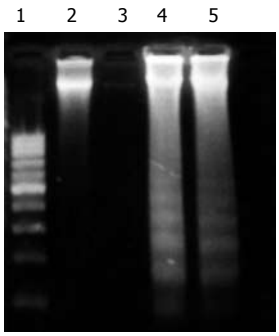

Figure 5 Determination of cell apoptosis by DNA fragment analysis. 1: Marker; 2: Blank group; 3: Ad-lacZ group; 4, 5: Ad-p27mt group.

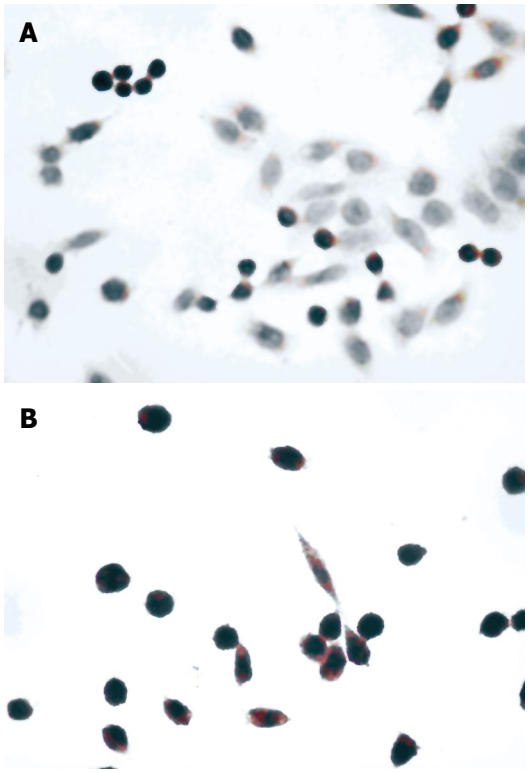

Figure 6 Detection of cell apoptosis by the TUNEL method. A: Blank group; B: Ad-p27mt.

Detection of DNA fragments

The results of DNA electrophoresis showed that the gene bands were intact in the Ad-LacZ and normal control group, while there were obvious 180-200 bp diploid "trapezia" bands in the Ad-p27mt infected group, which was in concordance with the characteristic changes of apoptosis (Figure 5).

Detection of cell apoptosis by the TUNEL method

The nuclei of apoptotic cells were dark stained, the cytoplasm was concentrated and the cells had shrunk. The AI of the Ad-p27mt and the control group were (82.6% ± 3.2%) and (5.0% ± 3.5%), respectively and showed a significant difference ($P < 0.05$). This demonstrated that Ad-p27mt could obviously induce apoptosis in colorectal cancer cells (Figure 6).

Table 1 The effect of Ad-p27mt on the cell cycle of Lovo cells (mean ± SD)

Group	G_0/G_1	S	G_2/M
Blank group	25.29 ± 1.04	41.12 ± 1.19	33.34 ± 1.55
Ad-LacZ group	27.57 ± 0.45[b]	38.21 ± 0.44[b]	34.22 ± 0.92[b]
Ad-p27mt group	77.96 ± 2.20[d]	8.98 ± 0.17[d]	13.06 ± 2.35[d]

Hypodiploid cells were not included ([b]$P < 0.01$ *vs* Ad-LacZ group, [d]$P < 0.01$ *vs* Blank group).

The effect of exogenous p27mt on the cell cycle (Table 1)

The cell cycle of Lovo cells after the various treatments are shown in Table 1. It can be seen that in the Ad-LacZ and blank control groups, the number of cells in the G_0/G_1 phase decreased gradually and the percentage of cells in the S phase increased, which indicated that the transition time of the cell cycle was shortened and cell proliferation was active. However, the percentage of cells in the G_0/G_1 phase decreased and the percentage of cells in the S phase increased and the cell cycle was arrested in the G_0/G_1 phase in the Ad-p27mt group, which was significantly different from the blank and Ad-LacZ groups ($P < 0.01$).

DISCUSSION

Currently, functional reconstruction of anti-oncogenes is a reasonable strategy for tumor gene therapy. p27 protein degradation is mainly caused by phosphorylation of the 187th threonine of *p27* which is mediated by ubiquitin[15-17]. Park *et al*[18,19] replaced the 187th threonine and the 188th praline of the wild-type *p27* with methionine and isoleucine, respectively, by which the target phosphorylation site of CDK would be protected from phosphorylation, and thus the mutant *p27* was prepared. These authors constructed a replication-deficient recombinant adenovirus which carried *p27mt* and *p27wt*, respectively and proved that the inhibition and apoptotic effects in cancer cells was more obvious in the mutant *p27 (p27mt)* than in the wild-type *p27 (p27wt)*.

This study constructed a replication-deficient recombinant adenovirus which successfully carried *p27mt* (Ad-p27mt). Ad-p27mt was then transfected into Lovo cells. When the MOI ⩾ 50, the infection efficiency was 100%. Using Western blotting, high expression of *p27* was observed, and using FACS, the rate of apoptosis was up to 41.0% in the Ad-p27mt group which was significantly different compared to the control group ($P < 0.01$). DNA analysis showed a 180-200 bp DNA ladder, and using the TUNEL technique, the apoptotic index was sharply upregulated to 82.6% which was significantly different compared to the control group ($P < 0.05$). These results showed that *p27mt* is an important gene and is related to the incidence of colorectal carcinoma. The downregulation of *p27* may be the main cause of cell differentiation dysfunction and apoptosis dysfunction. Mutant *p27* promoted the expression of *p27* in Lovo cells, which led to apoptosis in tumor cells. This may be a potential new therapy for colorectal carcinoma.

The concentration of cyclin/CDK is the key factor for cells passing the G_1-S threshold. Cell cycle analysis showed that the cleavage of tumor cells was stopped at the G_1 stage by *p27mt* suppressing the activity of the cyclin/CDK kinase. Hurteau *et al*[20] reported that the accumulation of *p27* played a role in the cell cycle arrest mechanism at the initiation of cell differentiation. A related report[21] in China showed that the *p27* gene suppressed DNA replication and protein synthesis and reduced cell mitosis division and inhibited cell generation.

In our study, apoptosis of colorectal carcinoma cells was successfully induced by the application of the mutant gene p27. The apoptosis rate was significantly higher than that of wild-type p27 reported in our previous study[21], which serves as a very useful experimental support for tumor suppression function reconstruction in the gene therapy of colorectal carcinoma. The efficacy of this method *in vivo* and the mechanism of apoptosis should be determined in future studies.

ACKNOWLEDGMENTS

We thank Dr. Xiao-Jun Yang for his excellent technical assistance.

COMMENTS

Background

Along with the improvement in living standards and a change in diet, there has been a gradual increase in the incidence of colorectal cancer in China. However, no effective therapeutic modalities are available for this condition. Gene therapy for the restoration of *p27* expression is a promising therapy. A mutant type *p27* gene, with a mutation of Thr-187/Pro-188 to Met-187/Ile-188, can inhibit degradation of p27 protein by the ubiquitin-mediated pathway. Inhibition of mutant *p27* (*p27mt*) in tumor cells was stronger than that in wild-type *p27* (*p27wt*), which was demonstrated by cells arresting in the G_0/G_1 phase. In addition, the apoptosis promoting activity of *p27mt* was also stronger. However, few studies on the *p27* gene in colorectal cancer have been reported.

Research frontiers

p27, as a cyclin-dependent kinase inhibitor, tumor suppressor gene, and promoter of apoptosis, has been widely investigated in malignancies such as skin, liver, bladder, thyroid, breast, prostate and endometrium cancer. However, the apoptotic bioactivity of *p27mt* has not been studied in colorectal cancer.

Innovations and breakthroughs

The study indicates that Ad-*p27mt* has a strong apoptosis inducing bioactivity as well as a cell cycle inhibitory effect in colorectal cancer *in vitro*.

Peer review

This is a nice article. This *in vitro* effect of *p27mt* should be examined *in vivo* to determine the safety and efficacy.

REFERENCES

1 **Sherr CJ**, Roberts JM. CDK inhibitors: positive and negative regulators of G1-phase progression. *Genes Dev* 1999; **13**: 1501-1512

2 **Tchernev G**, Orfanos CE. Downregulation of cell cycle modulators p21, p27, p53, Rb and proapoptotic Bcl-2-related proteins Bax and Bak in cutaneous melanoma is associated with worse patient prognosis: preliminary findings. *J Cutan Pathol* 2007; **34**: 247-256

3 **Matsuda Y**, Ichida T. p16 and p27 are functionally correlated during the progress of hepatocarcinogenesis. *Med Mol Morphol* 2006; **39**: 169-175

4 **Shariat SF**, Ashfaq R, Sagalowsky AI, Lotan Y. Predictive value of cell cycle biomarkers in nonmuscle invasive bladder transitional cell carcinoma. *J Urol* 2007; **177**: 481-487;

discussion 487
5 **Saltman B**, Singh B, Hedvat CV, Wreesmann VB, Ghossein R. Patterns of expression of cell cycle/apoptosis genes along the spectrum of thyroid carcinoma progression. *Surgery* 2006; **140**: 899-905; discussion 905-906
6 **Tan P**, Cady B, Wanner M, Worland P, Cukor B, Magi-Galluzzi C, Lavin P, Draetta G, Pagano M, Loda M. The cell cycle inhibitor p27 is an independent prognostic marker in small (T1a,b) invasive breast carcinomas. *Cancer Res* 1997; **57**: 1259-1263
7 **Tsihlias J**, Kapusta LR, DeBoer G, Morava-Protzner I, Zbieranowski I, Bhattacharya N, Catzavelos GC, Klotz LH, Slingerland JM. Loss of cyclin-dependent kinase inhibitor p27Kip1 is a novel prognostic factor in localized human prostate adenocarcinoma. *Cancer Res* 1998; **58**: 542-548
8 **Lahav-Baratz S**, Ben-Izhak O, Sabo E, Ben-Eliezer S, Lavie O, Ishai D, Ciechanover A, Dirnfeld M. Decreased level of the cell cycle regulator p27 and increased level of its ubiquitin ligase Skp2 in endometrial carcinoma but not in normal secretory or in hyperstimulated endometrium. *Mol Hum Reprod* 2004; **10**: 567-572
9 **Wang Z**, Yu BW, Rahman KM, Ahmad F, Sarkar FH. Induction of growth arrest and apoptosis in human breast cancer cells by 3,3-diindolylmethane is associated with induction and nuclear localization of p27kip. *Mol Cancer Ther* 2008; **7**: 341-349
10 **Craig C**, Wersto R, Kim M, Ohri E, Li Z, Katayose D, Lee SJ, Trepel J, Cowan K, Seth P. A recombinant adenovirus expressing p27Kip1 induces cell cycle arrest and loss of cyclin-Cdk activity in human breast cancer cells. *Oncogene* 1997; **14**: 2283-2289
11 **Montagnoli A**, Fiore F, Eytan E, Carrano AC, Draetta GF, Hershko A, Pagano M. Ubiquitination of p27 is regulated by Cdk-dependent phosphorylation and trimeric complex formation. *Genes Dev* 1999; **13**: 1181-1189
12 **Sheaff RJ**, Groudine M, Gordon M, Roberts JM, Clurman BE. Cyclin E-CDK2 is a regulator of p27Kip1. *Genes Dev* 1997; **11**: 1464-1478
13 **Wang JN**, Huang YZ, Kong X, Guo LY. The construction of recombinant adenoviral plasmid by homologous recombination in bacteria and the preparation of recombinant adenovirus expressing β-galactosidase. *Yunyang Yixueyuan Xuebao* 2004; **23**: 1-5
14 **Cortin V**, Thibault J, Jacob D, Garnier A. High-titer adenovirus vector production in 293S cell perfusion culture. *Biotechnol Prog* 2004; **20**: 858-863
15 **Kwon TK**, Park JW. Low levels of cyclin D and nonfunctional Rb protein affect cdk6 association with cyclin-dependent kinase inhibitor p27 (Kip1). *Biochem Biophys Res Commun* 2001; **284**: 106-111
16 **Tsvetkov LM**, Yeh KH, Lee SJ, Sun H, Zhang H. p27 (Kip1) ubiquitination and degradation is regulated by the SCF (Skp2) complex through phosphorylated Thr187 in p27. *Curr Biol* 1999; **9**: 661-664
17 **Bloom J**, Pagano M. Deregulated degradation of the cdk inhibitor p27 and malignant transformation. *Semin Cancer Biol* 2003; **13**: 41-47
18 **Park KH**, Seol JY, Kim TY, Yoo CG, Kim YW, Han SK, Shim YS, Lee CT. An adenovirus expressing mutant p27 showed more potent antitumor effects than adenovirus-p27 wild type. *Cancer Res* 2001; **61**: 6163-6169
19 **Park KH**, Lee J, Yoo CG, Kim YW, Han SK, Shim YS, Kim SK, Wang KC, Cho BK, Lee CT. Application of p27 gene therapy for human malignant glioma potentiated by using mutant p27. *J Neurosurg* 2004; **101**: 505-510
20 **Hurteau JA**, Brutkiewicz SA, Wang Q, Allison BM, Goebl MG, Harrington MA. Overexpression of a stabilized mutant form of the cyclin-dependent kinase inhibitor p27 (Kip1) inhibits cell growth. *Gynecol Oncol* 2002; **86**: 19-23
21 **Zhang WG**, Yu JP, Wu QM, Tong Q, Li SB, Wang XH, Xie GJ. Inhibitory effect of ubiquitin-proteasome pathway on proliferation of esophageal carcinoma cells. *World J Gastroenterol* 2004; **10**: 2779-2784

S- Editor Tian L **L- Editor** Webster JR **E- Editor** Ma WH

Online Submissions: wjg.wjgnet.com
wjg@wjgnet.com
doi:10.3748/wjg.15.2800

World J Gastroenterol 2009 June 14; 15(22): 2800-2804
World Journal of Gastroenterology ISSN 1007-9327

BRIEF ARTICLES

Expression of semaphorin 5A and its receptor plexin B3 contributes to invasion and metastasis of gastric carcinoma

Guo-Qing Pan, Hong-Zheng Ren, Shu-Fang Zhang, Xi-Mei Wang, Ji-Fang Wen

Guo-Qing Pan, Hong-Zheng Ren, Ji-Fang Wen, Department of Pathology, Xiangya Medical College, Central South University, Changsha 410008, Hunan Province, China
Guo-Qing Pan, Department of Pathology, the first Affiliated Hospital of Kunming Medical College, Kunming 530032, Yunnan Province, China
Shu-Fang Zhang, Central Laboratory, Affiliated Haikou Hospital of Xiangya Medical College, Central South University, Haikou 570208, Hainan Province, China
Xi-Mei Wang, Department of Basic Medicine, Huaihua Medical College, Huaihua 418000, Hunan Province, China
Author contributions: Pan GQ and Ren HZ contributed equally to this work; Pan GQ designed the research and wrote the manuscript; Ren HZ analyzed the data by Western blotting and RT-PCR; Zhang SF dealt with the statistical data; Wang XM collected the samples; Wen JF revised the manuscript.
Correspondence to: Ji-Fang Wen, Professor, Department of Pathology, Xiangya Medical College, Central South University, Changsha 410008, Hunan Province, China. jifangwen@hotmail.com
Telephone: +86-731-2650400 Fax: +86-731-2650400
Received: October 23, 2008 Revised: May 5, 2009
Accepted: May 12, 2009
Published online: June 14, 2009

Abstract

AIM: To investigate the protein and mRNA expression of semaphorin 5A and its receptor plexin B3 in gastric carcinoma and explore its role in the invasion and metastasis of gastric carcinoma.

METHODS: Expression of semaphorin 5A and its receptor plexin B3 in 48 samples of primary gastric carcinoma, its corresponding non-neoplastic mucosa, and matched regional lymph node metastasis was assayed by reverse transcription-polymerase chain reaction (RT-PCR), real-time RT-PCR and Western blotting.

RESULTS: The protein and mRNA expression of semaphorin 5A and its receptor plexin B3 increased gradually in non-neoplastic mucosa, primary gastric carcinoma and lymph node metastasis ($P < 0.05$). Moreover, the expression of semaphorin 5A was closely correlated with that of plexin B3.

CONCLUSION: Semaphorin 5A and its receptor plexin B3 play an important role in the invasion and metastasis of gastric carcinoma.

Key words: Semaphorin 5A; Plexin B3; Gastric carcinoma; Invasion; Metastasis

Peer reviewer: Robin G Lorenz, Associate Professor, Department of Pathology, University of Alabama at Birmingham, 845 19th Street South BBRB 730, Birmingham, AL 35294-2170, United States

Pan GQ, Ren HZ, Zhang SF, Wang XM, Wen JF. Expression of semaphorin 5A and its receptor plexin B3 contributes to invasion and metastasis of gastric carcinoma. *World J Gastroenterol* 2009; 15(22): 2800-2804 Available from: URL: http://www.wjgnet.com/1007-9327/15/2800.asp DOI: http://dx.doi.org/10.3748/wjg.15.2800

INTRODUCTION

Gastric cancer is the leading cause of cancer-related death in some Asian countries including China and Japan. Despite the advances in treatment and research efforts over the past few decades, the outcome of gastric cancer remains poor. The overall 5-year survival rate of gastric cancer patients is 5%-15% in the United States and most other Western countries, largely because many gastric cancers are diagnosed at an advanced stage. The aggressive nature of human gastric carcinoma is related to a variety of intracellular events, including activation of various oncogenes, inactivation of tumor suppressor genes. Therefore, great attention has been given to endogenous factors of tumors, which appear to be responsible for tumor cell growth, progression, and invasion. Identification of such endogenous factors not only leads to a better understanding of the carcinogenesis and development of gastric cancer, but also provides new strategies for developing agents that specifically suppress this process.

Semaphorins are the products of a large family of genes currently containing more than 30 members, all of which share a conserved N-terminal domain called the "sema" domain, a segment of approximately 400-500 amino acids[1]. Based on sequence similarity and distinctive structural features, these genes have been grouped into eight subclasses[1-8], of which classes 3-7 are the products of vertebrate semaphorins. Plexins

are identified as the best characterized semaphorin receptors, which are segregated into four sub-families containing nine members. It has been shown that some vertebrate semaphorins belonging to classes 4-7 can bind directly to plexins and activate plexin-mediated signal transduction[2,3]. These semaphorins and plexins have been originally characterized as constituents of the complex regulatory system responsible for the guidance of axons during the development of the central nervous system[4,5]. However, a growing body of evidence suggests that certain semaphorins, through interacting with its receptors, play a regulatory role in the occurrence and development of tumor[6-9]. Semaphorin 5A is a member of class 5 semaphorins. Plexin B3, belonging to class B plexin subfamily, is a receptor for semaphorin 5A[10]. However, it is unclear whether semaphorin 5A exerts certain biological functions in the progression of human cancers including gastric carcinoma through plexin B3.

In the present study, we investigated the protein and mRNA expression of semaphorin 5A, plexin B3 in primary gastric carcinoma as well as in its corresponding non-neoplastic mucosa and matched regional lymph node metastasis, and preliminarily analyzed their relation with the invasion and metastasis of gastric cancer.

MATERIALS AND METHODS

Patients and specimens

Forty-eight advanced gastric adenocarcinoma (TNM stage Ⅲ-Ⅳ) patients (28 male and 20 female) with lymph node metastasis diagnosed by postoperative pathology were investigated in this study. Their mean age was 58.7 years (range 45-68 years). The patients received neither chemotherapy nor radiation therapy prior to tumor resection and provided their consent for use of tumor tissue. Tissue blocks of non-neoplastic mucosa (> 5 cm away from the edge of tumor), primary tumor and its corresponding metastatic lymph nodes were obtained within 30 min after they were removed from the patients. Each block was cut into two pieces, one for routine pathologic diagnosis and the other for molecular analysis. Samples were frozen in liquid nitrogen immediately and stored at -260℃ until use.

Reverse transcription-polymerase chain reaction (RT-PCR)

Tissues were lysed using Trizol reagent (Invitrogen, Carlsbad, CA), and total RNA was isolated using chloroform and isopropyl alcohol according to the manufacturer's instructions. After RNA was quantified, 1-5 μg of RNA was annealed to Oligo (dT) at 65℃ for 5 min and cooled at room temperature. Using a proSTAR first strand RT-PCR kit (Stratagene, La Jolla, CA, USA), reverse transcriptase and dNTPs were added to the RNA-Oligo (dT) mixture and the reaction was performed at 42℃ for 1 h. Each single-strand cDNA was used for subsequent PCR amplification of semaphorin 5A, plexin B3 and β-actin with the latter used as a quantitative control. PCR was carried out in a reaction volume of 25 μL under the following conditions: an initial denaturation at 95℃ for 5 min, followed by 30 cycles at 94℃ for 30 s, at 55℃ for 50 s, at 72℃ for 40 s, and a final extension at 72℃ for 5 min on an authorized thermal cycler. The primer sequences used amplification are 5'-CTCAGTCGCTGTGAGCG TTAT-3' and 5'-CAGATGTTGGACCGCCAAATA-3' for semaphorin 5A, 5'-TCTGCTGCTGCGGTTCTG-3' and 5'-CCTCTCCACCATCTGCTTGTAG-3' for plexin B3, 5'-CGCACCACTGGCATTGTCAT-3' and 5'-TTC TCCTTGATGTCACGCAC-3' for β-actin, respectively. The primer sequences were synthesized by Beijing Genomics Institute (China). The PCR products were resolved in 1.5 % agarose gels and visualized by staining with ethidium bromide. To quantify the PCR products, bands representing the amplified products were analyzed by Quantity One Analysis Software (BIO-RAD Co., USA).

Real-time PCR

The reaction mixture volume was made up to 50 μL. Quantitative RT-PCR was performed using SYBR GreenER qPCR SuperMix reagents (Invitrogen) and a Bio-Rad iCycler. Relative transcript quantities were calculated using the ΔΔCt method with β-actin as the endogenous reference gene amplified from the samples. PCR conditions were as follows: an initial melting step at 95℃ for 1 min followed by 35 cycles at 95℃ for 90 s, at 60℃ for 30 s, at 72℃ for 30 s, and a final extension at 72℃ for 10 min. The primers used for RT-PCR are 5'-GGTACTGTTCTAGCGACGGC-3' and 5'-ATACTTGGGTTCGGGGTTGT-3' for semaphorin 5A, 5'-AAAGCCACCGAGGAGCCAGAA-3' and 5'-ACTTGACGGCGATGGGGATG-3' for plexin B3, 5'-TGACGTGGACATCCGCAAAG-3' and 5'-CTGGA AGGTGGACAGCGAGG-3' for β-actin, respectively.

Western blotting

Frozen specimens were homogenized in a lysis buffer [50 mmol/L Tris-HCl (pH 7.5), 150 mmol/L NaCl, 1 mmol/L EDTA, 0.25 % sodium deoxycholate, 1 % Triton X-100, 0.1 % sodium dodecyl sulfate (SDS), 1 mmol/L NaF, 1 mmol/L Na_3VO_4], and protease inhibitors (10 mg/L aprotinin and 1 mmol/L phenylmethylsulfonyl fluoride) were added to obtain total protein. An equal amount of protein, quantified with a bicinchoninic acid protein assay kit (Pierce Biotechnology, Rockford, IL, USA), was subjected to 10% SDS-polyacrylamide gel electrophoresis, and transferred to polyvinylidene difluoride membrane. The membranes were blocked with 5 % nonfat milk in Tris buffered saline with Tween 20 [TBST, 50 mmol/L Tris-HCl (pH 7.6), 150 mmol/L NaCl, 0.1 % Tween 20] for 2 h at room temperature, and subsequently incubated with primary anti-rabbit polyclonal antibody (anti-semaphorin 5A diluted at 1:400 and plexin B3 diluted at 1:500 and β-actin diluted at 1:2000 were purchased from Santa Cruz Biotechnology) in a blocking buffer at 4℃ overnight. Following a

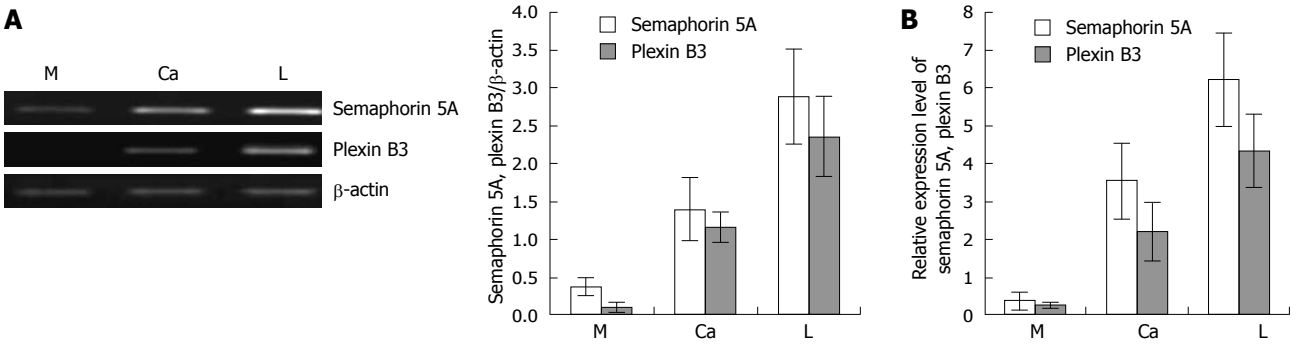

Figure 1 Expression of semaphorin 5A and plexin B3 mRNA in 48 samples of primary gastric carcinoma tissues and its corresponding non-neoplastic mucosa as well as matched regional lymph node metastasis. A: A representative result (left panel) and summary (right panel) of semaphorin 5A and plexin B3 expression in 48 samples of primary gastric carcinoma (Ca) and its corresponding nonneoplastic mucosa (M) as well as matched regional lymph node metastasis (L) examined by RT-PCR. The expression of β-actin was used as an internal control; B: Real time RT-PCR for relative expression levels of semaphorin 5A and plexin B3 in 48 samples of primary gastric carcinoma (Ca) and its corresponding nonneoplastic mucosa (M) as well as matched regional lymph node metastasis (L).

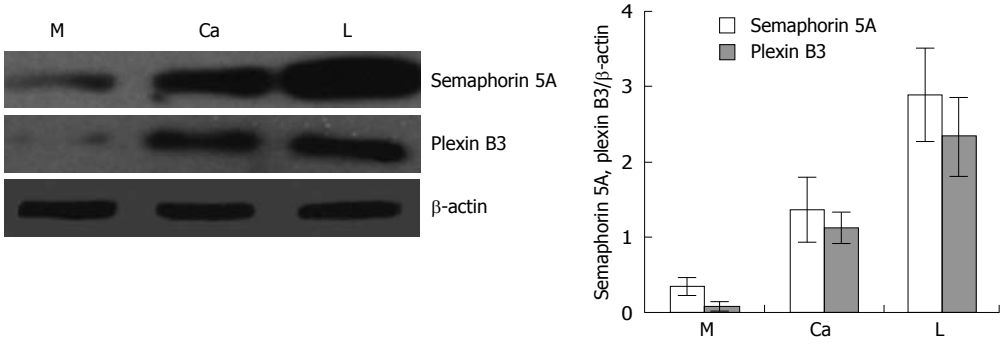

Figure 2 A representative result (left panel) and summary (right panel) of semaphorin 5A and plexin B3 protein expression in 48 samples of primary gastric carcinoma (Ca) and its corresponding nonneoplastic mucosa (M) as well as matched regional lymph node metastasis (L) examined by Western blotting. The expression of β-actin was used as an internal control.

washing with TBST, the membranes were incubated with horseradish peroxidase-conjugated rabbit anti-mouse secondary antibody (1:1000, Dako, Glostrup, Denmark) for 2 h at room temperature. The membranes were washed with TBST, and protein bands were visualized with enhanced chemiluminescence according to its manufacturer's instructions (KPL, Gaithersburg, USA). β-actin bands were taken as a loading control. Protein quantity was analyzed using the UTHSCSA Image Tool 3.0. Target protein expression was evaluated using the relative intensity ratio of target protein/loading control.

Statistical analysis

Results were expressed as mean ± SD. Statistical differences between different groups were assessed by ANOVA using SPSS12.0 statistical software. $P < 0.05$ was considered statistically significant.

RESULTS

Semaphorin 5A and plexin B3 mRNA expression

To infer the status of semaphorin 5A and plexin B3 in the invasion and metastasis of gastric carcinogenesis, we evaluated the mRNA expression of semaphorin 5A and plexin B3 using semi-quantitative RT-PCR in 48 samples of primary gastric carcinoma tissue and its corresponding non-neoplastic mucosa as well as matched regional lymph node metastasis. A representative result of RT-PCR for semaphorin 5A and plexin B3 expression is shown in Figure 1A. The expression of semaphorin 5A and plexin B3 mRNA gradually increased in nonneoplastic mucosa, primary gastric carcinoma and lymph node metastasis ($P < 0.05$). Moreover, the expression of semaphorin 5A was closely correlated with that of plexin B3. To confirm the RT-PCR result of semaphorin 5A and plexin B3, we performed real-time RT-PCR analysis in 20 samples of cDNAs from primary gastric cancer and non-neoplastic mucosa as well as matched regional lymph node metastasis. Similar results were observed (Figure 1B).

Semaphorin 5A and plexin B3 protein expression

The expression levels of semaphorin 5A, and plexin B3 were also measured by Western blotting in primary gastric carcinoma tissue and its corresponding nonneoplastic mucosa as well as matched regional lymph node metastasis. A representative result of Western blotting for the expression of semaphorin 5A and plexin B3 is shown in Figure 2. After normalization with β-actin, the expression of Semaphorin 5A and plexin B3 protein gradually increased in non-neoplastic mucosa, primary gastric carcinoma and lymph node metastasis ($P < 0.05$), which was consistent with the result from RT-PCR analysis.

DISCUSSION

Semaphorin 5A is a member of class 5 semaphorins which are anchored to cell membranes and characterized by seven type 1 thrombospondin repeats. Plexin B3,

belonging to class B plexin subfamily, was identified as a specific and functional receptor for semaphorin 5A. Semaphorin 5A and plexin B3 have been originally characterized as constituents of the complex regulatory system responsible for the wiring of neural networks during the development of the central nervous system, and subsequently found to participate in the activities outside of the nervous system such as migration of neural crest cells and heart development to name but a few examples[11,12]. However, very little is known about the expression and role of semaphorin 5A and plexin B3 in human cancers including gastric carcinoma. A random p-element insertion screen has been used to identify genes that modulate tumor progression and tumorigenicity in Drosophila study[13]. One of the genes identified in this screen is the Drosophila homologue of semaphorin 5C, with which semaphorin 5A shares a high sequence similarity[13]. In addition, experiments performed by Paolo Conrotto and co-workers revealed that semaphorin 5A, through plexin B3, stimulates the tyrosine kinase activity of Met and RON which has been shown to play a role in tumor progression[14,15]. Most importantly, there is cumulative evidence that certain semaphorins and their receptors implicated in axonal path finding in the developing nervous system are expressed in multiple types of cancer cells, modulate the behavior of cancer cells, promote tumor angiogenesis and progression by multiple mechanisms[16]. Taken together, these observations implicate that semaphorin 5A may play a role in the development and progression of human tumors by interacting with plexin B3.

To explore whether semaphorin 5A and plexin B3 are associated with the invasion and metastasis of gastric cancer and exert certain biological functions outside of the nervous system, we investigated the protein and mRNA expression of semaphorin 5A and plexin B3 in primary gastric carcinoma and its corresponding nonneoplastic mucosa as well as matched regional lymph node metastasis by RT-PCR and Western blotting assay. Our experimental results showed that the protein and mRNA expression level of semaphorin 5A was the lowest in normal gastric mucosa, moderate in primary gastric carcinoma, and the highest in lymph nodes with metastatic gastric carcinoma, respectively ($P < 0.05$). In contrast, plexin B3 and semaphorin 5A had a similar expression pattern, suggesting that the expression of plexin B3 is closely correlated with that of semaphorin 5A. These findings demonstrate that the expression of semaphorin 5A and its receptor plexin B3 increased gradually with gastric cancer procession, indicating that semaphorin 5A may play an important role in the invasion and metastasis of gastric carcinoma through plexin B3, displaying a novel expression and function of semaphorin 5A and plexin B3 outside of the nervous system. To our knowledge, this is the first report on the expression of semaphorin 5A and plexin B3 mRNA and protein in gastric carcinoma, and the functional role of semaphorin 5A and plexin B3 in the invasion and metastasis of gastric cancer.

In conclusion, semaphorin 5A and plexin B3 expression increases significantly with gastric carcinoma progression, and semaphorin 5A and plexin B3 may be involved in the processes of gastric cancer invasion and metastasis. Therefore, the novel expression and function of semaphorin 5A and plexin B3 outside of the nervous system not only add more knowledge about semaphorin 5A and plexin B3, but also shed some lights on the pathogenesis of gastric carcinoma, and probably represent a new therapeutic target for gastric carcinoma.

ACKNOWLEDGMENTS

The authors thank Dr. Xue-Shuang Huang for kindly revising our paper.

COMMENTS

Background

Gastric carcinoma is one of the most common malignant tumors in China. Invasion and metastasis are the main cause of cancer-related death. Therefore, it is necessary to investigate the mechanism underlying invasion and metastasis of malignant tumors. Semaphorin 5A and its receptor plexin B3 have been originally described in the nervous system, and are important in axon migration and proper central nervous system development. However, very little is known about the expression and role of semaphorin 5A and plexin B3 in human cancers including gastric carcinoma.

Research frontiers

Experiments were performed to study the expression of semaphorin 5A and plexin B3 in gastric carcinoma and its relation with tumor invasion and metastasis. This study showed that the expression of semaphorin 5A and plexin B3 increased gradually in non-neoplastic mucosa, primary gastric carcinoma, and lymph node metastasis, suggesting that the expression of semaphorin 5A and plexin B3 is closely correlated to the invasion and metastasis of gastric cancer.

Innovations and breakthroughs

This is the first report on the expression of semaphorin 5A and plexin B3 in gastric carcinoma, and the relation of semaphorin 5A and plexin B3 with the invasion and metastasis of gastric cancer.

Peer review

The authors studied the expression of semaphorin 5A and plexin B3 in gastric carcinoma and its relation with tumor invasion and metastasis, and showed that the expression level increased gradually in non-neoplastic mucosa, primary gastric carcinoma, and lymph node metastasis, and was positively related to tumor invasion and metastasis, which can be used in research of gastric carcinoma, and provide a new target for gastric carcinoma treatment.

REFERENCES

1 **Gherardi E**, Love CA, Esnouf RM, Jones EY. The sema domain. *Curr Opin Struct Biol* 2004; **14**: 669-678
2 **Yazdani U**, Terman JR. The semaphorins. *Genome Biol* 2006; **7**: 211
3 **Luo Y**, Raible D, Raper JA. Collapsin: a protein in brain that induces the collapse and paralysis of neuronal growth cones. *Cell* 1993; **75**: 217-227
4 **Negishi M**, Oinuma I, Katoh H. Plexins: axon guidance and signal transduction. *Cell Mol Life Sci* 2005; **62**: 1363-1371
5 **Kruger RP**, Aurandt J, Guan KL. Semaphorins command cells to move. *Nat Rev Mol Cell Biol* 2005; **6**: 789-800
6 **Potiron VA**, Roche J, Drabkin HA. Semaphorins and their receptors in lung cancer. *Cancer Lett* 2009; **273**: 1-14
7 **Sun Q**, Nawabi-Ghasimi F, Basile JR. Semaphorins in vascular development and head and neck squamous cell carcinoma-induced angiogenesis. *Oral Oncol* 2008; **44**: 523-531
8 **Neufeld G**, Kessler O. The semaphorins: versatile regulators of tumour progression and tumour angiogenesis. *Nat Rev*

Cancer 2008; **8**: 632-645
9 **Roth L**, Koncina E, Satkauskas S, Crémel G, Aunis D, Bagnard D. The many faces of semaphorins: from development to pathology. *Cell Mol Life Sci* 2009; **66**: 649-666
10 **Artigiani S**, Conrotto P, Fazzari P, Gilestro GF, Barberis D, Giordano S, Comoglio PM, Tamagnone L. Plexin-B3 is a functional receptor for semaphorin 5A. *EMBO Rep* 2004; **5**: 710-714
11 **Kantor DB**, Chivatakarn O, Peer KL, Oster SF, Inatani M, Hansen MJ, Flanagan JG, Yamaguchi Y, Sretavan DW, Giger RJ, Kolodkin AL. Semaphorin 5A is a bifunctional axon guidance cue regulated by heparan and chondroitin sulfate proteoglycans. *Neuron* 2004; **44**: 961-975
12 **Goldberg JL**, Vargas ME, Wang JT, Mandemakers W, Oster SF, Sretavan DW, Barres BA. An oligodendrocyte lineage-specific semaphorin, Sema5A, inhibits axon growth by retinal ganglion cells. *J Neurosci* 2004; **24**: 4989-4999
13 **Woodhouse EC**, Fisher A, Bandle RW, Bryant-Greenwood B, Charboneau L, Petricoin EF 3rd, Liotta LA. Drosophila screening model for metastasis: Semaphorin 5c is required for l(2)gl cancer phenotype. *Proc Natl Acad Sci USA* 2003; **100**: 11463-11468
14 **Conrotto P**, Corso S, Gamberini S, Comoglio PM, Giordano S. Interplay between scatter factor receptors and B plexins controls invasive growth. *Oncogene* 2004; **23**: 5131-5137
15 **Giordano S**, Corso S, Conrotto P, Artigiani S, Gilestro G, Barberis D, Tamagnone L, Comoglio PM. The semaphorin 4D receptor controls invasive growth by coupling with Met. *Nat Cell Biol* 2002; **4**: 720-724
16 **Neufeld G**, Shraga-Heled N, Lange T, Guttmann-Raviv N, Herzog Y, Kessler O. Semaphorins in cancer. *Front Biosci* 2005; **10**: 751-760

S- Editor Li LF **L- Editor** Wang XL **E- Editor** Zheng XM

Online Submissions: wjg.wjgnet.com
wjg@wjgnet.com
doi:10.3748/wjg.15.2805

World J Gastroenterol 2009 June 14; 15(22): 2805-2808
World Journal of Gastroenterology ISSN 1007-9327

CASE REPORT

Ligation-assisted endoscopic mucosal resection of gastric heterotopic pancreas

Mouen A Khashab, Oscar W Cummings, John M DeWitt

Mouen A Khashab, John M DeWitt, Division of Gastroenterology and Hepatology, Department of Medicine, Indiana University School of Medicine, IN 46202, United States
Oscar W Cummings, Department of Pathology, Indiana University School of Medicine, Indianapolis, IN 46202, United States
Author contributions: Khashab MA, DeWitt JM wrote and edited the manuscript; Cummings OW edited the pathology section of the manuscript.
Correspondence to: John M DeWitt, MD, Division of Gastroenterology and Hepatology, Department of Medicine, Indiana University, School of Medicine, IN 46202, United States. jodewitt@iupui.edu
Telephone: +1-317-2741113 Fax: +1-317-2788144
Received: October 13, 2008 Revised: November 26, 2008
Accepted: December 3, 2008
Published online: June 14, 2009

Abstract

Heterotopic pancreas is a congenital anomaly characterized by ectopic pancreatic tissue. Treatment of heterotopic pancreas may include expectant observation, endoscopic resection or surgery. The aim of this report was to describe the technique of ligation-assisted endoscopic mucosal resection (EMR) for resection of heterotopic pancreas of the stomach. Two patients (both female, mean age 32 years) were referred for management of gastric subepithelial tumors. Endoscopic ultrasound in both disclosed small hypoechoic masses in the mucosa and submucosa. Band ligation-assisted EMR was performed in both cases without complications. Pathology from the resected tumors revealed heterotopic pancreas arising from the submucosa. Margins were free of pancreatic tissue. Ligation-assisted EMR is technically feasible and may be considered for the endoscopic management of heterotopic pancreas.

Key words: Endoscopic mucosal resection; Endoscopic ultrasound; Heterotopic pancreas

Peer reviewers: Atsushi Nakajima, Professor, Division of Gastroenterology, Yokohama City University Graduate School of Medicine, 3-9 Fuku-ura, Kanazawa-ku, Yokohama 236-0004, Japan; Dr. Mitsuhiro Fujishiro, Department of Gastroenterology, Faculty of Medicine, University of Tokyo, 7-3-1 Hongo, Bunkyo-ku, Tokyo, Japan; Dr. Peter Draganov, University of Florida, 1600 SW Archer Rd., Gainesville, FL 32610, United States

Khashab MA, Cummings OW, DeWitt JM. Ligation-assisted endoscopic mucosal resection of gastric heterotopic pancreas. *World J Gastroenterol* 2009; 15(22): 2805-2808 Available from: URL: http://www.wjgnet.com/1007-9327/15/2805.asp DOI: http://dx.doi.org/10.3748/wjg.15.2805

INTRODUCTION

Heterotopic pancreas (HP), also known as pancreatic rest, was first described in 1727 when it was found in an ileal diverticulum[1]. It refers to an uncommon congenital anomaly characterized by the presence of ectopic pancreatic tissue far from the pancreas and without any anatomical or vascular communication with this organ. It occurs in 2% of the general population[2] and is more common in males than females[3]. HP may occur throughout the gastrointestinal tract but has a proclivity for involving the stomach and proximal small intestine. Most affected patients are asymptomatic although a minority may present with a variety of symptoms, most common being epigastric pain[2]. Options for treatment for heterotopic pancreas in the stomach include surgery[2-4], endoscopic resection[5-8] or conservative management. This report describes the first two cases of HP treated with band ligation-assisted endoscopic mucosal resection (EMR).

CASE REPORT

Case 1

A 49-year-old white female presented to her primary gastroenterologist with abdominal bloating and constipation. She was report anemic and found to have heme-occult positive stools. Work-up included a computer tomography (CT) scan of the abdomen and pelvis, colonoscopy and esophagogastroduodenoscopy (EGD). CT revealed small liver cysts but no other abnormalities. Colonoscopy demonstrated two small polyps that were removed. EGD showed a small, firm, umbilicated subepithelial antral mass. The mucosa overlying the mass was biopsied and showed chronic gastritis with no submucosal tissue present. The patient was referred to our endoscopy unit for upper endoscopic ultrasonography (EUS) of the antral lesion.

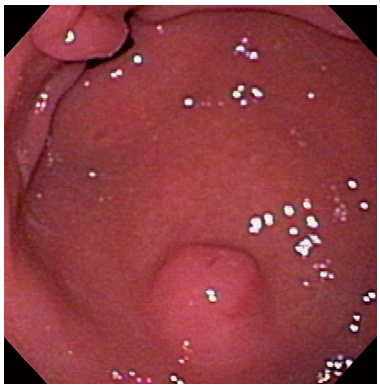

Figure 1 Endoscopic view of heterotopic pancreas of the stomach showing a medium-sized subepithelial nodule with central umbilication and normal overlying mucosa. The pylorus is visible distally.

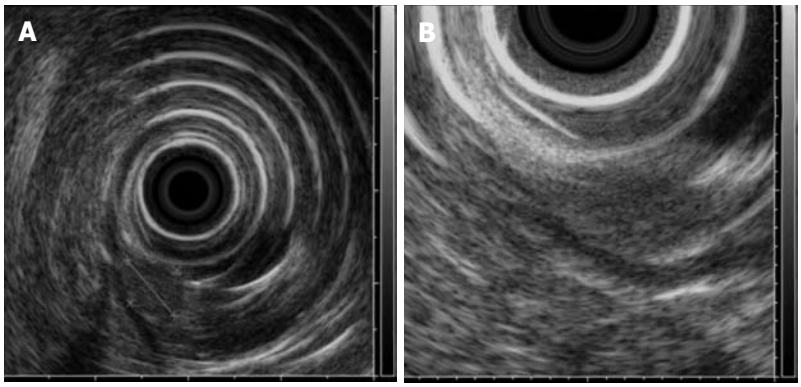

Figure 2 Radial EUS images. A pancreatic rest showing an 8 mm × 6 mm hypoechoic subepithelial mass appearing to involve the mucosa (A) and submucosa (B). The tumor was confirmed as submucosal in origin after resection without involvement of the mucosa.

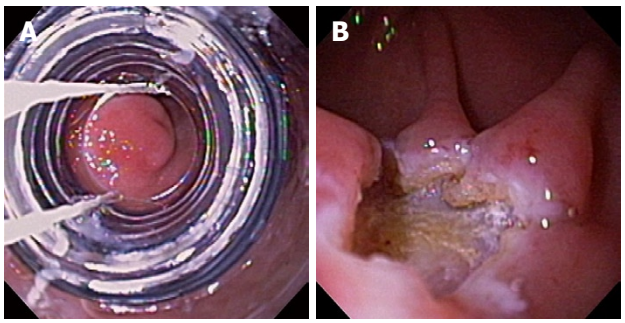

Figure 3 Ligation-assisted EMR of pancreatic rest. The banding device was positioned over the target lesion (A), suction was applied and a band was deployed. The lesion was then resected using electrocautery snare. Residual ulcer is shown (B).

She denied abdominal pain, nausea, vomiting, overt gastrointestinal bleeding or weight loss. Her physical examination revealed a healthy middle-aged white female in no apparent distress. Her abdominal examination was normal without tenderness. Prior to EUS, she was informed that the lesion most likely represented a pancreatic rest and that if suspected diagnosis was confirmed, then conservative management would be reasonable. Nevertheless, the patient expressed her preference for resection of the mass if possible. Informed consent was obtained and sedation was performed using a combination of intravenous midazolam and propofol. Initial EGD confirmed a single medium-sized subepithelial nodule along the greater curvature of the gastric antrum (Figure 1). The patient was then placed into the right lateral decubitus position and water was instilled into the distal stomach. Radial endosonography (GF-UE160-AL5; Olympus America Inc., Center Valley PA; USA) revealed a well-defined hypoechoic lesion from the deep mucosa/submucosa that measured 8 mm × 6 mm in maximal diameter (Figure 2A and B). There was no evidence of peritumoral adenopathy. Ligator-assisted EMR (Duette Multi-Band Mucosectomy; Cook Medical Inc., Winston-Salem, NC; USA) of the tumor was successfully performed using one band (Figure 3). The residual ulcer was closed using three endoclips (Resolution Clip; Boston Scientific Inc., Natick MA; USA). There were no complications. Surgical pathology from the resected specimen revealed heterotopic pancreatic tissue confined to the submucosa (Figure 4).

Case 2

A 15-year-old white female presented to her primary gastroenterologist with left upper quadrant abdominal pain. EGD showed a small subepithelial antral mass. The mucosa overlying the tumor was normal and biopsies showed only mild gastritis. The patient was then referred for an upper EUS. She denied nausea, vomiting, overt gastrointestinal bleeding or weight loss. Physical examination including abdominal examination was normal. Prior to EUS, review of endoscopic pictures from outside EGD suggested a pancreatic rest. Information was provided to the patient and parents that if suspected diagnosis was confirmed, then conservative management would be reasonable. Nevertheless, the patient and parents both expressed preference for tumor resection, if possible. Initial EGD confirmed a single medium-sized subepithelial nodule along the greater curvature of the prepyloric stomach (Figure 5). The patient was then placed into the right lateral decubitus position and water was instilled into the distal stomach. Radial endosonography revealed a well-defined 9 mm × 7 mm hypoechoic lesion from the deep mucosa and submucosa (Figure 6). The outer endosonographic borders were well defined. Ligator-assisted EMR of the tumor was successfully performed using one band (Figure 7). There were no complications. The resected specimen was submitted for pathologic examination, which revealed the presence of HP tissue confined to the submucosa with negative margins.

DISCUSSION

Heterotopic pancreas (HP), also known as pancreatic rest, is most often detected as an incidental finding during routine upper endoscopy. The typical endoscopic appearance in the stomach is as a firm round or oval umbilicated subepithelial nodule along the greater curvature situated

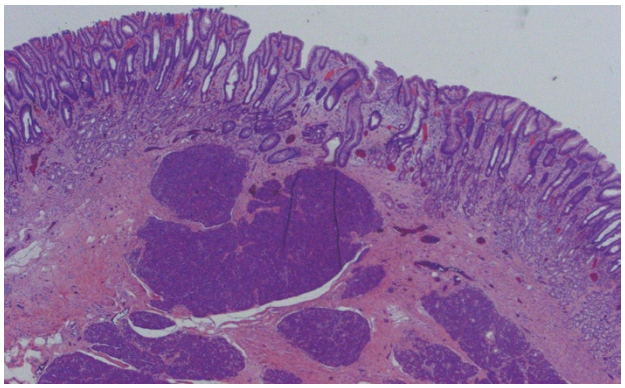

Figure 4 Photomicrograph of the resection specimen showing pancreatic tissue within the gastric submucosa (HE, × 10).

Figure 5 Endoscopic view of heterotopic pancreas of the stomach showing a medium-sized subepithelial nodule with central umbilication and normal overlying mucosa. The pylorus is visible distally.

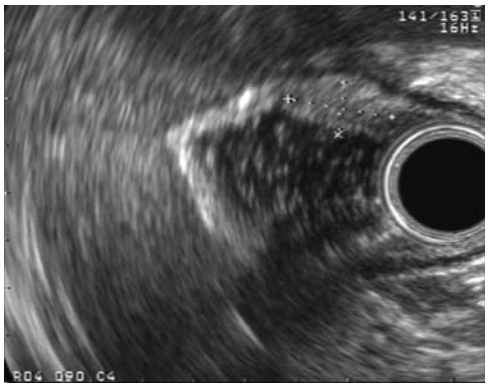

Figure 6 Radial EUS images of a pancreatic rest showing a 9 mm × 7 mm hypoechoic subepithelial mass appearing to involve the deep mucosa and submucosa. The tumor was confirmed as submucosal in origin after resection without involvement of the mucosa.

Figure 7 Ligation-assisted EMR of pancreatic rest.

several centimeters proximal to the pylorus. Most patients are asymptomatic, but symptoms may rarely occur due to the irritative effect of the hormones and enzymes secreted by the HP at a particular site[3]. Histologically, pancreatic rests vary from resembling the normal pancreas (acini, ducts and islets of Langerhans) to widely separated ducts within a muscular stroma[4,9]. Hence, complications in HP resemble those seen with the pancreas itself including acute pancreatitis[10,11], pancreatic cancer[12], cystic degeneration[13] and islet cell tumors[14]. Other rare reported complications include gastrointestinal bleeding[15], gastric outlet obstruction[16], jaundice[13] and abscess formation[10]. Asymptomatic HP can generally be followed expectantly with treatment reserved for patients who are symptomatic, have enlarging lesions or to ensure diagnostic certainty. Both pancreatic rests in these two patients were incidentally discovered during EGD for investigation of anemia and left upper quadrant pain, respectively. Nevertheless, removal was requested by both patients to ensure the suspected pre-procedural diagnosis.

The diagnosis of HP is not straightforward. Although umbilication is characteristic, the specificity of this endoscopic finding for HP remains unknown. The typical EUS image of a pancreatic rest in the stomach is a hypoechoic, heterogeneous submucosal mass, although the muscularis propria and mucosa may be occasionally involved. A ductal structure may also be discernible within the lesion. Although these endosonographic findings are suggestive of HP, the accuracy of EUS for the diagnosis of subepithelial tumors (other than gastrointestinal stromal tumors such as HP) is limited[7,17]. This fact is illustrated in our cases as the mucosa was incorrectly predicted to be involved in both patients.

Since HP is usually a submucosal tumor, pinch mucosal biopsies are invariably non-diagnostic. Nevertheless, Shalaby *et al*[18] reported a case of esophageal HP diagnosed with biopsies obtained with a jumbo forceps. Teixeira[19] has described the use of ethanol injection to create an artificial ulcer that then facilitated the removal of sufficient submucosal tissue to establish the diagnosis of HP. Goto *et al*[20] reported a case of esophageal HP diagnosed by EUS-guided FNA. Historically, the diagnosis of HP was often made by histological examination of surgical specimens. Some authors believe that it is difficult to obtain a definitive diagnosis of HP preoperatively[21] and therefore advocate surgical resection[3].

Although there are some reports of surgical resection of HP[2-4], EMR may be an attractive, less invasive option for resection of accessible lesions. However, there have only been a few reports[5-8] that describe the use EMR for HP resection (Table 1). Two groups have described the use of cap-assisted EMR[5,6]. The "inject, lift and cut", or "strip biopsy" EMR technique[7] was reported for the resection of 6 HP submucosal masses. Finally, Sun *et al*[8]

Table 1 Literature summary of HP cases treated with EMR

Author	Yr	Number of tumors	Mean tumor size (mm)	Tumor location	EMR technique	Follow-up[1] (mo)
Lee *et al*[5]	1999	1	Small	Stomach	CAP-assisted	NR
Faigel *et al*[6]	2001	1	10	Stomach	CAP-assisted	6
Kojima *et al*[7]	1999	6	13.5	Stomach	Strip biopsy	15
Sun *et al*[8]	2002	2	NR	Stomach	Inject and cut	12-17
Khashab *et al* (current study)	2008	2	8.5	Stomach	Ligation-assisted	NR

EMR: Endoscopic mucosal resection; NR: Not reported. [1]All cases with reported follow-up were without any recurrence.

studied the use of EUS-guided injection and the "inject and cut" EMR technique for the resection of 16 upper gastrointestinal submucosal tumors, two of which were gastric HP tumors. Ligation-assisted EMR may be more operator-friendly than the other EMR techniques. It requires neither saline injection nor snare prepositioning, and the concept of tissue capture is similar to the familiar variceal ligation technique. The current series, to our knowledge, is the first to describe the use of ligation-assisted EMR for gastric HP. This technique permitted a histologic confirmation of the suspected diagnosis and in both cases achieved a margin-negative resection without complication.

REFERENCES

1 **Elfving G**, Hästbacka J. Pancreatic heterotopia and its clinical importance. *Acta Chir Scand* 1965; **130**: 593-602
2 **Lai EC**, Tompkins RK. Heterotopic pancreas. Review of a 26 year experience. *Am J Surg* 1986; **151**: 697-700
3 **Ormarsson OT**, Gudmundsdottir I, Mårvik R. Diagnosis and treatment of gastric heterotopic pancreas. *World J Surg* 2006; **30**: 1682-1689
4 **Dolan RV**, ReMine WH, Dockerty MB. The fate of heterotopic pancreatic tissue. A study of 212 cases. *Arch Surg* 1974; **109**: 762-765
5 **Lee TH**, Wang HP, Huang SF, Wang TH, Lin JT. Endoscopic mucosal resection for treatment of heterotopic pancreas in the stomach. *J Formos Med Assoc* 1999; **98**: 643-645
6 **Faigel DO**, Gopal D, Weeks DA, Corless C. Cap-assisted endoscopic submucosal resection of a pancreatic rest. *Gastrointest Endosc* 2001; **54**: 782-784
7 **Kojima T**, Takahashi H, Parra-Blanco A, Kohsen K, Fujita R. Diagnosis of submucosal tumor of the upper GI tract by endoscopic resection. *Gastrointest Endosc* 1999; **50**: 516-522
8 **Sun S**, Wang M, Sun S. Use of endoscopic ultrasound-guided injection in endoscopic resection of solid submucosal tumors. *Endoscopy* 2002; **34**: 82-85
9 **DeBord JR**, Majarakis JD, Nyhus LM. An unusual case of heterotopic pancreas of the stomach. *Am J Surg* 1981; **141**: 269-273
10 **Kaneda M**, Yano T, Yamamoto T, Suzuki T, Fujimori K, Itoh H, Mizumoto R. Ectopic pancreas in the stomach presenting as an inflammatory abdominal mass. *Am J Gastroenterol* 1989; **84**: 663-666
11 **Matsushita M**, Hajiro K, Takakuwa H. Acute pancreatitis occurring in gastric aberrant pancreas accompanied by paralytic ileus. *Am J Gastroenterol* 1997; **92**: 2121-2122
12 **Jeng KS**, Yang KC, Kuo SH. Malignant degeneration of heterotopic pancreas. *Gastrointest Endosc* 1991; **37**: 196-198
13 **Fléjou JF**, Potet F, Molas G, Bernades P, Amouyal P, Fékété F. Cystic dystrophy of the gastric and duodenal wall developing in heterotopic pancreas: an unrecognised entity. *Gut* 1993; **34**: 343-347
14 **Rose C**, Kessaram RA, Lind JF. Ectopic gastric pancreas: a review and report of 4 cases. *Diagn Imaging* 1980; **49**: 214-218
15 **Endo Y**, Yazumi S, Kimura Y, Uza N, Matsuura M, Kodama Y, Nakase H, Chiba T. A case of ileal heterotopic pancreas with repeated melena. *Gastrointest Endosc* 2007; **65**: 156-157; discussion 157
16 **Shaib YH**, Rabaa E, Feddersen RM, Jamal MM, Qaseem T. Gastric outlet obstruction secondary to heterotopic pancreas in the antrum: case report and review. *Gastrointest Endosc* 2001; **54**: 527-530
17 **Brand B**, Oesterhelweg L, Binmoeller KF, Sriram PV, Bohnacker S, Seewald S, De Weerth A, Soehendra N. Impact of endoscopic ultrasound for evaluation of submucosal lesions in gastrointestinal tract. *Dig Liver Dis* 2002; **34**: 290-297
18 **Shalaby M**, Kochman ML, Lichtenstein GR. Heterotopic pancreas presenting as dysphagia. *Am J Gastroenterol* 2002; **97**: 1046-1049
19 **Teixeira CR**, Haruma K, Shimamoto T, Tsuda T, Okamoto S, Sumii K, Kajiyama G. Heterotopic pancreas diagnosed by endoscopic ultrasonography and endoscopic injection of ethanol to make a histologic diagnosis. *J Clin Gastroenterol* 1992; **15**: 52-54
20 **Goto J**, Ohashi S, Okamura S, Urano F, Hosoi T, Ishikawa H, Segawa K, Hirooka Y, Ohmiya N, Itoh A, Hashimoto S, Niwa Y, Goto H. Heterotopic pancreas in the esophagus diagnosed by EUS-guided FNA. *Gastrointest Endosc* 2005; **62**: 812-814
21 **Hsia CY**, Wu CW, Lui WY. Heterotopic pancreas: a difficult diagnosis. *J Clin Gastroenterol* 1999; **28**: 144-147

S- Editor Tian L **L- Editor** Logan S **E- Editor** Yin DH

Online Submissions: wjg.wjgnet.com
wjg@wjgnet.com
doi:10.3748/wjg.15.2809

World J Gastroenterol 2009 June 14; 15(22): 2809-2811
World Journal of Gastroenterology ISSN 1007-9327

CASE REPORT

Meckel's diverticulum masked by a long period of intermittent recurrent subocclusive episodes

Daniela Codrich, Andrea Taddio, Jurgen Schleef, Alessandro Ventura, Federico Marchetti

Daniela Codrich, Jurgen Schleef, Department of Pediatric Surgery, Institute of Child Health, IRCCS Burlo Garofolo, 34137 Trieste, Italy
Andrea Taddio, Alessandro Ventura, Federico Marchetti, Department of Pediatrics, Institute of Child Health, IRCCS Burlo Garofolo, 34137 Trieste, Italy
Author contributions: All authors contributed to the intellectual content and approved the final version; Schleef J, Ventura A and Marchetti F designed the study; Taddio A and Marchetti F performed the research; Codrich D, Taddio A and Marchetti F wrote the paper.
Correspondence to: Daniela Codrich, MD, Department of Pediatric Surgery, Institute of Child Health, IRCCS Burlo Garofolo, Trieste. Via dell'Istria 65/1, 34137 Trieste, Italy. codrich@yahoo.com
Telephone: +39-40-3785217 Fax: +39-40-3785537
Received: February 19, 2009 Revised: May 11, 2009
Accepted: May 18, 2009
Published online: June 14, 2009

Abstract

Meckel's diverticulum (MD) is the most frequent congenital abnormality of the small bowel and it is often difficult to diagnose. It is usually asymptomatic but approximately 4% are symptomatic with complications such as bleeding, intestinal obstruction, and inflammation. The authors report a case of a 7-year-old boy with a one-year history of recurrent periumbilical colicky pain with associated alimentary vomiting, symptoms erroneously related to a cyclic vomiting syndrome but not to MD. The clinical features and the differential diagnostic methods employed for diagnosis of MD are discussed.

Key words: Meckel diverticulum; Abdominal pain; Recurrent subocclusive episodes, Diagnostic imaging

Peer reviewer: Dr. Lee Bouwman, Leiden University Medical Centre, Department of surgery, Albinusdreef 2, PO Box 9600, 230 RC Leiden, The Netherlands

Codrich D, Taddio A, Schleef J, Ventura A, Marchetti F. Meckel's diverticulum masked by a long period of intermittent recurrent subocclusive episodes. *World J Gastroenterol* 2009; 15(22): 2809-2811 Available from: URL: http://www.wjgnet.com/1007-9327/15/2809.asp DOI: http://dx.doi.org/10.3748/wjg.15.2809

INTRODUCTION

Meckel's diverticulum (MD) occurs in about 2% of the population, making it the most prevalent congenital abnormality of the gastrointestinal tract. It can be asymptomatic or mimic common abdominal disorders. We report a case of a child with an intraoperative diagnosis of MD, with a long history of recurrent abdominal pain and vomiting misdiagnosed as a cyclic vomiting syndrome.

CASE REPORT

A 7-year-old boy was referred with a one-year history of periumbilical colicky pain with associated alimentary vomiting. The frequency of the episodes increased from one per month to weekly and then daily vomiting. The pain usually spontaneously disappeared within a few hours. During the weeks before our visit, the painful episodes lasted longer and were reported to occur also at night. The child lost one kilogram in one month. No diarrhoea was reported, the boy was rather constipated. Previous medical investigations, abdominal ultrasonography and plain abdominal film were negative.

Neither abdominal tenderness, nor liver or spleen enlargement, nor abdominal masses were identified at palpation. Intestinal bacterial overgrowth and celiac disease were excluded by laboratory tests. Complete blood cell count, electrolytes, glycemia, blood ammonia, renal and hepatic function, pancreatic enzymes, C-reactive protein, erythrocyte sedimentation rate, and gamma globulins were within normal ranges.

A plain abdominal film was unremarkable, and a small bowel enema indicated normal transit and normal appearance of the intestinal loops. An abdominal ultrasound (US) revealed a supravesical anechoic mass of about 4 cm × 3 cm × 2 cm, with fluid inside (Figure 1).

Pelvic magnetic resonance imaging (MRI) confirmed the presence of the 4 cm mass, located above and behind the bladder, slightly to the right of the midline, with liquid content (Figure 2).

With the suspicion of a mesenteric cyst or an intestinal duplication, the child underwent an exploratory laparoscopy. The intraoperative macroscopic finding was that of MD. Diagnosis was confirmed by histological features.

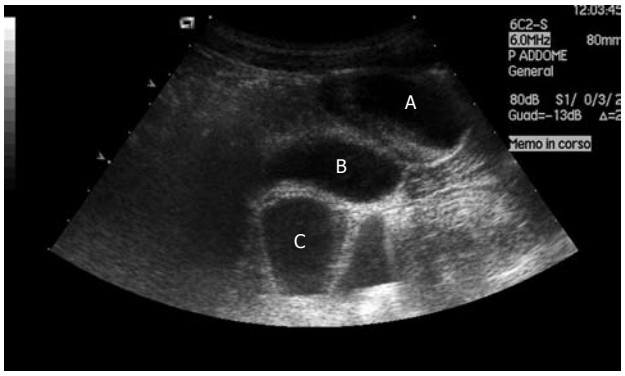

Figure 1 Abdominal ultrasound: anechoic oval supravesical lesion with fluid-fluid level (A); bladder (B); bowel (C).

Figure 2 Abdominal MRI; T1 weighted sequence with fat-suppression (SPIR) after contrast medium, saggital plane: hypointense oval supravesical lesion with air-fluid level and thin enhanced wall (A); bladder (B); rectum (C).

DISCUSSION

MD is the most common congenital anomaly of the gastrointestinal tract. The "rule of two" can remind us of some of its main features: occurs in 2% of the population; usually discovered before 2 years of age; occurs within 2 feet of the ileocecal valve; is 2 inches long and 2 cm in diameter[1]. It is the result of an incomplete atrophy of the omphalomesenteric duct. The location of the diverticulum is on the antimesenteric border of the small intestine, most frequently between 30 cm and 90 cm from the ileocecal valve; there can be a fibrous connection to the umbilicus, as the remnant of the partially obliterated vitelline duct.

MD is a true diverticulum, composed of all layers of the intestinal wall, and is lined by normal small intestine epithelium. Gastric heterotopias can be found in roughly 50% of cases, and pancreatic, duodenal, colonic, or biliary mucosa have rarely been reported.

MD can be silent all through a lifetime: clinical symptoms arise from complications (MD carriers have a 4% lifetime risk of developing a complication)[2]. Hemorrhage is the result of peptic ulceration of the ileal mucosa next to an acid-producing gastric mucosal heterotopia: the presentation of the blood loss varies from recurrent minimal intestinal bleeding, to a massive, shock-producing hemorrhage, and it is usually painless. Diverticulitis can mimic an acute appendicitis: pain is frequently localized in the midline or slightly to the right and, as in appendiceal disease, inflammation can progress until perforation. The diverticulum can invert into the ileal lumen and become the starting point of an ileo-ileal or ileo-ileo-colic intussusception: symptoms can not be discriminated from those ascribed to idiopathic intussusception, even though the onset of the former is described to occur at an earlier age. A further mechanism by which MD can produce intestinal obstruction is to turn around a fibrous remnant: symptoms may vary from intermittent recurrent subocclusive episodes, as in our patient, to frank occlusion with strangulation features if a complete volvulus occurs[3]. "Littre hernia" occurs when a MD protrudes into a potential abdominal opening such as umbilical, inguinal, or femoral, and can be accompanied in some cases by entrapment, inflammation, and necrosis[1]. Tumors are reported in 0.5% to 3% of symptomatic diverticula in adulthood (carcinomas in one third of the cases)[3].

Preoperative diagnosis of a complicated MD can be challenging and often difficult to establish because clinical symptoms and imaging features overlap with those of other disorders causing acute abdominal pain or gastrointestinal bleeding[4].

Initially, our case was misdiagnosed as a cyclic vomiting syndrome and a functional abdominal pain, since neither inflammatory nor bleeding clinical features were present, and laboratory tests were substantially within normal ranges. If any bleeding episode had been reported, a 99mTc-pertechnetate scintigraphy would have been indicated: the principle is that a bleeding diverticulum consists of ulcerated ectopic gastric mucosa that can be revealed with 99mTc-pertechnetate. This concentrates in gastric tissue leading to a reported sensitivity of between 60% and 80%[5].

The progressive worsening of painful episodes, however, prompted us to exclude causes of pain and vomiting requiring surgery, such as intestinal malrotation, which was ruled out by a normal small bowel enema. It is reported in the literature that enteroclysis may be of help in detecting MD but in our case the diverticular image was missed[6].

The US findings of a cyst supported the suspicion of a surgery-indicated cause for the painful episodes, but other gut malformations such as mesenteric cysts or enteric duplications, both of which can present with subocclusive symptoms, were taken into account in the differential diagnoses of our child. US and computed tomography are reported in the literature to be valuable radiological investigations in MD patients without the classical history of painless hemorrhage[7,8].

Complicated MD has a spectrum of radiological features which may help in the preoperative investigations, but are not always diagnostic[7-9]. Our rationale in choosing MRI as a second-line radiological examination lay in the fact that we needed a better anatomical definition of what we suspected was a pelvic mass, without further irradiation of the child: there is no evidence for the use of MRI to detect MD in the literature. Final diagnosis is almost always done at surgery: exploratory laparoscopy is recommended because it affords the possibility of simultaneous surgical resection, which is the definitive cure of a symptomatic MD[10].

In conclusion, Although MD is the most prevalent congenital abnormality of the gastrointestinal tract, it is often difficult to diagnose. The diagnosis of MD should be considered in children with intestinal bleeding, unexplained recurrent abdominal pain, and nausea and vomiting suggestive of cyclic vomiting syndrome.

REFERENCES

1 **Skandalakis PN**, Zoras O, Skandalakis JE, Mirilas P. Littre hernia: surgical anatomy, embryology, and technique of repair. *Am Surg* 2006; **72**: 238-743

2 **Martin JP**, Connor PD, Charles K. Meckel's diverticulum. *Am Fam Physician* 2000; **61**: 1037-1042, 1044

3 **Yahchouchy EK**, Marano AF, Etienne JC, Fingerhut AL. Meckel's diverticulum. *J Am Coll Surg* 2001; **192**: 658-662

4 **McCollough M**, Sharieff GQ. Abdominal pain in children. *Pediatr Clin North Am* 2006; **53**: 107-137, vi

5 **Poulsen KA**, Qvist N. Sodium pertechnetate scintigraphy in detection of Meckel's diverticulum: is it usable? *Eur J Pediatr Surg* 2000; **10**: 228-231

6 **Sommers S**. Congenital and developmental abnormalities of the small bowel. In: Gourtsoyiannis NC, editor. Radiological imaging of the small intestine. Berlin-Heidelberg: Springer, 2002: 216-219

7 **Elsayes KM**, Menias CO, Harvin HJ, Francis IR. Imaging manifestations of Meckel's diverticulum. *AJR Am J Roentgenol* 2007; **189**: 81-88

8 **Thurley PD**, Halliday KE, Somers JM, Al-Daraji WI, Ilyas M, Broderick NJ. Radiological features of Meckel's diverticulum and its complications. *Clin Radiol* 2009; **64**: 109-118

9 **Daneman A**, Lobo E, Alton DJ, Shuckett B. The value of sonography, CT and air enema for detection of complicated Meckel diverticulum in children with nonspecific clinical presentation. *Pediatr Radiol* 1998; **28**: 928-932

10 **Shalaby RY**, Soliman SM, Fawy M, Samaha A. Laparoscopic management of Meckel's diverticulum in children. *J Pediatr Surg* 2005; **40**: 562-567

S- Editor Li LF **L- Editor** Cant MR **E- Editor** Ma WH

Online Submissions: wjg.wjgnet.com
wjg@wjgnet.com
www.wjgnet.com

World J Gastroenterol 2009 June 14; 15(22): 2812
World Journal of Gastroenterology ISSN 1007-9327

ACKNOWLEDGMENTS

Acknowledgments to reviewers of *World Journal of Gastroenterology*

Many reviewers have contributed their expertise and time to the peer review, a critical process to ensure the quality of *World Journal of Gastroenterology*. The editors and authors of the articles submitted to the journal are grateful to the following reviewers for evaluating the articles (including those published in this issue and those rejected for this issue) during the last editing time period.

Luigi Bonavina, Professor
Department of Surgery, Policlinico San Donato, University of Milano, via Morandi 30, Milano 20097, Italy

Nikolaus Gassler, Professor
Institute of Pathology, University Hospital RWTH Aachen, Pauwelsstrasse 30, 52074 Aachen, Germany

Edoardo G Giannini, Assistant Professor
Department of Internal Medicine, Gastroenterology Unit, Viale Benedetto XV, no. 6, Genoa, 16132, Italy

Ajay Goel, PhD
Department of Internal Medicine, Division of Gastroenterology, Baylor University Medical Center and Charles A Sammons Cancer Center, 3500 Gaston Avenue, Suite H-250, Dallas, TX 75246, United States

Maria Gutiérrez-Ruiz Concepción, PhD
Departamento de Ciencias de la Salud, Universidad Autónoma Metropolitana-Iztapalapa, DCBS, Av San Rafael Atlixco 186, Colonia Vicentina, México, DF 09340, México

Keiji Hirata, MD
Surgery 1, University of Occupational and Environmental Health, 1-1 Iseigaoka, Yahatanishi-ku, Kitakyushu 807-8555, Japan

Yik-Hong Ho, Professor
Department of Surgery, School of Medicine, James Cook University, Townsville 4811, Australia

Toru Ishikawa, MD
Department of Gastroenterology, Saiseikai Niigata Second Hospital, Teraji 280-7, Niigata, Niigata 950-1104, Japan

Robert J Korst, MD
Department of Cardiothoracic Surgery, Weill Medical College of Cornell University, Room M404, 525 East 68th Street, New York 10032, United States

James D Luketich, MD, Professor and Chief
Division of Thoracic and Foregut Surgery University of Pittsburgh Medical Center Pittsburgh, PA 15213, United States

Roberto Mazzanti, MD, Professor, Chair of Medical Oncology
Department of Internal Medicine, University of Florence, viale Morgagni, 85-50134 Florence, Italy

Atsushi Nakajima, Professor
Division of Gastroenterology, Yokohama City University Graduate School of Medicine, 3-9 Fuku-ura, Kanazawa-ku, Yokohama 236-0004, Japan

Vasiliy I Reshetnyak, MD, PhD, Professor
Scientist Secretary of the Scientific Research Institute of General Reanimatology, 25-2, Petrovka str., 107031, Moscow, Russia

Marco Romano, MD, Professor
Dipartimento di Internistica Clinica e Sperimentale-Gastroenterologia, II Policlinico, Edificio 3, II piano, Via Pansini 5, 80131 Napoli, Italy

Gerardo Rosati, MD
Medical Oncology Unit, "S. Carlo" Hospita, Via Potito Petrone, 1, Potenza 85100, Italy

Philip Rosenthal, MD, Professor of Pediatrics & Surgery
UCSF, 500 Parnassus Avenue, Box 0136, MU 4-East, San Francisco, CA 94143-0136, United States

Alain L Servin, PhD
Faculty of Pharmacy, French National Institute of Health and Medical Research, Unit 756, Rue J.-B. Clément, F-922296 Châtenay-Malabry, France

Bruno Stieger, Professor
Department of Medicine, Division of Clinical Pharmacology and Toxicology, University Hospital, Zurich 8091, Switzerland

Xiao-Feng Sun, Professor
Department of Oncology, Biomedicine and Surgery, Department of Oncology, Biomedicine and Surgery, Linköping University, Linköping 58185, Sweden

Simon D Taylor-Robinson, MD
Department of Medicine A, Imperial College London, Hammersmith Hospital, Du Cane Road, London W12 0HS, United Kingdom

Frank I Tovey, OBE, ChM, FRCS
Honorary Research Felllow, Department of Surgery, University College London, London, United Kingdom

Sun-Lung Tsai, MD, PhD, Professor, Director
Hepatogastroenterology Section, Department of Internal Medicine and Liver Research Unit, Department of Medical Research, Chi Mei Medical Center, 901 Chung Hwa Road, Young-Kang City, Tainan County 710 , Taiwan, China

Akihito Tsubota, Assistant Professor
Institute of Clinical Medicine and Research, Jikei University School of Medicine, 163-1 Kashiwa-shita, Kashiwa, Chiba 277-8567, Japan

Saúl Villa-Trevio, MD, PhD
Departamento de Biología Celular, Centro de Investigación y de Estudios Avanzados del IPN (Cinvestav), Ave. IPN No. 2508. Col. San Pedro, Zacatenco, CP 07360, México, DF, México

World J Gastroenterol 2009 June 14; 15(22): 2813
World Journal of Gastroenterology ISSN 1007-9327

Meetings

Events Calendar 2009

January 12-15, 2009
Hyatt Regency San Francisco, San Francisco, CA
Mouse Models of Cancer

January 21-24, 2009
Westin San Diego Hotel, San Diego, CA
Advances in Prostate Cancer Research

February 3-6, 2009
Carefree Resort and Villas, Carefree, AZ (Greater Phoenix Area)
Second AACR Conference
The Science of Cancer Health Disparities in Racial/Ethnic Minorities and the Medically Underserved

February 7-10, 2009
Hyatt Regency Boston, Boston, MA
Translation of the Cancer Genome

February 8-11, 2009
Westin New Orleans Canal Place, New Orleans, LA
Chemistry in Cancer Research: A Vital Partnership in Cancer Drug Discovery and Development

February 13-16, 2009
Hong Kong Convention and Exhibition Centre, Hong Kong, China
19th Conference of the APASL
http://www.apasl2009hongkong.org/en/home.aspx

February 27-28, 2009
Orlando, Florida
AGAI/AASLD/ASGE/ACG Training Directors' Workshop

February 27-Mar 1, 2009
Vienna, Austria
EASL/AASLD Monothematic: Nuclear Receptors and Liver Disease
www.easl.ch/vienna2009

March 13-14, 2009
Phoenix, Arizona
AGAI/AASLD Academic Skills Workshop

March 20-24, 2009
Marriott Wardman Park Hotel
Washington, DC
13th International Symposium on Viral Hepatitis and Liver Disease

March 23-26, 2009
Glasgow, Scotland
British Society of Gastroenterology (BSG) Annual Meeting
Email: bsg@mailbox.ulcc.ac.uk

April 8-9, 2009
Silver Spring, Maryland
2009 Hepatotoxicity Special Interest Group Meeting

April 18-22, 2009
Colorado Convention Center, Denver, CO
AACR 100th Annual Meeting 2009

April 22-26, 2009
Copenhagen, Denmark
the 44th Annual Meeting of the European Association for the Study of the Liver (EASL)
http://www.easl.ch/

May 17-20, 2009
Denver, Colorado, USA
Digestive Disease Week 2009

May 29-June 2, 2009
Orange County Convention Center
Orlando, Florida
45th ASCO Annual Meeting
www.asco.org/annualmeeting

May 30, 2009
Chicago, Illinois
Endpoints Workshop: NASH

May 30-June 4, 2009
McCormick Place, Chicago, IL
DDW 2009
http://www.ddw.org

June 17-19, 2009
North Bethesda, MD
Accelerating Anticancer Agent Development

June 20-26, 2009
Flims, Switzerland
Methods in Clinical Cancer Research (Europe)

June 24-27 2009
Barcelona, Spain
ESMO Conference: 11th World Congress on Gastrointestinal Cancer
www.worldgicancer.com

June 25-28, 2009
Beijing International Convention Center (BICC), Beijing, China
World Conference on Interventional Oncology
http://www.chinamed.com.cn/wcio2009/

July 5-12, 2009
Snowmass, CO, United States
Pathobiology of Cancer: The Edward A. Smuckler Memorial Workshop

July 17-24, 2009
Aspen, CO, United States
Molecular Biology in Clinical Oncology

August 1-7, 2009
Vail Marriott Mountain Resort, Vail, CO, United States
Methods in Clinical Cancer Research

August 14-16, 2009
Bell Harbor Conference Center, Seattle, Washington, United States
Practical Solutions for Successful Management
http://www.asge.org/index.aspx?id=5040

September 23-26, 2009
Beijing International Convention Center (BICC), Beijing, China
19th World Congress of the International Association of Surgeons, Gastroenterologists and Oncologists(IASGO)
http://iasgo2009.org/en/index.shtml

September 27-30, 2009
Taipei, China
Asian Pacific Digestive Week
http://www.apdwcongress.org/2009/index.shtml

October 7-11, 2009
Boston Park Plaza Hotel and Towers, Boston, MA, United States
Frontiers in Basic Cancer Research

October 13-16, 2009
Hyatt Regency Mission Bay Spa and Marina, San Diego, CA, United States
Advances in Breast Cancer Research: Genetics, Biology, and Clinical Applications

October 20-24, 2009
Versailles, France
Fifth International Conference on Tumor Microenvironment: Progression, Therapy, and Prevention

October 30-November 3, 2009
Boston, MA, United States
The Liver Meeting

November 15-19, 2009
John B. Hynes Veterans Memorial Convention Center, Boston, MA, United States
AACR-NCI-EORTC Molecular Targets and Cancer Therapeutics

November 21-25, 2009
London, UK
Gastro 2009 UEGW/World Congress of Gastroenterology
www.gastro2009.org

Global Collaboration for Gastroenterology

For the first time in the history of gastroenterology, an international conference will take place which joins together the forces of four pre-eminent organisations: Gastro 2009, UEGW/WCOG London. The United European Gastroenterology Federation (UEGF) and the World Gastroenterology Organisation (WGO), together with the World Organisation of Digestive Endoscopy (OMED) and the British Society of Gastroenterology (BSG), are jointly organising a landmark meeting in London from November 21-25, 2009. This collaboration will ensure the perfect balance of basic science and clinical practice, will cover all disciplines in gastroenterology (endoscopy, digestive oncology, nutrition, digestive surgery, hepatology, gastroenterology) and ensure a truly global context; all presented in the exciting setting of the city of London. Attendance is expected to reach record heights as participants are provided with a compact "all-in-one" programme merging the best of several GI meetings. Faculty and participants from all corners of the earth will merge to provide a truly global environment conducive to the exchange of ideas and the forming of friendships and collaborations.

Online Submissions: wjg.wjgnet.com
wjg@wjgnet.com
www.wjgnet.com

World J Gastroenterol 2009 June 14; 15(22): 2814-2816
World Journal of Gastroenterology ISSN 1007-9327

Instructions to authors

GENERAL INFORMATION

World Journal of Gastroenterology (*World J Gastroenterol* ISSN 1007-9327 CN 14-1219/R) is a weekly open-access (OA) peer-reviewed journal supported by an editorial board consisting of 1179 experts in gastroenterology and hepatology from 60 countries.

The biggest advantage of the OA model is that it provides free, full-text articles in PDF and other formats for experts and the public without registration, which eliminates the obstacle that traditional journals possess and usually delays the speed of the propagation and communication of scientific research results. The open access model has been proven to be a true approach that may achieve the ultimate goal of the journals, i.e. the maximization of the value to the readers, authors and society.

Maximization of the value of the readers can be comprehended in two ways. First, the journal publishes articles that can be directly read or downloaded free of charge at any time, which attracts more readers. Second, the readers can apply the knowledge in clinical practice without delay after reading and understanding the information in their fields. In addition, the readers are encouraged to propose new ideas based on those of the authors, or to provide viewpoints that are different from those of the authors. Such discussions or debates among different schools of thought will definitely boost advancements and developments in the fields. Maximization of the value of the authors refers to the fact that these journals provide a platform that promotes the speed of propagation and communication to a maximum extent. This is also what the authors really need. Maximization of the value of the society refers to the maximal extent of the social influences and impacts produced by the high quality original articles published in the journal. This is also the main purpose of many journals around the world.

The major task of *WJG* is to rapidly report the most recent results in basic and clinical research on gastroenterology, hepatology, endoscopy and gastrointestinal surgery fields, specifically including autoimmune, cholestatic and biliary disease, esophageal, gastric and duodenal disorders, cirrhosis and its complications, celiac disease, dyspepsia, gastroesophageal reflux disease, esophageal and stomach cancers, carcinoma of the colon and rectum, gastrointestinal bleeding, gastrointestinal infection, intestinal inflammation, intestinal microflora and immunity, irritable bowel syndrome; liver biology/pathobiology, liver failure, growth and cancer; liver failure/cirrhosis/portal hypertension, liver fibrosis; *Helicobacter pylori*, hepatitis B and C virus, hepatology elsewhere; pancreatic disorders, pancreas and biliary tract disease, pancreatic cancer; transplantation, genetics, epidemiology, microbiology and inflammatory disorders, molecular and cell biology, nutrition; geriatric gastroenterology, pediatric gastroenterology, steatohepatitis and metabolic liver disease; diagnosis and screening, endoscopy, imaging and advanced technology.

The columns in the issues of *WJG* will be adjusted in 2009, which will include: (1) Editorial: To introduce and comment on the substantial advance and its importance in the fast-developing areas; (2) Frontier: To review the most representative achievements and comment on the current research status in the important fields, and propose directions for the future research; (3) Topic Highlight: This column consists of three formats, including (A) 10 invited review articles on a hot topic, (B) a commentary on common issues of this hot topic, and (C) a commentary on the 10 individual articles; (4) Observation: To update the development of old and new questions, highlight unsolved problems, and provide strategies on how to solve the questions; (5) Guidelines for Basic Research: To provide Guidelines for basic research; (6) Guidelines for Clinical Practice: To provide guidelines for clinical diagnosis and treatment; (7) Review: To systemically review the most representative progress and unsolved problems in the major scientific disciplines, comment on the current research status, and make suggestions on the future work; (8) Original Articles: To originally report the innovative and valuable findings in gastroenterology and hepatology; (9) Brief Articles: To briefly report the novel and innovative findings in gastroenterology and hepatology; (10) Case Report: To report a rare or typical case; (11) Letters to the Editor: To discuss and make reply to the contributions published in *WJG*, or to introduce and comment on a controversial issue of general interest; (12) Book Reviews: To introduce and comment on quality monographs of gastroenterology and hepatology; (13) Guidelines: To introduce Consensuses and Guidelines reached by international and national academic authorities worldwide on basic research and clinical practice in gastroenterology and hepatology.

Indexed and abstracted in

Current Contents®/Clinical Medicine, Science Citation Index Expanded (also known as SciSearch®) and Journal Citation Reports/Science Edition, Index Medicus, MEDLINE and PubMed, Chemical Abstracts, EMBASE/Excerpta Medica, Abstracts Journals, PubMed Central, Digital Object Identifier, CAB Abstracts and Global Health. ISI JCR 2003-2000 IF: 3.318, 2.532, 1.445 and 0.993.

Published by

The WJG Press and Baishideng

SUBMISSION OF MANUSCRIPTS

Manuscripts should be typed in 1.5 line spacing and 12 pt. Book Antiqua with ample margins. Number all pages consecutively, and start each of the following sections on a new page: Title Page, Abstract, Introduction, Materials and Methods, Results, Discussion, Acknowledgments, References, Tables, Figures, and Figure Legends. Neither the editors nor the publisher are responsible for the opinions expressed by contributors. Manuscripts formally accepted for publication become the permanent property of The WJG Press and Baishideng, and may not be reproduced by any means, in whole or in part, without the written permission of both the authors and the publisher. We reserve the right to copy-edit and put onto our website accepted manuscripts. Authors should follow the relevant guidelines for the care and use of laboratory animals of their institution or national animal welfare committee. For the sake of transparency in regard to the performance and reporting of clinical trials, we endorse the policy of the International Committee of Medical Journal Editors to refuse to publish papers on clinical trial results if the trial was not recorded in a publicly-accessible registry at its outset. The only register now available, to our knowledge, is http://www.clinicaltrials.gov sponsored by the United States National Library of Medicine, and we encourage all potential contributors to register with it. However, in the event that other registers become available, you will be duly notified. A letter of recommendation from each author's organization should be provided with the contributed article to ensure the privacy and secrecy of research is protected.

Authors should retain one copy of the text, tables, photographs and illustrations because rejected manuscripts will not be returned to the corresponding author(s) and the editors will not be responsible for loss or damage to photographs and illustrations sustained during mailing.

Online submissions

Manuscripts should be submitted through the Online Submission System at: http://wjg.wjgnet.com/wjg. Authors are highly recommended to consult the ONLINE INSTRUCTIONS TO AUTHORS (http://www.wjgnet.com/wjg/help/instructions.jsp) before attempting to submit online. For assistance, authors encountering problems with the Online Submission System may send an email describing the problem to submission@wjgnet.com, or by telephone: +86-10-85381892. If you submit your manuscript online, do not make a postal contribution. Repeated online submission for the same manuscript is strictly prohibited.

MANUSCRIPT PREPARATION

All contributions should be written in English. All articles must be submitted using word-processing software. All submissions must be typed in 1.5 line spacing and 12 pt. Book Antiqua with ample margins. Style should conform to our house format. Required information for each of the manuscript sections is as follows:

Title page

Title: Title should be less than 12 words.

Running title: A short running title of less than 6 words should be provided.

Authorship: Authorship credit should be in accordance with the standard proposed by International Committee of Medical Journal Editors, based on (1) substantial contributions to conception and design, acquisition of data, or analysis and interpretation of data; (2) drafting the article or revising it critically for important intellectual content; and (3) final approval of the version to be published. Authors should meet conditions 1, 2, and 3.

Institution: Author names should be given first, then the complete name of institution, city, province and postcode. For example, Xu-Chen Zhang, Li-Xin Mei, Department of Pathology, Chengde Medical College, Chengde 067000, Hebei Province, China. One author may be represented from two institutions, for example, George Sgourakis, Department of General, Visceral, and Transplantation Surgery, Essen 45122, Germany; George Sgourakis, 2nd Surgical Department, Korgialenio-Benakio Red Cross Hospital, Athens 15451, Greece

Author contributions: The format of this section should be: Author contributions: Wang CL and Liang L contributed equally to this work; Wang CL, Liang L, Fu JF, Zou CC, Hong F and Wu XM designed the research; Wang CL, Zou CC, Hong F and Wu XM performed the research; Xue JZ and Lu JR contributed new reagents/analytic tools; Wang CL, Liang L and Fu JF analyzed the data; and Wang CL, Liang L and Fu JF wrote the paper.

Supportive foundations: The complete name and number of

supportive foundations should be provided, e.g., Supported by National Natural Science Foundation of China, No. 30224801

Correspondence to: Only one corresponding address should be provided. Author names should be given first, then author title, affiliation, the complete name of institution, city, postcode, province, country, and email. All the letters in the email should be in lower case. A space interval should be inserted between country name and email address. For example, Montgomery Bissell, MD, Professor of Medicine, Chief, Liver Center, Gastroenterology Division, University of California, Box 0538, San Francisco, CA 94143, United States. montgomery.bissell@ucsf.edu

Telephone and fax: Telephone and fax should consist of +, country number, district number and telephone or fax number, e.g., Telephone: +86-10-59080039, Fax: +86-10-85381893

Peer reviewers: All articles received are subject to peer review. Normally, three experts are invited for each article. Decision for acceptance is made only when at least two experts recommend an article for publication. Reviewers for accepted manuscripts are acknowledged in each manuscript, and reviewers of articles which were not accepted will be acknowledged at the end of each issue. To ensure the quality of the articles published in *WJG*, reviewers of accepted manuscripts will be announced by publishing the name, title/position and institution of the reviewer in the footnote accompanying the printed article. For example, reviewers: Professor Jing-Yuan Fang, Shanghai Institute of Digestive Disease, Shanghai, Affiliated Renji Hospital, Medical Faculty, Shanghai Jiaotong University, Shanghai, China; Professor Xin-Wei Han, Department of Radiology, The First Affiliated Hospital, Zhengzhou University, Zhengzhou, Henan Province, China; and Professor Anren Kuang, Department of Nuclear Medicine, Huaxi Hospital, Sichuan University, Chengdu, Sichuan Province, China.

Abstract

There are unstructured abstracts (no more than 256 words) and structured abstracts (no more than 480). The specific requirements for structured abstracts are as follows:

An informative, structured abstracts of no more than 480 words should accompany each manuscript. Abstracts for original contributions should be structured into the following sections. AIM (no more than 20 words): Only the purpose should be included. Please write the aim as the form of "To investigate/study/…; MATERIALS AND METHODS (no more than 140 words); RESULTS (no more than 294 words): You should present *P* values where appropriate and must provide relevant data to illustrate how they were obtained, e.g. 6.92 ± 3.86 *vs* 3.61 ± 1.67, $P < 0.001$; CONCLUSION (no more than 26 words). Available from:http://www.wjgnet.com/wjg/help/8.doc

Key words

Please list 5-10 key words, selected mainly from *Index Medicus*, which reflect the content of the study.

Text

For articles of these sections, original articles, rapid communication and case reports, the main text should be structured into the following sections: INTRODUCTION, MATERIALS AND METHODS, RESULTS and DISCUSSION, and should include appropriate Figures and Tables. Data should be presented in the main text or in Figures and Tables, but not in both. The main text format of these sections, editorial, topic highlight, case report, letters to the editors, can be found at: http://www.wjgnet.com/wjg/help/instructions.jsp.

Illustrations

Figures should be numbered as 1, 2, 3, *etc*., and mentioned clearly in the main text. Provide a brief title for each figure on a separate page. Detailed legends should not be provided under the figures. This part should be added into the text where the figures are applicable. Figures should be either Photoshop or Illustrator files (in tiff, eps, jpeg formats) at high-resolution. Examples can be found at: http://www.wjgnet.com/1007-9327/13/4520.pdf; http://www.wjgnet.com/1007-9327/13/4554.pdf; http://www.wjgnet.com/1007-9327/13/4891.pdf; http://www.wjgnet.com/1007-9327/13/4986.pdf; http://www.wjgnet.com/1007-9327/13/4498.pdf. Keeping all elements compiled is necessary in line-art image. Scale bars should be used rather than magnification factors, with the length of the bar defined in the legend rather than on the bar itself. File names should identify the figure and panel. Avoid layering type directly over shaded or textured areas. Please use uniform legends for the same subjects. For example: Figure 1 Pathological changes in atrophic gastritis after treatment. A: ...; B: ...; C: ...; D: ...; E: ...; F: ...; G: …*etc*. It is our principle to publish high resolution-figures for the printed and E-versions.

Tables

Three-line tables should be numbered 1, 2, 3, *etc*., and mentioned clearly in the main text. Provide a brief title for each table. Detailed legends should not be included under tables, but rather added into the text where applicable. The information should complement, but not duplicate the text. Use one horizontal line under the title, a second under column heads, and a third below the Table, above any footnotes. Vertical and italic lines should be omitted.

Notes in tables and illustrations

Data that are not statistically significant should not be noted. $^{a}P < 0.05$, $^{b}P < 0.01$ should be noted ($P > 0.05$ should not be noted). If there are other series of *P* values, $^{c}P < 0.05$ and $^{d}P < 0.01$ are used. A third series of *P* values can be expressed as $^{e}P < 0.05$ and $^{f}P < 0.01$. Other notes in tables or under illustrations should be expressed as ^{1}F, ^{2}F, ^{3}F; or sometimes as other symbols with a superscript (Arabic numerals) in the upper left corner. In a multi-curve illustration, each curve should be labeled with ●, ○, ■, □, ▲, △, *etc*., in a certain sequence.

Acknowledgments

Brief acknowledgments of persons who have made genuine contributions to the manuscript and who endorse the data and conclusions should be included. Authors are responsible for obtaining written permission to use any copyrighted text and/or illustrations.

REFERENCES

Coding system

The author should number the references in Arabic numerals according to the citation order in the text. Put reference numbers in square brackets in superscript at the end of citation content or after the cited author's name. For citation content which is part of the narration, the coding number and square brackets should be typeset normally. For example, "Crohn's disease (CD) is associated with increased intestinal permeability[1,2]". If references are cited directly in the text, they should be put together within the text, for example, "From references[19,22-24], we know that..."

When the authors write the references, please ensure that the order in text is the same as in the references section, and also ensure the spelling accuracy of the first author's name. Do not list the same citation twice.

PMID and DOI

Pleased provide PubMed citation numbers to the reference list, e.g. PMID and DOI, which can be found at http://www.ncbi.nlm.nih.gov/sites/entrez?db=pubmed and http://www.crossref.org/SimpleTextQuery/, respectively. The numbers will be used in E-version of this journal.

Style for journal references

Authors: the name of the first author should be typed in bold-faced letters. The family name of all authors should be typed with the initial letter capitalized, followed by their abbreviated first and middle initials. (For example, Lian-Sheng Ma is abbreviated as Ma LS, Bo-Rong Pan as Pan BR). The title of the cited article and italicized journal title (journal title should be in its abbreviated form as shown in PubMed), publication date, volume number (in black), start page, and end page [PMID: 11819634 DOI: 10.3748/wjg.13.5396].

Style for book references

Authors: the name of the first author should be typed in bold-faced letters. The surname of all authors should be typed with the initial letter capitalized, followed by their abbreviated middle and first initials. (For example, Lian-Sheng Ma is abbreviated as Ma LS, Bo-Rong Pan as Pan BR) Book title. Publication number. Publication place: Publication press, Year: start page and end page.

Format

Journals

English journal article (list all authors and include the PMID where applicable)

1 **Jung EM**, Clevert DA, Schreyer AG, Schmitt S, Rennert J, Kubale R, Feuerbach S, Jung F. Evaluation of quantitative contrast harmonic imaging to assess malignancy of liver tumors: A prospective controlled two-center study. *World J Gastroenterol* 2007; **13**: 6356-6364 [PMID: 18081224 DOI: 10.3748/wjg.13.6356]

Chinese journal article (list all authors and include the PMID where applicable)

2 **Lin GZ**, Wang XZ, Wang P, Lin J, Yang FD. Immunologic effect of Jianpi Yishen decoction in treatment of Pixu-diarrhoea. *Shijie Huaren Xiaohua Zazhi* 1999; **7**: 285-287

In press

3 **Tian D**, Araki H, Stahl E, Bergelson J, Kreitman M. Signature of balancing selection in Arabidopsis. *Proc Natl Acad Sci USA* 2006; In press

Organization as author

4 **Diabetes Prevention Program Research Group**. Hypertension,

insulin, and proinsulin in participants with impaired glucose tolerance. *Hypertension* 2002; **40**: 679-686 [PMID: 12411462 PMCID:2516377 DOI:10.1161/01.HYP.0000035706.28494.09]

Both personal authors and an organization as author

5 **Vallancien G**, Emberton M, Harving N, van Moorselaar RJ; Alf-One Study Group. Sexual dysfunction in 1274 European men suffering from lower urinary tract symptoms. *J Urol* 2003; **169**: 2257-2261 [PMID: 12771764 DOI:10.1097/01.ju.0000067940.76090.73]

No author given

6 21st century heart solution may have a sting in the tail. *BMJ* 2002; **325**: 184 [PMID: 12142303 DOI:10.1136/bmj.325.7357.184]

Volume with supplement

7 **Geraud G**, Spierings EL, Keywood C. Tolerability and safety of frovatriptan with short- and long-term use for treatment of migraine and in comparison with sumatriptan. *Headache* 2002; **42** Suppl 2: S93-99 [PMID: 12028325 DOI:10.1046/j.1526-4610.42.s2.7.x]

Issue with no volume

8 **Banit DM**, Kaufer H, Hartford JM. Intraoperative frozen section analysis in revision total joint arthroplasty. *Clin Orthop Relat Res* 2002; (**401**): 230-238 [PMID: 12151900 DOI:10.1097/00003086-200208000-00026]

No volume or issue

9 Outreach: Bringing HIV-positive individuals into care. *HRSA Careaction* 2002; 1-6 [PMID: 12154804]

Books

Personal author(s)

10 **Sherlock S**, Dooley J. Diseases of the liver and billiary system. 9th ed. Oxford: Blackwell Sci Pub, 1993: 258-296

Chapter in a book (list all authors)

11 **Lam SK**. Academic investigator's perspectives of medical treatment for peptic ulcer. In: Swabb EA, Azabo S. Ulcer disease: investigation and basis for therapy. New York: Marcel Dekker, 1991: 431-450

Author(s) and editor(s)

12 **Breedlove GK**, Schorfheide AM. Adolescent pregnancy. 2nd ed. Wieczorek RR, editor. White Plains (NY): March of Dimes Education Services, 2001: 20-34

Conference proceedings

13 **Harnden P**, Joffe JK, Jones WG, editors. Germ cell tumours V. Proceedings of the 5th Germ cell tumours Conference; 2001 Sep 13-15; Leeds, UK. New York: Springer, 2002: 30-56

Conference paper

14 **Christensen S**, Oppacher F. An analysis of Koza's computational effort statistic for genetic programming. In: Foster JA, Lutton E, Miller J, Ryan C, Tettamanzi AG, editors. Genetic programming. EuroGP 2002: Proceedings of the 5th European Conference on Genetic Programming; 2002 Apr 3-5; Kinsdale, Ireland. Berlin: Springer, 2002: 182-191

Electronic journal (list all authors)

15 Morse SS. Factors in the emergence of infectious diseases. Emerg Infect Dis serial online, 1995-01-03, cited 1996-06-05; 1(1): 24 screens. Available from: URL: http//www.cdc.gov/ncidod/EID/eid.htm

Patent (list all authors)

16 **Pagedas AC**, inventor; Ancel Surgical R&D Inc., assignee. Flexible endoscopic grasping and cutting device and positioning tool assembly. United States patent US 20020103498. 2002 Aug 1

Statistical data

Write as mean ± SD or mean ± SE.

Statistical expression

Express *t* test as *t* (in italics), *F* test as *F* (in italics), chi square test as χ^2 (in Greek), related coefficient as *r* (in italics), degree of freedom as υ (in Greek), sample number as *n* (in italics), and probability as *P* (in italics).

Units

Use SI units. For example: body mass, m (B) = 78 kg; blood pressure, p (B) = 16.2/12.3 kPa; incubation time, t (incubation) = 96 h, blood glucose concentration, c (glucose) 6.4 ± 2.1 mmol/L; blood CEA mass concentration, p (CEA) = 8.6 24.5 μg/L; CO_2 volume fraction, 50 mL/L CO_2, not 5% CO_2; likewise for 40 g/L formaldehyde, not 10% formalin; and mass fraction, 8 ng/g, *etc*. Arabic numerals such as 23, 243, 641 should be read 23 243 641.

The format for how to accurately write common units and quantums can be found at: http://www.wjgnet.com/wjg/help/14.doc.

Abbreviations

Standard abbreviations should be defined in the abstract and on first mention in the text. In general, terms should not be abbreviated unless they are used repeatedly and the abbreviation is helpful to the reader. Permissible abbreviations are listed in Units, Symbols and Abbreviations: A Guide for Biological and Medical Editors and Authors (Ed. Baron DN, 1988) published by The Royal Society of Medicine, London. Certain commonly used abbreviations, such as DNA, RNA, HIV, LD50, PCR, HBV, ECG, WBC, RBC, CT, ESR, CSF, IgG, ELISA, PBS, ATP, EDTA, mAb, can be used directly without further explanation.

Italics

Quantities: *t* time or temperature, *c* concentration, *A* area, *l* length, *m* mass, *V* volume.
Genotypes: *gyrA*, *arg* 1, *c myc*, *c fos*, *etc*.
Restriction enzymes: *Eco*RI, *Hin*dI, *Bam*HI, *Kbo* I, *Kpn* I, *etc*.
Biology: *H pylori*, *E coli*, *etc*.

SUBMISSION OF THE REVISED MANUSCRIPTS AFTER ACCEPTED

Please revise your article according to the revision policies of *WJG*. The revised version including manuscript and high-resolution image figures (if any) should be copied on a floppy or compact disk. The author should send the revised manuscript, along with printed high-resolution color or black and white photos, copyright transfer letter, and responses to the reviewers by courier (such as EMS/DHL).

Editorial Office

World Journal of Gastroenterology

Editorial Department: Room 903, Building D,
Ocean International Center,
No.62 Dongsihuan Zhonglu,
Chaoyang District, Beijing 100025, China
E-mail: wjg@wjgnet.com
http://www.wjgnet.com
Telephone: +86-10-59080039
Fax: +86-10-85381893

Language evaluation

The language of a manuscript will be graded before it is sent for revision. (1) Grade A: priority publishing; (2) Grade B: minor language polishing; (3) Grade C: a great deal of language polishing needed; (4) Grade D: rejected. Revised articles should reach Grade A or B.

Copyright assignment form

Please download a Copyright assignment form from http://www.wjgnet.com/wjg/help/10.doc.

Responses to reviewers

Please revise your article according to the comments/suggestions provided by the reviewers. The format for responses to the reviewers' comments can be found at: http://www.wjgnet.com/wjg/help/9.doc.

Proof of financial support

For paper supported by a foundation, authors should provide a copy of the document and serial number of the foundation.

Links to documents related to the manuscript

WJG will be initiating a platform to promote dynamic interactions between the editors, peer reviewers, readers and authors. After a manuscript is published online, links to the PDF version of the submitted manuscript, the peer-reviewers' report and the revised manuscript will be put on-line. Readers can make comments on the peer reviewer's report, authors' responses to peer reviewers, and the revised manuscript. We hope that authors will benefit from this feedback and be able to revise the manuscript accordingly in a timely manner.

Science news releases

Authors of accepted manuscripts are suggested to write a science news item to promote their articles. The news will be released rapidly at EurekAlert/AAAS (http://www.eurekalert.org). The title for news items should be less than 90 characters; the summary should be less than 75 words; and main body less than 500 words. Science news items should be lawful, ethical, and strictly based on your original content with an attractive title and interesting pictures.

Publication fee

Authors of accepted articles must pay a publication fee.
EDITORIAL, TOPIC HIGHLIGHTS, BOOK REVIEWS and LETTERS TO THE EDITOR are published free of charge.